LEUPHANA
UNIVERSITÄT LÜNEBURG

Identifikation, Strukturaufklärung und Eigenschaften von Transformations-produkten ausgewählter organischer UV-Filter-Substanzen

Von der Fakultät Nachhaltigkeit

der Leuphana Universität Lüneburg zur Erlangung des Grades

Doktorin der Naturwissenschaft

– Dr. rer. nat. –

genehmigte Dissertation von

Franziska Schneider (geb. Jentzsch)

geboren am 04. Juli 1988 in Leipzig

Eingereicht am:	04. Dezember 2023
Mündliche Verteidigung (Disputation) am:	12. Juni 2024
Betreuer und Erstgutachter:	Prof. Dr. Klaus Kümmerer Leuphana Universität Lüneburg
Zweitgutachter:	Prof. Dr. Ralf Ebinghaus Leuphana Universität Lüneburg
Drittgutachter:	Prof. Dr. Kai Bester Aarhus Universität, Roskilde, Dänemark

Die einzelnen Beiträge des kumulativen Dissertationsvorhabens sind wie folgt veröffentlicht:

F. Jentzsch, *et al.* (2016) doi: *https://doi.org/10.1016/j.scitotenv.2016.08.017*.

F. Jentzsch, *et al.* (2019) doi: *https://doi.org/10.1016/j.scitotenv.2019.134048*.

F. Jentzsch, *et al.* (2023) doi: *https://doi.org/10.1111/ics.12908*.

Veröffentlichungsjahr: 2024

„Wir können den Wind nicht ändern, aber die Segel anders setzen.“

Aristoteles

Zusammenfassung

Ultraviolett- (UV-)Filter-Substanzen werden vielfach eingesetzt. In Körperpflegeprodukten hat die Verwendung von UV-Filtern das Ziel die Haut vor schädlicher UV-Strahlung – und somit auch vor strahlungsbedingten Krankheiten wie Hautkrebs – zu schützen. Dem Nutzen steht jedoch die steigende Besorgnis bezüglich der Auswirkung von direkten wie indirekten Einträgen von UV-Filtern in die Umwelt gegenüber. Im Fokus der Besorgnis stehen die hormonellen Aktivitäten, das Bioakkumulationspotential und die Stabilität der UV-Filter. Letzteres ist sowohl in der Umwelt als auch während herkömmlicher (Ab-) Wasserbehandlungsverfahren relevant. Ein bewährtes dezentrales Verfahren zur Eliminierung von UV-Filtern ist die Bestrahlung mit UV-Licht, welches ebenfalls zur Desinfektion eingesetzt wird. Nicht selten haben solche erweiterten Oxidationsverfahren die Bildung von Transformationsprodukten (TP) zur Folge, deren Identität sowie Eigenschaften ebenso wichtig sind wie ihr Nachweis. Um die hervorgerufenen Umweltschäden einzudämmen, gewinnt die Untersuchung der Vielzahl der gebildeten TP zunehmend an Bedeutung, da die Erkenntnisse dabei helfen u.a. zukünftigen Strategien und Gesetzgebungen umzusetzen. Durch die Erforschung von TP können Datenlücken identifiziert bzw. geschlossen und anwendbare Methoden bereitgestellt werden, die der Vielzahl an TP gewachsen sind. Durch die Bewertung von TP kann das Ziel einer nicht-toxischen Umwelt im Sinne des „Europäischen Grünen Deals“ verfolgt und vorangebracht werden.

Die vorliegende Doktorarbeit geht den Fragen nach: *Was für TP entstehen, wenn UV-Filter in wässriger Lösung photolytisch eliminiert werden? Geht von den TP eine gleiche, geringere oder höhere Besorgnis aus als von ihren Ausgangssubstanzen? Wie sollen TP – ob bekannt oder noch unbekannt – grundsätzlich erfasst und bewertet werden?*

Um die Fragen zu beantworten, wurde in dieser Doktorarbeit untersucht, welche TP von organischen UV-Filtern bereits identifiziert wurden und welches Umweltverhalten – insbesondere die leichte biologische Abbaubarkeit – die TP aufwiesen. Zunächst wurden jene TP durch Auswertung von Studien aus der Literatur zusammengetragen, welche aus abiotischen und biotischen Prozessen stammen und deren chemische Struktur in den Studien aufgeklärt beziehungsweise vorgeschlagen wurden. Ausgehend von den gefundenen TP wurden außerdem Informationen zu deren Stabilität recherchiert, da die Bildung von stabilen TP nachteilig für ihre Eliminierung aus der Umwelt ist. Dabei wurde eine umfangreiche Datenlücke bezüglich der Verfügbarkeit von Informationen zur leichten biologischen Abbaubarkeit von TP von UV-Filtern offengelegt. Neben der Notwendigkeit in Zukunft neue Daten bereitzustellen, leitet sich aus den Ergebnissen der Bedarf eines neuen kombinierten Ansatzes zur Datengenerierung für relevante UV-Filter und TP ab.

Darüber hinaus wurde das Abbauverhalten und die Transformation zweier prominenter Vertreter organischer UV-Filter – namentlich 2-Ethylhexyl-4-methoxycinnamat (EHMC) und Octocrylene (OCR) – während der wässrigen Photolyse mittels UV-C-Strahlung untersucht. Neben der Abbaukinetik unter verschiedenen Versuchsbedingungen und dem analytischen Nachweis von TP, wurden außerdem die chemischen Strukturen der TP von EHMC aufgeklärt. Auf Basis der Strukturvorschläge für die TP von EHMC wurden die Eigenschaften der TP mit computergestützten Methoden vorhergesagt. Der Nachweis von TP erfolgte dabei zunächst über Flüssigkeitschromatographie mit UV-Detektion (HPLC-UV). Die Strukturen der TP von EHMC wurden anschließend mittels Flüssigkeitschromatographie-Tandem-Massenspektrometrie (LC-MS/MS) aufgeklärt. Zur Vorhersage der Eigenschaften von TP wurde Software zur Analyse quantitativer Struktur-Wirkungs-Beziehungen (engl. "*quantitative structure-activity relationship*", QSAR) verschiedener Anbieter eingesetzt. Da in realen Proben häufig mehr als ein Spurenstoff gleichzeitig vorliegt, wurde zudem untersucht, ob die Bestrahlung einer Mischung aus EHMC und OCR mit UV-C-Licht in wässriger Lösung zu Mischungseffekten führt.

Ein Ergebnis dieser Doktorarbeit ist der erstmals zusammengestellte Überblick über 177 TP, die aus der Transformation von elf UV-Filtern während abiotischer und biotischer Prozesse hervorgehen. Eine Analyse zeigt die ungleichmäßige Verteilung der Studien über die UV-Filter und die Prozessarten. Um einen besseren Überblick über die Eigenschaften der TP zu erlagen, wird die Fachliteratur sowie die Datenbank der Europäischen Chemikalien Agentur (ECHA) auf Informationen und Daten zur Stabilität der TP geprüft. Die Auswertung deckt eine große Datenlücke auf, da die Daten zur leichten biologischen Abbaubarkeit für mehr als 80 % der TP von UV-Filtern nicht verfügbar sind.

Die Ergebnisse dieser Doktorarbeit zeigen neue Erkenntnisse zur Bildung von TP der beiden getesteten UV-Filter während der wässrigen Photolyse mit UV-C-Bestrahlung. Die Strukturvorschläge der TP von EHMC beinhalten sowohl bereits bekannte TP von EHMC als auch neue TP, welche erstmalig nachgewiesen worden sind. Anhand der Strukturvorschläge wird mithilfe von QSAR-Vorhersagen abgeschätzt, welche der TP gleich bzw. toxischer als EHMC sind und daher weiterer Forschung bedürfen. Im Fall von OCR wurde erstmals die Eliminierung der Ausgangssubstanz sowie die Bildung von TP mittels HPLC-UV nachgewiesen. Zudem werden in den photolytischen Versuchen mit der Mischung aus EHMC und OCR erstmals UV-Filter-UV-Filter-Wechselwirkungen zwischen OCR und EHMC und die Bildung von Mischungs-TP aufgezeigt.

Die Doktorarbeit dient als Grundlage für weitere Forschung zur TP-Bewertung: Zum einen werden Wissenslücken zum unvollständigen abiotischen Abbau der beiden UV-Filter EHMC und OCR und der möglichen Bildung von Photo-TP gefüllt. Zum anderen werden neue

Wissenslücken zu Eigenschaften von TP aus UV-Filtern im Allgemeinen aufgezeigt. Die Ergebnisse zeigen, dass die Eliminierung eines kritischen Stoffes nicht das alleinige Ziel einer Behandlung spurenstoffhaltiger Medien durch erweiterte oxidative Prozesse ist. TP müssen nachgewiesen, identifiziert und charakterisiert werden. Es wird außerdem deutlich, dass ein harmonisiertes Vorgehen benötigt wird, nach dem TP erfasst und bewertet werden. Der Nachweis der Mischungs-TP zeigt zudem, dass die vorliegenden Ergebnisse dieser Forschung wichtige Hinweise für die praktische Anwendung von Bestrahlung zur Spurenstoffeliminierung unter realen Bedingungen liefern.

Die angewendete Trennmethode mittels LC eignet sich gut für die Übertragung auf LC-HRMS zur *non-target*-Analyse von TP in wässrigen Lösungen. Eine Übertragung der Methode auf komplexere Proben bedarf jedoch einer optimierten Probenvorbereitung und ggf. Anreicherung der Analyten. Beim Nachweis von TP mit HPLC-UV liegt die Grenze bei der UV-Aktivität der Analyten. Allerdings kann die Identifizierung über hochauflösende Massenspektrometrie erfolgen. Diese Technik sollte in Zukunft angewendet werden. Weiterentwickelt werden muss auch die Messbarkeit des Mineralisierungsgrades für lipophile Verbindungen, die nur mit Lösungsvermittler in wässrige Lösung gebracht werden können.

Nichtsdestotrotz zeigt diese Doktorarbeit, wie im Sinne des 6. Ziels der nachhaltigen Entwicklung („sauberes Wasser“) und des „Europäischen Grünen Deals“ der Verschmutzung von Gewässern und der Umwelt durch Spurenstoffe von Vornherein entgegengewirkt werden kann.

Zusammenfassend zeigt diese Arbeit, dass, wenn dem Eintrag von besorgniserregenden Stoffen nicht vorgebeugt werden kann, der Eintrag von Spurenstoffen wie UV-Filtern sowie ihren TP zumindest reduziert werden sollte.

Abstract

Ultraviolet (UV) filter substances are widely used. The use of UV filters in personal care products aims to protect the skin from harmful UV radiation - and therefore also from radiation-related diseases such as skin cancer. However, this benefit is opposed by growing concern about the impact of direct and indirect releases of UV filters into the environment. The focus of concern is on hormonal activities, the bioaccumulation potential and the stability of UV filters. The latter is relevant both in the environment and during conventional (waste) water treatment processes. A proven decentralized process for eliminating UV filters is irradiation with UV light, which is also used for disinfection. Such extended oxidation processes often result in the formation of transformation products (TP), whose identity and properties are just as important as their detection. In order to contain the environmental damage caused, the investigation of the large number of TP formed is becoming increasingly important, as the findings help to implement future strategies and legislation, among other things. By researching TP, data gaps can be identified or closed and applicable methods can be provided that can cope with the large number of TP. Through the evaluation of TP, the goal of a non-toxic environment in the sense of the "European Green Deal" can be pursued and advanced.

This doctoral thesis examines the following questions: *What kind of TP are formed when UV filters are eliminated? Are the TP of equal, lesser or greater concern than their parent substances? How should TP - whether known or as yet unknown - be in general recorded and evaluated?*

In order to answer these questions, this doctoral thesis investigated which TP of organic UV filters have already been identified and which environmental behavior - in particular the ready biodegradability - the TP exhibited. First of all, those TP were compiled by evaluating studies from the literature which originate from abiotic and biotic processes and whose chemical structure was elucidated or proposed in the studies. Based on the TP found, information on their stability was also researched, as the formation of stable TP is detrimental to their elimination from the environment. This revealed an extensive data gap regarding the availability of information on the ready biodegradability of TP from UV filters. In addition to the need to provide new data in the future, the results indicate the need for a new combined approach to data generation for relevant UV filters and TP.

In addition, the degradation behavior and transformation of two prominent representatives of organic UV filters - namely 2-ethylhexyl-4-methoxycinnamate (EHMC) and octocrylene (OCR) - during aqueous photolysis using UV-C radiation were investigated. In addition to the degradation kinetics under different experimental conditions and the analytical detection of TP, the chemical structures of the TP of EHMC were also elucidated. Based on the proposed

structures of the TP of EHMC, the properties of the TP were predicted using computer-based methods. The detection of TP was initially carried out using liquid chromatography with UV detection (HPLC-UV). The structures of the TP of EHMC were then elucidated using liquid chromatography-tandem mass spectrometry (LC-MS/MS). Quantitative structure-activity relationship (QSAR) analysis software from various suppliers was used to predict the properties of TP. Since in real samples often more than one trace compound is present at the same time, it was also investigated whether irradiation of a mixture of EHMC and OCR with UV-C light in aqueous solution leads to mixture-effects.

One result of this doctoral thesis is the first compiled overview of 177 TP resulting from the transformation of eleven UV filters during abiotic and biotic processes. An analysis shows the uneven distribution of the studies across the UV filters and the process types. To obtain a better overview of the properties of TP, the scientific publications and the database of the European Chemicals Agency (ECHA) were reviewed for information and data on TP stability. The evaluation reveals a large data gap, as the data on ready biodegradability is not available for more than 80 % of the TP of UV filters.

The results of this doctoral thesis show new findings on the formation of TP of the two tested UV filters during aqueous photolysis with UV-C irradiation. The structure proposals of the TP of EHMC include both already known TP of EHMC and new TP, which have been detected for the first time. Based on the structural proposals, QSAR predictions are used to estimate which of the TP are the same or more toxic than EHMC and therefore require further research. In the case of OCR, the elimination of the starting substance and the formation of TP was demonstrated for the first time using HPLC-UV. In addition, the photolytic experiments with the mixture of EHMC and OCR show for the first time UV-filter-UV-filter interactions between OCR and EHMC and the formation of mixture-TP.

The doctoral thesis serves as a basis for further research on TP assessment: On the one hand, gaps in knowledge on the incomplete abiotic degradation of the two UV filters EHMC and OCR and the possible formation of photo-TP are filled. On the other hand, new knowledge gaps on the properties of TP from UV filters in general are identified. The results show that the elimination of a critical substance is not the sole aim of the treatment of media containing trace substances by extended oxidative processes. TP must be detected, identified and characterized. It is also clear that a harmonized approach is needed to detect and evaluate TP. The detection of mixed TP also shows that the available results of this research provide important information for the practical application of irradiation for trace substance elimination under real conditions.

The LC separation method used is well suited for transfer to LC-HRMS for non-target analysis of TP in aqueous solutions. However, transferring the method to more complex samples requires optimized sample preparation and, if necessary, enrichment of the analytes. When detecting TP with HPLC-UV, the limit lies in the UV-activity of the analytes. However, identification can be carried out using high-resolution mass spectrometry. This technique should be used in the future. The measurability of the degree of mineralization for lipophilic compounds, which can only be brought into aqueous solution with solubilizers, must also be further developed.

Nevertheless, this doctoral thesis shows how the pollution of water bodies and the environment by trace substances can be counteracted from the outset in line with the 6th Sustainable Development Goal ("clean water") and the "European Green Deal".

In summary, this work shows that if the input of substances of concern cannot be prevented, the input of trace substances such as UV filters and their TP should at least be reduced.

Danksagung

Ich danke meinem Doktorvater Prof. Klaus Kümmerer für die Möglichkeit diese Arbeit anzufertigen und die damit verbundene wissenschaftliche Betreuung.

Bei Prof. Dr. Ralf Ebinghaus und Prof. Dr. Kai Bester bedanke ich mich für dafür, dass Sie das Zweit- und Drittgutachten übernommen haben.

Mein herzlicher Dank geht an Dr. Oliver Olsson für die langjährige Unterstützung, seine konstruktiven Beiträge und die lebendigen Diskussionen. Dank seiner Tipps im Umgang mit Veröffentlichungsprozessen lernte ich schnell mich im Wissenschaftsdschungel zurecht zu finden und auf eigenen Beinen zu stehen. Seine Weisheiten haben mich nachhaltig geprägt und helfen mir noch heute das ein oder andere Mal über meinen Schatten zu springen.

Ich danke Prof. Matthias Gaßmann, der in der Anfangszeit mein Büronachbar war und dessen ruhige Art und Erfahrung mir die das Ankommen sehr erleichtert hat.

Ich danke auch allen aus der Arbeitsgruppe, die mich während meiner Zeit in Lüneburg freundlich aufgenommen und begleitet haben. Ihr seid zu einem Teil meines Weges geworden.

Ich danke meinen Freundinnen, die sich immer wieder Zeit für mich nehmen: Unsere gemeinsame Zeit gibt mir die Kraft durchzuhalten.

- Mein Dank geht an Eva, deren Engagements mich bis heute beeindrucken. Ich bin froh, dass sich unsere Wege in meiner Zeit in Lüneburg gekreuzt haben und wir uns bis heute nicht aus den Augen verloren haben.
- Ich danke auch Steffi die schönen Zeiten – auch außerhalb des Labors – und für den Tipp, der mich zu meinem heutigen Arbeitgeber geführt hat.
- Außergewöhnlicher Dank geht dabei an Elisa: Für unsere Freundschaft – egal auf welche Distanz – bin ich so dankbar! Ob ich wissenschaftlichen Rat oder eine Freundin suche, du bist für mich da.
- Mit dem Beginn meiner Anstellung am UBA kreuzten sich dann plötzlich unsere Wege und ich fragte mich, ob sie das vielleicht schon in Lüneburg getan haben. Ich danke daher Lena, die zu eine meiner besten Freundinnen geworden ist, für die gemeinsamen Jahre Tür an Tür in Dessau. Seit ich wieder in meiner Heimat Leipzig wohne, bist du eine meiner engsten Vertrauten geworden und bist immer für mich da.
- Maria danke ich insbesondere für unser Freundschaft, die wir jetzt schon seit unserem gemeinsamen Studium haben. Dein Feedback und deine ehrliche, direkte Art sind eine Bereicherung und ich schätze dich sehr.
- Außerdem danke ich meinen UBA-Kolleginnen dafür, dass sie immer für mich da sind.

Ich danke Hanni, Jule, Georg und Katha, die mich mit ihrer offenen Art in Ihrer Mitte aufgenommen haben.

Ob nah oder fern, Marcel ist für mich da, wenn ich ihn brauchte. Ich danke dir für deine Unterstützung.

Mein Dank geht auch an meine Familie, die nach meinem erschwerten Start für mich da waren.

Meinen Mann, Mario, danke ich für unsere langjährige Freundschaft und die schier endlose Liebe, aus der ich immer wieder Kraft schöpfe, um weiter für meine Träume zu kämpfen. Du hast so oft die richtigen Worte gefunden, die mich motiviert und meiner persönlichen Weiterentwicklung zu neuem Schwung verholfen haben. Du warst für mich da, als es am dunkelstem war und nun erleuchten wir uns gegenseitig den Weg in unsere gemeinsame Zukunft. Ich danke dir, dass du immer ein offenes Ohr hast und dass du dir die Zeit genommen hast zu verstehen, was diese Doktorarbeit für mich bedeutet.

Inhaltsverzeichnis

Abbildungsverzeichnis

Tabellenverzeichnis

Abkürzungsverzeichnis

3-BC	3-Benzylidencampher
4-MBA	4-Methoxybenzaldehyd
ACN	Acetonitril
BMDM	Avobenzon (INCI: Butylmethoxydibenzoylmethan)
BP-3	2-Hydroxy-4-methoxybenzophenon, auch bekannt als: Oxybenzon (INCI: Benzophenon-3)
CAS-Nr.	Registriernummer in der Datenbank des „Chemical Abstract Service“
DHHB	Diethylaminohydroxybenzoylhexylbenzoat (= INCI)
ECHA	Europäische Chemikalienagentur
EIC	Extrahiertes Ionenchromatogramm
EFSA	Europäische Behörde für Lebensmittelsicherheit (englisch “European Food Safety Authority”)
EHDP	2-Ethylhexyl-4-dimethylaminobenzoat, auch bekannt als: Padimate O, Octyldimethyl-PABA oder abgekürzt OD-PABA
EHMC	2-Ethylhexyl-4-methoxycinnamat (INCI: Ethylhexyl-methoxycinnamat), auch bekannt als: Octinoxat oder Octylmethoxycinnamat (abgekürzt: OMC)
Et-PABA	Benzocain oder *para*-Aminobenzoesäureethylester
EU	Europäische Union
HPLC	Hochleistungsflüssigkeitschromatographie (englisch “high performance liquid chromatography”)
HPLC-UV	Hochleistungsflüssigkeitschromatographie gekoppelt mit einem Ultraviolett-Detektor
IMC	4-Methoxyzimtsäure-3-methylbutylester (INCI: Isoamyl *p*-methoxycinnamat), auch bekannt als: Amiloxat
INCI	internationale Benennung kosmetischer Inhaltsstoffe (englisch “International Nomenclature Cosmetic Ingredients”)
LC-MS	Flüssigkeitschromatographie gekoppelt mit Massenspektrometrie

LC-MS/MS	Flüssigkeitschromatographie gekoppelt mit einem Tandem-Massenspektrometer
MBC	3-(4′-Methylbenzyliden)campher (INCI: 4-Methylbenzylidencampher), auch bekannt als: Enzacamen
MS	Massenspektrometrie
m/z	Masse-zu-Ladungsverhältnis
OCR	2-Ethylhexyl-2-cyano-3,3-diphenyl-acrylat (INCI: Octocrylene), auch bekannt als: Octocrilen
OD	außerhalb des Anwendungsbereichs (englisch “out-of-domain”)
OECD	Organisation für wirtschaftliche Zusammenarbeit und Entwicklung (englisch “Organisation for Economic Co-operation and Development”)
PABA	*para*-Aminobenzoesäure oder 4-Aminobenzoesäure
PBSA	2-Phenylbenzimidazol-5-sulfonsäure (INCI: Phenylbenzimidazolsulfonsäure), auch bekannt als: Ensulizol
Photo-TP	Photo-Transformationsprodukt(e)
QSAR	quantitative Struktur-Wirkungs-Beziehung (englisch “quantitative structure-activity relationship”)
TOC	Gesamter organischer Kohlenstoff (englisch “total organic carbon”)
TP	Transformationsprodukt(e)
UV	Ultraviolett
v/v	Volumenanteil φ

Publikationsverzeichnis

Veröffentlichungen in Fachzeitschriften

F. Jentzsch, O. Olsson, J. Westphal, M. Reich, C. Leder, K. Kümmerer (2016) Photodegradation of the UV filter ethylhexyl methoxycinnamate under ultraviolet light: Identification and in silico assessment of photo-transformation products in the context of grey water reuse. *Science of the Total Environment* 572: 1092-1100. DOI: https://doi.org/10.1016/j.scitotenv.2016.08.017

F. Jentzsch, M. Reich, K. Kümmerer, O. Olsson (2019) Photolysis of mixtures of UV filters octocrylene and ethylhexyl methoxycinnamate leads to formation of mixed transformation products and different kinetics. *Science of the Total Environment* 134048. DOI: https://doi.org/10.1016/j.scitotenv.2019.134048

F. Jentzsch, K. Kümmerer, O. Olsson (2023) Status quo on identified transformation products of organic ultraviolet filters and their persistence. *International Journal of Cosmetic Science* 45 (Suppl. 1): 101–126. DOI: https://doi.org/10.1111/ics.12908

Konferenz- und Tagungsbeiträge

F. Jentzsch, O. Olsson, K. Kümmerer (Mai 2015) Identification and Assessment of Photo Transformation Products of the UV Filters Octocrylene and Ethylhexyl methoxycinnamate Present in Grey Water Intended for Water Reuse. Society of Environmental Toxicology and Chemistry (SETAC) Europe 25th Annual Meeting, 03. – 07. Mai 2015, Barcelona, Spanien, Poster.

F. Jentzsch, C. Leder, K. Kümmerer, O. Olsson (September 2015) Identification and Assessment of Photo Transformation Products of the UV Filter Ethylhexyl Methoxycinnamate Present in Grey Water Intended for Water Reuse. 15th EuCheMS International Conference on Chemistry and the Environment (ICCE) 20. – 24. September 2015, Leipzig, Deutschland, Poster.

Sonstige Veröffentlichungen, Konferenzbeiträge und Vorträge

Umweltbundesamt (UBA): K. Adlunger, J. M. Anke, G. Bachem, H. Banning, A. Biegel-Engler, K. Blondzik, U. Braun, A. Eckhardt, D. Gildemeister, F. Hilliges, G. Hoffmann, **F. Jentzsch**, S. Klitzke, J. Kuckelkorn, K. Martens, A. Müller, C. Pickl, U. Pirntke, J. Rechenberg, D. Sättler, U. Schmidt, G. Speichert, I. Warnke, J. Wehner, R. Wischer, *Redaktion*: K. Adlunger, H. Banning, **F. Jentzsch** (in alphabetischer Reihenfolge) (November 2021) Chemikalieneintrag in Gewässer vermindern – Trifluoracetat (TFA) als persistente und mobile Substanz mit vielen Quellen: Quellen, Eintragspfade, Umweltkonzentrationen von TFA und regulatorische Ansätze. *UBA Hintergrund: Chemikalien, Wirtschaft | Konsum, Boden | Landwirtschaft, Wasser*, https://www.umweltbundesamt.de/publikationen/chemikalieneintrag-in-gewaesser-vermindern

European Food Safety Authority (EFSA): M. Egsmose, G. Fait, W. Janzen, **F. Jentzsch**, R. Lava, C. Lythgo, L. Padovani, C. Pickl, J. Priegnitz (in alphabetischer Reihenfolge) (15. März 2022) Scientific guidance on soil phototransformation products in groundwater – consideration, parameterisation and simulation in the exposure assessment of plant protection products. *EFSA Journal*, 20 (3): e07119. DOI: https://doi.org/10.2903/j.efsa.2022.7119

F. Jentzsch, M. Diehle, H. Banning, C. Pickl (Mai 2022) Trifluoroacetate leaching potential from fluorinated herbicides – a balancing and FOCUS modelling approach. Society of Environmental Toxicology and Chemistry (SETAC) Europe 32nd Annual Meeting, 15. – 19. Mai 2022, Kopenhagen, Dänemark, Vortrag.

F. Jentzsch, W. Janzen, C. Pickl (Juni 2022) Latest development on the assessment of soil photo transformation products in groundwater – making of and status quo on the new EFSA Guidance Document. 24th International Akademie Fresenius AGRO Conference – Behaviour of Pesticides in Air, Soil and Water, 08. – 09. Juni 2022, Online, Vortrag.

Umweltbundesamt (UBA): K. Adlunger, J. M. Anke, G. Bachem, H. Banning, A. Biegel-Engler, K. Blondzik, U. Braun, A. Eckhardt, D. Gildemeister, F. Hilliges, G. Hoffmann, **F. Jentzsch**, S. Klitzke, J. Kuckelkorn, K. Martens, A. Müller, C. Pickl, U. Pirntke, J. Rechenberg, D. Sättler, U. Schmidt, G. Speichert, I. Warnke, J. Wehner, R. Wischer, *Redaktion*: K. Adlunger, H. Banning, **F. Jentzsch** (in alphabetischer Reihenfolge) (September 2022) Reducing the input of chemicals into waters: trifluoroacetate (TFA) as a persistent and mobile substance with many sources. *UBA Background: Chemicals Economy |*

Consumption Soil | Agriculture Water, https://www.umweltbundesamt.de/publikationen/reducing-the-input-of-chemicals-into-waters

S. Sturm, U. Karges, F. Freeling, F. Brauer, T. Vollmer, T. aus der Beek, **F. Jentzsch** (2023) TFA im Wasserkreislauf: Ursachen – Einträge –Minimierung. Spurenstoffe und Krankheitserreger im Wasserkreislauf (SUK) 27. - 28. März 2023, Frankfurt am Main, Deutschland, Poster.

1 Einleitung

1.1 Organische UV-Filter im Spannungsfeld zwischen Schutzfunktion und schädlichen Umweltauswirkungen

Sonnenschutzmittel im Besonderen und einige Körperpflegeprodukte im Allgemeinen haben zum Ziel die Haut des Menschen vor der schädlichen Strahlung der Sonne zu schützen. Aus diesem Grund enthalten diese Produkte Ultraviolett- (UV-) Filter Substanzen. Diese verhindern entweder mittels Reflexion (physikalischer UV-Filter, z.B. TiO_2 oder ZnO) oder durch Absorption der Strahlung (chemische bzw. organische UV-Filter) Schädigungen unserer Haut. In Deutschland stieg die Zahl der Krankenhausbehandlungen aufgrund von Hautkrebs in den Jahren 2000 bis 2020 um rund 81 % (Statistisches Bundesamt, 2023). Das zeigt, dass mit den sich verändernden Sonnenstunden aufgrund des Klimawandels auch der Bedarf nach Sonnenschutz wächst und mehr Information zur Prävention notwendig ist.

Parallel dazu nimmt seit einigen Jahren die wissenschaftliche, öffentliche und regulatorische Besorgnis über das Vorhandensein von organischen UV-Filtern in der Umwelt zu (de Miranda *et al.*, 2021; Germer *et al.*, 2020; Huang *et al.*, 2021; Murawski *et al.*, 2021; Nagorka und Duffek, 2021). Diese Besorgnis bezüglich der Gefahren, die von UV-Filtern ausgehen, zieht auf globaler Ebene mittlerweile erste Konsequenzen nach sich. So verbietet seit 2021 ein Gesetz im US-Bundesstaat Hawaii den Verkauf und die Verbreitung von Sonnenschutzmitteln, die Benzophenon-3 (BP-3) oder 2-Ethylhexyl-4-methoxycinnamat (EHMC) enthalten. Auf diese Weise sollen die umliegenden Riffe des Inselstaats Hawaii geschützt werden (Abou-Dahech *et al.*, 2022; Downs *et al.*, 2022). Neben den Restriktionen im US-Bundesstaat Hawaii wurde der Verkauf und die Verwendung von BP-3 haltigen Sonnenschutzmitteln außerdem in Ländern wie Palau, den Marshallinseln, Thailand, in einigen Karibikinseln (u.a. Aruba und Bonaire) und den amerikanischen Jungferninseln gesetzlich verboten (Downs *et al.*, 2022). Da die VerbraucherInnen weltweit auf die Gefahren von BP-3 für die Meere aufmerksam geworden sind, ist die Verwendung dieses UV-Filters in Sonnenschutzmitteln in den letzten Jahren deutlich zurück gegangen (Downs *et al.*, 2022).

UV-Filter werden trotz ihrer besorgniserregenden Eigenschaften angewendet, um Menschen vor den Auswirkungen solarer Strahlung zu schützen. Ausschlaggebend für die Besorgnis sind die Auswirkung von direkten wie indirekten Einträgen von UV-Filtern in die Umwelt (Cadena-Aizaga et al., 2020; Fent *et al.*, 2008), wobei insbesondere aquatische Ökosysteme unter der Wirkung der in großen Mengen eingetragenen UV-Filter leiden (Boyd *et al.*, 2021; Díaz-Cruz und Barceló, 2009). Die Probleme ergeben sich dabei unter anderem aus den hormonellen Aktivitäten (Huang *et al.*, 2021), dem Bioakkumulationspotential (Bachelot *et al.*, 2012; Gago-Ferrero *et al.*, 2015) und der Stabilität der UV-Filter (Apel *et al.*, 2018).

Diese Arbeit betrachtet zwei ausgewählte organische UV-Filter im Detail: EHMC, dessen Einsatz wie zuvor beschrieben aufgrund seiner bedenklichen Eigenschaften in Hawaii verboten wurde, und Octocrylene (OCR). EHMC und OCR gehören zu den häufig in Körperpflegeprodukten eingesetzten UV-Filtern (Kupper *et al.*, 2006; Sharma *et al.*, 2017). Auf zwei Pfaden gelangen EHMC und OCR in die Umwelt. Der indirekte Eintrag erfolgt über Kläranlagen durch Abrieb oder Abwaschen nach der Anwendung über die Haut. Zudem werden beide Verbindungen direkt durch Freizeitaktivitäten im Wasser freigesetzt (He *et al.*, 2019). Im Fall der indirekten Einträge ist bekannt, dass EHMC und OCR mit den derzeit verfügbaren Behandlungsverfahren nicht vollständig entfernbar sind und somit in die Umwelt gelangen (Balmer *et al.*, 2005; Rodil und Möder, 2008; Hernández-Leal *et al.*, 2010, 2011; Magi *et al.*, 2013; Tsui *et al.*, 2014a; Molins-Delgado *et al.*, 2018). In Folge der Einträge in die Umwelt wurde EHMC aufgrund seiner hohen Lipophilie in Biota nachgewiesen: in Fischen (Blüthgen *et al.*, 2014; Gago-Ferrero *et al.*, 2013) und in wirbellosen Tieren wie Muscheln (Bachelot *et al.*, 2012). Darüber hinaus wurde nachgewiesen, dass EHMC sich in menschlicher Muttermilch (Hany und Nagel, 1995) durch Bioakkumulation anreichert. Dies ist besonders besorgniserregend, da EHMC hormonaktiv wirkt, also ein sogenannter endokriner Disruptor ist. In *in vivo* Tests in Fischen (Tsui *et al.*, 2014a,b) und Ratten (Schlumpf *et al.*, 2004) wirkt EHMC östrogenartig und *in vitro* wurde nachgewiesen, dass EHMC vielfältige hormonelle Wirkungen auf menschliche Rezeptoren hat (Kunz und Fent, 2006; Schreurs *et al.*, 2005). Das photostabile OCR (Ricci *et al.*, 2003; Rodil *et al.*, 2009) wurde ebenfalls wiederholt in der aquatischen Umwelt (Poiger *et al.*, 2004; Balmer *et al.*, 2005; Cuderman und Heath, 2007; Rodil und Möder, 2008) und in aquatischen Lebewesen (Balmer *et al.*, 2005; Buser *et al.*, 2006; Fent *et al.*, 2010; Bachelot *et al.*, 2012; Gago-Ferrero *et al.*, 2013) nachgewiesen. Durch den stark lipophilen Charakter ist auch OCR in der Lage, in der Umwelt zu akkumulieren (Li *et al.*, 2007). *In vitro* wurde die endokrine (insbesondere antiöstrogene und antiandrogene) Aktivität von OCR nachgewiesen (Kunz und Fent, 2006; Fent *et al.*, 2008; Bachelot *et al.*, 2012). Die zunehmende Besorgnis über OCR in der Umwelt basiert somit auf den hohen verwendeten Mengen in Körperpflegeprodukten, dem Vorkommen in der aquatischen Umwelt sowie dem Nachweis in Fischen und Muscheln, der Fähigkeit zur Bioakkumulation und der nachgewiesenen endokrinen Aktivität.

1.2 Herausforderungen in Folge von Abbau und Transformation organische UV-Filter

Die Stabilität bestimmt nicht nur die Langlebigkeit von UV-Filtern in der Umwelt, sondern erschwert – wie zuvor bereits erwähnt – zudem die Entfernung von UV-Filtern während herkömmlichen Prozessen zur (Ab-)Wassereinigung. In den letzten Jahren wurde vermehrt gezeigt, dass einige Techniken (UV-Bestrahlung, Oxidation) in der Lage sind UV-Filter zu entfernen (Hernández-Leal *et al.*, 2010, 2011; Seo *et al.*, 2019; Tran *et al.*, 2022). Die

Bestrahlung mit UV-Licht zielt beispielsweise primär auf das Hygienisieren von vorbehandeltem Abwasser ab. Sekundär kann die Bestrahlung mit UV-Licht zur Entfernung von UV-Filtern angewendet werden. Nicht selten haben die angewendeten Eliminierungsprozesse – insbesondere die Oxidationsverfahren – die Bildung von Transformationsprodukten (TP) zur Folge. Potentielle Probleme können dabei entweder von den gebildeten TP oder von der unvollständig entfernten Ausgangssubstanz ausgehen (Maimon *et al.*, 2014). Die TP, welche bei (photolytischen) Reaktionen von Spurenstoffen gebildet werden, haben meist eine unbekannte Toxizität und können noch toxischer sein als ihre Ausgangsverbindungen (La Farré *et al.*, 2008; Michael *et al.*, 2014; Santiago-Morales *et al.*, 2013). Um eine Gefährdung durch Bildung von TP durch die UV-Behandlung auszuschließen, werden daher neue Erkenntnisse über die Transformationswege benötigt.

Aus früheren Studien ist bekannt, dass EHMC in wässriger Lösung unter Sonnenlichtbestrahlung (λ = 290 nm; u. a. MacManus-Spencer *et al.*, 2011; Rodil *et al.*, 2009) oder mit monochromatischem UV-Licht (λ_{max} = 254, 365 oder 313 nm; u. a. Santiago-Morales *et al.*, 2013; Vione *et al*., 2015) photolytisch abgebaut wird. Jedoch konzentrieren sich nur wenige dieser Studien auf die Bildung von (teilweise stabilen) Photo-Transformationsprodukten (Photo-TP) in Wasser (MacManus-Spencer *et al.*, 2011; Rodil *et al.*, 2009; Vione *et al.*, 2015). Bisher fehlten allerdings noch Studien, welche die Photolyse von EHMC unter Multiwellenlängen Bestrahlung (200–400 nm) oder die Auswirkungen der Versuchsbedingungen auf den Abbau von EHMC und die Bildung von TP untersuchten. Die Toxizität der bekannten TP von EHMC ist weitgehend unbekannt. In einigen Fällen wurde die Toxizität von photolytischen Mischungen bzw. deren Bestandteile getestet, z. B. im *Vibrio fischeri* microtox assay für 4-Methoxybenzaldehyd (4-MBA), welches eine höhere Toxizität als EHMC zeigte (Vione *et al.*, 2015). Außerdem ist der Verbleib der bei der UV-Behandlung gebildeten TP von EHMC unbekannt. Bisher lag der Fokus bei der Erforschung von TP aus UV-Filtern eher bei EHMC als bei OCR.

Die Herausforderungen der TP sind vielfältig. Mit jedem Eliminationsprozess, in dem neue TP entstehen, deren Eigenschaften oftmals nicht bekannt sind, wächst nicht nur die Stoffvielfalt, sondern auch das Risiko für die (aquatische) Umwelt. Mit zunehmender Anzahl an Stoffen, welche alle bewertet werden müssen, wächst somit auch die Zahl der Endpunkte. Jedoch stehen viele TP nicht als Standards zur Verfügung, was eine experimentelle Analyse der Toxizität einzelner Substanzen erschwert. Darüber hinaus sind toxikologische Experimente kostenintensiv. Zudem werden diese Verbindungen in der Regel nur in geringen Konzentrationen in komplexen Matrices gebildet, sodass die Isolierung und Reinigung sehr aufwendig und teuer sind. Darüber hinaus ist die gezielte Synthese von TP, welche für die Identifikation als Standard eingesetzt werden können, teuer und zeitaufwendig, was zu

Datenlücken bei der Strukturaufklärung oder dem Verhalten in der Umwelt führt (Hensen *et al.*, 2018). Eine Herangehensweise zur Lösung dieser Probleme ist die Generierung von *in silico* Daten über quantitative Struktur-Wirkungs-Beziehungen (*quantitative structure-activity relationship*, QSAR). Der Ansatz QSAR-Modelle zu verwenden, gewinnt zunehmend an Bedeutung, insbesondere für die Analyse und Bewertung von Umwelt-TP (Gutowski *et al.*, 2015; Khaleel *et al.*, 2019; Rastogi *et al.*, 2014; Westphal *et al.*, 2020). In Anbetracht der Grenzen von QSAR-Modellen (beispielsweise der Anwendbarkeitsdomain) kann der Einsatz von *in silico* Methoden nicht die abschließende Lösung sein. QSAR Modelle dienen als ein erstes Screening dem jedoch in einem gestuften Ansatz weitere experimentelle Versuche folgen sollten (Hensen *et al.*, 2020).

1.3 Diskurs über Umgang mit und Vermeidung von Chemikalieneinträgen

Die Zunahme an Chemikalien in der aquatischen Umwelt mit teils unbekannten Eigenschaften gewinnt zunehmend an Bedeutung. Durch den Einsatz immer energieintensiver oder aufwendiger Techniken zur (Ab-)Wasserbehandlung wird am Ende der Ereigniskette eingegriffen, um (Ab-)Wasser von Spurenstoffen zu befreien und auf diese Weise sauberes Wasser zu erhalten. Gleichzeitig wird das gesellschaftliche Bewusstsein und Bestreben nach einer nicht-toxischen Umwelt immer stärker. Die Strategie, bei der die Verschmutzung von Gewässern und der Umwelt durch Spurenstoffe vermieden werden soll, setzt somit am Anfang des Problems an. Die folgenden, aktuellen Beispiele für Bestrebungen der internationalen Gemeinschaft verfolgen ebenfalls beide Ansätze des Eingriffs am Anfang sowie am Ende des Problems:

(1) Die Vereinten Nationen erklären im sechsten Ziel der nachhaltigen Entwicklung („sauberes Wasser“) der „Agenda 2030 für nachhaltige Entwicklung“, dass der Zugang zu sauberem Wasser gewährleistet werden soll (Vereinte Nationen, 2023).
(2) Die europäische Kommission hat den „Europäischen Grünen Deal“ (Europäische Kommission, 2023a) geschlossen und
(3) die europäische Kommission verfolgt mit dem „Aktionsplan zur Schadstofffreiheit von Luft, Wasser und Boden“ (auch “*Zero Pollution Action Plan*“) (Europäische Kommission, 2023b) u.a. das Ziel Verschmutzungen zu vermeiden und zu reduzieren.

Die Erkenntnisse aus der Forschung werden dabei genutzt, um zukünftige Strategien zu entwickeln und gewonnenes Wissen in die Gesetzgebungen zu implementieren. Im Falle der Bewertung von TP trägt die Forschung zu den Strategien bei und hilft diese voranzubringen, indem Datenlücken gefüllt und anwendbare Methoden bereitgestellt werden, um die Vielzahl an TP handhaben zu können (Hensen *et al.*, 2020). Sofern folglich bei der Eliminierung von UV-Filtern neue Verbindungen entstehen, sollte gewährleistet werden, dass diese nicht giftig sind, um Umwelt- und Gesundheitsprobleme zu vermeiden.

2 Ziele und Aufbau der Arbeit

2.1 Ziele

Das Ziel der Arbeit ist der Erkenntnisgewinn bezüglich der Fragen: *Was für TP entstehen, wenn UV-Filter in wässriger Lösung photolytisch eliminiert werden? Geht von den TP eine gleiche, geringere oder höhere Besorgnis aus als von ihren Ausgangssubstanzen? Wie sollen TP – ob bekannt oder noch unbekannt – grundsätzlich erfasst und bewertet werden?*

UV-Filter werden durch eine Vielzahl abiotischer und biotischer Prozesse in TP umgewandelt. Ein Indikator zur Beurteilung der Stabilität bzw. Persistenz der TP ist deren biologische Abbaubarkeit. Ein Ziel der Arbeit war daher die Erstellung eines Überblicks über die bereits bekannten TP, welche aus der Umwandlung von UV-Filter-Substanzen in abiotischen und biotischen Prozessen hervorgehen. Zudem sollten die Daten zur Stabilität (insbesondere der leichten biologischen Abbaubarkeit) der in der Fachliteratur beschriebenen TP von UV-Filtern ermittelt und verglichen werden.

Die vorliegende Arbeit soll außerdem der Frage der Verringerung beziehungsweise Verhinderung des Eintrags von UV-Filtern in die (aquatische) Umwelt nachgehen. Aufgrund ihrer besorgniserregenden Eigenschaften (z.B. Persistenz oder endokrine Wirksamkeit) sollte der indirekte Eintrag von UV-Filtern in die (aquatische) Umwelt vermieden werden. Eine Möglichkeit zur Eliminierung stellt die Bestrahlung mit UV-C-Strahlung dar. Diese Technik kommt primär bei dezentralen Abwassertechnologien mit dem Ziel des Hygienisierens zum Einsatz. Am Beispiel ausgewählter UV-Filter-Substanzen (EHMC & OCR) sollen daher die Effekte des Einsatzes von UV-C-Strahlung auf das Abbauverhalten und die Bildung von TP untersucht werden.

Ein weiteres Ziel dieser Arbeit war in Konsequenz die Untersuchung des Abbauverhaltens und der Transformation der organischen UV-Filter-Substanzen EHMC und OCR während der wässrigen Photolyse mittels UV-C-Bestrahlung. Wird der UV-Filter nicht vollständig mineralisiert, sondern werden stattdessen TP gebildet, so gilt es diese nachzuweisen. Am Beispiel von EHMC sollte zudem durch die Kombination von geeigneten analytischen Methoden sowohl die Strukturaufklärung der TP als auch mittels *in silico* Methoden die Vorhersage der Stoffeigenschaften der TP erfolgen.

Da in (Ab-)Wasserproben häufig mehr als ein Spurenstoff gleichzeitig vorliegt, wurde darüber hinaus untersucht, ob es bei der Bestrahlung von EHMC und OCR mit UV-C-Licht in wässriger Lösung zu UV-Filter-UV-Filter-Wechselwirkungen kommt und ob dadurch neue Mischungs-TP entstehen.

2.2 Aufbau

Die praktischen Arbeiten wurden von Juni 2013 bis Mai 2017 an der Leuphana Universität Lüneburg am Institut für Nachhaltige Chemie und Umweltchemie durchgeführt. Das Publikationsverzeichnis gibt einen Überblick zu allen Veröffentlichungen die im Rahmen dieser Arbeit und parallel dazu entstanden sind. Die folgenden drei Artikel (veröffentlicht in internationalen, wissenschaftlichen Zeitschriften mit Peer-Review-Verfahren) spiegeln dabei die Ergebnisse der Arbeit wider. In den nachfolgenden Kapiteln werden die Artikel zusammengefasst und diskutiert.

Artikel 1

Franziska Jentzsch, Oliver Olsson, Janin Westphal, Marco Reich, Christoph Leder, Klaus Kümmerer (2016) Photodegradation of the UV filter ethylhexyl methoxycinnamate under ultraviolet light: Identification and in silico assessment of photo-transformation products in the context of grey water reuse. *Science of the Total Environment* 572: 1092-1100. DOI: https://doi.org/10.1016/j.scitotenv.2016.08.017

Artikel 2

Franziska Jentzsch, Marco Reich, Klaus Kümmerer, Oliver Olsson (2019) Photolysis of mixtures of UV filters octocrylene and ethylhexyl methoxycinnamate leads to formation of mixed transformation products and different kinetics. *Science of the Total Environment* 134048. DOI: https://doi.org/10.1016/j.scitotenv.2019.134048

Artikel 3

Franziska Jentzsch, Klaus Kümmerer, Oliver Olsson (2023) Status quo on identified transformation products of organic ultraviolet filters and their persistence. *International Journal of Cosmetic Science* 45 (Suppl. 1): 101–126. https://doi.org/10.1111/ics.12908

2.3 Themenschwerpunkte

In Abbildung 1 ist das zentrale Thema der Arbeit sowie die jeweiligen Themenschwerpunkte der einzelnen Artikel dargestellt. Im Einzelnen wurden die folgenden Methoden angewendet:

- Überprüfung der Konsequenzen der Bildung von TP des UV-Filters EHMC durch Bestrahlung mit UV-Licht (Photolyse) durch Nachweis der Photo-TP mittels Hochleistungsflüssigkeitschromatographie mit UV-Detektor (HPLC-UV) sowie Identifikation der Photo-TP mittels Flüssigkeitschromatographie gekoppelt mit einem Tandem-Massenspektrometer (LC-MS/MS) mit dem Ziel des Vergleichs der Eigenschaften der Photo-TP und denen der Ausgangssubstanz EHMC auf Grundlage der computerbasierten quantitativen Struktur-Wirkungs-Beziehung (QSAR) (Artikel 1).
- Untersuchung von UV-Filter-UV-Filter-Wechselwirkungen anhand des Vergleichs der unter Bestrahlung mit UV-Licht (photolytisch) entstehenden TP der UV-Filter EHMC und OCR im Einzelnen sowie als Mischung durch den Vergleich der mittels HPLC-UV nachgewiesenen Photo-TP (Artikel 2).
- Recherche nach Transformationsprodukten (TP) von elf organischen UV-Filtern, für die in der Fachliteratur strukturaufgeklärte Produkte aus abiotischen und biotischen Prozessen beschrieben wurden, zum Zwecke der Erstellung einer Liste der bekannten TP und anschließenden Analyse des Wissen zur (biologischen) Stabilität der 177 bekannten TP aus UV-Filtern (Artikel 3) als Literaturübersichtsartikel.

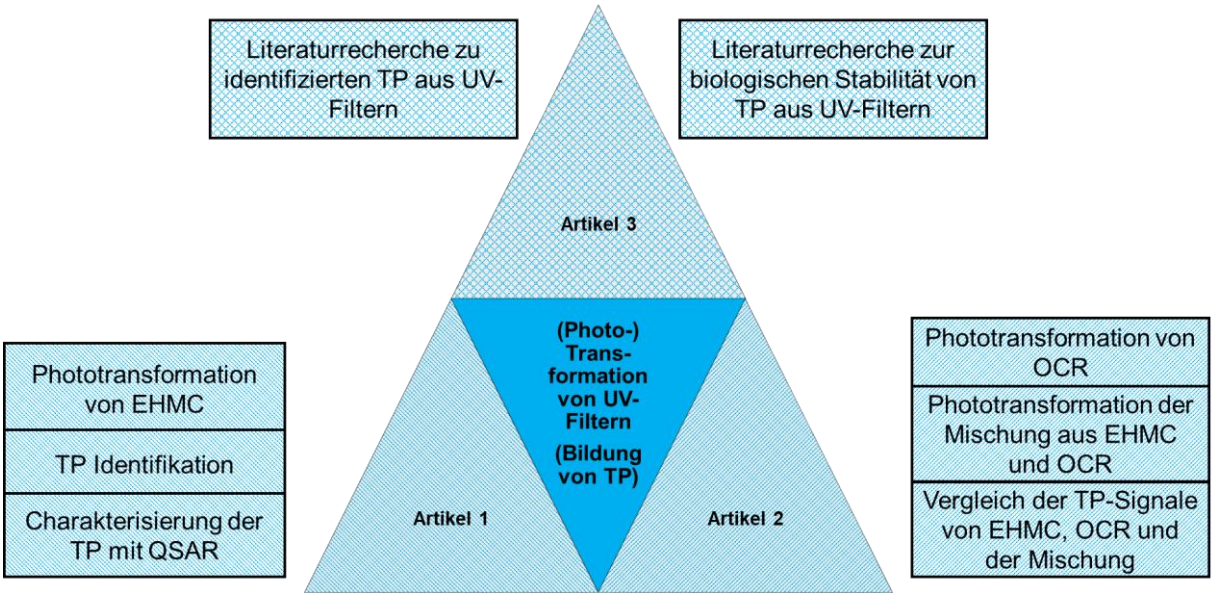

Abbildung 1: Übersicht über die Themen der Arbeit. Das zentrale Thema der Arbeit ist die Transformation von ausgewählten organischen UV-Filtern durch die Bestrahlung mit UV-Licht (Photolyse), die daraus hervorgehenden Photo-Transformationsprodukte (Photo-TP) sowie Transformationsprodukte (TP) von UV-Filtern im weiteren Sinne.

3 Methoden

3.1 Substanzauswahl

In dem Literaturübersichtsartikel (Artikel 3) wurden in einem ersten Schritt 27 organischen UV-Filter ausgewählt, deren Nutzung in kosmetischen Produkten in der Europäischen Union (EU) gemäß Kosmetikverordnung (EG) Nr. 1223/2009 (Europäische Union, 2009) zulässig ist. Darüber hinaus wurden zwei UV-Filter (3-Benzylidencampher (3-BC) und *para*-Aminobenzoesäure (PABA)) in den Literaturübersichtsartikel als Ergänzung der EU-weit genutzten UV-Filter mit einbezogen. Die Verwendung von 3-BC ist seit 2016 in der EU nicht mehr zugelassen und PABA darf nur in den Vereinigten Staaten von Amerika, Japan und auf dem Mercosur (dem sogenannten „Gemeinsamen Markt des Südens“ in Lateinamerika) in kosmetischen Produkten verwendet werden. Die beiden Substanzen (3-BC und PABA) wurden als Ergänzung ausgewählt, da sie häufig in Produkten angewendet wurden und/oder regelmäßig in der Umwelt gefunden wurden. Somit standen insgesamt 29 Substanzen im Fokus der Literaturrecherche. Um im Literaturübersichtsartikel näher betrachtet zu werden, mussten die Studien zu den 29 UV-Filtern nachfolgende Auswahlkriterien erfüllen. Als Hauptkriterium musste in den Studien ein oder mehrere TP identifiziert worden sein, die durch Transformation der organischen UV-Filter in abiotischen und biotischen Prozessen gebildet wurden. Zu den UV-Filtern, die das Hauptkriterium erfüllen, zählen (in alphabetischer Reihenfolge der Abkürzungen, sowie unter Angabe der jeweiligen Registriernummer des *chemical abstract services*, CAS) folgende Substanzen:

- Avobenzon (BMDM, CAS-Nr.: 70356-09-1),
- Oxybenzon (BP-3, CAS-Nr.: 131-57-7),
- Diethylaminohydroxybenzoylhexylbenzoat (DHHB, CAS-Nr.: 302776-68-7),
- 2-Ethylhexyl-4-dimethylaminobenzoat (EHDP, CAS-Nr.: 21245-02-3),
- 2-Ethylhexyl-4-methoxycinnamat (EHMC, CAS-Nr.: 5466-77-3 und 83834-59-7),
- Benzocain (Et-PABA, CAS-Nr.: 94-09-7),
- Amiloxat (IMC, CAS-Nr.: 71617-10-2),
- Enzacamen (MBC, CAS-Nr.: 36861-47-9).
- Octocrylene (OCR, CAS-Nr.: 6197-30-4),
- *para*-Aminobenzoesäure (PABA, CAS-Nr.: 150-13-0) und
- Phenylbenzimidazolsulfonsäure (PBSA, CAS-Nr.: 27503-81-7).

Für den experimentellen Teil der Arbeit (veröffentlicht in Artikel 1 und Artikel 2) wurden zwei organische UV-Filter ausgewählt: 2-Ethylhexyl-4-methoxycinnamat (EHMC) und Octocrylene (OCR) (Abbildung 2).

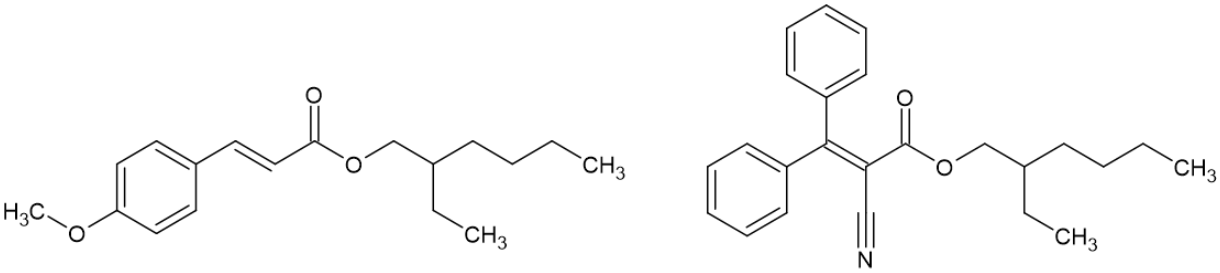

Abbildung 2: Darstellung der chemischen Strukturen von EHMC (links) und OCR (rechts) (Strukturformeln generiert mit ACD/ChemSketch 2023.1.1).

Für die Auswahl der Substanzen EHMC und OCR als Modellsubstanzen waren die folgenden drei Faktoren ausschlaggebend:

(1) aus der Literatur geht hervor, dass EHMC und OCR sich bei Photolyseversuchen mit sichtbarem Licht unterschiedlich verhalten,

(2) beide UV-Filter zeigen im Vergleich zu anderen UV-Filtern (z. B. BP-3) eine geringe Anzahl an Studien zur Photolyse auf und

(3) da in der Literatur bereits UV-Filter-UV-Filter-Wechselwirkungen (Dondi *et al.*, 2006) und die Dimerisierung von EHMC über die vorhandene Doppelbindung beschrieben wurde (MacManus-Spencer *et al.*, 2011; Rodil *et al.*, 2009; Vione *et al.*, 2015), wurde bei der Substanzauswahl auf eine chemisch ähnliche Struktur (in Form der Doppelbindung, welche in beiden Molekülen vorhanden ist) geachtet.

3.2 Zusammenstellung und Stabilität von TP organischer UV-Filter aus biotischen und abiotischen Prozessen (Artikel 3)

In einer Recherche wurden jene in der Literatur bekannten TP ermittelt, welche in Versuchen mit organischen UV-Filtern unter biotischen und abiotischen Bedingungen gebildet wurden. Voraussetzung für die Aufnahme in die Liste war, dass die TP analytisch nachgewiesen wurden und dass für die TP auch ein Strukturvorschlag vorliegt. Das exakte Vorgehen kann Artikel 3 entnommen werden.

Ausgehend von der Liste bekannter TP, die aus UV-Filtern in abiotischen und biotischen Prozessen gebildet werden, wurde die Datenlage zur Stabilität der TP geprüft. Zunächst wurde dazu jede Studie, in welcher TP identifiziert wurden, untersucht, ob in diese Studie auch die Stabilität der TP näher untersucht wurde. Darüber hinaus wurden die TP mit den Einträgen zur leichten biologischen Abbaubarkeit in der Datenbank der Europäischen Chemikalienagentur (ECHA) abgeglichen.

3.3 Photolytischer Abbau der UV-Filter-Substanzen EHMC und OCR (Artikel 1 und 2)

Aufgrund der geringen Löslichkeit wurde gemäß den Angaben in der Testleitlinie Nr. 316 der Organisation für wirtschaftliche Zusammenarbeit und Entwicklung (OECD) mit einem Lösungsvermittler (0,1 %, 0,2 % bzw. 0,5 % (v/v) Acetonitril (ACN)) gearbeitet (Organisation für wirtschaftliche Zusammenarbeit und Entwicklung, 2008). Für die Photolyseversuche wurde Reinstwasser mit den in reinem ACN gelösten Testsubstanzen (EHMC und OCR) versetzt, sodass eine nominale Konzentration des UV-Filters von 1 mg/L, 2,5 mg/L bzw. 5 mg/L erreicht wurde. Die Experimente wurden zunächst mit jedem UV-Filter separat und anschließend noch zwei Mal mit der Mischung aus beiden Substanzen (in einer jeweils gleichhohen Konzentration von 2,5 mg/L und 5 mg/L) durchgeführt. Die Testlösung wurde in den Photoreaktor gegeben und für 256 min mit einer polychromatischen Mitteldruck-Quecksilberdampflampe (TQ150, 150 W, UV Consulting Peschl, Mainz, Deutschland) bestrahlt. Die Lampe emittiert Licht im UV-A, -B und -C-Bereich (200–400 nm). Vor Versuchsbeginn (zum Zeitpunkt: 0 min) und nach 2, 4, 8, 16, 32, 64, 96, 128, 192 und 256 min wurden Proben aus den Photoreaktor entnommen.

Zusätzlich zu den Photolyseversuchen wurde das Emissionsspektrum der verwendeten Lampe und die Absorptionsspektren der Testsubstanzen bestimmt.

Die zur Bestrahlung eingesetzte Lampe wurde bezüglich ihres Photonenflusses und der Quantenausbeute charakterisiert. Die Methode, die dabei zum Einsatz kam, ist in Artikel 1 und Artikel 2 detailliert beschrieben.

3.4 Nachweis von Photo-Transformationsprodukten (Artikel 1 und 2)

Die analytische Methode der HPLC-UV wurde eingesetzt, um die Eliminierung von EHMC und OCR während der Photolyse zu monitoren und um die Kinetik des photolytischen Abbaus der UV-Filter zu ermitteln.

Zudem wurde mittels HPLC-UV geprüft, ob in den Proben aus den photolytischen Abbauversuchen neue Substanz-Signale als Indikator für die Entstehung von Photo-TP nachweisbar waren. Neben dem reinen Nachweis von Photo-TP wurden die HPLC-UV-Peaks verschiedener Photolyseversuche (EHMC, OCR und Mischung aus EHMC und OCR) verglichen mit dem Ziel der Überprüfung, ob UV-Filter-UV-Filter-Wechselwirkungen auftreten. Mit Hilfe des Nachweises von Photo-TP über die HPLC-UV-Signale, die ausschließlich im Mischungsexperiment detektiert wurden, wurde die Bildung von Mischungs-Transformationsprodukten während der Photolyse-Experimente abgeleitet.

3.5 Strukturaufklärung von Photo-Transformationsprodukten (Artikel 1)

Für Artikel 1 wurden Proben (aus der Photolyse von 5 mg L^{-1} EHMC in 0,5 % (v/v) wässriger ACN-Lösung), in denen Photo-TP mittels HPLC-UV nachgewiesen wurden, einer zusätzlichen Analytik zugeführt, um die Struktur der Photo-TP auf zu klären. Die Bildung von Photo-TP wurde dabei mittels Massenspektrometrie (MS) verfolgt. Um die Photo-TP zu identifizieren wurden zunächst die UV-Signale potentieller Photo-TP mit neu auftretenden Masse-zu-Ladungsverhältnis (m/z)-Signalen verglichen. Außerdem wurden die zeitlichen Verläufe der m/z-Signale mittels extrahierter Ionenchromatogramme (EIC) überprüft. Die Informationen zum eingesetzten System der Flüssigkeitschromatographie mit gekoppelter Ionenfalle (Bruker Daltonic Esquire 6000+, Karlsruhe, Deutschland) (LC-MS) sind im Anhang zu Artikel 1 zusammengefasst. Kurz zusammengefasst wurde für die chromatographische Trennung eine C_{18}-Phase und somit Umkehrphasenchromatographie genutzt.

Um die Struktur neu aufgetretener Massen aufzuklären und potentiellen Photo-TP zuzuordnen, wurden bekannte Strukturen aus der Literatur herangezogen. Darüber hinaus wurde – mit der computergestützten, regelbasierten, *in silico* Software MetaPC v.1.8.1 (MultiCASE Inc.) – die chemische Transformation von EHMC vorhergesagt. Mithilfe der Vorhersagen wurden zum einen die mittels LC-MS neu nachgewiesenen m/z-Signale mit den vorgeschlagenen *in silico* TP verglichen und zum anderen nach dem Auftreten von weiteren m/z-Signalen gesucht.

Für die Entscheidung, welche m/z-Signale strukturell aufgeklärt werden, wurde die maximale beobachtete relative Peakfläche A/A_0 des Photo-TP herangezogen. Nur wenn die Fläche A unter dem Peak des Photo-TP zu einem beliebigen Zeitpunkt des Experiments mindestens 0,5 % von A_0 – also der Fläche unter dem EHMC-Peak zum Zeitpunkt 0 min – ist, wurde für die Photo-TP eine Strukturvorhersage vorgenommen. Jede vorgeschlagene Struktur eines Photo-TP wurde mit dem m/z-Verhältnis beschriftet, wobei Strukturisomere einen alphabetischen Index erhielten. Bei m/z-Signalen verschiedener Addukte ein und des gleichen Moleküls wurde das $[M+H]^+$ Addukt für die Benennung des Strukturvorschlags verwendet.

3.6 Charakterisierung der Photo-Transformationsprodukten mit quantitativer Struktur-Wirkungs-Beziehung (Artikel 1)

Die *in silico* Vorhersage der Toxizität (Mutagenität, Gentoxizität und Ökotoxizität) von EHMC und seinen Photo-TP wurde mit unterschiedlicher Software durchgeführt, um die Stärken und Schwächen der verschiedenen Algorithmen und Übungsdatensätzen auszugleichen.

Mit CASE Ultra v.1.5.2.0 (MultiCASE Inc.) kam eine Fragment-basierte Software zum Einsatz. Bei der zweiten Anwendung, Oasis Catalogic v.5.11.6 TB (Labor für Mathematische Chemie,

Universität Burgas, Bulgarien), handelt es sich um eine Kombination aus einer statistischen und einer Regel-basierten Software. Als drittes wurde die statistische QSAR-Software von Leadscope v.3.2.6-1 verwendet, welche auf Übungsdatensätze aus der SAR Genotox Datenbank von 2012 zurückgreift.

Ergänzend zur Toxizität wurde das Umweltverhalten von EHMC und seinen Photo-TP in Artikel 1 mit *in silico* Anwendungen vorhergesagt. Dazu wurden EHMC und seine Photo-TP auf leichte biologische Abbaubarkeit nach OECD 301C, also einem MITI-I (*Ministry of International Trade and Industry*, Japan) Test, mit *in silico* Modellen von Oasis Catalogic v.5.11.6 TB (Catabol und Catalogic) sowie mit dem AU6 Modell von CASE Ultra getestet.

Die Prognosen von CASE Ultra, Oasis Catalogic und Leadscope unterscheiden sich in „positiv“, „negativ“ und „*out-of-domain* (OD)“ (wobei OD so viel heißt wie „außerhalb des Anwendungsbereichs des Modells“). Im Fall von CASE Ultra kann es zu Prognosen kommen, die *'inconclusive*‘ sind, d.h. das Ergebnis ist unklar. In diesen Fällen ist dies ein Hinweis darauf, dass ein signifikanter struktureller Teil der getesteten Chemikalie unbekannte Strukturfragmente aufweist.

4 Ergebnisse

In den nachfolgenden Kapiteln werden die wichtigsten Erkenntnisse und Ergebnisse aus den Artikeln 1, 2 und 3 vorgestellt.

4.1 Zusammenstellung und Stabilität der bekannten TP aus UV-Filtern

Artikel 3 fasst die TP, von denen bekannt ist, dass sie aus UV-Filtern in abiotischen und biotischen Prozessen gebildet werden, zusammen. In Summe gehen aus der Literaturrecherche 177 individuelle TP hervor, welche nicht nur nachgewiesen wurden, sondern deren Struktur auch ermittelt bzw. vorgeschlagen wurde. Insgesamt wurden in 42 Studien 46 abiotische und biotische Prozesse mit elf UV-Filtern und einer UV-Filter-Mischung für den Literaturreview herangezogen. Die Verteilung der Anzahl der Prozesse pro UV-Filter und der Art der Prozesse ist sehr variabel (Tabelle 1).

Von den 42 herangezogenen Studien beschrieben acht Studien neben der Bildung und Strukturaufklärung der TP auch deren Stabilität. Die daraufhin zusätzlich durchgeführte Analyse der ECHA-Datenbank bezüglich der Frage, welche der 177 individuellen TP Informationen zu ihrem Umweltverhalten – in Form von Studien zur Stabilität bzw. Persistenz – aufweisen, kam zu dem Ergebnis, dass 3,4 % (sechs TP) nicht leicht biologisch abbaubar und 13 % (23 TP) leicht biologisch abbaubar waren. Zu mehr als 83 % der individuellen TP sind in der verwendeten ECHA Datenbank entweder gar kein Eintrag hinterlegt oder sofern Einträge existieren, lagen keine Informationen zum leichten biologischen Abbauverhalten vor.

Tabelle 1: Überblick über die 46 abiotischen und biotischen Prozesse der elf UV-Filter, welche in 42 Studien publiziert wurden (n = Anzahl der untersuchten Prozesse) (nach Artikel 3).

UV-Filter	Prozesse													Summe der untersuchten Prozesse
	Photolyse		Erweiterte Oxidation (Advanced oxidation processes, AOP)						Biologischer Abbau					
	künstliches UV-Licht*	Sonnen-simulator	Licht/ TiO_2/ H_2O_2	Licht/ H_2O_2	Licht/ TiO_2	Photo-Fenton (Fe^{3+})	Licht/ O_3	O_3	Algen	Pilze	Biofilm	Klär-schlamm	marines Sediment	
BMDM	4	2	0	0	0	0	0	0	0	0	0	0	0	**6**
BP-3	2	0	2	2	0	0	0	1	1	1	0	2	0	**11**
DHHB	1	0	0	0	0	0	0	0	0	0	0	0	0	**1**
PABA	1	0	1	0	0	1	0	0	0	0	0	0	0	**3**
EHDP	4	1	0	1	0	0	1	0	0	0	0	1	1	**9**
Et-PABA	0	0	0	0	1	0	0	0	0	0	0	0	0	**1**
PBSA	2	0	0	0	0	0	0	0	0	0	0	0	0	**2**
MBC	0	0	0	0	0	0	0	0	0	1	0	0	1	**2**
EHMC	5	1	0	0	0	0	0	1	0	0	0	1	0	**8**
IMC	1	0	0	0	0	0	0	0	0	0	0	0	0	**1**
OCR	0	0	0	0	0	0	0	1	0	0	1	0	0	**2**
Summe	**20**	**4**	**3**	**3**	**1**	**1**	**1**	**3**	**1**	**2**	**1**	**4**	**2**	**46**

* vor allem UV-A, UV-C oder UV-C/Vakuum-UV

4.2 Photolytischer Abbau, Nachweis und Strukturvorschläge von TP aus UV-Filtern

4.2.1. Eliminierung von EHMC und OCR während der wässrigen Photolyse

In den Artikeln 1 und 2 werden die Ergebnisse rund um die Versuche zum photolytischen Abbau von EHMC und OCR im Detail dargestellt. Die Basis für den photolytischen Abbau bildet dabei die Überlappung der Emission der verwendeten UV-Lampe und der Absorptionsspektren der beiden Testsubstanzen EHMC und OCR (Abbildung 3).

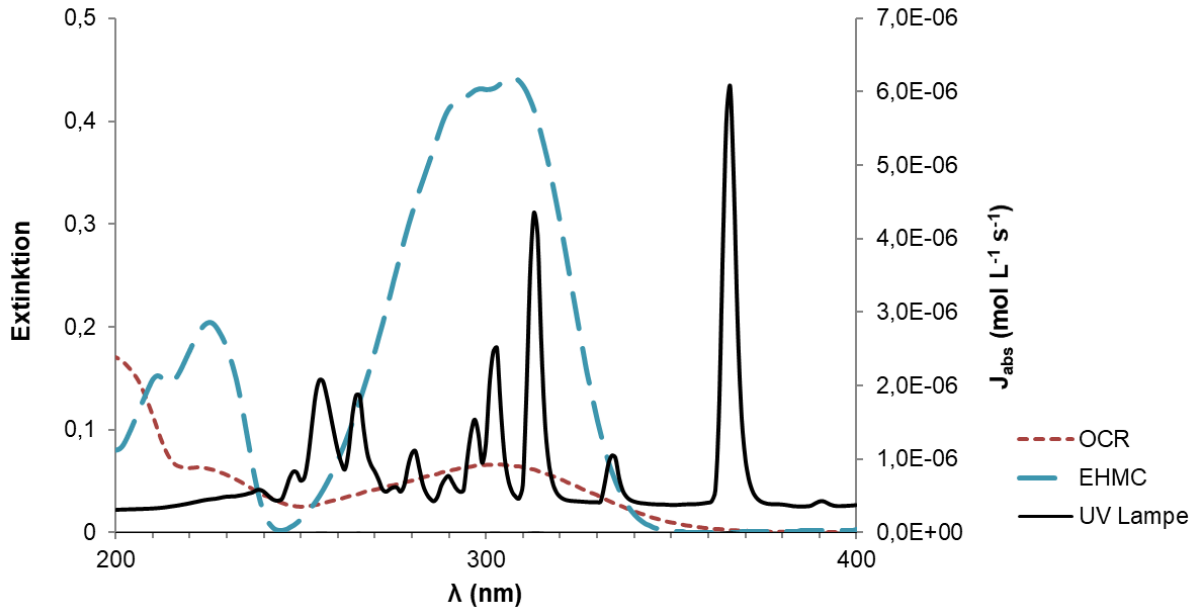

Abbildung 3: Absoluter Photonenfluss J_{abs} der Mitteldruck-Quecksilberdampflampe (schwarz, durchgehende Linie) sowie UV/vis-Spektren von EHMC (blau, lange Striche) und OCR (rot, kurze Stiche) gelöst in 100% Acetonitril (nach Artikel 2).

In den ersten beiden Artikeln wurde nachgewiesen, dass unter den getesteten Bedingungen EHMC (Artikel 1) und OCR (Artikel 2) im Verlauf des photolytischen Abbaus primär eliminiert werden. Der Abbau folgte dabei einer Kinetik erster Ordnung. Da ACN als Lösungsvermittler verwendet wurde, konnte keine Bestimmung des gesamten organischen Kohlenstoffs (TOC) durchgeführt werden, um den Mineralisierungsgrad der Testsubstanzen zu untersuchen. Folglich kann über den Grad der Mineralisierung keine Aussage getroffen und an dieser Stelle mit Sicherheit nur von einer Eliminierung gesprochen werden. Die photolytischen Abbauversuche mit unterschiedlichen Konzentrationen an Lösungsvermittler zeigen, dass beim Einsatz von geringen Mengen ACN (im Bereich von unter einem Volumenprozent) kein Einfluss auf das Abbauverhalten festzustellen ist.

Die Konzentrationsänderungen der Testsubstanzen OCR und EHMC im Verlauf der photolytischen Abbauversuche wurden in Artikel 2 gegenübergestellt (Abbildung 4). Hierbei zeigte sich, dass die Konzentration von EHMC deutlich schneller abnimmt als die von OCR. EHMC ist in der hohen Konzentration nach 64 min bereits eliminiert (bzw. nicht mehr nachweisbar), wohingegen OCR zu Versuchsende (256 min) immer noch detektierbar war.

Die ermittelten Geschwindigkeitskonstanten belegen, dass EHMC unter gleichen Versuchsbedingungen schneller eliminiert wird als OCR.

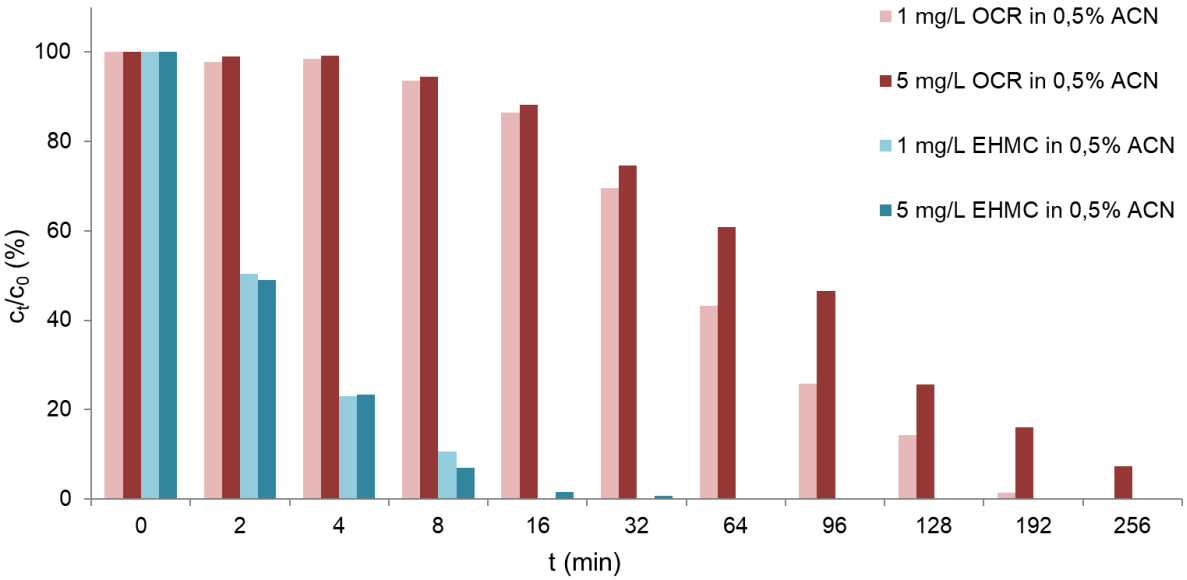

Abbildung 4: Vergleich des photolytischen Abbaus von 1 mg/L und 5 mg/L der UV-Filter EHMC (blau) und OCR (rot) in wässriger Lösung mit 0,5 % (v/v) Acetonitril als Lösungsvermittler (nach Artikel 2).

4.2.2. Photolytische Stabilität und Strukturvorschläge für Photo-TP aus EHMC

In Summe wurden in den Proben der Versuche mit 5 mg/L EHMC 15 verschiedene Signale massenspektrometrisch nachgewiesen, welche zu verschiedenen Retentionszeiten auftraten. 14 dieser Signale wurden sechs m/z zugeordnet (Abbildung 5), was für die Bildung von Strukturisomeren mit der gleichen molaren Masse spricht. Das 15. Signal wurde durch nachträgliche Messung eines kommerziell verfügbaren, analytischen Standards der Verbindung 4-MBA eindeutig zugeordnet (TP_{137c} in Abbildung 6). Die Gegenüberstellung der massenspektrometrisch bestimmten Peakflächen A zum Zeitpunkt t zu den Peakflächen der TP zum Zeitpunkt 0 min (A_0) ergeben die relative Peakfläche A/A_0 in %. Die Darstellung der relativen Peakflächen über den zeitlichen Verlauf der photolytischen Abbauversuche von EHMC veranschaulicht die Bildung und die Eliminierung der TP (Abbildung 5). Da alle Graphen gegen Ende der Versuche abfallen, ist davon auszugehen, dass es sich um (unter den Versuchsbedingungen) photo-labile TP handelt.

Ausgehend von den HPLC-UV- und den LC-MS/MS-Messdaten sowie den Vorschlägen für TP der MetaPC-Software sind in Abbildung 6 die Strukturvorschläge für Photo-TP von EHMC dargestellt. Da es sich bei dem Signal m/z 322 um das $[M+NH_4]^+$ Addukt von m/z 305 ($[M+H]^+$) handelt, sind die Signale für m/z 322 mit den Strukturvorschlägen für die Strukturisomere $TP_{305a\text{-}g}$ in Abbildung 6 abgedeckt.

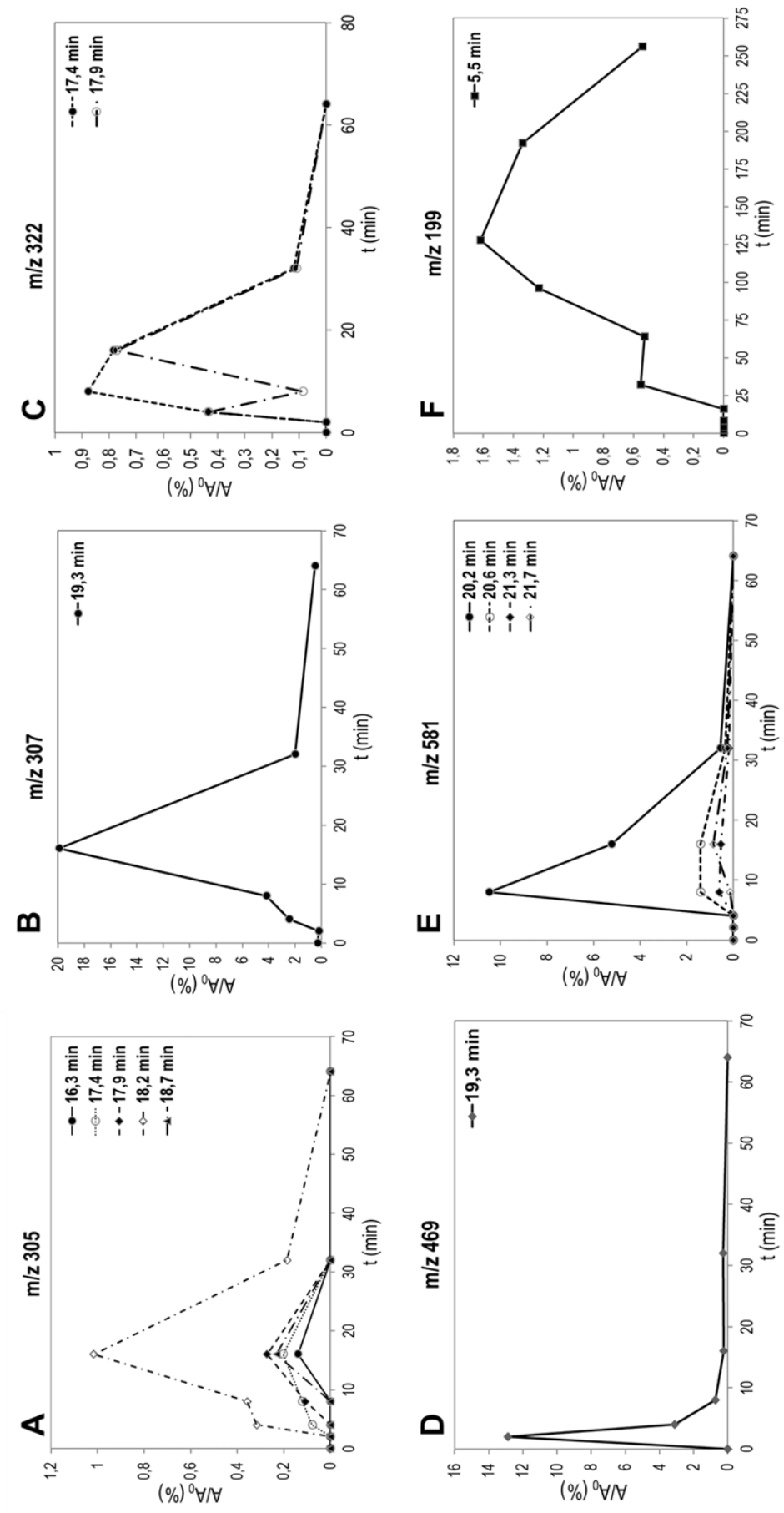

Abbildung 5: Relative Peakflächen A/A_0 der mittels LC-MS/MS bestimmten TP aus dem photolytischem Abbau von 5 mg/L EHMC, wobei A_0 die Peakfläche zu Versuchsbeginn (Zeitpunkt: 0 min) und A zum Zeitpunkt t darstellt. Die Kurven werden durch die m/z-Verhältnisse und die Retentionszeiten (in min) charakterisiert. Die unterschiedlichen Retentionszeiten pro m/z in den Abbildungen entsprechen der Anzahl an möglichen Isomeren. Man beachte, dass die Skalen variieren (nach Artikel 1).

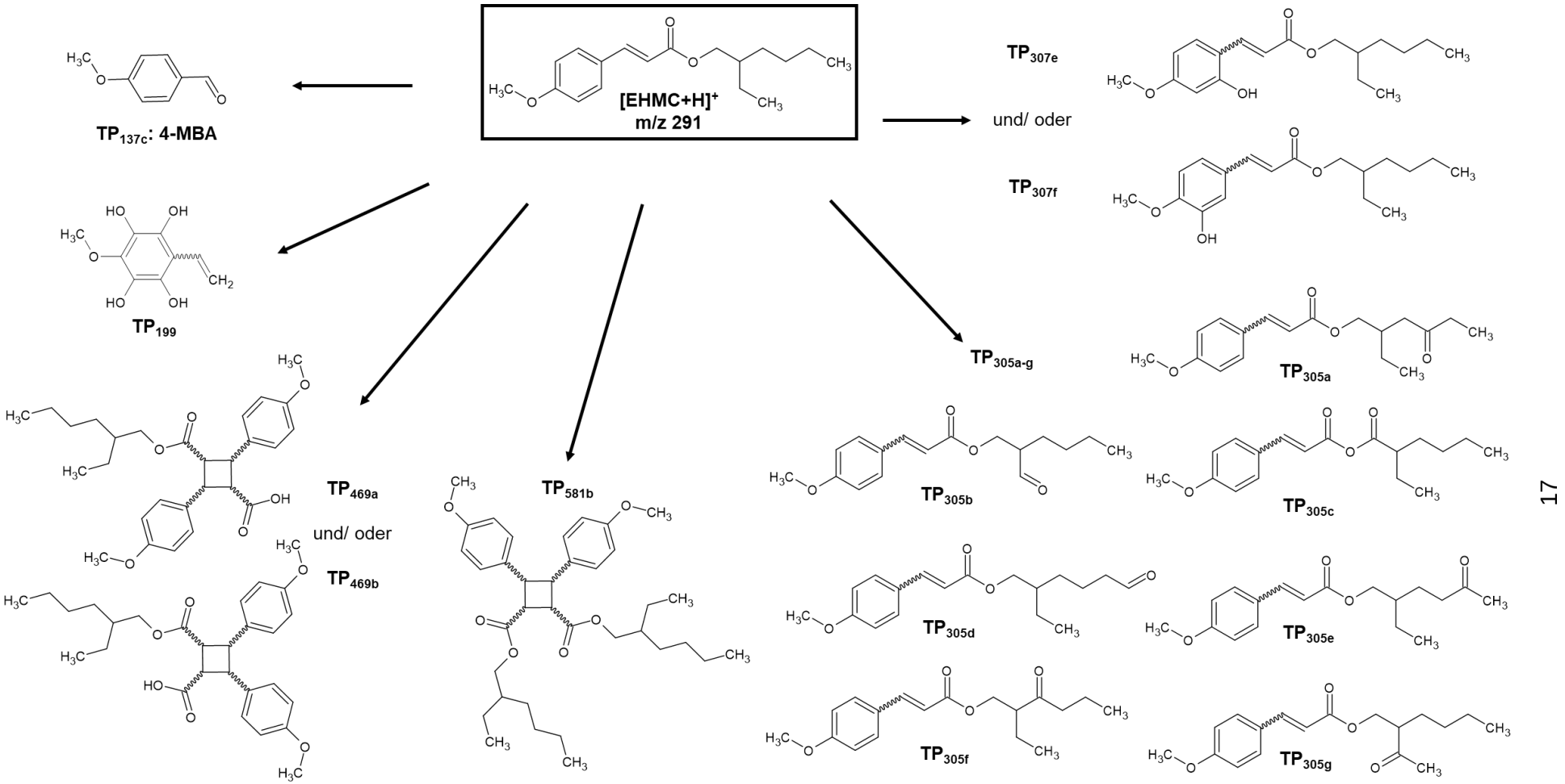

Abbildung 6: Strukturvorschläge für die Photo-TP von EHMC (nach Artikel 1).

4.2.3. Nachgewiesene Photo-TP aus OCR

In Artikel 2 wurde erstmals (mittels HPLC-UV Analyse) gezeigt, dass mit der verwendeten analytischen Methode vier TP nachweisbar waren, die während der wässrigen Photolyse von OCR gebildet werden (Abbildung 7). Da die TP zu jeweils kürzeren Retentionszeiten als OCR detektiert wurden, ist davon auszugehen, dass es sich - im Vergleich zu OCR – um polarere Verbindungen handelt.

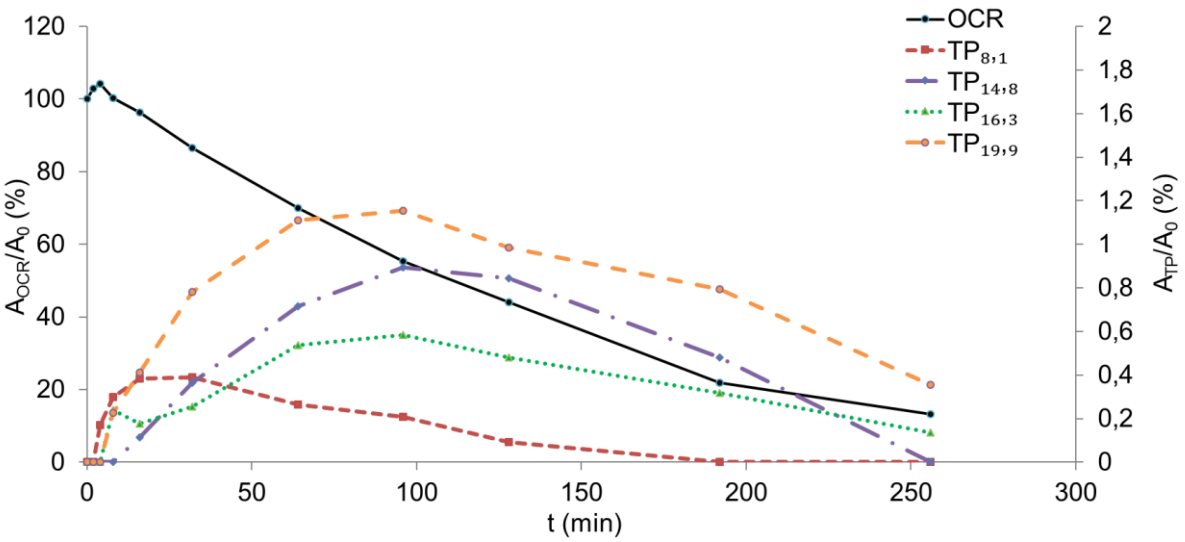

Abbildung 7: Primäre Eliminierung von OCR und die Verläufe der relativen Peakflächen der Photo-TP von OCR gemessen mittels HPLC-UV Analyse. Die TP werden charakterisiert durch ihre Retentionszeiten in min (nach Artikel 2).

4.3 UV-Filter-UV-Filter-Wechselwirkung während der Photolyse der EHMC-OCR-Mischung

Bereits in Abbildung 4 wurde deutlich, dass die schnellste Elimination von EHMC und OCR nicht zum gleichen Zeitpunkt stattfindet. Dieser Umstand wurde in Artikel 2 genutzt, um die Kinetik von EHMC und OCR während des photolytischen Abbaus einer wässrigen Lösung aus beiden Testsubstanzen zu bestimmen (Abbildung 8). Im Vergleich zu den Versuchen mit den einzelnen UV-Filtern wurde die Elimination von EHMC verlangsamt und von OCR beschleunigt als diese in einer Mischung bestrahlt wurden.

Die Proben, die während der Bestrahlung der wässrigen UV-Filter-Mischung entnommen und mittels HPLC-UV analysiert wurden, zeigten eine Vielzahl von Peaks zu verschiedenen Retentionszeiten auf. Der Vergleich dieser Peaks bezüglich ihrer Verläufe und ihrer Retentionszeiten mit den Daten aus den photolytischen Abbauversuchen von EHMC bzw. OCR ergab, dass weitere TP gebildet wurden, die weder mit den TP aus den EHMC- noch mit den TP aus den OCR-Versuchen übereinstimmen. Zusammenfassend wurde in Artikel 2 nachgewiesen, dass es (unter den getesteten Bedingungen) zu Mischungseffekten kommt, die

einen Einfluss auf die Kinetik des photolytischen Abbaus von EHMC und OCR und die Bildung von sieben weiteren detektierten TP zur Folge haben.

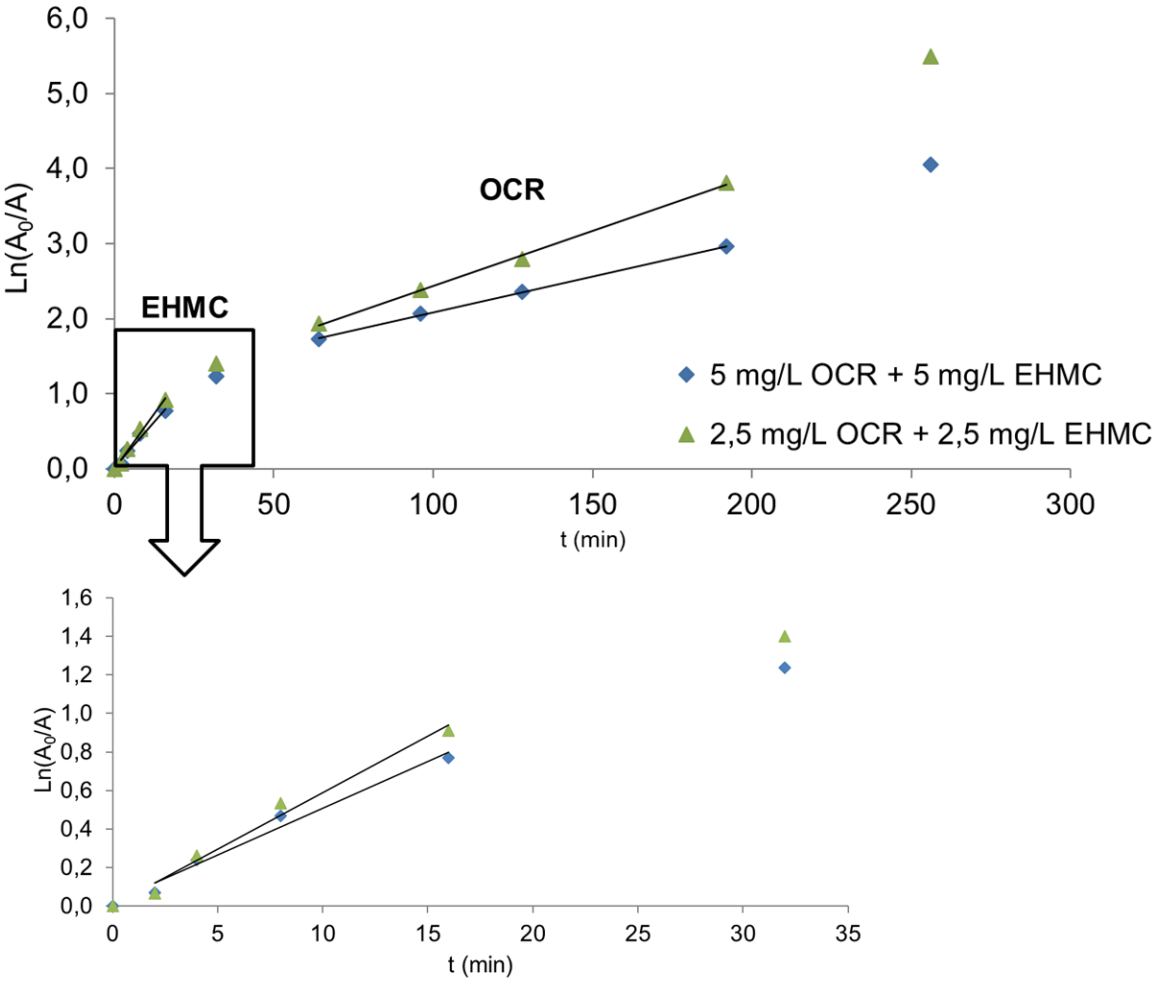

Abbildung 8: Auswertung der Kinetik von EHMC und OCR für den photolytischen Abbau der Mischung beider Substanzen. Oben sind die relativen Peakflächen (A_0/A) als natürlicher Logarithmus (gemessen mittels HPLC-UV Analyse) gegen den Zeitpunkt der Probennahme dargestellt. Unten ist die Vergrößerung für das Zeitfenster 0–35 min abgebildet, welches für die Auswertung für EHMC herangezogen wurde (nach Artikel 2).

4.4 QSAR-Prognosen für EHMC und seine Photo-TP

In Artikel 1 wurden die Vorhersagen aus QSAR-Modellen genutzt, um die leichte biologische Abbaubarkeit und die Toxizität von EHMC und seinen TP (vgl. Strukturvorschläge in Abbildung **6**) zu vergleichen. Die Vorhersage der *in silico* Eigenschaften von EHMC und seine TP ergaben in Bezug auf die leichte biologische Abbaubarkeit, dass sowohl für EHMC als auch für die meisten seiner TP eine leichte biologische Abbaubarkeit vorhergesagt wird. Die Ausnahme stellt TP_{199} dar, welches laut der Vorhersage mit dem CASE Ultra Modell AU6 nicht leicht biologisch abbaubar sei. Die Auswertung der Ergebnisse der Oasis Software (für die Modelle Catabol und Catalogic 301C) ergab, dass für die meisten Strukturvorschläge keine

Vorhersagen möglich sind, da die Strukturen außerhalb der Domain liegen. Die Ausnahme stellt TP_{137c} dar, welches zum Trainingssatz des verwendeten Modells gehört.

Die computerbasierte Vorhersage der Toxizität von EHMC und seinen Photo-TP ermöglicht die Identifizierung von im Vergleich zu EHMC toxischeren Molekülen, die während des photolytischen Abbaus von EHMC entstehen. Folglich sind TP_{137c}, TP_{199}, TP_{305a}, TP_{305e}, TP_{305f} und TP_{305g} jene Produkte, die mehr Aufmerksamkeit erfordern. Im Fall von TP_{199}, TP_{305f} und TP_{305g} ist zum Beispiel der Humankarzinogenität-Endpunkt auffällig: Die Vorhersage für EHMC von CASE Ultra für die Humankarzinogenität ergibt, dass der UV-Filter nicht krebserregend sei. Die drei genannten TP (TP_{199}, TP_{305f} und TP_{305g}) hingegen zeigen positive Warnmeldungen mit Wahrscheinlichkeiten in der Grauzone des Modells (40–60 %), woraus sich ein nicht eindeutiges Ergebnis ableiten lässt. Für den Endpunkt Genotoxizität sagen die Modelle für EHMC keine Toxizität voraus, wobei das Modell von Leadscope für TP_{199} Mikronucleustoxizität anzeigt. Die Daten aus der Vorhersage der Genotoxizität durch Chromosomenaberrationen zeigen, dass die Aussage für EHMC nicht schlüssig ist, wohingegen positive Vorhersagen für die Genotoxizität von TP_{137c} und TP_{305a} vorliegen.

5 Diskussion

Im folgenden Kapitel werden die Ergebnisse der Artikel 1, 2 und 3 diskutiert.

5.1 Überblick über bekannte TP von UV-Filtern und ihrer Persistenz

Das Ziel einen Überblick über bereits bekannte TP von UV-Filtern, welche in abiotischen und biotischen Prozessen gebildet werden, zu erstellen wurde mit der in Artikel 3 veröffentlichten Liste von 177 individuellen TP aus UV-Filtern erreicht. Die Liste stellt einen wichtigen Ausgangspunkt für zukünftige Fragestellungen dar, wie beispielsweise der Analyse von Eigenschaften von TP z.B. mit *in silico* Methoden oder Laborversuchen.

Zudem wurden in Artikel 3 die Daten zur leichten biologischen Abbaubarkeit – sofern vorhanden – zusammengetragen. Aufgrund der schlechten Datenlage ist der Vergleich der Daten zur leichten biologischen Abbaubarkeit nur bedingt möglich und ist mit einer hohen Unsicherheit behaftet.

Die Dokumentation bzw. Darstellung der TP in den ausgewerteten Studien war sehr unterschiedlich und teilweise unvollständig. Einige der vorab ausgeschlossenen Artikel legten den Schwerpunkt ihrer Untersuchungen nur auf die primäre Eliminierung. Zudem weist die Tatsache, dass nur sehr wenige Informationen zum biologischen Abbauverhalten verfügbar sind, auf den Handlungsbedarf in diesem Forschungsfeld hin. Wird nichts verändert, so ist mit einer größer werdenden Wissenslücke über die Existenz und Identität der TP von UV-Filtern zu rechnen. Eine Maßnahme, um die fehlenden Daten in Zukunft zu genieren und eine zunehmende Wissenslücke zu umgehen, stellt die Einführung eines harmonisierten Prüfsystems mit mehreren Schritten dar. Dieses System sollte die nachfolgenden Schritte umfassen: Entfernung des UV-Filters, Analyse des Transformationsprozesses inkl. des Nachweises und der Strukturaufklärung der gebildeten TP und eine abschließende Bewertung der Eigenschaften der TP. Auf diese Weise kann die Wissenslücke über die Eigenschaften (wie der leichten biologische Abbaubarkeit) von TP in der Umwelt geschlossen und ausreichend Kenntnis über den Verbleib von TP in der Umwelt generiert werden, um die Risikobewertung und Regulierung zukünftig besser aus zu gestalten. In der ersten Ebene könnte z.B. eine Methode angewendet werden, die leicht zugänglich ist. Auf der höheren Ebene können spezifische Tests angewandt werden, die komplexer sind (Hensen *et al.*, 2020). Die Testanleitung sollte darüber hinaus neu bewertet und an den aktuellen Stand von Wissenschaft und Technik angepasst werden. Dabei ist hervorzuheben, dass kein Mangel an Testmethoden oder das Fehlen von abgestuften Testverfahren besteht, sondern dass die Testanleitung hauptsächlich auf die Ausgangsverbindungen und nicht auf die TP angewendet wird.

In Artikel 3 wurden nur Studien, in denen TP identifiziert wurden, für die Auswertung herangezogen. Daraus folgt jedoch nicht, dass nur die Eigenschaften der identifizierten TP weiter untersucht werden sollten. Vielmehr sollen auch die Strukturen und Eigenschaften der TP, die bisher nur entdeckt – aber nicht strukturell aufgeklärt – wurden, erforscht werden.

5.2 Eliminierung und Transformation von EHMC und OCR durch wässrige Photolyse

Das Ziel der Arbeit war die Untersuchung des Verhaltens der beiden UV-Filter EHMC und OCR während der Bestrahlung mit einer Mitteldruck-Quecksilberdampflampe. Eine detaillierte Diskussion aller Ergebnisse des photolytischen Abbaus von EHMC, OCR und der Mischung aus beiden UV-Filtern ist in Artikel 1 und Artikel 2 veröffentlicht. Die nachfolgende Diskussion der wichtigsten Ergebnisse soll einen Einblick in die Erkenntnisse aus Artikel 1 und Artikel 2 geben.

Die experimentell bestimmte Kinetik erster Ordnung von EHMC stimmt mit der ermittelten Kinetik anderer Studien überein (Rodil *et al.*, 2009). Von allen vorgeschlagenen Strukturen der TP von EHMC wurde TP_{137c} durch die Analyse eines kommerziell verfügbaren Standards als 4-MBA bestätigt. Von den strukturaufgeklärten TP aus dem photolytischen Abbauversuch von EHMC wurden TP_{199}, das hydrolysierte Cyclodimer TP_{469a}, die hydroxylierten Monomere TP_{307e} und TP_{307f}, die oxidierten Monomere TP_{305a}, TP_{305b}, TP_{305c}, TP_{305d}, TP_{305e}, TP_{305f} und TP_{305g} erstmalig beschrieben. Im Gegensatz dazu wurde die Bildung von 4-MBA, des Cyclodimers TP_{581b}, des hydrolysierten Cyclodimers TP_{469b} und eines hydrolysierten Monomers bereits in anderen Studien dokumentiert (Broadbent *et al.*, 1996; MacManus-Spencer *et al.*, 2011; Rodil *et al.*, 2009; Vione *et al.*, 2015). Die Verläufe der relativen Peakflächen der TP weisen darauf hin, dass diese photo-labil sind. Im Gegensatz dazu wurde in anderen Studien unter Verwendung von simuliertem Sonnenlicht bzw. nach der Bestrahlung mit UV-A- und UV-B-Strahlung z.B. 4-MBA, das hydroxylierte Monomer und Cyclodimere nachgewiesen, welche jedoch nicht nach 128 min bzw. 240 min Photolyse eliminiert wurden (MacManus-Spencer *et al.*, 2011; Vione *et al.*, 2015). Gleichzeitig wurde das EHMC-Dimer, dem eine der Ethylhexyl-Gruppen fehlt, als nicht photo-stabil unter UV-B-Licht beschrieben (Vione *et al.*, 2015). Die Unterschiede zwischen den erwähnten Studien und den Ergebnissen der vorliegenden Arbeit sind auf unterschiedliche Überlappungen zwischen den Absorptionsspektren der TP und dem Emissionsspektrum der verwendeten Bestrahlungsquellen zurückzuführen. Der Einfluss der Überlappung der Spektren ist ein bekanntes Phänomen und wurde bereits in der Literatur beschrieben (Hensen *et al.*, 2019; Westphal *et al.*, 2020).

Ausgehend von den Bedingungen der HPLC und den ermittelten Retentionszeiten wurde bezüglich der Polarität der TP von EHMC der Schluss gezogen, dass die meisten TP polarer sind als ihrer Ausgangssubstanz. Die Ausnahme stellen die beiden TP_{581} dar, welche,

aufgrund ihrer – im Vergleich zu EHMC – späteren Retentionszeit, unpolarer sind. Diese Erkenntnisse decken sich mit den Ergebnissen aus früheren Arbeiten (MacManus-Spencer *et al.*, 2011). Die Polarität von Molekülen hat einen Einfluss auf deren Mobilität in der Umwelt, wobei Stoffe mit höheren Polaritäten eine höhere Mobilität in der aquatischen Umwelt aufweisen (Knepper *et al.*, 2003). Es können daher stärker polare und somit mobilere TP gebildet werden (Boxall, 2009).

In Artikel 2 wurde erstmals die primäre Eliminierung von OCR nachgewiesen, welche einer Kinetik erster Ordnung folgt. Zuvor wurde OCR als photostabil beschrieben (Gaspar und Maia Campos, 2006). In den Studien wurden andere Strahlungsquellen (künstliches Sonnenlicht einer Halogenlampe, 290 – 800 nm (Rodil *et al.*, 2009), beziehungsweise UV-A-Lampe (Ricci *et al.*, 2003)) eingesetzt. Eine Erklärung für die neue Beobachtung ist die stärkere Überlappung des Absorptionsspektrums von OCR mit dem Emissionsspektrum der verwendeten Lampe (200 – 400 nm).

In Artikel 2 wird erstmalig den Nachweis von TP nach der Bestrahlung einer wässrigen OCR-Lösung beschrieben. Aufgrund der beobachteten Retentionszeiten der mittels HPLC-UV-Analyse nachgewiesenen TP von OCR, ist davon auszugehen, dass die vier TP polarer sind als OCR. Für die TP von OCR gilt folglich, dass die höhere Polarität eines TP einer höheren Mobilität der Substanz in der aquatischen Umwelt im Vergleich zur Ausgangsverbindung (Boxall, 2009; Knepper *et al*., 2003; Reemtsma *et al.*, 2016) gleich kommt. Dies kann zu einer Gefahr für Mensch und die Umwelt führen, da die toxischen Eigenschaften der TP in der Regel unbekannt sind (Stein *et al.*, 2017; Kümmerer *et al.*, 2018, 2019).

5.3 Effekte während der Photolyse einer UV-Filter-Mischung

Die Beobachtung, dass EHMC in Gegenwart von OCR langsamer eliminiert wird, steht im Einklang mit zuvor beschriebenen Effekten zur Anwesenheit von OCR (Gaspar und Maia Campos, 2006). Somit scheint OCR stabilisierend zu wirken. Dass umgekehrt OCR in Gegenwart von EHMC schneller zersetzt wird, ist auf die Radikale von EHMC, welches zuerst abgebaut wurde, zurückzuführen. Auf Grund dieser Reaktion wird OCR bei der Photolyse der Mischung schneller eliminiert. Bei der Wasseraufbereitung durch Nachbehandlung mittels UV-Bestrahlung muss daher berücksichtigt werden, dass es bei Mischungen von Spurenstoffen zu Wechselwirkungen zwischen diesen miteinander kommt. Somit sind Ergebnisse aus Versuchen mit den einzelnen Verbindungen nicht direkt auf die Gemische übertragbar und die Generierung von Daten zu den Gemischen selbst ist unerlässlich. Allerdings können aus den Versuchen der Einzelsubstanzen grundlegende Erkenntnisse zu deren Umweltverhalten abgeleitet werden.

Ein noch deutlicherer Effekt, der auf die Wechselwirkung der UV-Filter während der Bestrahlung zurückzuführen ist, ist die Bildung von sieben weiteren Mischungs-TP, welche erstmals für die Mischung aus EHMC und OCR nachgewiesen wurden. Die Formulierung „UV-Filter-UV-Filter-Wechselwirkung“ stellt dabei eine Vereinfachung der Situation dar, da die Mischungs-TP nicht nur aus der Wechselwirkung zwischen EHMC und OCR entstanden sein können, sondern auch durch die Reaktion von TP untereinander oder durch die Reaktion von TP mit den Ausgangsverbindungen.

Fakt ist, dass die Behandlung von Mischungen mehrerer Spurenstoffe mehr und bisher unbekannte TP entstehen lässt. Im hier untersuchten Gemisch liegt der Vorteil darin, dass alle TP, die im Mischungsversuch auftraten, während der Bestrahlungszeit wieder eliminiert wurden. Somit gilt es bei der Planung von Behandlungen durch Bestrahlung eine geeignete Bestrahlungsdauer zu ermitteln sowie eine ausreichend große Überlappung der Spektren der Verbindungen und der verwendeten Lampe zu gewährleisten, um alle gebildeten TP wieder zu entfernen.

5.4 Einordnung der QSAR Ergebnisse der TP von EHMC

Die Ergebnisse aus dem Vergleich der computergestützten Vorhersagen für EHMC und seine TP zeigen, dass die Oasis-Software für die Vorhersage der leichten biologischen Abbaubarkeit von Strukturvorschlägen aus Untersuchungen seltener oder neuartiger Strukturen nur bedingt bzw. nicht geeignet ist. Obwohl für EHMC eine leichte biologische Abbaubarkeit vorhergesagt wurde, wurde vielfach über den Nachweis von EHMC in der aquatischen Umwelt berichtet (Balmer *et al.*, 2005; Cuderman und Heath, 2007; Díaz-Cruz *et al.*, 2012; Poiger *et al.*, 2004; Rodil und Möder, 2008). Eine Erklärung bietet die Betrachtung der Eintragsmengen und Kontinuität. Da EHMC kontinuierlich eingetragen wird, spricht man von einem pseudo-persistenten Stoff (Gago-Ferrero *et al.*, 2013). Darüber hinaus kann nicht ausgeschlossen werden, dass die *in silico* Methoden z.T. nicht geeignet war, da manche der Moleküle zu groß bzw. komplex waren für die Anwendungsdomain.

Bei der Vorhersage der Toxizität hingegen wurde deutlich, dass TP_{137c}, TP_{199}, TP_{305a}, TP_{305e}, TP_{305f} und TP_{305g} als toxischer vorhergesagt wurden als die Ausgangssubstanz. Zur Absicherung der Vorhersagen und zur Feststellung, ob die TP krebserregend oder genotoxisch sind, sind weitere Tests wie beispielsweise ein *in vivo* Mikronucleus Tests mit EHMC nötig. Hierfür werden kommerziellen Standards u.a. für TP_{199} essentiell. Alternativ kann die photolytische Mischung untersucht werden. Die Ursache für die vorhergesagte Genotoxizität durch Chromosomenaberrationen für TP_{137c} und TP_{305a} und die unschlüssige Aussage bezüglich der Genotoxizität von EHMC für diesen Endpunkt ist möglicherweise auf unterschiedliche Aktivitäten in den Molekülen zurückzuführen. Die vorhergesagten

Genotoxizitäten können somit verändert sein, da verschiedene Warnmeldungen zu unterschiedlichen Aktivitäten auf einen bestimmten Endpunkt führen können. Es ist somit anzunehmen, dass einige TP toxischere Eigenschaften als EHMC aufweisen und weitere Untersuchungen zur Verifizierung notwendig sind.

Eine aktuelle Studie mit EHMC in umweltrelevanten Konzentrationen und dem TP 4-MBA bestätigt durch experimentelle Daten die Auswirkungen auf die Genexpression von Fischen: Beide Substanzen verändern antioxidative Gene in der Leber von Zebrafischen (Nataraj *et al.*, 2022). Somit kann ein Einfluss auf die Süßwasserfauna nicht ausgeschlossen werden, wenn EHMC und/oder 4-MBA in die aquatische Umwelt gelangen und sich in dieser ausbreiten.

5.5 Methodendiskussion

Die ausgewählten methodischen Herangehensweisen sind die Basis für den Erkenntnisgewinn dieser Arbeit.

Die Nutzung der Daten aus der ECHA-Datenbank war hilfreich für die Erarbeitung von Artikel 3, da auf diese Weise Daten zu TP ergänzt werden konnten, zu denen keine Informationen in den ausgewerteten Studien veröffentlicht waren. Jedoch hat diese Methode ihre Grenze dahingehend erreicht, dass nicht zu allen TP Daten zur leichten biologischen Abbaubarkeit hinterlegt waren. Teilweise war nicht einmal der Eintrag zu den entsprechenden TP vorhanden. Das Fehlen einiger Verbindungen in der Datenbank begründet sich vorrangig damit, dass nur registrierungspflichtige Stoffe des europäischen Wirtschaftsraums gelistet werden, welche das Produktionsvolumen von einer Tonne pro Jahr pro Hersteller bzw. Importeur überschreiten.

Ein harmonisiertes Testsystem für TP einschließlich ihrer Eigenschaften ist erforderlich, um eine systematische Untersuchung der Stabilität von TP zu ermöglichen. Standardisierte Verfahren, wie die bereits etablierten Verfahren zur Bewertung der biologischen Abbaubarkeit sollten angewandt oder entwickelt werden, sofern diese noch nicht vorhanden sind. In Fällen, bei denen keine Laborversuche durchführbar sind, kann eine systematische Untersuchung der Stabilität oder anderen Eigenschaften der TP einschließlich eines Pre-Screenings mit Hilfe von QSAR-Analysen oder mittels *Read Across* durchgeführt werden. Das harmonisierte System sowie die alternativen Ansätze sind auch auf Substanzen jenseits von UV-Filtern übertragbar.

Bei der Frage nach der geeigneten chromatographische Trenntechnik für die Analytik der TP von UV-Filtern fiel die Entscheidung auf HPLC bzw. LC-MS, da noch unbekannte TP mittels *non-target*-Analytik identifiziert werden sollten. Eine HPLC hat bei der Fragestellung der TP Analytik einige Vorteile gegenüber einer gaschromatographischen Trennung: Die HPLC eignet sich besonders für thermisch labile und sich leicht zersetzende Substanzen besser als eine Gaschromatographie. Mittels HPLC können auch schwerflüchtige oder nicht flüchtige

Verbindungen analysiert werden. Außerdem können mit einer HPLC auch Substanzen mit einem hohen Molekulargewicht (> 500 g/mol) untersucht werden, was eine Detektion von UV-Filter-UV-Filter-Wechselwirkungs-TP ermöglicht. Da TP oft polarer sind als ihre Ausgangssubstanz sind, die bessere Auftrennung polarer Substanzen der größte Vorteil der HPLC.

Aufgrund der gewählten Methoden ist zudem zu berücksichtigen, dass der alleinige Nachweis des Verschwindens von TP in der Photolyse eine unvollständige Mineralisierung nicht ausschließt. Mit der eingesetzten photolytischen Methode werden möglicherweise einige weitere Ausgangsverbindungen und TP entfernt, jedoch nicht alle von ihnen. Insbesondere die Ergebnisse von Artikel 2 zeigen, dass nicht alle nachgewiesenen TP von OCR nach 256 min Bestrahlungszeit eliminiert wurden. Daher empfiehlt sich zunächst die Auswahl einer angemessenen Bestrahlungsdauer, während derer alle TP vollständig eliminiert werden. Darüber hinaus weist die in Artikel 2 verwendete Nachweismethode blinde Flecken auf. Die Frage, ob und welche TP von OCR gebildet werden, wurde nur unvollständig beantwortet. Mit der verwendeten Methode (HPLC-UV) können nur UV-aktiven TP nachgewiesen werden und die UV-Detektion eignet sich auch nicht zur Strukturaufklärung. In künftigen Arbeiten empfiehlt es sich daher, eine zusätzliche Analyse mittels hochaufgelöster Massenspektrometrie zu nutzen, um auch nicht UV-aktive TP von OCR nachweisen und die nachgewiesenen TP identifizieren zu können.

Die experimentellen Ergebnisse wurden in Versuchen mit wässrigen Lösungen im Labormaßstab gewonnen. Die Übertragung der Ergebnisse auf reale Bedingungen ist somit mit Unsicherheiten behaftet. Ein nächster Schritt in Richtung der realistischen Bedingungen ist beispielsweise eine Versuchsreihe in größerer Dimension als der Labormaßstab. Außerdem sollten komplexere (ggf. künstliche) Probenlösungen erforscht werden, wobei jedoch zusätzliche Reinigungs- und Konzentrationsschritte notwendig sind. Sobald die Probenvorbereitung für die komplexeren Proben optimiert ist, sollten Umweltproben untersucht werden. Eine Möglichkeit zum Umgang mit komplexeren Proben stellt der Einsatz von analytischen Methoden z.B. mit radioaktiven Markierungen dar, da zum einen auch geringen Stoffkonzentrationen detektiert und zum anderen Transformationsmechanismen nachvollzogen werden können.

End-of-Pipe-Konzepte wie die erweiterten Verfahren zur (Ab-)Wasseraufbereitung werden bereits routinemäßig eingesetzt. Dennoch sind diese Techniken nicht in der Lage, die meisten Verunreinigungen vollständig zu entfernen und stoßen somit an ihre Grenzen. Daher wird zunehmend diskutiert, dass sich das Verständnis über die Eliminierung von Spurenstoffen grundlegend ändern und die Maßnahmen am Anfang ergriffen werden müssen (Kümmerer *et al.*, 2015). Idealerweise wird dem Eintrag von Spurenstoffen in den Wasserkreislauf und

deren Vermeidung von vorherein mehr Aufmerksamkeit gewidmet und das Wasser gar nicht erst verunreinigt.

Eine Übertragbarkeit der angewendeten Methoden auf andere Spurenstoffe, wie Pharmazeutika, ist denkbar. Zu berücksichtigen ist dabei, dass in dieser Arbeit mit EHMC und OCR sehr lipophile Substanzen untersucht wurden. Dadurch war der Einsatz von Lösungsvermittlern notwendig, wodurch eine TOC-Analyse nicht möglich war. Für deutlich wasserlöslichere Analyten empfiehlt sich in jedem Fall eine TOC-Analyse, da auf diese Weise der Grad der Mineralisierung der Testsubstanz(en) nachverfolgt werden kann.

6 Schlussfolgerungen und Ausblick

Das erste Ziel der vorliegenden Arbeit war die Untersuchung von TP, die in Folge der Eliminierung von UV-Filtern entstehen. Dazu wurde zum einen eine Literaturrecherche durchgeführt, mit dem Ziel alle TP zusammen zu tragen, die in abiotischen oder biotischen Transformationsprozessen aus UV-Filtern gebildet wurden. Zum anderen wurde anhand der beiden UV-Filter EHMC und OCR untersucht, ob die UV-Filter infolge der Bestrahlung mit UV-C-Licht in wässriger Lösung eliminiert werden und ob TP entstehen. Die gebildeten TP wurden mittels HPLC-UV nachgewiesen. Für EHMC wurde zudem die Strukturen der TP mittels LC-MS/MS untersucht und Strukturvorschläge für die nachgewiesenen TP gemacht. Um der Frage nach Mischungseffekten nachzugehen wurden die beiden Testsubstanzen EHMC und OCR zusammen in wässriger Lösung mit UV-C-Licht bestrahlt und die gebildeten TP mit HPLC-UV nachgewiesen.

Das zweite Ziel der Arbeit beschäftigt sich mit den Eigenschaften von TP und ob von TP aus UV-Filtern eine gleiche, geringere oder höhere Besorgnis ausgeht als von ihren Ausgangssubstanzen. Zu diesem Zweck wurden zum einen Daten zur leichte biologische Abbaubarkeit der TP, die während der Literaturrecherche ermittelt wurden, analysiert. Zum anderen wurden die Eigenschaften der TP von EHMC mit QSAR vorhergesagt.

Der dritte Aspekt der Arbeit widmet sich der Frage, wie mit TP grundsätzlich umgegangen werden soll. Als Antwort auf diese Frage wird gefordert, dass die Regularien weiterentwickelt und harmonisierte, stufenweise Ansätze eingeführt werden. Denn durch eine harmonisierte Untersuchung der TP wird die Datengrundlage verbessert und Datenlücken werden geschlossen.

Die Untersuchungen des Abbauverhaltens und der Transformation der beiden UV-Filter EHMC und OCR ergab, dass EHMC im Verlauf der Experimente vollständig eliminiert wurde. Außerdem wurde erstmals die Eliminierung von OCR während einer Bestrahlung mit UV-Licht nachgewiesen. Für beide UV-Filter konnte die Bildung von TP nachgewiesen werden. Da die Eliminierung von OCR erstmalig beobachtet wurde, wurden auch zum ersten Mal TP für OCR aus einem abiotischen Abbau nachgewiesen. Aufgrund des Nachweises von TP unter den verwendeten Bedingungen und im untersuchten Zeitfenster fand bei der Eliminierung der beiden UV-Filter keine vollständige Mineralisierung statt. Im Fall von EHMC wurden die TP zusätzlich identifiziert und ermöglichten somit einen Abgleich mit bereits in der Literatur beschriebenen TP. Dieser Vergleich zeigte, dass nicht nur bekannte TP identifiziert, sondern für einige TP von EHMC zum ersten Mal ein Strukturvorschlag beschrieben wurde. Für sechs der Photo-TP von EHMC wurden mit Hilfe von *in silico* Methoden Hinweise gefunden, dass eine höhere oder andere, bedenklichere Toxizität als für EHMC vorliegen könnte. Die QSAR-Vorhersagen zur Toxizität geben einen wichtigen Anhaltspunkt, welche der TP mehr

Aufmerksamkeit in zukünftigen Untersuchungen erfordern (TP_{137c}, TP_{199}, TP_{305a}, TP_{305e}, TP_{305f} und TP_{305g}). Im Fokus künftiger Aktivitäten sollte daher die Bestätigung der vorhergesagten Toxizität z.B. einer veränderten Genotoxizität der vorgeschlagenen TP stehen. Dazu ist es notwendig, dass ausreichende Mengen der Substanzen für eine experimentelle Überprüfung zur Verfügung stehen. Die hier vorgestellten *in silico* Ergebnisse können genutzt werden, um zu entscheiden mit welchen Verbindungen begonnen werden sollte.

Die Ergebnisse aus den photolytischen Experimenten mit der Mischung von EHMC und OCR belegen erstmals, dass nicht nur bekannte TP (aus den Versuchen mit den Einzelsubstanzen) gebildet werden. Die Ergebnisse machen deutlich, dass aufgrund von Wechselwirkungen der UV-Filter untereinander zusätzliche, neue TP gebildet werden. Vergleichbare Mischungseffekte waren von anderen Substanzen bereits bekannt, jedoch wurden die Effekte sowie die Bildung der Mischungs-TP zum ersten Mal für die Mischung von EHMC und OCR nachgewiesen.

Erstmals wurden im Rahmen der Literaturrecherche 177 individuelle Substanzen gelistet, welche durch Transformation in abiotischen oder biotischen Prozessen aus elf UV-Filtern hervorgegangen sind. Der Überblick enthält dabei nur identifizierte und strukturell aufgeklärte TP. Zusätzlich wurde ein Überblick über die Verteilung der Prozesse, die zur Bildung der TP aus UV-Filtern führen, erstellt. Die Verteilung dieser Prozesse, bei denen eine der oben genannten 177 Substanzen als TP gebildet wurde, ist sehr variabel. Manche UV-Filter wurden intensiver untersucht als andere. Daraus leitet sich ab, dass jene UV-Filter, die bisher nicht im Mittelpunkt der Forschung standen, ebenfalls intensiver untersucht werden sollten. In Anbetracht des hohen Aufwandes für weitere Untersuchungen empfiehlt sich eine Priorisierung, gemäß dieser z.B. stark genutzte oder besonders problematische UV-Filter zuerst untersucht werden.

Bei der Selektion geeigneter Studien zur Transformation von UV-Filtern in abiotischen und biotischen Prozessen fiel auf, dass das Vorgehen weder einheitlich, noch systematisch war. Darüber hinaus wurden die TP häufig nicht vollständig untersucht, d.h. oft wurde gar nicht erst nach TP gesucht und wenn TP nachgewiesen wurden, dann fehlte die Strukturaufklärung. Die Eigenschaften der TP wurden in den seltensten Fällen untersucht. Aus diesem Grund wurden sowohl in der Literatur als auch in der ECHA-Datenbank nach Informationen zur leichten biologischen Abbaubarkeit der TP recherchiert. Die Ergebnisse dieser Arbeit zeigen dabei deutlich, dass nur sehr wenige Informationen zur biologischen Abbaubarkeit von TP zu finden sind (für mehr als 80 % der TP waren keine Informationen verfügbar). Da nur für wenige TP Daten zu ihren Eigenschaften vorlagen, wurde erstmals eine umfangreichen Datenlücke bezüglich der Information zur leichten biologischen Abbaubarkeit von TP aus UV-Filtern identifiziert. Die Auswertung der vorhandenen Daten deutet zwar eine Tendenz zur leichteren

biologischen Abbaubarkeit der TP im Vergleich zu ihren Ausgangssubstanzen an. Jedoch kann dieses Ergebnis – aufgrund der geringen Zahl verfügbarer Daten – nicht wirklich als Trend bezeichnet werden und ist mit großen Unsicherheiten behaftet. Die Ergebnisse zeigen deutlich, dass in weiteren Forschungsarbeiten nicht nur der Nachweis von TP erfolgen sollte, sondern auch die Strukturaufklärung und, was noch wichtiger ist, die Untersuchung der Eigenschaften der TP, z.B. in Form der Bewertung der leichten biologischen Abbaubarkeit. Die Bewertung der leichten biologischen Abbaubarkeit identifizierter TP sollte dabei nach einem harmonisierten Ansatz folgen, um eine bessere Zuverlässigkeit zu gewährleisten, Verständnis und den Vergleich der Ergebnisse zu ermöglichen. Außerdem hat sich gezeigt, dass es wichtig ist, Wissen zu generieren über die biologische Abbaubarkeit der gebildeten TP, um sicherzustellen, dass die eingesetzten Prozesse zu einer vollständigen Mineralisierung der TP führen. Die vorliegende Arbeit leistet somit einen Beitrag zu den aktuellen Strategien der internationalen Gemeinschaft zum Umgang mit Chemikalien in der Umwelt („Europäischer Grüner Deal“ und „Aktionsplan Schadstofffreiheit“/ “*Zero Pollution Action Plan*“). Diese Strategien streben eine nicht-toxische Umwelt an, indem der Eintrag von (anthropogenen) Spurenstoffen von vornherein zu vermeiden ist. Ist dies nicht möglich, so sollen Einträge zumindest reduziert werden. Die Ergebnisse der vorliegenden Arbeit stehen im Zeichen der aktuellen Strategien; denn auch wenn die Methoden am Ende der Fragestellung zum Eintrag und Verbleib von Chemikalien in der Umwelt ansetzen, so sind die Ergebnisse doch wichtige Wegweiser für weiteres Vorgehen.

Der Ansatz Einträge besorgniserregender Chemikalien von vorherein zu vermeiden, bekommt umso mehr Gewicht, je deutlicher man sich die zu erwartenden Auswirkungen des Klimawandels in den nächsten Jahrzehnten zum Beispiel auf die Ressource Wasser vor Augen führt. Je weniger (Süß-) Wasserressourcen zur Verfügung stehen, desto relevanter wird der Zugang zu sauberem Wasser. Weltweit ist Wasser schon heutzutage eine wertvolle Ressource, deren Wert sich in Zukunft noch steigern wird. Jedoch werden mit zunehmenden Effekten des Klimawandels nicht nur die Wasserressourcen knapper, sondern werden auch die Sonnenstunden weltweit steigen, sodass auch ein steigender Verbrauch von Sonnencremes und anderen Körperpflegeprodukten mit Lichtschutzfaktor zu erwarten ist. Dies führt wiederrum zu einem gesteigerten Eintrag der UV-Filtern.

Die vorliegende Arbeit macht deutlich, dass die Eliminierung eines kritischen Stoffes nicht das alleinige Ziel einer Behandlung durch Bestrahlung sein kann. Wie schon so oft führte die Bestrahlung mit UV-C-Licht zur Bildung mehrerer TP, deren Eigenschaften unbekannt oder sogar schlechter sind als die des Ausgangsstoffes. Daher müssen die Eigenschaften der gebildeten TP genauer betrachtet werden. Ohne Daten zu den Eigenschaften besteht die Gefahr besorgniserregende TP zu übersehen und dass durch eine vermeidliche Lösung eines

Problems neue, oder sogar schwerwiegendere Probleme auftreten. Die Ergebnisse zeigen deutlich wie uneinheitlich UV-Filter auf TP untersucht werden. Um die Gefahr von TP für den Menschen und die Umwelt einzuschätzen, empfiehlt sich bei Transformationsprozessen nicht nur zu prüfen, ob die Ausgangsverbindung eliminiert wird, sondern ob und welche TP entstehen, um anschließend Untersuchungen zum Umweltverhalten durchführen zu können.

7 Literatur

Abou-Dahech, M.; Boddu, S. H. S.; Bachu, R. D.; Babu, R. J.; Shahwan, M.; Al-Tabakha, M. M.; Tiwari A. K. (2022) A mini-review on limitations associated with UV filters. *Arabian Journal of Chemistry* 15 (11): 104212. https://doi.org/10.1016/j.arabjc.2022.104212

Apel, C.; Joerss, H.; Ebinghaus, R. (2018) Environmental occurrence and hazard of organic UV stabilizers and UV filters in the sediment of European North and Baltic Seas. *Chemosphere* 212: 254–261. https://doi.org/10.1016/j.chemosphere.2018.08.105

Bachelot, M.; Li, Z.; Munaron, D.; Le Gall, P.; Casellas, C.; Fenet, H.; Gomez, E. (2012) Organic UV filter concentrations in marine mussels from French coastal regions. *Science of The Total Environment* 420: 273–279. https://doi.org/10.1016/j.scitotenv.2011.12.051

Balmer, M. E.; Buser, H.-R.; Müller, M. D.; Poiger, T. (2005) Occurrence of some organic UV filters in wastewater, in surface waters, and in fish from Swiss Lakes. *Environmental Science & Technology* 39 (4): 953–962. https://doi.org/10.1021/es040055r

Blüthgen, N.; Meili, N.; Chew, G.; Odermatt, A.; Fent, K. (2014) Accumulation and effects of the UV-filter octocrylene in adult and embryonic zebrafish (*Danio rerio*). *Science of The Total Environment* 476–477: 207–217. https://doi.org/10.1016/j.scitotenv.2014.01.015

Boxall, A. B. A. (2009) Transformation products of synthetic chemicals in the environment. The Handbook of Environmental Chemistry 2 (Part P), 194 Springer, Berlin Heidelberg. https://doi.org/10.1007/978-3-540-88273-2

Boyd, A.; Stewart, C. B.; Philibert, D. A.; How, Z. T.; El-Din, M. G.; Tierney, K. B.; Blewett, T. A. (2021) A burning issue: The effect of organic ultraviolet filter exposure on the behaviour and physiology of Daphnia magna. *Science of The Total Environment* 750: 141707 https://doi.org/10.1016/j.scitotenv.2020.141707

Broadbent, J. K.; Martincigh, B. S.; Raynor, M. W.; Salter, L. F.; Moulder, R.; Sjöberg, P.; Markides, K. E. (1996) Capillary supercritical fluid chromatography combined with atmospheric pressure chemical ionisation mass spectrometry for the investigation of photoproduct formation in the sunscreen absorber 2-ethylhexyl-p-methoxycinnamate. *Journal of Chromatography A* 732 (1): 101–110. https://doi.org/10.1016/0021-9673(95)01199-4

Buser, H.-R.; Balmer, M. E.; Schmid, P.; Kohler, M. (2006) Occurrence of UV filters 4-methylbenzylidene camphor and octocrylene in fish from various Swiss Rivers with inputs from wastewater treatment plants. *Environmental Science & Technology* 40: 1427–1431. https://doi.org/10.1021/es052088s

Cadena-Aizaga, M. I.; Montesdeoca-Esponda, S.; Torres-Padrón, M. E.; Sosa-Ferrera, Z.; Santana-Rodríguez, J. J. (2020) Organic UV filters in marine environments: An update of analytical methodologies, occurrence and distribution. *Trends in Environmental Analytical Chemistry* e00079 https://doi.org/10.1016/j.teac.2019.e00079

Cuderman, P.; Heath, E. (2007) Determination of UV filters and antimicrobial agents in environmental water samples. *Analytical and Bioanalytical Chemistry* 387 (4): 1343–1350. https://doi.org/10.1007/s00216-006-0927-y

de Miranda, L.; Harvey, K.; Ahmed, A.; Harvey, S. C. (2021) UV-filter pollution: current concerns and future prospects. *Environmental Monitoring & Assessment* 193: 840. https://doi.org/10.1007/s10661-021-09626-6

Díaz-Cruz, M. S.; Barceló, D. (2009) Chemical analysis and ecotoxicological effects of organic UV-absorbing compounds in aquatic ecosystems. *Trends in Analytical Chemistry* 28 (6): 708-717. https://doi.org/10.1016/j.trac.2009.03.010

Díaz-Cruz, M. S.; Gago-Ferrero, P.; Llorca, M.; Barceló, D. (2012) Analysis of UV filters in tap water and other clean waters in Spain. *Analytical and Bioanalytical Chemistry* 402: 2325–2333. https://doi.org/10.1007/s00216-011-5560-8

Dondi, D.; Albini, A.; Serpone, N. (2006) Interactions between different solar UVB/UVA filters contained in commercial suncreams and consequent loss of UV protection. *Photochemical & Photobiological. Sciences*. 5: 835–843. https://doi.org/10.1039/b606768a

Downs, C. A.; Bishop, E.; Díaz-Cruz M. S.; Haghshenas, S. A.; Stien, D.; Rodrigues, A. M. S.; Woodley, C. M.; Sunyer-Caldú, A.; Doust, S. N.; Espero, W.; Ward., G.; Farhangmehr, A.; Samimi, S. M. T.; Risk, M. J.; Lebaron, P.; DiNardo, J. C. (2022) Oxybenzone contamination from sunscreen pollution and its ecological threat to Hanauma Bay, Oahu, Hawaii, U.S.A.. *Chemosphere* 291 (2): 132880. https://doi.org/10.1016/j.chemosphere.2021.132880

Europäische Kommission (2023a) Europäischer Grüner Deal - Erster klimaneutraler Kontinent werden. online verfügbar https://commission.europa.eu/strategy-and-policy/priorities-2019-2024/european-green-deal_de 25.09.2023, 15:10 Uhr.

Europäische Kommission (2023b) Zero pollution action plan - Towards zero pollution for air, water and soil. Online verfügbar https://environment.ec.europa.eu/strategy/zero-pollution-action-plan_de#objectives 01.07.2023, 16:05 Uhr.

Europäische Union (2009) Verordnung (EG) Nr. 1223/2009 des europäischen Parlaments und des Rates vom 30. November 2009 über kosmetische Mittel (Neufassung).

Fent, K.; Kunz, P. Y.; Gomez, E. (2008) UV filters in the aquatic environment induce hormonal effects and affect fertility and reproduction in fish. *Chimia* 62 (5): 368–375. https://doi.org/10.2533/chimia.2008.368

Fent, K.; Zenker, A.; Rapp, M. (2010) Widespread occurrence of estrogenic UV-filters in aquatic ecosystems in Switzerland. *Environmental Pollution* 158 (5): 1817–1824. https://doi.org/10.1016/j.envpol.2009.11.005

Gago-Ferrero, P.; Díaz-Cruz, M. S.; Barceló, D. (2013) Multi-residue method for trace level determination of UV filters in fish based on pressurized liquid extraction and liquid chromatography–quadrupole-linear ion trap-mass spectrometry. *Journal of Chromatography A* 1286: 93–101. https://doi.org/10.1016/j.chroma.2013.02.056

Gago-Ferrero, P.; Díaz-Cruz, M. S.; Barceló, D. (2015) UV filters bioaccumulation in fish from Iberian river basins. *Science of The Total Environment* 518–519: 518–525. https://doi.org/10.1016/j.scitotenv.2015.03.026

Gaspar, L. R.; Maia Campos, P. M. B. G. (2006) Evaluation of the photostability of different UV filter combinations in a sunscreen. *International Journal of Pharmaceutics* 307 (2): 123–128. https://doi.org/10.1016/j.ijpharm.2005.08.029

Germer, S.; Schalles, S.; Kaßner, F.; Hassold, E.; Stock, F.; Schulze, J.; Arning, J. (2020) UV-Filter in Sonnenschutzmitteln – Bewertung hormonähnlicher Eigenschaften und möglicher Gefahren für die Umwelt. UMID: Umwelt und Mensch – Informationsdienst 02/2020: 17–24. https://www.umweltbundesamt.de/sites/default/files/medien/4031/publikationen/umid-02-20-uv-filter_in_sonnenschutzmitteln.pdf, 24.09.2023, 20:08 Uhr.

Gutowski, L.; Olsson, O.; Leder, C.; Kümmerer, K. (2015) A comparative assessment of the transformation products of S-metolachlor and its commercial product Mercantor Gold® and their fate in the aquatic environment by employing a combination of experimental and in silico methods. *Science of The Total Environment* 506–507: 369–379. https://doi.org/10.1016/j.scitotenv.2014.11.025

Hany, J.; Nagel, R. (1995) Nachweis von UV-Filtersubstanzen in Muttermilch. *Deutsche Lebensmittelrundschau* 91: 341–345.

He, K.; Hain, E.; Timm, A.; Tarnowski, M.; Blaney, L. (2019) Occurrence of antibiotics, estrogenic hormones, and UV-filters in water, sediment, and oyster tissue from the Chesapeake Bay. *Science of the Total Environment* 650: 3101–3109. https://doi.org/10.1016/j.scitotenv.2018.10.021

Hensen, B.; Lange, J.; Jackisch, N.; Zieger, F.; Olsson, O.; Kümmerer, K. (2018) Entry of biocides and their transformation products into groundwater via urban stormwater infiltration systems. *Water Research* 144: 413–423. https://doi.org/10.1016/j.watres.2018.07.046

Hensen, B.; Olsson, O.; Kümmerer, K. (2019) The role of irradiation source setups and indirect phototransformation: Kinetic aspects and the formation of transformation products of weakly sunlight-absorbing pesticides. *Science of The Total Environment* 695: 133808. https://doi.org/10.1016/j.scitotenv.2019.133808

Hensen, B.; Olsson, O.; Kümmerer, K. (2020) A strategy for an initial assessment of the ecotoxicological effects of transformation products of pesticides in aquatic systems following a tiered approach *Environment International* 137: 105533. https://doi.org/10.1016/j.envint.2020.105533

Hernández-Leal, L.; Vieno, N.; Temmink, H.; Zeeman, G.; Buisman, C. J. N. (2010) Occurrence of xenobiotics in gray water and removal in three biological treatment systems. *Environmental Science & Technology* 44 (17): 6835–6842. https://doi.org/10.1021/es101509e

Hernández-Leal, L.; Zeeman, G.; Temmink, H.; Buisman, C. J. N. (2011) Grey water treatment concept integrating water and carbon recovery and removal of micropollutants. *Water Practice & Technology* 6 (2): wpt2011035. https://doi.org/10.2166/wpt.2011.035

Huang, Y.; Law, J. C.-F.; Lam, T.-K.; Leung, K. S.-Y. (2021) Risks of organic UV filters: a review of environmental and human health concern studies. *Science of The Total Environment* 755 (1): 142486. https://doi.org/10.1016/j.scitotenv.2020.142486

Khaleel, N. D. H.; Mahmoud, W. M. M.; Olsson, O.; Kümmerer, K. (2019) Studying the fate of the drug Chlorprothixene and its photo transformation products in the aquatic environment: Identification, assessment and priority setting by application of a combination of experiments and various *in silico* assessments. *Water Research* 149: 467–476. https://doi.org/10.1016/j.watres.2018.10.075

Knepper, T. P.; de Voogt, P.; Barceló, D. (2003) Analysis and fate of surfactants in the aquatic environment. Comprehensive Analytical Chemistry. vol. XL. Elsevier Science, Amsterdam, S. 808.

Kümmerer, K.; Dionysiou, D. D.; Fatta-Kassinos, D. (2015). Long-Term Strategies for Tackling Micropollutants. In: Fatta-Kassinos, D.; Dionysiou, D.; Kümmerer, K. (eds) Advanced

Treatment Technologies for Urban Wastewater Reuse. The Handbook of Environmental Chemistry, Vol. 45. Springer, Cham. https://doi.org/10.1007/698_2015_447

Kümmerer, K.; Dionysiou, D. D.; Olsson, O.; Fatta-Kassions, D. (2018) A path to clean water. *Science* 361 (6399): 222–224. https://doi.org/10.1126/science.aau2405.

Kümmerer, K.; Dionysiou, D. D.; Olsson, O.; Fatta-Kassions, D. (2019). Reducing aquatic micropollutants – increasing the focus on input prevention and integrated emission management. *Science of The Total Environment* 652: 836–850. https://doi.org/10.1016/j.scitotenv.2018.10.219

Kunz, P. Y.; Fent, K. (2006) Multiple hormonal activities of UV filters and comparison of *in vivo* and *in vitro* estrogenic activity of ethyl-4-aminobenzoate in fish. *Aquatic Toxicology* 79: 305–324. https://doi.org/10.1016/j.aquatox.2006.06.016

Kupper, T.; Plagellat, C.; Brändli, R.; Alencastro, L. de; Grandjean, D.; Tarradellas, J. (2006) Fate and removal of polycyclic musks, UV filters and biocides during wastewater treatment. *Water Research* 40 (14): 2603–2612; https://doi.org/10.1016/j.watres.2006.04.012

La Farré, M.; Pérez, S.; Kantiani, L.; Barceló, D. (2008) Fate and toxicity of emerging pollutants, their metabolites and transformation products in the aquatic environment. *Trends in Analytical Chemistry* 27 (11): 991–997. https://doi.org/10.1016/j.trac.2008.09.010

Li, W.; Ma, Y.; Guo, C.; Hu, W.; Liu, K.; Wang, Y.; Zhu, T. (2007) Occurrence and behavior of four of the most used sunscreen UV filters in a wastewater reclamation plant. *Water Research* 41 (15): 3506–3512. https://doi.org/10.1016/j.watres.2007.05.039

MacManus-Spencer, L. A.; Tse, M. L.; Klein, J. L.; Kracunas, A. E. (2011) Aqueous photolysis of the organic ultraviolet filter chemical octylmethoxycinnamate. *Environmental Science & Technology* 45: 3931–3937. https://doi.org/10.1021/es103682a

Magi, E.; Scopolla, C.; Di Carro, M.; Rivaro, P.; Nguyen, K. T. N. (2013) Emerging Pollutants in Aquatic Environments: Monitoring of UV Filters in Uraban Wastwater Treatment Plants. *Analytical Methods* 5: 428–433. https://doi.org/10.1039/C2AY26163D

Maimon, A.; Friedler, E.; Gross, A. (2014) Parameters affecting greywater quality and its safety for reuse. *Science of The Total Environment* 487 (1): 20–25. https://doi.org/10.1016/j.scitotenv.2014.03.133

Michael, I.; Vasquez, M. I.; Hapeshi, E.; Haddad, T.; Baginska, E.; Kümmerer, K.; Fatta-Kassinos, D. (2014) Metabolites and transformation products of pharmaceuticals in the aquatic environment as contaminants of emerging concern. In: Lambropoulou, D. A.; Nollet, L. M. L. (Eds.), Transformation Products of Emerging Contaminants in the Environment: Analysis, Processes, Occurrence, Effects and Risks. John Wiley and Sons Ltd., Chichester, Vereinigtes Königreich, 413–458. https://doi.org/10.1002/9781118339558.ch14

Molins-Delgado, D.; Muñoz, R.; Nogueira, S.; Alonso, M. B.; Torres, J. P.; Malm, O.; Ziolli, R. L.; Hauser-Davis, R. A.; Eljarrat, E:; Barceló, D.; Díaz-Cruz, M. S. (2018) Occurrence of organic UV filters and metabolites in lebranche mullet (Mugil liza) from Brazil. *Science of The Total Environment* 618: 451-459. https://doi.org/10.1016/j.scitotenv.2017.11.033

Murawski, A.; Schmied-Tobies, M. I. H.; Rucic, E.; Schmidtkunz, C.; Küpper, K.; Leng, G.; Eckert, E., Kuhlmann, L.; Göen, T.; Daniels, A.; Schwedler, G.; Kolossa-Gehring, M. (2021) Metabolites of 4-methylbenzylidene camphor (4-MBC), butylated hydroxytoluene (BHT), and tris(2-ethylhexyl) trimellitate (TOTM) in urine of children and adolescents in Germany –

human biomonitoring results of the German Environmental Survey GerES V (2014–2017). *Environmental Research* 192: 110345. https://doi.org/10.1016/j.envres.2020.110345

Nagorka, R.; Duffek, A. (2021) Under the influence of regulations: spatio-temporal trends of the UV filter 2-Ethylhexyl-4-methoxycinnamate (EHMC) in German rivers. *Environmental Science Europe* 33 (8) https://doi.org/10.1186/s12302-020-00448-w

Nataraj, B.; Maharajan, K.; Malafaia, G.; Hemalatha, D.; Ahmed, M. A. I.; Ramesh, M. (2022) Gene expression profiling in liver of zebrafish exposed to ethylhexyl methoxycinnamate and its photoproducts. *Science of The Total Environment* 826: 154046. https://doi.org/10.1016/j.scitotenv.2022.154046

Organisation für wirtschaftliche Zusammenarbeit und Entwicklung (2008) Guideline for Testing of Chemicals - Test No. 316: Phototransformation of Chemicals in Water – Direct Photolysis. https://doi.org/10.1787/9789264067585-en

Poiger, T.; Buser, H.-R.; Balmer, M. E.; Bergqvist, P.-A.; Müller, M. D. (2004) Occurrence of UV filter compounds from sunscreens in surface waters: regional mass balance in two Swiss lakes. *Chemosphere* 55 (7): 951–963. https://doi.org/10.1016/j.chemosphere.2004.01.012

Rastogi, T.; Leder, C.; Kümmerer, K. (2014) Qualitative environmental risk assessment of photolytic transformation products of iodinated X-ray contrast agent diatrizoic acid. *Science of The Total Environment* 482–483 (1): 378–388. https://doi.org/10.1016/j.scitotenv.2014.02.139

Reemtsma, T.; Berger, U.; Arp, H. P. H.; Gallard, H.; Knepper, T. P.; Neumann, M.; Quintana, J. B.; de Voogt, P. (2016) Mind the gap: persistent and mobile organic compounds — water contaminants that slip through. *Environmental Science & Technology* 50 (19): 10308–10315. https://doi.org/10.1021/acs.est.6b03338

Ricci, A.; Chrétien, M. N.; Maretti, L.; Scaiano, J. C. (2003) TiO_2-promoted mineralization of organic sunscreens in water suspension and sodium dodecyl sulfate micelles. *Photochemical & Photobiological Sciences* 2: 487–492. https://doi.org/10.1039/b212815b

Rodil, R.; Möder, M. (2008) Development of a method for the determination of UV filters in water samples using stir bar sorptive extraction and thermal desorption–gas chromatography–mass spectrometry. *Journal of Chromatography A* 1179 (2): 81–88. https://doi.org/10.1016/j.chroma.2007.11.090

Rodil, R.; Möder, M.; Altenburger, R.; Schmitt-Jansen, M. (2009) Photostability and phytotoxicity of selected sunscreen agents and their degradation mixtures in water. *Analytical and Bioanalytical Chemistry* 395: 1513–1524. https://doi.org/10.1007/s00216-009-3113-1

Santiago-Morales, J.; Gómez, M. J.; Herrera-López, S.; Fernández-Alba, A. R.; García-Calvo, E.; Rosal, R. (2013) Energy efficiency for the removal of non-polar pollutants during ultraviolet irradiation, visible light photocatalysis and ozonation of a wastewater effluent. *Water Research* 47: 5546–5556. https://doi.org/10.1016/j.watres.2013.06.030

Schlumpf, M.; Schmid, P.; Durrer, S.; Conscience, M.; Maerkel, K.; Henseler, M.; Gruetter, M.; Herzog, I.; Reolon, S.; Ceccatelli, R.; Faass, O.; Stutz, E.; Jarry, H.; Wuttke, W., Lichtensteiger, W. (2004) Endocrine activity and developmental toxicity of cosmetic UV filters—an update. *Toxicology* 205: 113–122. https://doi.org/10.1016/j.tox.2004.06.043

Schreurs, R. H. M. M.; Sonneveld, E.; Jansen, J. H. J.; Seinen, W.; Van der Burg, B. (2005) Interaction of polycyclic musks and UV filters with the estrogen receptor (ER), androgen receptor (AR), and progesterone receptor (PR) in reporter gene bioassays. *Toxicological Science* 83: 264–272. https://doi.org/10.1093/toxsci/kfi035

Seo, C.; Shin, J.; Lee, M.; Lee, W.; Yoom, H.; Son, H.; Jang, S.; Lee, Y. (2019) Elimination efficiency of organic UV filters during ozonation and UV/H_2O_2 treatment of drinking water and wastewater effluent. *Chemosphere* 230: 248 – 257. https://doi.org/10.1016/j.chemosphere.2019.05.028

Sharma, A.; Bányiová, K.; Babica, P.; El Yamani, N.; Collins, A. R.; Čupr, P. (2017) Different DNA damage response of cis and trans isomers of commonly used UV filter after the exposure on adult human liver stem cells and human lymphoblastoid cells. *Science of The Total Environment* 593–594: 18-26. https://doi.org/10.1016/j.scitotenv.2017.03.043

Statistisches Bundesamt (Destatis) (2023) Pressemitteilung: Hautkrebs führte im Jahr 2020 zu 81 % mehr Krankenhausbehandlungen und 53 % mehr Todesfällen als im Jahr 2000. Online Verfügbar unter https://www.destatis.de/DE/Presse/Pressemitteilungen/2022/04/PD22_N018_231.html 07.08.2023, 10:41 Uhr.

Stein, H. V.; Berg, C. J.; Maung, J. N.; O'Connor, L. E.; Pagano, A. E.; MacManus-Spencer, L. A.; Paulick, M. G. (2017) Photolysis and cellular toxicities of the organic ultraviolet filter chemical octylmethoxycinnamate and its photoproducts. *Environmental Science: Processes & Impacts* 19: 851–860. https://doi.org/10.1039/C7EM00059F

Tran, T.; Dang, B. T.; Thuy, L. T. T.; Hoang, H.-G.; Bui, X.-T.; Le, V.-G.; Lin, C.; Nguyen, M.-K.; Nguyen, K.-Q.; Nguyen, P.-T.; Binh, Q. A.; Thuy Bui T.-P. (2022) Advanced Treatment Technologies for the Removal of Organic Chemical Sunscreens from Wastewater: A Review. *Current Pollution Reports* 8: 288–302. https://doi.org/10.1007/s40726-022-00221-y

Tsui, M. M. P.; Leung, H. W.; Wai, T.-C.; Yamashita, N.; Taniyasu, S.; Liu, W.; Lam, P. K. S.; Murphy, M. B. (2014a) Occurrence, distribution and ecological risk assessment of multiple classes of UV filters in surface waters from different countries. *Water Research* 67: 55–65. https://doi.org/10.1016/j.watres.2014.09.013

Tsui, M. M. P.; Leung, H. W.; Lam, P. K. S.; Murphy, M. B. (2014b) Seasonal occurrence, removal efficiencies and preliminary risk assessment of multiple classes of organic UV filters in wastewater treatment plants. *Water Research* 53: 58–67. https://doi.org/10.1016/j.watres.2014.01.014

Vereinte Nationen (2023) Ziele für nachhaltige Entwicklung. Online Verfügbar unter https://unric.org/de/17ziele/, 30.06.2023, 13:32 Uhr.

Vione, D.; Calza, P.; Galli, F.; Fabbri, D.; Santoro, V.; Medana, C. (2015) The role of direct photolysis and indirect photochemistry in the environmental fate of ethylhexyl methoxy cinnamate (EHMC) in surface waters. *Science of The Total Environment* 537: 58–68. https://doi.org/10.1016/j.scitotenv.2015.08.002

Westphal, J.; Kümmerer, K.; Olsson, O. (2020) Experimental and in silico assessment of fate and effects of the UV filter 2-phenylbenzimidazole 5-sulfonic acid and its

phototransformation products in aquatic solutions. *Water Research* 171: 115393. https://doi.org/10.1016/j.watres.2019.115393

8 Artikel zur kumulativen Dissertation

Artikel 1

Franziska Jentzsch, Oliver Olsson, Janin Westphal, Marco Reich, Christoph Leder, Klaus Kümmerer (2016) Photodegradation of the UV filter ethylhexyl methoxycinnamate under ultraviolet light: Identification and in silico assessment of photo-transformation products in the context of grey water reuse. *Science of the Total Environment* 572: 1092-1100.

DOI: https://doi.org/10.1016/j.scitotenv.2016.08.017

Artikel 2

Franziska Jentzsch, Marco Reich, Klaus Kümmerer, Oliver Olsson (2019) Photolysis of mixtures of UV filters octocrylene and ethylhexyl methoxycinnamate leads to formation of mixed transformation products and different kinetics. *Science of the Total Environment* 134048.

DOI: https://doi.org/10.1016/j.scitotenv.2019.134048

Artikel 3

Franziska Jentzsch, Klaus Kümmerer, Oliver Olsson (2023) Status quo on identified transformation products of organic ultraviolet filters and their persistence. *International Journal of Cosmetic Science* 45 (Suppl. 1): 101–126.

DOI: https://doi.org/10.1111/ics.12908

Tabelle 2: Beitrag der Autoren zu den Veröffentlichungen

Artikel Nr.	Titel	Individuelle wissenschaftliche Leistung aller Autoren*	Klassifizierung des eigenen Anteils	Status der Veröf-fentlichung
1	Photodegradation of the UV filter ethylhexyl methoxycinnamate under ultraviolet light: Identification and in silico assessment of photo-transformation products in the context of grey water reuse.	**FJ**: Konzeption des Forschungsansatzes, Entwicklung der Forschungsmethoden, Erhebung und Aufbereitung von Daten, Durchführung der Forschung, Analyse/Interpretation von Daten oder Zwischenergebnissen, Schreiben und Überarbeitung des Manuskripts **OO**: inhaltliche Überarbeitung des Manuskripts **JW**: Entwicklung der Forschungsmethoden, Erhebung von Daten **MR**: Entwicklung der Forschungsmethoden **CL**: Erhebung von Daten **KK**: inhaltliche Überarbeitung des Manuskripts	Ko-Autorenschaft: überwiegender Anteil. Wichtung: 1	Veröffentlicht: Science of the Total Environment (2016) 572: 1092-1100.
2	Photolysis of mixtures of UV filters octocrylene and ethylhexyl methoxycinnamate leads to formation of mixed transformation products and different kinetics.	**FJ**: Konzeption des Forschungsansatzes, Entwicklung der Forschungsmethoden, Erhebung und Aufbereitung von Daten, Durchführung der Forschung, Analyse/Interpretation von Daten oder Zwischenergebnissen, Schreiben und Überarbeitung des Manuskripts **MR**: Entwicklung der Forschungsmethoden **KK**: inhaltliche Überarbeitung des Manuskripts **OO**: inhaltliche Überarbeitung des Manuskripts	Ko-Autorenschaft: überwiegender Anteil. Wichtung: 1	Veröffentlicht: Science of the Total Environment (2019) 134048.
3	Status quo on identified transformation products of organic ultraviolet filters and their persistence	**FJ**: Konzeption des Forschungsansatzes, Entwicklung der Forschungsmethoden, Erhebung und Aufbereitung von Daten, Durchführung der Forschung, Analyse/Interpretation von Daten oder Zwischenergebnissen, Schreiben und Überarbeitung des Manuskripts **KK**: inhaltliche Überarbeitung des Manuskripts **OO**: inhaltliche Überarbeitung des Manuskripts	Ko-Autorenschaft: überwiegender Anteil. Wichtung: 1	Veröffentlicht International Journal of Cosmetic Science (2023) 45 (Suppl. 1): 101–126.

Abkürzungen der einzelnen Autoren: FJ – Franziska Schneider (geb. Jentzsch), OO – Oliver Olsson, JW – Janin Westphal, MR – Marco Reich, CL – Christoph Leder, KK – Klaus Kümmerer.

***Zugehörigkeit der Autoren*:** Institut für Nachhaltige und Umweltchemie, Leuphana Universität Lüneburg, Lüneburg.

Artikel 1

Franziska Jentzsch, Oliver Olsson, Janin Westphal, Marco Reich, Christoph Leder, Klaus Kümmerer.

Photodegradation of the UV filter ethylhexyl methoxycinnamate under ultraviolet light: Identification and in silico assessment of photo-transformation products in the context of grey water reuse

Science of the Total Environment (2016) 572: 1092-1100.

DOI: https://doi.org/10.1016/j.scitotenv.2016.08.017

Science of the Total Environment 572 (2016) 1092–1100

Contents lists available at ScienceDirect

Science of the Total Environment

journal homepage: www.elsevier.com/locate/scitotenv

Photodegradation of the UV filter ethylhexyl methoxycinnamate under ultraviolet light: Identification and *in silico* assessment of photo-transformation products in the context of grey water reuse

F. Jentzsch, O. Olsson *, J. Westphal, M. Reich, C. Leder, K. Kümmerer

Sustainable Chemistry and Material Resources, Institute of Sustainable and Environmental Chemistry, Faculty of Sustainability, Leuphana University of Lüneburg, Scharnhorststraße 1/C13, DE-21335 Lüneburg, Germany

HIGHLIGHTS

- Examination of the photochemical properties of EHMC
- Different initial concentrations of EHMC were exposed to UV light.
- A tentative photodegradation pathway of EHMC is proposed.
- Identification of known and new photo-transformation products (TPs) of EHMC
- *In silico* assessment of the toxicity of EHMC's TPs showed, *e.g.* genotoxic effects.

GRAPHICAL ABSTRACT

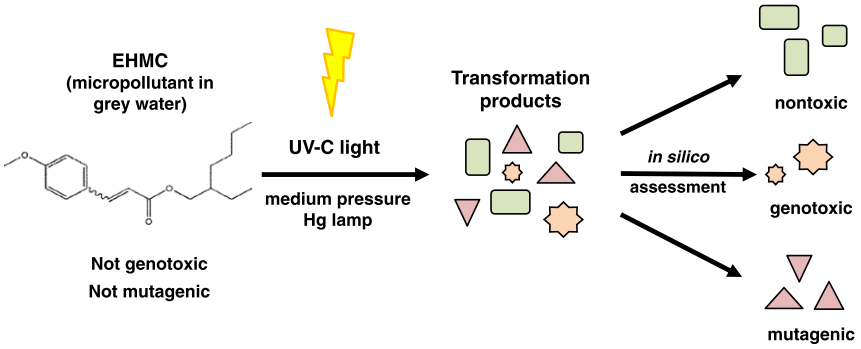

ARTICLE INFO

Article history:
Received 31 March 2016
Received in revised form 2 August 2016
Accepted 3 August 2016
Available online 13 August 2016

Editor: Adrian Covaci

Keywords:
Grey water
Personal care products
Photolysis
Transformation
UV treatment
Quantitative structure-activity relationship

ABSTRACT

To prevent water shortages in the future and to reduce domestic water consumption, decentralized grey water (GW) reuse has become increasingly important. This water has, however, to be free of pollutants. Conventional treatment of GW does not fully eliminate micropollutants such as the UV filter substance ethylhexyl methoxycinnamate (EHMC). EHMC, which is commonly used in sunscreens and personal care products, is an endocrine disruptor and shows potential to bioaccumulation, which is also reflected in its low water solubility. Photolysis has been proposed as an alternative treatment method for other micropollutants, but it is not clear yet whether it can also be used to eliminate EHMC. One goal of this study was to better understand the basic pathways involved in this process. It aimed to identify photo-transformation products (photo-TPs) by using, in the test conditions, an initial concentration of EHMC higher than those expected in the environment. Acetonitrile (ACN) was added in low concentrations to the aqueous solution to overcome the low aquatic solubility of EHMC. The influence of this co-solvent on the degradation kinetics was studied. The photolysis experiments were carried out using a medium pressure mercury lamp, which emits UV light in the range of 200–400 nm. The quantum yield of the photolysis of EHMC was 0.0042 and 0.0023 mol·Einstein^{-1} (for 0.2 and 0.5% ACN (v/v), respectively), and the relative and absolute UV photon fluxes were determined. HPLC was used to monitor the elimination kinetics of EHMC, which followed first-order kinetics. The results of LC-MS^n analyses revealed that beside others, several oxidized and hydroxylized EHMC isomers were formed as photo-TPs in aqueous

* Corresponding author at: Institute of Sustainable and Environmental Chemistry, Faculty of Sustainability, Leuphana University of Lüneburg, Scharnhorststraße 1 - C.13.313a, D-21335 Lüneburg, Germany.
E-mail addresses: Franziska.Jentzsch@leuphana.de, F_Jentzsch@gmx.de (F. Jentzsch), oliver.olsson@leuphana.de (O. Olsson), Janin.Westphal@leuphana.de (J. Westphal), marco.reich@leuphana.de (M. Reich), christoph.leder@leuphana.de (C. Leder), klaus.kuemmerer@leuphana.de (K. Kümmerer).

http://dx.doi.org/10.1016/j.scitotenv.2016.08.017

solution. Using a set of *in silico* quantitative structure-activity relationship (QSAR) models, this study also offered new insights concerning the environmental fate and toxicity of the TPs of EHMC.

1. Introduction

Water has become an increasingly precious resource around the world, wherefore grey water (GW) could be an alternative source, which comprises 50–70% of domestic wastewater (Eriksson et al., 2002; Friedler, 2004). In some contexts, GW has been used as a substitute for potable water, especially in arid and semi-arid zones (Fatta-Kassinos et al., 2016; Oron et al., 2014). Before it can be a contribution to a more sustainable use of water in urban areas, GW has to be free of contaminants. Therefore, treatment systems have to ensure the complete degradation of substances into non-toxic compounds to avoid environmental and health problems originating either from transformation products (TPs) or from the incomplete removal of the parent compound (Maimon et al., 2014). Recent studies have shown that personal care products (PCP) are only partially eliminated by conventional (biological) GW treatment (*e.g.*, Buchberger, 2011; Eriksson et al., 2010; Martínez-Hernández et al., 2014). One group of PCP ingredients found in treated GW includes UV filter substances such as 2-ethylhexyl 4-methoxycinnamate (EHMC) with concentration range of 0.16–1.5 μg L^{-1} (Eriksson et al., 2003, 2010; Hernández-Leal et al., 2010). EHMC showed poor removal during aerobic but also anaerobic and combined aerobic and anaerobic sludge treatments (Hernández-Leal et al., 2010, 2011). However, for decentralized (*i.e.*, on-site) GW treatment, an anaerobic system followed by an aerobic post-treatment unit for water disinfection (*e.g.* by UV irradiation) may be a sustainable option to achieve high level of removal of persistent pollutants from GW (Ghaitidak and Yadav, 2013).

Previous studies reported photodegradation of EHMC in aqueous solution under sun light irradiation ($\lambda > 290$ nm; i.a., MacManus-Spencer et al., 2011; Rodil et al., 2009) or with monochromatic UV light (λ_{max} 254, 365 or 313 nm; i.a., Santiago-Morales et al., 2013; Vione et al., 2015). However, only a few of these studies focused on the formation of partly stable photo-TPs in water (MacManus-Spencer et al., 2011; Rodil et al., 2009; Vione et al., 2015). But until now, no one performed the photolysis of EHMC under multiwavelength irradiation (200–400 nm) and analyzed the effect of these conditions on EHMC degradation and formation of TPs. However, an evaluation of UV treatment as an option for decentralized post-treatment of GW needs urgently further insights concerning the pathways and outcomes of this kind of treatment. This should comprise the analysis of the degradation efficiency of EHMC, the identification of TPs, and their assessment (Herrmann et al., 2015; Mahmoud et al., 2014).

Because of its high lipophilicity, EHMC has potential to bioaccumulate in fish (Blüthgen et al., 2014; Gago-Ferrero et al., 2013), invertebrates (Bachelot et al., 2012), and human breast milk (Hany and Nagel, 1995). This is of major concern because it has been shown to act as an endocrine disruptor, *in vivo*, EHMC acts estrogenically in fish (Tsui et al., 2014a,b) and rats (Schlumpf et al., 2004) and, *in vitro*, it has been shown to have multiple hormonal effects on human receptors (Kunz and Fent, 2006; Schreurs et al., 2005). The toxicity of known TPs of EHMC is mostly unknown. In some cases the toxicity of photolytic mixtures was tested, *e.g. Vibrio fischeri* microtox assay for 4-methoxybenaldehyde that showed higher toxicity than EHMC (Vione et al., 2015). Besides, the environmental fate of the TPs of EHMC formed during UV treatment is unknown. In general, TPs created during photolytic reactions of micropollutants have mostly unknown properties and toxicity and can be even more toxic than their parent compounds (La Farré et al., 2008; Michael et al., 2014; Santiago-Morales et al., 2013). Many TPs are not available commercially, which makes an experimental analysis of the toxicity of individual substances difficult. In addition, toxicological experiments are costly. Furthermore, these compounds are usually formed only in low concentrations within complex matrices so that isolation and purification is very tedious and challenging. Solving these problems by generating data based on QSAR is an approach that has become increasingly important, especially for the analysis and assessment of environmental TPs (Gutowski et al., 2015; Rastogi et al., 2014a).

This paper examines the effect of UV irradiation on EHMC in aquatic solutions and the properties of its TPs. Specifically, we hypothesize (I) that EHMC will be degraded under polychromatic UV light, (II) TPs will be formed, and (III) using QSAR can provide an useful *in silico* assessment of toxicity of the TPs. The findings, in turn, can serve as the basis for further toxicity assessment and the development of an aerobic GW post-treatment method. Due to the hydrophobicity of EHMC and the fact that several studies showed the improved solubility when solutions of EHMC in acetonitrile (ACN) or methanol were used to spike water for the photolysis (MacManus-Spencer et al., 2011; Rodil et al., 2009; Vione et al., 2015). ACN was used and assessed as solubilizer in this study. Although the effects of different solubilizers on the degradation were examined (Serpone et al., 2002; Vione et al., 2015), no study addressed the influence of the solvent concentration on the degradation kinetics which should be as low as possible. For this reason, the influence of the co-solvent had to be taken into account and examined while looking at the elimination kinetics during the photodegradation process. Determining the quantum yield of a photolysis under laboratory conditions is important if one intends to draw on lab data for practical application. Previously, only a few articles have examined the quantum yield of EHMC either in water or water methanol mixtures with a very low organic solvent content (MacManus-Spencer et al., 2011; Serpone et al., 2002; Vione et al., 2015), but not in aqueous solutions with a minimal ACN content (<1%). In addition, the role of reactive oxygen species (ROS) was studied. The TPs formed were monitored and identified by HPLC with UV detection and LC-ESI-MS^n. QSAR prediction tools were applied a) to support structure elucidation of the generated photoproducts identified with LC–UV–MS^n and b) to enable an initial assessment of TPs toxicity.

2. Materials and method

2.1. Chemicals and reagents

The parent compound EHMC (purity: 98%, racemate, CAS 5466-77-3) and the standard for the only available TP of those hypothesized to form from EHMC, namely *p*-methoxybenzaldehyde (4-MBA, purity: ≥99%, CAS 123-11-5), were purchased from Sigma Aldrich (Germany). ACN (HiPerSolv CHROMANORM®; LC-MS grade) and ammonium acetate (HiPerSolv CHROMANORM® for HPLC) were obtained from VWR International (Germany) and 2-propanol (ROTISOLV® HPLC) was obtained from Carl Roth (Karlsruhe, Germany). EHMC and 4-MBA stock solutions were prepared in ACN (1 g L^{-1}). All chemicals were analytical grade and were used without further purification. Ultrapure water was used for the preparation of all solutions for analytical measurement and photodegradation tests.

2.2. Simulated UV treatment (direct UV photolysis)

As EHMC is only barely soluble in water, the photolysis experiments were performed with 800 mL aqueous solution spiked with EHMC

dissolved in the solubilizer ACN (according to OECD 316) to increase the solubility of the EHMC. Methanol was not applied as solubilizer because pretests showed changes in absorption (maximum) and hydrolysis of EHMC in methanol–water-mixtures. The photo-degradation of acetonitrile in water was tested and the non-purgeable organic carbon (NPOC) was measured which was constant during 256 min irradiation. Therefore, we expect no reaction of acetonitrile with EHMC or the TPs. In order to examine the influence of the solubilizer content on the degradation kinetics, various concentrations of ACN (0.1, 0.2 and 0.5% (v/v)) were analyzed. In line with the literature (Broadbent et al., 1996; MacManus-Spencer et al., 2011; Rodil et al., 2009; Vione et al., 2015), a significantly higher concentration of EHMC was applied during photolysis compared to the concentration of EHMC in GW or surface water to facilitate the identification of TPs. Therefore, the initial nominal concentration of EHMC was adjusted either to (i) 1 mg L^{-1}, in order to investigate the kinetics and to determine the quantum yield, or to (ii) 5 mg L^{-1}, in order to identify the TPs. The role of ROS during the photolysis process was studied according to procedure (i), but with the EHMC dissolved in ultrapure water dosed with 0.1% (v/v) 2-propanol.

UV photolysis experiments of EHMC were performed in a 1 L batch photo-reactor. Magnetic stirring ensured continuous mixing of the solution. Constant temperature (20 ± 1 °C) was guaranteed using a cooling system (WKL230, LAUDA, Berlin, Germany). A polychromatic medium pressure (MP) Hg lamp (TQ150, 150 W, UV Consulting Peschl, Mainz, Germany) emitting light in the range of UVA, B and C (200–400 nm) surrounded by an ilmasil quartz immersion tube was used in the irradiation experiments. The emission spectrum of polychromatic light measured before performing the photolysis and the absorbance spectrum of EHMC is shown in Fig. S1, Supplementary material (SM).

The photolysis experiment was conducted for 256 min. Samples for each test concentration were collected before irradiation (0 min), and after 2, 4, 8, 16, 32, 64, 96, 128, 192 and 256 min of irradiation time. The samples were analyzed by HPLC-UV detection in order to follow the kinetics of transformation of the EHMC. The monitoring of the primary elimination and TP formation was performed by HPLC-UV and LC-ESI-MS^n (ion-trap), respectively. During photodegradation the influence of the solvent composition on pH development was monitored with a pH-electrode (Sen Tix 41, WTW, Weilheim, Germany), and peroxide test stripes screened hydrogen peroxide (H_2O_2) formation, an indicator for ROS (MQuant, Merck Chemicals GmbH, Schwalbach, Germany). On the test stripes peroxidase transfers peroxide oxygen to an organic redox indicator. This produces a blue oxidation product. The peroxide concentration is measured semi quantitatively by visual comparison of the reaction zone of the test strip with the fields of a color scale.

The methods for measuring and calculating the first-order degradation rate constant k, the half-life $t_{1/2}$, the molar extinction coefficient of EHMC by UV–VIS spectroscopy, the photon flux rate of the MP Hg lamp and the quantum yield are described in Text S1, SM. The relative photon flux of UV lamp was measured with a radiometer (Black Comet, Stellar.Net, Tampa, USA) and two chemical actinometers (metamitrone and terbuthylazine) were treated with the UV lamp to calculate the absolute photon flux (Text S1, SM). The quantum yield was determined for 0.2 and 0.5% ACN (v/v) content, but the spectra of the solutions with 0.1% ACN (v/v) only showed very low absorption since the concentration of EHMC was limited by the concentration of the stock solution.

2.3. Analytical methods

The main procedure developed here to analyze EHMC and its possible TPs, which were expected to be more polar compared to the parent compound. A Shimadzu Prominence-20 HPLC system (Duisburg, Germany) equipped with a UV-detector was used to determine the concentration of the parent compound. Chromatographic separation was performed on an RP 18plus column (EC 150/3 NUCLEOSHELL® 2.7 μm, Macherey-Nagel, Düren, Germany) using a binary gradient program consisting of 10 mM ammonium acetate in ultrapure water (eluent A) and ACN (eluent B). The gradient started at 20% B (from 0 up to 1 min), increased until 15 min to 97% B maintained for 2 min, then decreased until 25 min to the initial conditions, equilibrated for 2 min. The flow rate, column oven temperature and injection volume were set to 0.3 mL min^{-1}, 20 °C and 10 μL, respectively. The detector wavelengths were set to 285 and 305 nm in accordance to spectral analysis data for the substance (see Fig. S1, SM). The quantification and determination of the degradation kinetics and of the corresponding parameters were performed at 305 nm as this was more sensitive. EHMC eluted after 21.0 min. For quantitative analysis *via* external calibration, calibration standards of EHMC were made up at eight different concentration levels, ranging from 78.125 μg L^{-1} to 10 mg L^{-1}. The final concentrations were achieved by diluting the stock solution with ACN. The method showed good linearity for EHMC between 78.125 μg L^{-1} and 10 mg L^{-1} (correlation coefficient 0.999) and reproducibility RSD <2.0%. The limit of detection for EHMC was found <10 ng L^{-1} at 305 nm.

In order to test if the measured signals of the TP with mass to charge ratio (*m/z*) 137 (TP_{137}) coincide with the proposed structure, calibration standards of 4-MBA were prepared as outlined above and analyzed with HPLC-UV.

The identification and structural elucidation of the possible TPs were performed by an Agilent 1100 HPLC system (Agilent Technologies, Waldbronn, Germany) coupled to a Bruker Esquire 6000plus ion-trap mass spectrometer (IT-MS, Bruker Daltonics, Bremen, Germany) with ESI interface. The abovementioned LC parameters were adopted for the elution of EHMC and its TPs, but injection volume was increased (20 μL). The MS parameters were optimized for the hydrogen, ammonium and sodium adducts of EHMC (mass to charge ratio (m/z) 291, 308, 313) (Table S1, SM). The MS conditions of the m/z 291-optimized method were most sensitive so this method was used to investigate the photo-TPs. The mass spectrometer was operated in positive mode at −4300 V capillary voltage, 300 °C, 12 L·min^{-1} dry gas and 45 psi nebulizer pressure. Full scan analysis was performed from m/z 100–700. The photo-TPs generated during UV treatment were identified by comparing 0 min irradiated samples (the parent compound itself) to other photolyzed samples. The structures were elucidated by interpreting MS^n spectra.

2.4. In silico prediction of environmental fate and toxicity

For the *in silico* prediction of the chemical transformation of EHMC and the environmental fate and toxicity of EHMC and its TPs, a range of software packages were used to allow for the strengths and weaknesses of different algorithms and training sets. This software included the fragment-based CASE Ultra V.1.5.2.0 and the rule-based MetaPC V.1.8.1 (both MultiCASE Inc.) (Chakravarti et al., 2012; Saiakhov et al., 2013; Sedykh et al., 2001), the combined statistical and rule-based Oasis Catalogic software V.5.11.6 TB from the Laboratory of Mathematical Chemistry, University Bourgas, Bulgaria (Laboratory of Mathematical Chemistry, 2012) and the statistical QSAR Leadscope software V.3.2.6-1. The models of Leadscope use training sets from 2012 SAR Genotox Database. The photodegradation pathway of EHMC and the head-to-head (truxinates) and head-to-tail (truxillates) dimers were predicted by MetaPC for comparison to the experimental results in order to provide additional support for the chemical analysis by moving from unknown to more probable analysis, as no reference compounds were available.

The EHMC and the TPs were tested for ready biodegradability according to OECD 301C MITI-I test (Ministry of International Trade and Industry, Japan), using *in silico* models from Oasis Catalogic software (V.5.11.6 TB, Catabol and Catalogic, Laboratory of Mathematical Chemistry, University Bourgas, Bulgaria) and the CASE Ultra platform (model AU6, Chakravarti et al., 2012).

For EHMC and the photo-TPs, the mutagenicity, genotoxicity and ecotoxicity were predicted by the models listed in Table S2 (SM).

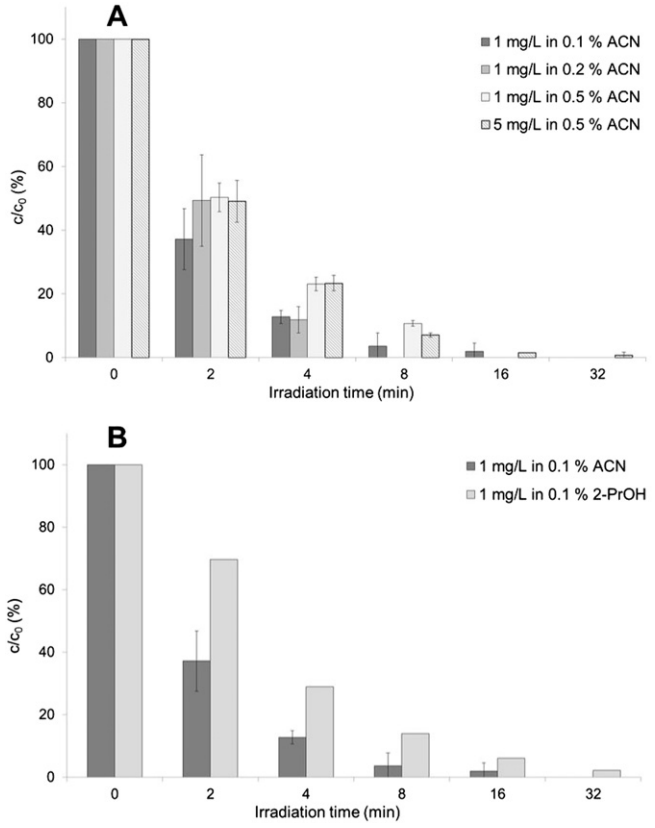

Fig. 1. The elimination of EHMC during photolysis with A: 1 mg L^{-1} and 5 mg L^{-1} initial (nominal) concentrations of EHMC in aqueous solution and varying ACN concentrations (0.1, 0.2, 0.5%) performed in duplicates and for B: 1 mg L^{-1} EHMC in aqueous solution with 0.1% (v/v) of ACN and 2-propanol.

CASE Ultra, Oasis Catalogic and Leadscope software provide positive, negative and out-of-domain (OD) estimations for the selected models. OD means that the test chemical is not within the applicability domain of the respective model. CASE Ultra software may evaluate models as 'Inconclusive', indicating that a significant structural part of the test chemical has unknown structural fragments.

3. Results and discussion

3.1. UV photolysis: primary elimination and mineralization

The primary elimination of EHMC for different experimental conditions is shown in Fig. 1. The lamp warmed up to maximum irradiation after 2 min. This explains the wide standard deviations of the samples at 2 min irradiation time. In all experiments, EHMC was completely removed (primary elimination) *via* UV treatment after 64 min at the latest. The degradations followed first-order kinetics for all experiments which agrees with data in the literature (Rodil et al., 2009). The analysis of the EHMC concentrations at the beginning of the photolysis revealed that the ACN concentration of 0.2% (v/v) led to the best recoveries while also having the lowest influence on the degradation kinetics. Table 1 lists the rate constants, half-lives and quantum yields for the different EHMC and ACN concentrations. The photodegradation constants for the 0.1 and 0.2% ACN (v/v) experiments showed no significant difference, whereas the application of 0.5% ACN (v/v) caused a slight reduction in the photolysis rate (Table 1, Fig. 1A). This dose-dependent effect of ACN may be due to the involvement of ROS such as hydroxyl radicals (·OH). The decreased reactivity of ·OH in the presence of dipolar, aprotic solvents was previously reported (Mitroka et al., 2010). To confirm the impact of indirect photolysis by ·OH, photolysis with the ·OH scavenger 2-propanol (Adam et al., 2000; Georgaki et al., 2014) was performed. The results showed a significantly reduced photolysis rate (Table 1). The formation of H_2O_2 during photolysis of the aqueous solutions can also indicate if the reaction mechanism is affected by ·OH. The maximum H_2O_2 concentrations (0.5–2 mg L^{-1}) occurred after 32 min irradiation. Finally, a comparison between the appearance trajectories of most TPs (*vide infra*) (Fig. 2A–E) and the concentration maximum of H_2O_2 after 32 min suggest that, after EHMC and the TPs degrade, the remaining free ·OH radicals react to form H_2O_2. The quantum yield of EHMC for 0.2 and 0.5% ACN (v/v) (Table 1) agreed with that reported in the literature (MacManus-Spencer et al., 2011). The quantum yield was slightly lower for the higher ACN content, which may be because of the differences in the degradation rate constant and/or the influence of the ACN content on the absorption spectra. The elimination rate for 5 mg L^{-1} EHMC in 0.5% ACN (v/v) was even lower than for 1 mg L^{-1} in 0.5% ACN (v/v) (Table 1, Fig. 1A), which indicates that the degradation was affected not only by scavenging of ·OH radicals, but also by the high initial concentration. MacManus-Spencer et al. (2011) also reported a reduction of EHMC's photodegradation rate constant with increasing initial concentration under simulated sunlight conditions. A possible explanation for this is the molecules close to the lamp shielding those behind from the irradiation. Additionally, the higher initial concentrations led to higher concentrations of TPs that compete for the absorption of light, depending on their individual absorption spectra (Ding et al., 2013; Herrmann et al., 2015). But the latter circumstances will have only a minor effect because EHMC is removed by >90% after 8 min (Fig. 1) while most of the TPs gain their maximum concentration between 8 and 32 min (Fig. 2).

The high lipophilic character in combination with the moderate recoveries of the initial EHMC concentration indicate that sorption on the wall of the reactor might be an issue. Vione et al. (2015) also reported problems with sorption of EHMC but achieved desorption by adding methanol, allowing a nearly quantitative recovery. The application of this procedure was not possible here given the batch reactor conditions. Otherwise, we assume that EHMC could float on the aqueous phase.

3.2. Time trend and structure elucidation of EHMC photo-TPs

The formation of photo-TPs was investigated for an initial, nominal concentration of 5 mg L^{-1} EHMC in 0.5% ACN (v/v). The appearance of new peaks during HPLC analysis of samples that were taken at different times revealed the generation of photo-TPs. The structural elucidation of the photoproducts was firstly done comparing new UV peaks with new *m/z* whose time trends were checked with extracted ion chromatograms (EIC, Fig. S2, SM). Masses that newly turned up during photolysis

Table 1
Overview of kinetic rate constants, half-lives and quantum yields of the photolysis of EHMC under various experimental conditions with MP Hg lamp.

c_{EHMC} [mg L^{-1}]	Solvent	Amount of solvent [%] (v/v)	k [min^{-1}]	$t_{1/2}$ [min]	Φ [mol $Einstein^{-1}$]
1	ACN	0.1	0.48 ± 0.21[a]	1.59 ± 0.70[a]	–
1	ACN	0.2	0.54 ± 0.09[a]	1.30 ± 0.21[a]	0.0042 ± 0.0007[a]
1	ACN	0.5	0.37 ± 0.02[a]	1.89 ± 0.12[a]	0.0023 ± 0.0001[a]
5	ACN	0.5	0.33 ± 0.01[a]	2.09 ± 0.05[a]	–
1	2-Propanol	0.1	0.26	2.71	–

[a] Error estimated from standard deviations of two separate experiments.

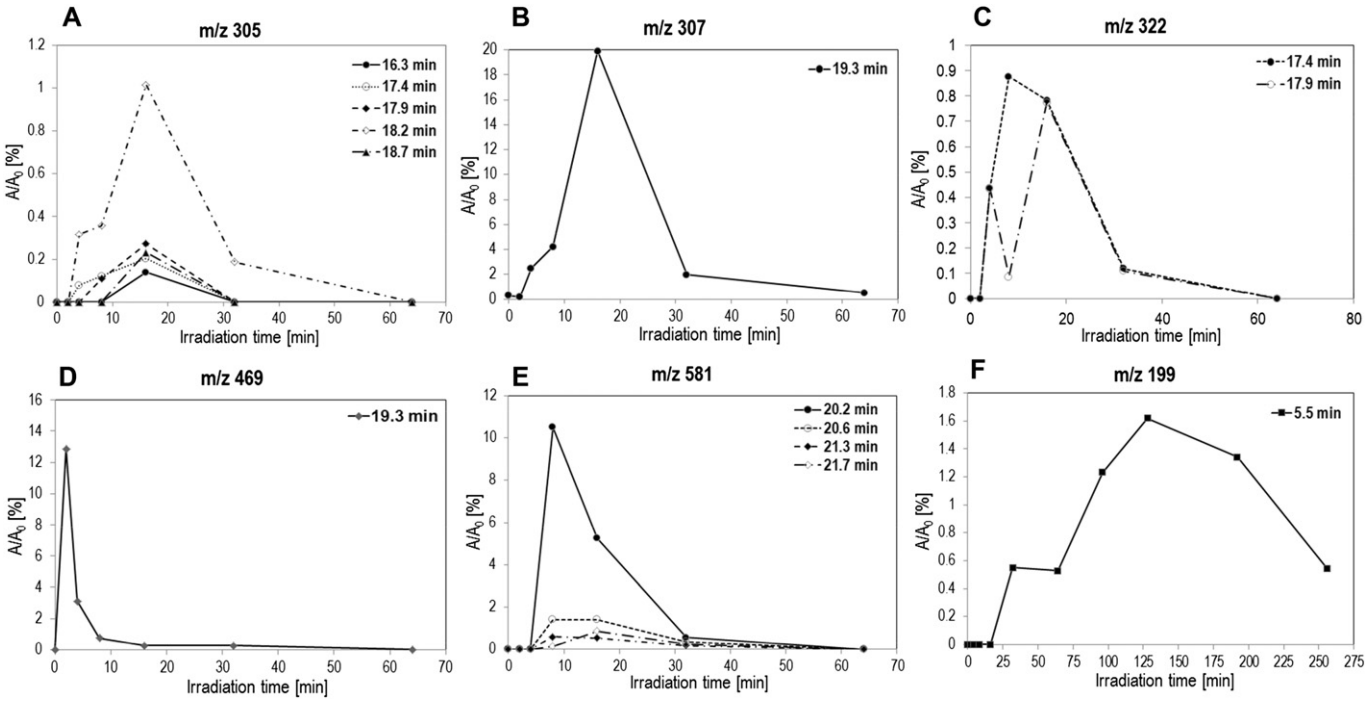

Fig. 2. Relative peak area A/A_0 [%] of TPs of EHMC photolysis with initial EHMC concentration of 5 mg L^{-1} (A_0 is the peak area of EHMC at 0 min; A is the peak area of the TP at a defined time point); trajectories identified by LC-MS. Curves are identified by retention time and *m/z*. Note that the scale varies.

were compared with those reported in literature or proposed by MetaPC software as well as m/z of TPs from literature and proposed by MetaPC software were checked for their appearance. Table 2 shows the TPs with corresponding retention times (RTs), product ions and the maximum observed relative peak areas A/A_0 of the photo-TPs during photolysis, the MS peak area A of the photo-TP being related to EHMC's MS peak area A_0 at time point 0 min. Only photo-TPs exceeding 0.5% of A/A_0 were structurally elucidated by LC-MS^n as MS signals below this value were insufficient. In total, 13 MS peaks at different RTs that could be related to six different m/z values were detected (the m/z values are used as labels in the sequel) (Table 2). Table S3 (SM) lists all potential TP structures, with possible structural isomers of the TPs (*i.e.* those possessing identical m/z values) receiving alphabetical indices. Fig. 3 summarizes the suggested TPs based on HPLC analysis, LC/MS-MS data and TP structures predicted by the MetaPC software. TP_{199} (3-ethenyl-6-methoxybenzene-1, 2, 4, 5-tetraol), the hydrolyzed cyclodimer TP_{469a}, the hydroxylated monomers TP_{307e} and TP_{307f} and the oxidized monomers TP_{305a}, TP_{305b}, TP_{305c}, TP_{305d}, TP_{305e}, TP_{305f}, and TP_{305g} were found in our study for the first time, while 4-MBA, the cyclodimer TP_{581b}, the hydrolyzed cyclodimer TP_{469b} and a hydrolyzed monomer were previously reported (Broadbent et al., 1996; MacManus-Spencer et al., 2011; Rodil et al., 2009; Vione et al., 2015).

For completeness, the more dilute photolysis experiments, as dilute as 1 mg L^{-1} initial concentration of EHMC, were also checked for TPs and TP_{469} and TP_{581} were also detected under this condition. The formation of TP_{581b} was also previously reported for several initial EHMC concentrations, the most dilute of which was 2.9 mg L^{-1} (MacManus-Spencer et al., 2011). Future experiments will be conducted with even lower initial concentrations of EHMC, which are closer to environmental conditions, in order to see if the dimer can still be detected.

The trajectories of the TPs' appearances reveal that almost all the TPs were formed and underwent further transformation between 2 min and 32 min (Fig. 2A–E). The single exception was TP_{199}, which was formed after 32 min and was still incompletely eliminated after 256 min irradiation (Fig. 2F). In contrast, other research, for both simulated sunlight and irradiation with UV-A and UV-B, found some of the same TPs as in

Table 2
EHMC and its photo-TPs chronologically by LC-MS retention times (RT), listing the highest observed A/A0 during photolysis with corresponding RT (A0 is the EHMC MS peak area at time point 0 min; A is the TP MS peak area). TPs are labelled by m/z value.

EHMC/TPs	LC-MS RT [min]	Highest observed A/A0 [%]	Main precursor ion [m/z]	Precursor ion species	Product ions [m/z], % of relative abundance in brackets
TP199	5.5	1.6	199.2	$[M + H]^+$	172.0 (100)
TP_{137}	12.3	0.5	137.1	$[M + H]^+$	–[a]
TP_{305}	16.3	0.1	305.2	$[M + H]^+$	–[a]
TP_{305}	17.4	0.9	322.2	$[M + NH4]^+$	305.0 (100), 127.1 (74.5)
TP_{305}	17.9	0.8	322.2	$[M + NH4]^+$	305.0 (100), 127.1 (68.2)
TP_{305}	18.2	1.0	305.2	$[M + H]^+$	161.0 (100), 179.0 (15.1)
TP_{305}	18.7	0.2	305.2	$[M + H]^+$	–[a]
TP_{307}	19.3	19.9	307.2	$[M + H]^+$	194.9 (100), 135.1 (48.1)
TP_{469}	19.6	12.9	469.2	$[M + H]^+$	161.0 (100), 451.2 (82.5)
TP_{581}	20.2	10.5	581.2	$[M + H]^+$	451.1 (100), 241.0 (14.8)
TP_{581}	20.6	1.4	581.2	$[M + H]^+$	451.1 (100), 241.0 (23.7), 469.0 (14.6)
EHMC	21.2	100.0	291.2	$[M + H]^+$	178.9 (100), 161.1 (35.7)
TP_{581}	21.3	0.6	581.2	$[M + H]^+$	451.1 (100), 469.0 (29.1), 241.0 (29.0), 291.0 (11.8)
TP_{581}	21.7	0.9	581.2	$[M + H]^+$	451.1 (100), 241.0 (32.2), 469.0 (30.8)

[a] No MS/MS product ions detected.

the present work, *e.g.* 4-MBA, the hydroxylated monomer and cyclodimers, but these were not eliminated after 128 min and 240 min photolysis, respectively (MacManus-Spencer et al., 2011; Vione et al., 2015). Otherwise, the EHMC dimer with the loss of one ethylhexyl group was not photostable under UV-B light (Vione et al., 2015). The differences between the previous and present results and may result from different overlaps between the TPs' absorption spectra and emission spectrum of the MP Hg lamp used here and of other irradiation sources.

The LC conditions and RTs of most of the TPs indicated that they were more polar than the EHMC. Only two TP_{581} MS peaks had higher RTs than EHMC and so appear to be more nonpolar substances (Table 2). These findings are consistent with previous work (MacManus-Spencer et al., 2011). As TPs with higher polarity have higher mobility in aquatic environments (Knepper et al., 2003), such TPs, which are possibly generated during GW treatment, will be more mobile than the parent compound (Boxall, 2009).

The product ion of TP_{199} (Table 2) showed a loss of 27 Da. This indicates the presence of a $HC{=}CH_2$ moiety. For that reason, the formation of 3-ethenyl-6-methoxybenzene-1, 2, 4, 5-tetraol was designated TP_{199} (Fig. 3) as it seems to involve cleavage directly next to the double bond and a fourfold hydroxylation of the benzyl ring. This is supported by the findings of Rastogi et al. (2014b), which reported that TPs were generated by a multiple hydroxylation of an aromatic ring during photodegradation with an MP Hg lamp.

TP_{137} had a significantly more intense UV signal than any other TP, but its MS peak with *m/z* 137 was too small to permit LC-MS^n analysis (Fig. S3, SM). This may be the result of poor ionization, as the MS method was optimized for EHMC. M/z 137 is not shown in Fig. 2 because it was detected only once in the sample after 16 min. Two structures (TP_{137a} and TP_{137b}) were predicted by MetaPC software as degradation products with m/z 137 when EHMC's aryl moiety is attacked by hydroxyl radicals. In contrast, TP_{137c} (4-MBA, Fig. 3) was previously reported as a photodegradation product of EHMC under artificial sunlight (MacManus-Spencer et al., 2011). The analysis of commercially available 4-MBA *via* HPLC-UV and LC-MS verified the proposed structure of TP_{137c} by the match between the detected RTs of TP_{137} and 4-MBA. Further confirmation of 4-MBA was impossible because the analysis of the precursor ion *m/z* 137 by LC-MS^n showed only the mass peak but no fragments (Table 2).

The formation of TP_{307} is proposed to occur through attack of EHMC by ·OH radicals. For TP_{307e} and/or TP_{307f} (Fig. 3) the detection of the product ion m/z 194.9, which signifies a loss of the ethylhexyl group that was not hydroxylated, excludes the attack of ·OH on that part of the molecule. The second product ion m/z 135.1 indicates the loss of CO_2 so that a hydroxylated aromatic ring remains. It was not possible to determine if the MS peak arises from TP_{307e}, TP_{307f} or both co-eluting. Contrary to Vione et al. (2015), hydroxylation of the aromatic ring and the ethylhexyl moiety is assumed, based on the results of MetaPC software.

The presumed structure of TP_{305} is the oxidized EHMC molecule, as predicted by the MetaPC software. LC-MS^n confirmed that the oxygen atom is located at the ethylhexyl moiety through the detection of the product ions m/z 161.0 and m/z 179.0, which reveal the loss of a $C_8H_{14}O$ group (Table S4, SM). However, the product ions did not allow differentiation between the structural isomers TP_{305a}, TP_{305b}, TP_{305c}, TP_{305d}, TP_{305e}, TP_{305f}, and TP_{305g} (Fig. 3). In addition, ammonium adducts of TP_{305} with m/z 322 were detected. Their respective product ions confirmed the ammonia loss (m/z 305.0) and indicated an oxidized ethylhexyl moiety (m/z 127.1, Table S4, SM). Information on the fragmentation pattern of LC-MS data of $[M + NH_4]^+$ was available, but differentiating the seven structural isomers was impossible.

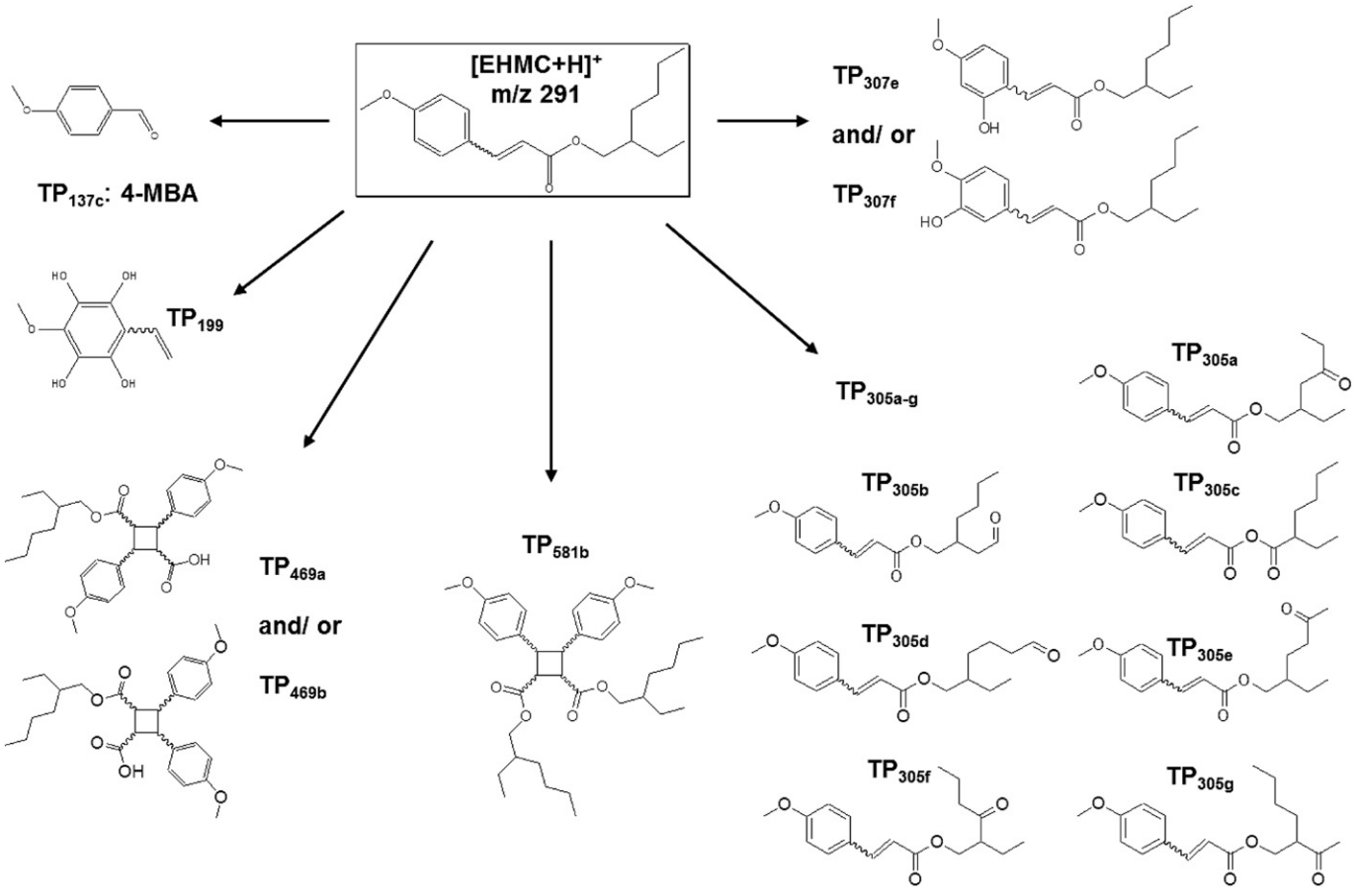

Fig. 3. Proposed photo-TPs of EHMC.

The peaks of TP_{581} appear to be dimers of EHMC formed by the dimerization of *E*- and *Z*-EHMC-monomers. The generation of 13 isomers of the dimer, eight truxinates and five truxillates, have been described in the literature as possible TPs formed under artificial sunlight, in dichloromethane (Broadbent et al., 1996) and in aqueous solution (MacManus-Spencer et al., 2011). For TP_{581}, LC-MS^n detected the product ion m/z 241.0 at the four RTs (Table 2), so it was assumed to be 4,4′-dimethoxystilbene (Table S4, SM). This supposition supports findings in the literature that formation of head-to-head-isomers (truxinates) was preferred (Broadbent et al., 1996; MacManus-Spencer et al., 2011; Rodil et al., 2009; Vione et al., 2015). The preference for truxinates during stereo selective photoreaction of cinnamic derivates in solutions was already reported as a consequence of steric factors and highest-occupied molecular orbital (HOMO)–lowest-occupied molecular orbital (LUMO) interactions (Egerton et al., 1981; Lewis et al., 1988), thus being a typical [2 + 2] photo-cyclo-addition reaction.

TP_{469} is 112 Da less than the dimers, which may be due to the hydrolysis of one ester moiety. The fragmentation by MS^n first led to the product ion m/z 451 which corresponds to the loss of water (18 Da) with simultaneous ring opening. Second, the main product ion m/z 161 corresponded to the loss of $C_{18}H_{26}O_3$ (290 Da). The respective degradations of TP_{581a} and TP_{581b} were predicted using MetaPC, which showed the hydrolyzed dimers TP_{469a} and TP_{469b} as outcomes, confirming the suggested structure. MacManus-Spencer et al. (2011) hypothesizes that for the photolysis of EHMC with simulated sunlight, TP_{469b} was formed by the hydrolysis of one dimer, in addition to cyclodimers, leading to the assumption that only TP_{469b} is formed. This study showed another outcome. The MP Hg lamp reached its irradiation maximum at 2 min. The time trajectories of TP_{469} and TP_{581} reached maximum A/A_0 at 2 min (Fig. 2D) and between 8 and 16 min (Fig. 2E) irradiation, respectively. Considering the previous findings and that the hydrolysis product of EHMC may already exist in the 0 min sample, the formation of the hydrolyzed cyclodimer is hypothesized to occur by the reaction between the monomer EHMC and its hydrolyzed monomer. Compared to the head-to-head cyclodimer TP_{581b}, which was confirmed by the LC-MS^n analysis, the fragments of TP_{469} did not allow TP_{469a} and TP_{469b} to be distinguished (Table S4, SM).

3.3. In silico prediction of EHMC and photo-TP biodegradability

Table S5 (SM) summarizes the *in silico* predictions for the ready biodegradability prediction of EHMC and its photo-TPs (Fig. 3). The CASE Ultra model AU6 predicted that EHMC and most of its TPs should be readily biodegradable. The single exception is TP_{199}, which was predicted to be not readily biodegradable and, thus, could persist as a dead-end product in the environment after photolysis. However, EHMC has been frequently detected in the aquatic environment (Balmer et al., 2005; Cuderman and Heath, 2007; Díaz-Cruz et al., 2012; Poiger et al., 2004; Rodil and Moeder, 2008). On the one hand, this could be due to continuous input into the environment, so that EHMC is a pseudo-persistent pollutant (Gago-Ferrero et al., 2013). On the other hand, it is possible that the prediction is not correct.

The Oasis software was used to provide additional confirming models. It should be noted that the applicability domains of the Catabol and Catalogic 301C models consist of a “global parameter range” determined by $\log K_{OW}$ and the molecular weight, and a “structural domain”, based on atom-centered fragments (ACFs). The global parameter requirements were in domain for all substances. In contrast, all structures were out of the structural domain, except of TP_{137c}, which belongs to the training set. Thus, the Oasis predictions might be unreliable and the Oasis models should be improved.

3.4. In silico prediction of EHMC and photo-TP toxicity

The aim of the *in silico* prediction of EHMC and its photo-TPs was to assess if the toxicity might be altered after photolysis for selected endpoints. The identification of novel toxicological activities in the molecule after photolysis allows evaluation of possible carcinogenicity or genotoxicity. Therefore, screening QSAR results for differences between the parent compound and its TPs is the main analytical process.

The detailed list of QSAR mutagenicity and toxicity predictions is summarized in Tables S6 and S7 (SM), respectively. CASE Ultra predicted the bacterial mutagenicity by rule-based (GT Expert) and statistical models (GT1 A7B, GT1 AT E coli, Pharm-E_coli and Pharm_Salm). This generates more reliable results than just one methodology. Using both types of method also complies with the ICH M7 guideline for assessment of the bacterial mutagenicity assessment of impurities of pharmaceuticals (Stavitskaya et al., 2015). The bacterial mutagenicity of EHMC was predicted to be known negative or negative by most models (Table S6, SM). Therefore, EHMC can most likely be classified as a non-mutagenic substance, which agrees with the literature on the toxicity of EHMC against *Salmonella typhimurium* (Zeiger et al., 1985). Furthermore, the TPs were also predicted to be not mutagenic by most Case Ultra, Oasis Catalogic and Leadscope models (Table S6, SM). However, the mutagenicity model V04 from Oasis Catalogic predicted positive alerts for EHMC, and its hydroxylated and oxidized products. In six cases, the structures were in domain. The varying prediction of the different software is likely due to the divergent training sets and databases.

Table 3 shows the results for carcinogenicity, genotoxicity and mutagenicity of EHMC and the TPs for selected endpoints. Since estimations for various TPs that showed positive alerts were inconclusive, the alert IDs for inconclusive estimations were detailed, as summarized in Table S8 (SM).

First of all, the human carcinogenesis CASE Ultra predicted EHMC as non-carcinogenic (Table 3, A). However, TP_{199}, TP_{305f} and TP_{305g} were inconclusive. They showed positive alerts with probabilities in the model's grey zone (40–60%). In addition, genotoxicity was predicted by the micronucleus *in vivo* model, whereas CASE Ultra showed no positive alerts at all, and Leadscope predicted EHMC to be non-genotoxic but indicated micronucleus toxicity for TP_{199} (Table 3, B). To differentiate between the varying predictions and to determine if the highlighted TPs might be carcinogenic or genotoxic, further testing is required, e.g. by performing *in vivo* micronucleus experiments with EHMC, a commercial standard of TP_{199}, and photolytic mixtures.

The prediction of the genotoxicity by chromosome aberration is inconclusive for EHMC (Table 3, C and D). The comparison of the alerts which are responsible for the positive and inconclusive predictions of

Table 3
In silico toxicity predictions by different CASE Ultra and Leadscope models for EHMC and the photo-TPs presented in Fig. 3.

$TP_{m/z}$	QSAR models						
	CASE Ultra				Leadscope		
	A	B	C	D	B	C	D
EHMC	−	−	IN	IN	−	+	+
TP_{137c}	−	−	+	−	−	+	+
TP_{199}	IN	−	−	−	+	+	+
TP_{305a}	−	−	+	IN	−	+	+
TP_{305b}	−	−	IN	IN	−	+	+
TP_{305c}	−	−	IN	IN	−	+	+
TP_{305d}	−	−	IN	IN	−	+	+
TP_{305e}	−	−	IN	+	−	+	+
TP_{305f}	IN	−	IN	IN	−	+	+
TP_{305g}	IN	−	IN	+	−	+	+
TP_{307e}	−	−	IN	IN	−	+	+
TP_{307f}	−	−	IN	IN	−	+	+
TP_{469a}	OD	OD	OD	OD	−	OD	OD
TP_{469b}	OD	OD	OD	OD	−	−	−
TP_{581b}	−	−	−	−	−	−	−

A – human carcinogenicity; B – micronucleus *in vivo* composite; C – chromosome aberration; D – chromosome aberration *in vitro* CHO; OD – out of domain: the test chemical is not in the applicability domain of the model; IN – inconclusive: the molecule contained too many unknown fragments; + – a positive prediction for corresponding activity; − - a negative prediction for corresponding activity.

EHMC and the TPs indicates alternative positive alerts for TP_{137c} and an additional alert for the prediction of genotoxicity of TP_{305a} (model A7U, Table S8, SM). In case of the positive predictions of the genotoxicity in Chinese Hamster Ovary (CHO) cells for TP_{305e} and TP_{305g} (CASE Ultra, D), additional alerts to the inconclusive positive alert for EHMC are predicted (model A7V, Table S8, SM). These data provide indications that the activities of various TPs on genotoxic endpoints might be altered compared to EHMC, since different alerts can lead to different activities on a given endpoint.

In general, there were indications that the TPs formed by photolysis of EHMC can be toxic *e.g.* genotoxicity (A7V, A7U and A64; Table S7, SM). Overall, the abovementioned toxicity endpoints of TPs TP_{137c}, TP_{199}, TP_{305a}, TP_{305e}, TP_{305f} and TP_{305g} need more attention. Therefore, confirming the predicted toxicity and the possibility of altered genotoxicity of the proposed TPs is recommended as soon as adequate amounts of the substances are available for experimental verification. The *in silico* results presented here can give guidance on which compounds to start with.

4. Conclusions

This study sought better understanding of the fate of EHMC in aqueous solution and mechanisms involved in its photo-transformation, with a view to assessing UV irradiation for GW post-treatment. This paper extended the knowledge of the effects of concentration of co-solvent ACN, initial concentration of EHMC, and presence of an ·OH radical scavenger on the degradation of EHMC under polychromatic UV light. The data of all performed tests indicate that EHMC was not fully mineralized as non-persistent photo-TPs formed and subsequently degraded.

Although photo-TPs were formed by UV treatment, it is important to note that they were identified under experimental conditions with high initial concentrations of EHMC, to allow more reliable structural elucidation, in the presence of ACN (<1%) as solubilizer. These experimental parameters may not replicate real-world conditions; nonetheless, the quantity of these substances must be investigated. The results serve as basis for an initial *in silico*-based evaluation of the TPs and complement investigations already performed under solar and monochromatic UV light conditions. Due to varying *in silico* results for TPs that are structural isomers this paper also raises the need for additional research to differentiate the possible isomers. The *in silico* tools proved helpful in identifying which TPs need further attention. Furthermore, the application of more than one model made the predictions more reliable.

The results of this assessment will be utilised in further studies of the applicability of UV treatment, *e.g.* to confirm the risk of the TPs to the environment or human health, and with artificial and, ultimately, real GW.

Acknowledgments

These results are derived from a collaborative project in Lower Saxony and Israel with financial support from the State of Lower Saxony (Ministry of Science and Culture) to research “Personal care products (PCPs) as source for micropollutants in Greywater – Identification, quantification and on-site treatment”, Project No. VWZN 2830. The authors also wish to acknowledge Multicase Inc. and Leadscope Inc. for generously providing the CASE Ultra, MetaPC and Leadscope QSAR software.

Appendix A. Supplementary data

Supplementary data to this article can be found online at http://dx.doi.org/10.1016/j.scitotenv.2016.08.017.

References

Adam, W., Hartung, J., Okamoto, H., Saha-Möller, C.R., Špehar, K., 2000. *N*-Hydroxy-4-(4-chlorophenyl)thiazole-2(3*H*)-thione as a photochemical hydroxyl-radical source: photochemistry and oxidative damage of DNA (strand breaks) and 2′-deoxyguanosine (8-oxodG formation). Photochem. Photobiol. 72 (5), 619–624. http://dx.doi.org/10.1562/0031-8655(2000)0720619NHCTHT2.0.CO2.

Bachelot, M., Li, Z., Munaron, D., Le Gall, P., Casellas, C., Fenet, H., Gomez, E., 2012. Organic UV filter concentrations in marine mussels from French coastal regions. Sci. Total Environ. 420, 273–279. http://dx.doi.org/10.1016/j.scitotenv.2011.12.051.

Balmer, M.E., Buser, H.-R., Müller, M.D., Poiger, T., 2005. Occurrence of some organic UV filters in wastewater, in surface waters, and in fish from Swiss lakes. Environ. Sci. Technol. 39 (4), 953–962. http://dx.doi.org/10.1021/es040055r.

Blüthgen, N., Meili, N., Chew, G., Odermatt, A., Fent, K., 2014. Accumulation and effects of the UV-filter octocrylene in adult and embryonic zebrafish (*Danio rerio*). Sci. Total Environ. 476–477, 207. http://dx.doi.org/10.1016/j.scitotenv.2014.01.015.

Boxall, A., 2009. Transformation products of synthetic chemicals in the environment. The Handbook of Environmental Chemistry vol. 2, Part P. Springer, Berlin Heidelberg, p. 194.

Broadbent, J.K., Martincigh, B.S., Raynor, M.W., Salter, L.F., Moulder, R., Sjöberg, P., et al., 1996. Capillary supercritical fluid chromatography combined with atmospheric pressure chemical ionisation mass spectrometry for the investigation of photoproduct formation in the sunscreen absorber 2-ethylhexyl-p-methoxycinnamate. J. Chromatogr. A 732 (1), 101–110. http://dx.doi.org/10.1016/0021-9673(95)01199-4.

Buchberger, W.W., 2011. Current approaches to trace analysis of pharmaceuticals and personal care products in the environment. J. Chromatogr. A 1218, 603–608. http://dx.doi.org/10.1016/j.chroma.2010.10.040.

Chakravarti, S.K., Saiakhov, R.D., Klopman, G., 2012. Optimizing predictive performance of CASE ultra expert system models using the applicability domains of individual toxicity alerts. J. Chem. Inf. Model. 52 (10), 2609–2618. http://dx.doi.org/10.1021/ci300111r.

Cuderman, P., Heath, E., 2007. Determination of UV filters and antimicrobial agents in environmental water samples. Anal. Bioanal. Chem. 387 (4), 1343–1350. http://dx.doi.org/10.1007/s00216-006-0927-y.

Díaz-Cruz, M.S., Gago-Ferrero, P., Llorca, M., Barceló, D., 2012. Analysis of UV filters in tap water and other clean waters in Spain. Anal. Bioanal. Chem. 402, 2325–2333. http://dx.doi.org/10.1007/s00216-011-5560-8.

Ding, S.-L., Wang, X.-K., Jiang, W.-Q., Meng, X., Zhao, R.-S., Wang, C., et al., 2013. Photodegradation of the antimicrobial triclocarban in aqueous systems under ultraviolet radiation. Environ. Sci. Pollut. Res. Int. 20 (5), 3195–3201. http://dx.doi.org/10.1007/s11356-012-1239-8.

Egerton, P.L., Hyde, E.M., Trigg, J., Payne, A., Beynon, P., Mijovic, M.V., et al., 1981. Photocycloaddition in liquide ethyl cinnamate and in ethyl cinnamate glasses. The photoreaction as a probe into the micromorphology of the solid. J. Am. Chem. Soc. (103), 3859–3863 http://dx.doi.org/10.1021/ja00403a039.

Eriksson, E., Auffarth, K., Henze, M., Ledin, A., 2002. Characteristics of grey wastewater. Urban Water 4, 85–104. http://dx.doi.org/10.1016/S1462-0758(01)00064-4.

Eriksson, E., Auffarth, K., Eilersen, A.-M., Henze, M., Ledin, A., 2003. Household chemicals and personal care products as sources for xenobiotic organic compounds in grey wastewater. Water SA 29 (2), 135–136.

Eriksson, E., Donner, E., Ledin, A., 2010. Presence of selected priority and personal care substances in an onsite bathroom greywater treatment facility. Water Sci. Technol. 62 (12), 2889–2898. http://dx.doi.org/10.2166/wst.2010.988.

Fatta-Kassinos, D., Dionysiou, D.D., Kümmerer, K., 2016. The Handbook of Environmental Chemistry 45: Advanced Treatment Technologies for Urban Wastewater Reuse. first ed. Springer, Cham.

Friedler, E., 2004. Quality of individual domestic greywater streams and its implication for on-site treatment and reuse possibilities. Environ. Technol. 25, 997–998. http://dx.doi.org/10.1080/09593330.2004.9619393.

Gago-Ferrero, P., Díaz-Cruz, M.S., Barceló, D., 2013. Multi-residue method for trace level determination of UV filters in fish based on pressurized liquid extraction and liquid chromatography–quadrupole-linear ion trap-mass spectrometry. J. Chromatogr. A 1286, 93–101. http://dx.doi.org/10.1016/j.chroma.2013.02.056.

Georgaki, I., Vasilaki, E., Katsarakis, N., 2014. A study on the degradation of carbamazepine and ibuprofen by TiO_2 & ZnO photocatalysis upon UV/visible-light irradiation. Am. J. Anal. Chem. 5, 518–534. http://dx.doi.org/10.4236/ajac.2014. 58060.

Ghaitidak, D.M., Yadav, K.D., 2013. Characteristics and treatment of greywater - a review. Environ. Sci. Pollut. Res. 20 (5), 2795–2799. http://dx.doi.org/10.1007/s11356-013-1533-0.

Gutowski, L., Olsson, O., Leder, C., Kümmerer, K., 2015. A comparative assessment of the transformation products of S-metolachlor and its commercial product Mercantor Gold® and their fate in the aquatic environment by employing a combination of experimental and *in silico* methods. Sci. Total Environ. 506–507, 369. http://dx.doi.org/10.1016/j.scitotenv.2014.11.025.

Hany, J., Nagel, R., 1995. Nachweis von UV-Filtersubstanzen in Muttermilch. Dtsch. Lebensmitt. Rundsch. 91, 341–345.

Hernández-Leal, L., Vieno, N., Temmink, H., Zeeman, G., Buisman, C.J.N., 2010. Occurrence of xenobiotics in gray water and removal in three biological treatment systems. Environ. Sci. Technol. 44 (17), 6835–6842. http://dx.doi.org/10.1021/es101509e.

Hernández-Leal, L., Zeeman, G., Temmink, H., Buisman, C.J.N., 2011. Grey water treatment concept integrating water and carbon recovery and removal of micropollutants. Water Pract. Technol. 6 (2). http://dx.doi.org/10.2166/wpt.2011.035.

Herrmann, M., Menz, J., Olsson, O., Kümmerer, K., 2015. Identification of phototransformation products of the antiepileptic drug gabapentin: biodegradability and initial assessment of toxicity. Water Res. 85 (11451), 11. http://dx.doi.org/10.1016/j.watres. 2015.08.004.

Knepper, T.P., de Voogt, P., Barceló, D., 2003. Analysis and fate of surfactants in the aquatic environment. Comprehensive Analytical Chemistry vol. XL. Elsevier Science, Amsterdam, p. 808.

Kunz, P.Y., Fent, K., 2006. Multiple hormonal activities of UV filters and comparison of in vivo and in vitro estrogenic activity of ethyl-4-aminobenzoate in fish. Aquat. Toxicol. 79, 305–324. http://dx.doi.org/10.1016/j.aquatox.2006.06.016.

La Farré, M., Pérez, S., Kantiani, L., Barceló, D., 2008. Fate and toxicity of emerging pollutants, their metabolites and transformation products in the aquatic environment. Trends Anal. Chem. 27 (11), 991–997. http://dx.doi.org/10.1016/j.trac.2008.09.010.

Laboratory of Mathematical Chemistry B, 2012. OASIS catalogic software V. 5.11.6 TB. http://oasis-lmc.org.

Lewis, F.D., Quillen, S.L., Hale, P.D., Oxman, J.D., 1988. Lewis acid catalysis of photochemical reactions. 7. Photodimerization and cross-cycloaddition of cinnamic esters. J. Am. Chem. Soc. 110, 1261–1267. http://dx.doi.org/10.1021/ja00212a039.

MacManus-Spencer, L.A., Tse, M.L., Klein, J.L., Kracunas, A.E., 2011. Aqueous photolysis of the organic ultraviolet filter chemical octyl methoxycinnamate. Environ. Sci. Technol. 45, 3931–3937. http://dx.doi.org/10.1021/es103682a.

Mahmoud, W.M.M., Toolaram, A.P., Menz, J., Leder, C., Schneider, M., Kümmerer, K., 2014. Identification of phototransformation products of thalidomide and mixture toxicity assessment: an experimental and quantitative structural activity relationships (QSAR) approach. Water Res. 49, 11–12. http://dx.doi.org/10.1016/j.watres.2013.11.014.

Maimon, A., Friedler, E., Gross, A., 2014. Parameters affecting greywater quality and its safety for reuse. Sci. Total Environ. 487 (1), 20–25. http://dx.doi.org/10.1016/j.scitotenv. 2014.03.133.

Martínez-Hernández, V., Meffe, R., Herrera, S., Arranz, E., de Bustamante, I., 2014. Sorption/desorption of non-hydrophobic and ionisable pharmaceutical and personal care products from reclaimed water onto/from a natural sediment. Sci. Total Environ. 472, 273–281. http://dx.doi.org/10.1016/j.scitotenv.2013.11.036.

Michael, I., Vasquez, M.I., Hapeshi, E., Haddad, T., Baginska, E., Kümmerer, K., et al., 2014. Metabolites and transformation products of pharmaceuticals in the aquatic environment as contaminants of emerging concern. In: Lambropoulou, D.A., Nollet, L.M.L. (Eds.), Transformation Products of Emerging Contaminants in the Environment: Analysis, Processes, Occurrence, Effects and Risks. John Wiley and Sons Ltd., Chichester, United Kingdom, pp. 413–458 http://dx.doi.org/10.1002/9781118339558.ch14.

Mitroka, S., Zimmeck, S., Troya, D., Tanko, J.M., 2010. How solvent modulates hydroxyl radical reactivity in hydrogen atom abstractions. J. Am. Chem. Soc. 132, 2907–2913. http://dx.doi.org/10.1021/ja903856t.

Oron, G., Adel, M., Agmon, V., Friedler, E., Halperin, R., Leshem, E., et al., 2014. Greywater use in Israel and worldwide: standards and prospects. Water Res. 58, 92–101. http://dx.doi.org/10.1016/j.watres.2014.03.032.

Poiger, T., Buser, H.-R., Balmer, M.E., Bergqvist, P.-A., Müller, M.D., 2004. Occurrence of UV filter compounds from sunscreens in surface waters: regional mass balance in two Swiss lakes. Chemosphere 55 (7), 951–953. http://dx.doi.org/10.1016/j.chemosphere.2004.01.012.

Rastogi, T., Leder, C., Kümmerer, K., 2014a. Qualitative environmental risk assessment of photolytic transformation products of iodinated X-ray contrast agent diatrizoic acid. Sci. Total Environ. 482–483 (1), 378. http://dx.doi.org/10.1016/j.scitotenv.2014.02.139.

Rastogi, T., Leder, C., Kümmerer, K., 2014b. Designing green derivatives of β-blocker metoprolol: a tiered approach for green and sustainable pharmacy and chemistry. Chemosphere 111, 493–499. http://dx.doi.org/10.1016/j.chemosphere.2014.03.119.

Rodil, R., Moeder, M., 2008. Development of a method for the determination of UV filters in water samples using stir bar sorptive extraction and thermal desorption–gas chromatography–mass spectrometry. J. Chromatogr. A 1179 (2), 81–88. http://dx.doi.org/10.1016/j.chroma.2007.11.090.

Rodil, R., Möder, M., Altenburger, R., Schmitt-Jansen, M., 2009. Photostability and phytotoxicity of selected sunscreen agents and their degradation mixtures in water. Anal. Bioanal. Chem. 395 (5), 1513–1524. http://dx.doi.org/10.1007/s00216-009-3113-1.

Saiakhov, R., Chakravarti, S., Klopman, G., 2013. Effectiveness of CASE ultra expert system in evaluating adverse effects of drugs. Mol. Inform. 32, 87. http://dx.doi.org/10.1002/minf. 201200081.

Santiago-Morales, J., Gómez, M.J., Herrera-López, S., Fernández-Alba, A.R., García-Calvo, E., Rosal, R., 2013. Energy efficiency for the removal of non-polar pollutants during ultraviolet irradiation, visible light photocatalysis and ozonation of a wastewater effluent. Water Res. 47, 5546. http://dx.doi.org/10.1016/j.watres.2013.06.030.

Schlumpf, M., Schmid, P., Durrer, S., Conscience, M., Maerkel, K., Henseler, M., et al., 2004. Endocrine activity and developmental toxicity of cosmetic UV filters—an update. Toxicology 205, 113–122. http://dx.doi.org/10.1016/j.tox.2004.06.043.

Schreurs, R.H.M.M., Sonneveld, E., Jansen, J.H.J., Seinen, W., Van der Burg, B., 2005. Interaction of polycyclic musks and UV filters with the estrogen receptor (ER), androgen receptor (AR), and progesterone receptor (PR) in reporter gene bioassays. Toxicol. Sci. 83, 264–272. http://dx.doi.org/10.1093/toxsci/kfi035.

Sedykh, A., Saiakhov, R., Klopman, G., 2001. META V. A model of photodegradation for the prediction of photoproducts of chemicals under natural-like conditions. Chemosphere 45, 971.

Serpone, N., Salinaro, A., Emeline, A.V., Horikoshi, S., Hidaka, H., Zhao, J., 2002. An *in vitro* systematic spectroscopic examination of the photostabilities of a random set of commercial sunscreen lotions and their chemical UVB/UVA active agents. Photochem. Photobiol. Sci. 1, 970–981. http://dx.doi.org/10.1039/b206338g.

Stavitskaya, L., Aubrecht, J., Kruhlak, N.L., 2015. Chemical structure-based and toxicogenomic models 20–22. In: Graziano, M.J., Jacobson-Kram, D. (Eds.), Genotoxicity and Carcinogenicity Testing of Pharmazeuticals, first ed. Springer.

Tsui, M.M.P., Leung, H.W., Lam, P.K.S., Murphy, M.B., 2014a. Seasonal occurrence, removal efficiencies and preliminary risk assessment of multiple classes of organic UV filters in wastewater treatment plants. Water Res. 53, 58–67. http://dx.doi.org/10.1016/j.watres.2014.01.014.

Tsui, M.M.P., Leung, H.W., Wai, T.-C., Yamashita, N., Taniyasu, S., Liu, W., et al., 2014b. Occurrence, distribution and ecological risk assessment of multiple classes of UV filters in surface waters from different countries. Water Res. 67, 55. http://dx.doi.org/10.1016/j.watres.2014.09.013.

Vione, D., Calza, P., Galli, F., Fabbri, D., Santoro, V., Medana, C., 2015. The role of direct photolysis and indirect photochemistry in the environmental fate of ethylhexyl methoxy cinnamate (EHMC) in surface waters. Sci. Total Environ. 537, 58. http://dx.doi.org/10.1016/j.scitotenv.2015.08.002.

Zeiger, E., Haworth, S., Mortelmans, K., Speck, W., 1985. Mutagenicity testing of di(2-ethylhexy1)phthalate and related chemicals in *Salmonella*. Environ. Mutagen. 7, 213–232. http://dx.doi.org/10.1002/em.2860070209.

Supplementary materials

Photodegradation of the UV filter ethylhexyl methoxycinnamate under ultraviolet light: identification and *in silico* assessment of photo-transformation products in the context of grey water reuse

F. Jentzsch, O. Olsson, J. Westphal, M. Reich, C. Leder, K. Kümmerer*

Sustainable Chemistry and Material Resources, Institute of Sustainable and Environmental Chemistry, Faculty of Sustainablilty, Leuphana University of Lüneburg, Scharnhorststraße 1/C13, DE-21335 Lüneburg, Germany

Tel.: +49 4131 677-2899

* Corresponding author address: Chair of Sustainable Chemistry and Material Resources, Institute of Sustainable and Environmental Chemistry, C.13, Scharnhorststraße 1, D-21335 Lüneburg, Germany. Tel.: +49 4131 677-2893.

E-mail addresses: Franziska.Jentzsch@leuphana.de, F_Jentzsch@gmx.de (F. Jentzsch), oliver.olsson@leuphana.de (O. Olsson), Janin.Westphal@leuphana.de (J. Westphal), marco.reich@leuphana.de (M. Reich), christoph.leder@leuphana.de (C. Leder), klaus.kuemmerer@leuphana.de (K. Kümmerer).

Characteristics of UV lamp and UV/vis spectra of EHMC

The relative photon flux of UV lamp was measured with a radiometer (Black Comet, Stellar.Net, Tampa, USA) and two chemical actinometers (metamitrone and terbuthylazine) were treated with the UV lamp to calculate the absolute photon flux (Figure S1) according to Text S1, SM. The absorption spectrum of EHMC (in acetonitrile) was measured with a *Lambda 20* spectrometer (Perkin Elmer Inc., Waltham, Massachusetts, USA) (Figure S1).

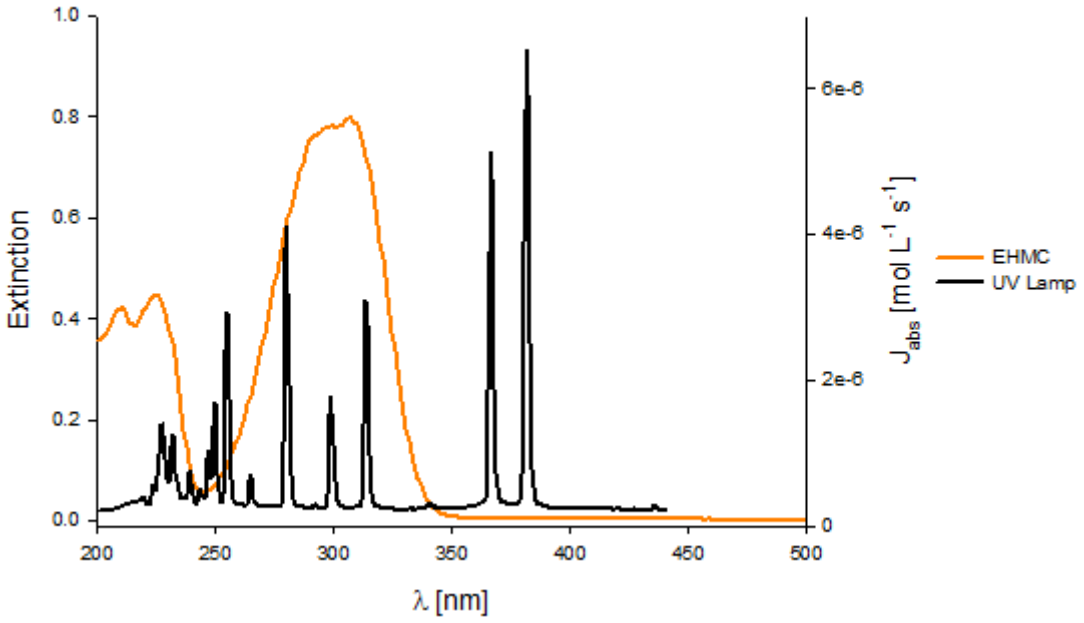

Figure S1, SM: Absolute photon flux J_{abs} of the medium pressure mercury vapor lamp (black line) and UV/vis absorption spectra of EHMC in 100% acetonitrile (orange line).

MS parameter for the identification of photo-TPs of EHMC

The mass spectrometer was operated in positive polarity. The LC parameters mentioned in chapter 2.3 were used while the MS parameters were optimized for EHMC (m/z 291, 308 and 313) by direct injection of a (50:50) 10 mmol L^{-1} ammonium acetate : acetonitrile (ACN) solution of 1 mg L^{-1} EHMC at a flow rate of 7 µL min^{-1} through a syringe pump.

Out of the three optimized methods the appropriate method was chosen by comparing the peak areas of the parent compound. The method that was optimized for m/z 291 showed the highest peak area and was consequently used for the investigation of the photo-TPs.

Table S1, SM: The operating parameters of the ESI and Iontrap (Bruker 6000) of the LC-ESI-IT-MS^n for EHMC proton, ammonia and sodium adducts determined by syringe pump experiments.

Parameter	**m/z 291 $[M+H]^+$**	**m/z 308 $[M+NH_4]^+$**	**m/z 313 $[M+Na]^+$**
Capillary voltage (V)	- 4300	- 5000	- 4433
End plate offset (V)	- 500	- 500	- 500
Nebulizer (psi)	45	45	45
Dry gas (L · min^{-1})	12	12	12
Dry temperature (°C)	300	300	300
Skimmer (V)	23.5	20.7	64.6
Capillary Exit (V)	50	50	120.8
Oct 1 DC (V)	8.56	10.02	12.46
Oct 2 DC (V)	2.13	2.25	2.01
Tap drive	35.8	34.9	47.1
Oct RF (V)	175.0	87.5	262.5
Lens 1 (V)	- 3.1	- 8.7	- 2.2
Lens 2 (V)	- 58.0	- 100.0	- 49.0

Text S1, SM: Determination of the kinetic parameters and quantum yield

The first-order degradation rate constant k was calculated from the slope of logarithm plot of the concentration ratio $c_t\ c_0^{-1}$ versus (irradiation) time in min according to equation (1):

$$\ln\frac{c_t}{c_0} = -k \cdot t \quad (1)$$

where c_0 is the initial concentration and c_t is the remaining concentration of EHMC at time t. In addition, the half-life $t_{1/2}$ was calculated from the photodegradation constant k with equation (2).

$$t_{\frac{1}{2}} = \frac{\ln(2)}{k} \quad (2)$$

The absolute photon flux (J_{abs}) of the source of radiation was examined by combining chemical actinometry and UV-VIS spectroscopy. A BlackComet UV-VIS spectrometer (StellartNet Inc., Tampa, USA) was applied to measure the relative photon flux (J_{rel}) from a distance of 5 cm and an integration time of 10 ms. For the conversion of J_{rel} into J_{abs} terbuthylazine (in 1% ACN) and metamitron were used as chemical actinometers via equation (3) and (4):

$$\mathrm{FACTOR} = \frac{\frac{dc}{dt}}{\Phi * \sum_{200\ nm}^{400\ nm} J_{rel} * 2{,}303 * c_0 * \varepsilon * l} \quad (3)$$

$$J_{abs} = \mathrm{FACTOR} * J_{rel} \quad (4)$$

where FACTOR is the conversion factor, dc/dt is the initial elimination rate of the actinometer, Φ is literature value of the quantum yield of the actinometer (Palm and Zetzsch 1996; Palm et al. 1997), c_0 is the initial concentration of the actinometer, ε is the molar absorption coefficient of the actinometer and l is the path length. For the calculation of J_{abs} the average conversion factor of the two actinometers ($1.1 \cdot 10^{-10}$) was used.

ε_{EHMC}, the extinction of EHMC (dissolved in 0.2% and 0.5% (v/v) ACN, respectively) in different concentrations was determined for every wavelength with a Perkin Elmer LAMBDA 20 UV-VIS spectral photometer (PerkinElmer LAS GmbH, Rodgau, Germany). As consequence of the sparse solubility the measured concentrations of EHMC differed from the initial nominal concentrations of all samples. Therefore, the exact concentrations were analyzed by HPLC-UV. The obtained data were used to calculate the molar extinction coefficient.

Equation (5) was applied for a wavelength range from 200-400 nm, due to the overlap of the emitted light of the lamp and the absorption spectra of EHMC (Fig. S1, SM), to calculate the quantum yield of EHMC (Φ_{EHMC}):

$$\Phi_{EHMC} = \frac{\frac{dc}{dt}}{2{,}303 * \sum_{200\ nm}^{400\ nm} \varepsilon_{EHMC} * J_{abs} * c_0 * l} \quad (5)$$

In equation (5), dc/dt represents the initial elimination rate of EHMC, ε_{EHMC} the molar absorption coefficient of EHMC, J_{abs} is the absolute photon flux, c_0 is the initial concentration of EHMC, and l is the path length (1 cm).

The calculated quantum yields were 0.0042 ± 0.0007 and 0.0023 ± 0.0001 EHMC dissolved in 0.2% and 0.5% (v/v) ACN, respectively, whereas the error represents the standard deviation of two separate photolysis experiments.

Table S2, SM: List of software and their respective QSAR models used for the prediction of the formation of TPs, the environmental fate and toxicity.

Activity	QSAR Software	Models	End points	References
Photodegradation products	MetaPC V. 1.8.1	Photodegradation	Photoproducts of chemicals under natural-like conditions	(Sedykh et al. 2001)
Environmental fate	OASIS Catalogic V.5.11.6TB	Catabol 301C	Ready biodegradability according to MITI-I test	(Laboratory of Mathematical Chemistry 2012)
		Catalogic 301C	Ready biodegradability according to MITI-I test	
	CASE Ultra V.1.5.2.0 (MultiCASE Inc.)	MITI-I test (OECD 301C, module AU6)	Ready biodegradability according to MITI-I test	(Chakravarti et al. 2012; Saiakhov et al. 2013)
Toxicity	OASIS Catalogic V.5.11.6TB	Mutagenicity v04 (Salmonella Catalogic (SC))	Bacterial mutagenicity	(Laboratory of Mathematical Chemistry 2012)
	CASE Ultra V.1.5.2.0 (MultiCASE Inc.)	A - Human carcinogenicity (A0J)	Carcinogenicity	(Chakravarti et al. 2012; Saiakhov et al. 2013)
		B - Micronucleus formation *in vivo* composite (A7S)	Genotoxicity	
		C - Chromosome aberration *in vitro* composite (A7U)	Genotoxicity	
		D - Chromosome aberration *in vitro* CHO (A7V)	Genotoxicity	
		Mutagenicity Ames (SALM2013)	Bacterial mutagenicity	

Table S2, SM: continued

Toxicity	CASE Ultra V.1.5.2.0 (MultiCASE Inc.)	*Salmonella* mutagenicity (GT1A7B)	Bacterial mutagenicity	(Chakravarti et al. 2012; Saiakhov et al. 2013)
		A-T mutation of *E. coli* and TA102 (GT1AT E coli)	Bacterial mutagenicity	
		Expert rules for genotoxicity (GT Expert)	Genotoxicity	
		E. coli mutagenicity (Pharm-E_coli)	Bacterial mutagenicity	
		Salmonella mutagenicity (Pharm_Salm)	Bacterial mutagenicity	
		Aneuploidy in Yeast (A6A)	Genotoxicity	
		Micronucleus Formation *in vivo* Mouse (A7T)	Genotoxicity	
		Rat Carcinogenicity (AOD)	Carcinogenicity	
		Mouse Lymphoma (ML)	Mammalian mutagenicity	
		Mouse Carcinogenicity (AO8)	Carcinogenicity	
		UDS Induction (A64)	Genotoxicity	

Table S2, SM: continued

Toxicity	Leadscope V. 3.2.6-1	Bacterial mutagenesis (BM)	Bacterial mutagenicity	Training sets from 2012 SAR Genetox Database provided by Leadscope (Roberts et al. 2000)
		Mammalian mutagenesis (MM)	Mammalian mutagenicity	
		B - *In vivo* micronucleus (IVMN)	Genotoxicity	
		C - *In vitro* chromosome aberration (IVCA)	Genotoxicity	
		D - Chromosome aberration *in vitro* CHO (A7V)	Genotoxicity	

Identification of photo-TPs

The identification and structural elucidation of the TPs were performed for an initial EHMC concentration of 5 mg L^{-1}. The A/A_0 ratios (as A is the MS peak area of photo-TP and A_0 is the MS peak area of EHMC at 0 min) were obtained from the extracted ion chromatograms (EIC, Fig. S2). Fig. S3 illustrates the correlation between the UV and the MS signal of TP_{137}.

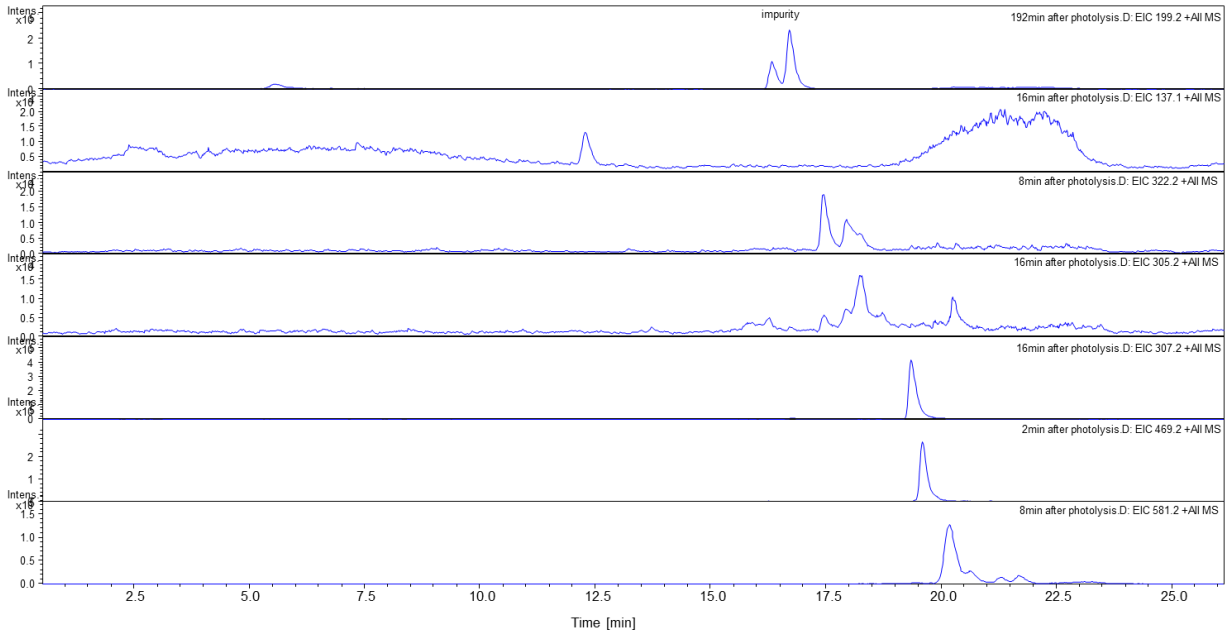

Figure S2, SM: EICs of the identified photo-TPs by LC-MS.

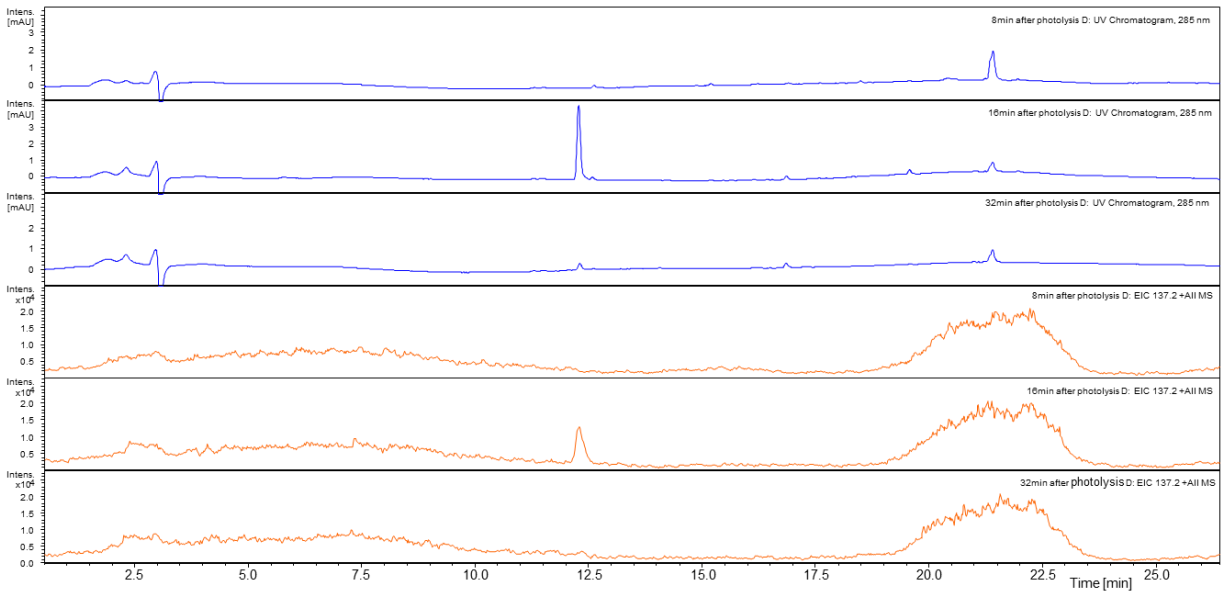

Figure S3, SM: UV chromatograms and EICs of the course appearance of the proposed TP_{137c} by LC-MS.

Table S3, SM: The proposed structures of the identified photo-TPs of EHMC.

Name		Chemical Formula	Structures
EHMC		$C_{18}H_{26}O_3$	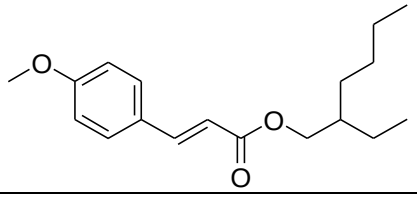
TP_{137}	a	$C_8H_8O_2$	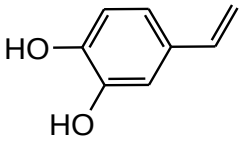
	b		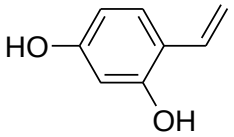
	c		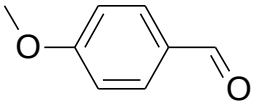
TP_{199}		$C_9H_{10}O_5$	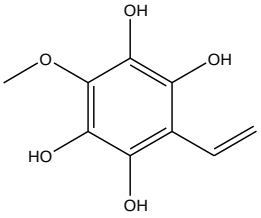
TP_{305}	a	$C_{18}H_{24}O_4$	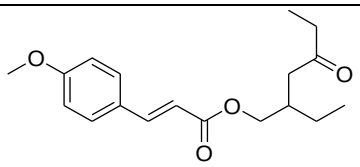
	b		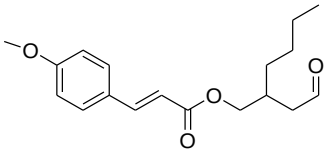
	c		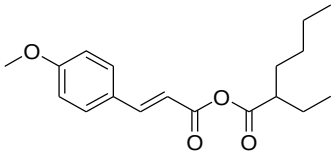
	d		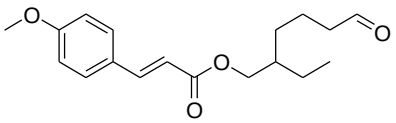
	e		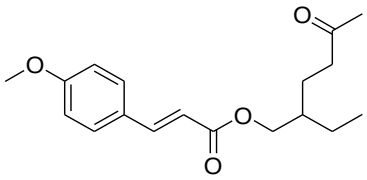

Table S3, SM: continued

TP_{305}	f	$C_{18}H_{24}O_4$	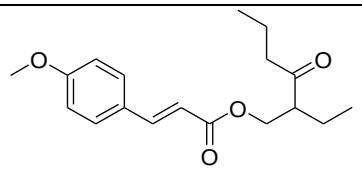
	g		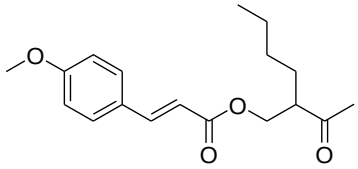
TP_{307}	a	$C_{18}H_{26}O_4$	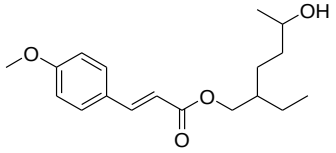
	b		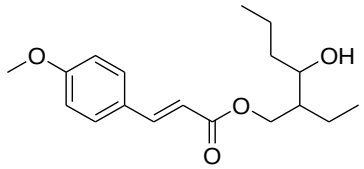
	c		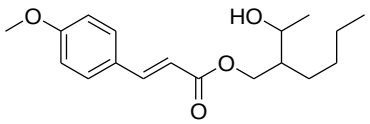
	d		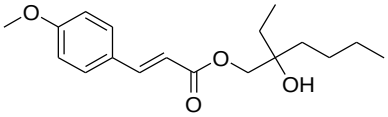
	e		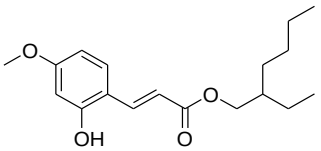
	f		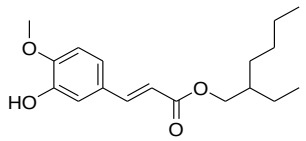
	g		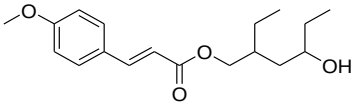
	h		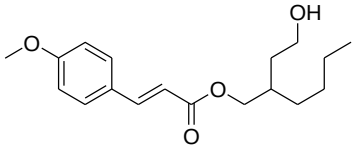
	I		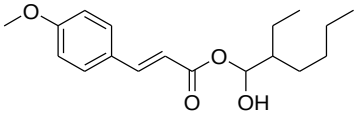
	k		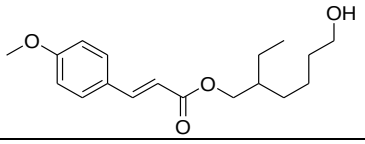

Table S3, SM: continued

TP_{469}	a	$C_{28}H_{36}O_6$	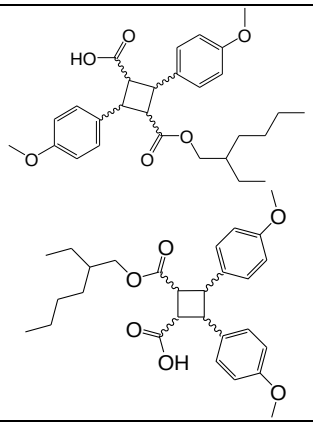
	b		
TP_{581}	a	$C_{36}H_{52}O_6$	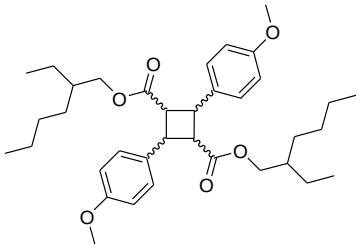
	b		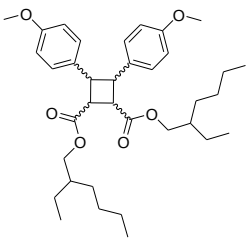

Table S4, SM: Product ions of the proposed TPs of EHMC formed during fragmentation with MS^n (autoMSn and MRM) (RT – retention time, m/z – mass to charge ratio, relative abundance in brackets).

Proposed TP	RT [min]	Precursor ion	Proposed structure
EHMC (m/z 291)	21.2	$[M+H]^+$	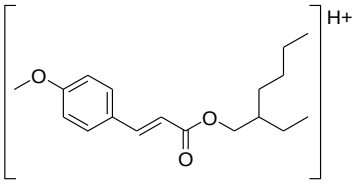
Product ions (intensity in brackets)			
178.9 (100)	$[M-C_8H_{16}]^+$		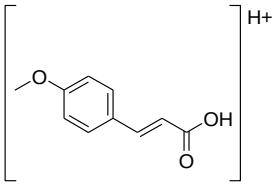
161.1 (35.7)	$[M-C_8H_{16}-H_2O]^{\bullet+}$		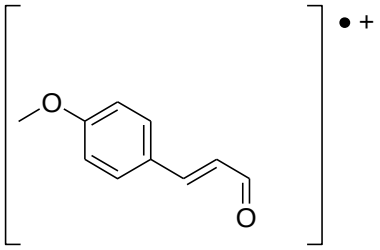

Proposed TP	RT [min]	Precursor ion	Proposed structure
TP_{199} (m/z 199)	5.5	$[M+H]^+$	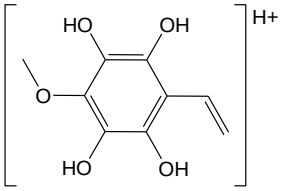
Product ions (intensity in brackets)			
172.0 (100)	$[M-C_2H_3]^{\bullet+}$		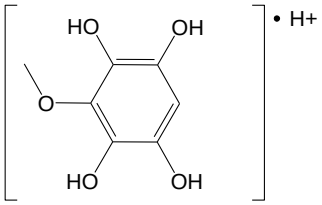

Table S4, SM: continued

Proposed TP	RT [min]	Precursor ion	Proposed structure
TP_{137} (m/z 137)	12.3	$[M+H]^+$	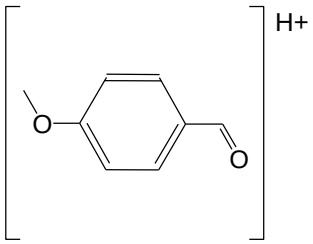
Product ions (intensity in brackets)			
–	–	–	

Proposed TP	RT [min]	Precursor ion	Proposed structure
TP_{305} (m/z 322)	17.4 17.9	$[M+NH_4]^+$	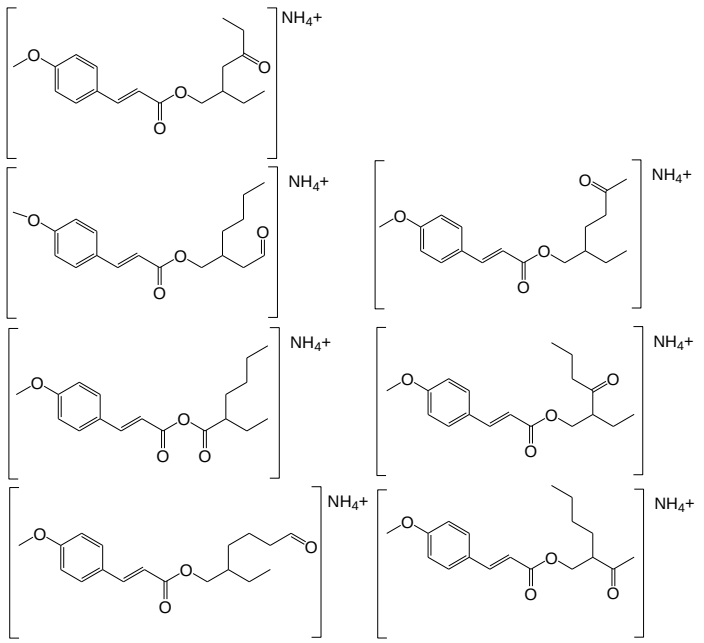
Product ions (intensity in brackets)			
305.0 (100)	$[M-NH_3]^+$	e.g. TP_{305f}:	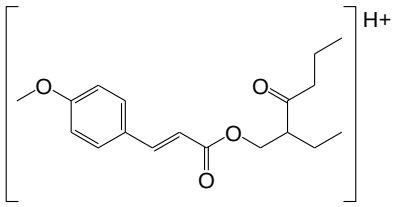
127.1 (17.4 min: 74.5) 127.1 (17.9 min: 68.2)	$[M-NH_3-C_{10}H_{10}O_3]^{\bullet+}$		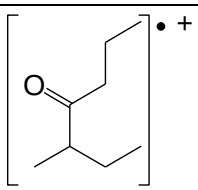

Table S4, SM: continued

Proposed TP	RT [min]	Precursor ion	Proposed structure
TP_{305} (m/z 305)	18.2	$[M+H]^+$	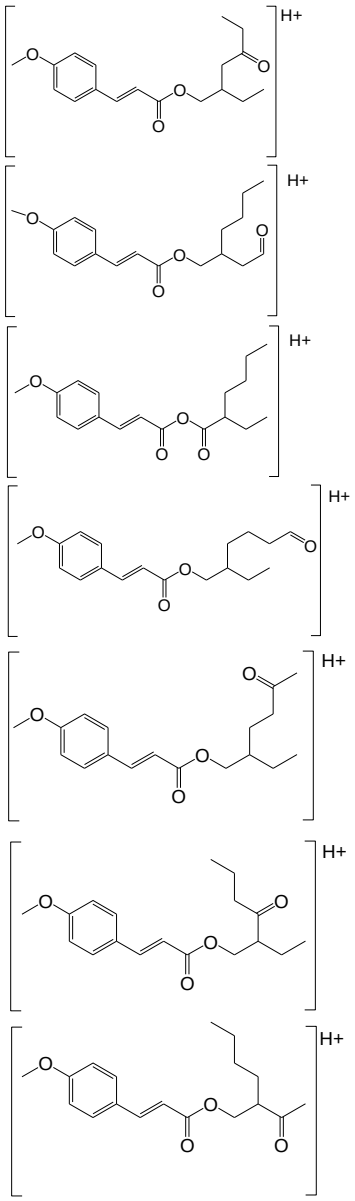
Product ions (intensity in brackets)			
161.0 (100)	$[M-C_8H_{14}O-H_2O]^{\bullet+}$	e.g. TP_{305f}:	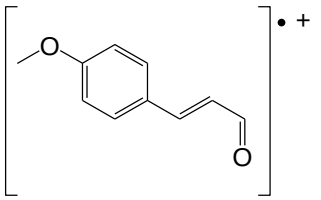
179.0 (15.1)	$[M-C_8H_{14}O]^+$		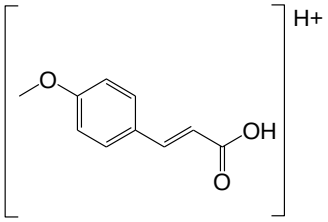

Table S4, SM: continued

Proposed TP	RT [min]	Precursor ion	Proposed structure
TP_{307} (m/z 307)	19.3	$[M+H]^+$	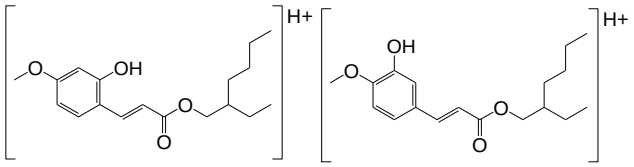
Product ions (intensity in brackets)			
194.9 (100)	$[M-C_8H_{16}]^+$		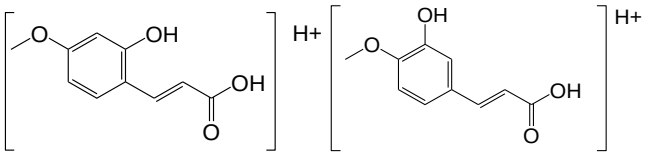
135.1 (48.1)	$[M-C_8H_{16}-CO_2-O]^+$		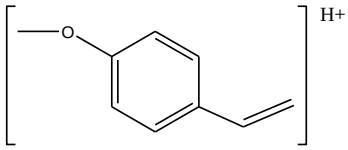

Table S4, SM: continued

Proposed TP	RT [min]	Precursor ion	Proposed structure
TP_{469} (m/z 469)	19.6	$[M+H]^+$	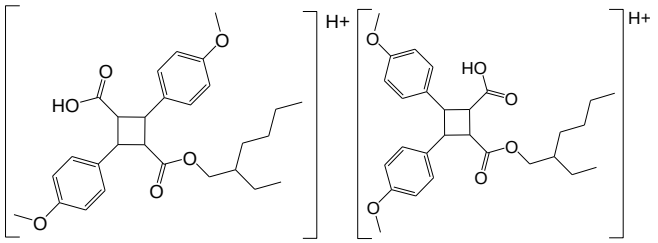
Product ions (intensity in brackets)			
161.0 (100)	$[M\text{-}H_2O\text{-}C_{18}H_{26}O_3]^{\bullet+}$		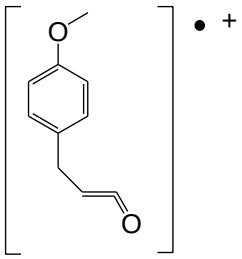
451.2 (82.5)	$[M\text{-}H_2O]^+$		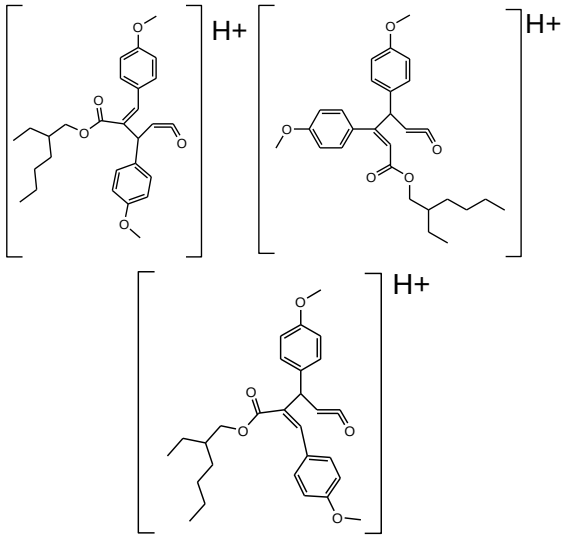

Table S4, SM: continued

Proposed TP	RT [min]	Precursor ion	Proposed structure
TP_{581} (m/z 581)	20.2 20.6 21.3 21.7	$[M+H]^+$	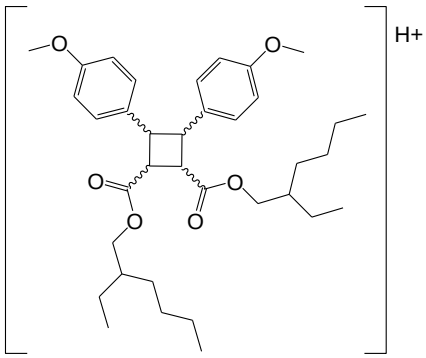
Product ions (intensity in brackets)			
451.1 (100)	$[M-C_8H_{16}-H_2O]^+$		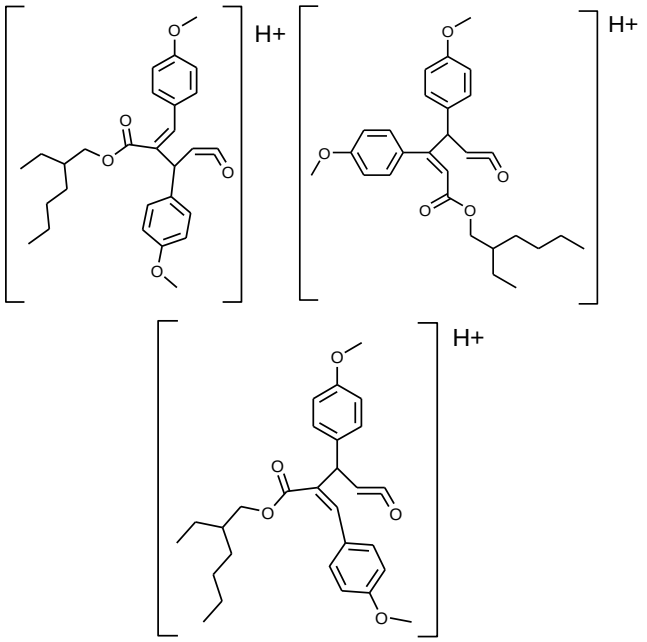
241.0 (20.2 min: 14.8; 20.6 min: 23.7; 21.3 min: 29.0; 21.7 min: 32.2)	$[M-C_8H_{16}-H_2O-C_{12}H_{18}O_3]^+$		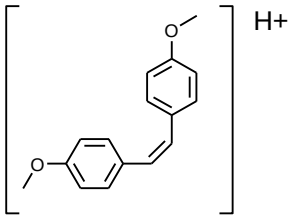
469.0 (20.6 min: 14.6; 21.3 min: 29.1; 21.7 min:30.8)	$[M-C_8H_{16}]^+$		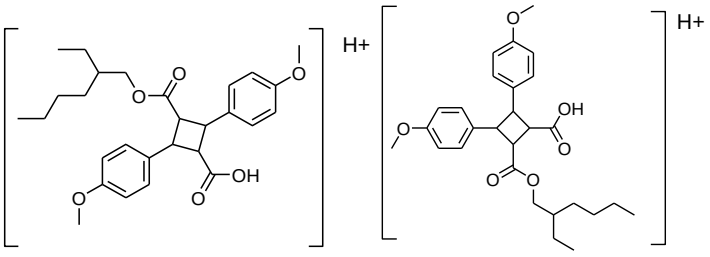

Table S4, SM: continued

291.0 (21.3 min: 11.8)	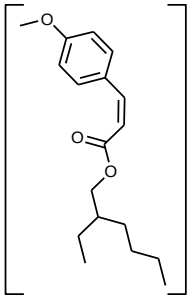 H+

Text S2, SM: Output from various *in silico* models used in the study

The ready biodegradability of EHMC and its photo-TPs was predicted with models based on data for OECD 301C MITI-I test (Ministry of International Trade and Industry, Japan) (OECD, 1992), which are usually not directly comparable to tests, but can provide orientation towards identifying the moieties of molecules responsible for ready biodegradability non-biodegradability. The OASIS Catalogic models predict the ready biodegradability as a numerical value between 1 and 0. A numeric value of 1 corresponds to 100% biodegradation and 0 represents 0 % biodegradation while numeric value of 0.6 corresponds to 60% biodegradation, which is a pass criterion for ready biodegradability under MITI-I tests conditions. CASE Ultra and Leadscope software provides a positive, negative and out-of-domain (OD) estimation for the selected models. OD means that the test chemical is not included in the applicability domain of the applied model. 'Inconclusive' estimation means that a significant portion of the test chemical is covered by unknown structural fragments and therefore a clear result cannot be provided. Tab. S2 enlists the software and their respective models used in the present study.

Table S5, SM: QSAR predictions for EHMC and its photo-TPs presented in Fig. 4 for biodegradation activity by different models and alert IDs for the activating alerts (CATABOL 301C model under MITI test condition biological oxygen demand (BOD) 28d, 2: CATALOGIC 301C model BOD 28d; CASE Ultra - Ready biodegradability under MITI test (AU6)).

	QSAR models				
Photo-TPs	**Catabol 301C model** [§]	**Catalogic 301C model** [§]	**estimation**[§]	**AU6** **Multicase activating alert: Alert ID**	**AU6** **Unknown fragment**
EHMC	0.6373 [OD]	0.6888 [OD]	+	2, 54, 79	–
TP_{137c}	0.6929 [OD]	0.7451	+	11, 79	–
TP_{199}	0.8486 [OD]	0.2182 [OD]	–	–	–
TP_{305a}	0.7088 [OD]	0.7800 [OD]	+	2, 39, 54, 79	–
TP_{305b}	0.5552 [OD]	0.7086 [OD]	+	2, 11, 54, 79	–
TP_{305c}	0.4465 [OD]	0.6616 [OD]	+	2, 11, 54, 79	–
TP_{305d}	0.5016 [OD]	0.6864 [OD]	+	2, 5, 39, 54, 79	–
TP_{305e}	0.7023 [OD]	0.7274 [OD]	+	54, 79	–
TP_{305f}	0.7428 [OD]	0.7965 [OD]	+	2, 39, 54, 79	–
TP_{305g}	0.6410 [OD]	0.7377 [OD]	+	2, 5, 54, 79	–
TP_{307e}	0.6390 [OD]	0.6654 [OD]	+	2, 13, 54, 79	–
TP_{307f}	0.4624 [OD]	0.6238 [OD]	+	2, 13, 54, 79	–

Table S5, SM: continued

TP_{469a}	0.2287 OD	0.2696 OD	+	2, 79	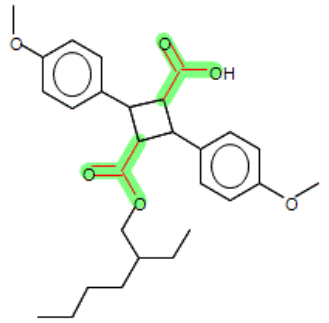
TP_{469b}	0.2488 OD	0.2697 OD	+	2, 79	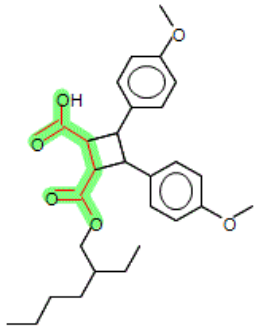
TP_{581b}	0.3173 OD	0.3389 OD	+	2, 79	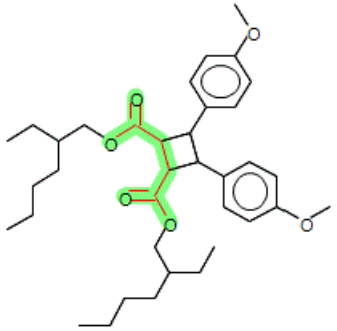

§: “100% biodegradation” was assigned a numeric value of 1 and “0% biodegradation” was assigned a numeric value of 0. Out-of-Domain (OD) means that the test chemical is not included in the applicability domain of the applied model. (+): positive prediction; (–): negative prediction.

Table S6, SM: Predicted mutagenic activities of EHMC and its TPs presented in Fig. 4 calculated by Case Ultra (MultiCASE Inc.), *Salmonella* mutagenicity (GT1 A7B), A-T mutation of *E. coli* and TA102 (GT1 AT E coli), Expert rules for genotoxicity (GT Expert), *E. coli* mutagenicity (Pharm-E_coli), *Salmonella* mutagenicity (Pharm_Salm) and other QSAR models mutagenicity model V04 (Salmonella Catalogic (SC), Oasis Catalogic), and Bacterial mutagenesis (BM, Leadscope).

	QSAR models*						
$TP_{m/z}$	**GT1 A7B[§]**	**GT1 AT E coli[§]**	**GT Expert[§]**	**Pharm-E_coli[§]**	**Pharm_Salm[§]**	**SC**	**BM**
EHMC	known neg.	–	known neg.	known neg.	known neg.	+	–
TP_{137c}	known neg.	known neg.	known neg.	known neg.	known neg.	–[OD]	–
TP_{199}	–	–	–	–	–	–[OD]	+
TP_{305a}	–	–	–	–	–	+	–
TP_{305b}	–	–	–	–	–	+	–
TP_{305c}	–	–	–	–	–	+[OD]	–
TP_{305d}	–	–	–	–	–	+	–
TP_{305e}	–	–	–	–	–	+[OD]	–
TP_{305f}	–	–	–	–	–	+[OD]	–
TP_{305g}	–	–	–	–	–	+[OD]	–
TP_{307e}	–	–	–	–	–	+	–
TP_{307f}	–	–	–	–	–	+	–
TP_{469a}	–	OD	–	–	–	–[OD]	–
TP_{469b}	–	OD	–	–	–	–[OD]	–
TP_{581b}	–	–	–	–	–	–[OD]	–

*Positive (+), negative (–), Out-of-domain (OD)

[§]ICH M7

Table S7, SM: Predicted toxicities of EHMC and the photo-TPs presented in Fig. 4 calculated with the following QSAR models: From CASE Ultra: Human Carcinogenicity (A0J), Aneuploidy in Yeast (A6A), Micronucleus Formation *in vivo* composite (A7S), Micronucleus Formation *in vivo* Mouse (A7T), Chromosome Aberrations *in vitro* composite (A7U), Chromosome Aberrations *in vitro* CHO cells (A7V), Rat Carcinogenicity (AOD), Mouse Lymphoma (ML), Mouse Carcinogenicity (AO8), UDS Induction (A64); From Leadscope: *In vitro* chromosome aberration (IVCA), Mammalian mutagenesis (MM), *in vivo* micronucleus (IVMN).

QSAR models:	**genotoxicity and mutagenicity**												
	A0J	**A6A**	**A7S**	**A7T**	**A7U**	**A7V**	**AOD**	**ML**	**AO8**	**A64**	**IVCA**	**MM**	**IVMN**
EHMC	–	OD	–	–	IN	IN	+	+	+	IN	+	+	–
TP_{137c}	–	OD	–	–	+	–	OD	**+**	–	IN	+	+	–
TP_{199}	IN	–	–	IN	–	–	–	IN	–	–	+	+	+
TP_{305a}	–	IN	–	–	+	IN	+	+	IN	IN	+	+	–
TP_{305b}	–	OD	–	–	IN	IN	+	+	+	IN	+	+	–
TP_{305c}	–	OD	–	–	IN	IN	+	+	+	IN	+	+	–
TP_{305d}	–	IN	–	–	IN	IN	+	+	IN	IN	+	+	–
TP_{305e}	–	OD	–	OD	IN	+	–	+	+	IN	+	+	–
TP_{305f}	IN	IN	–	–	IN	IN	+	+	IN	+	+	+	–
TP_{305g}	IN	OD	–	–	IN	+	+	+	+	+	+	+	–
TP_{307e}	–	OD	–	–	IN	IN	+	+	IN	IN	+	+	–
TP_{307f}	–	OD	–	–	IN	IN	+	+	+	IN	+	+	–
TP_{469a}	OD	OD	OD	OD	OD	OD	IN	+	+	OD	OD	–	–
TP_{469b}	OD	OD	OD	OD	OD	OD	IN	+	+	OD	–	–	–
TP_{581b}	–	OD	–	–	–	–	IN	+	+	OD	–	–	–

*Positive (+), known positive (**+**), negative (–), inconclusive (IN), Out-of-domain (OD)

Table S8, SM: Details of “inconclusive” predictions (alert IDs) of various endpoints with different models and highlighted molecular moiety for the activating alert (Leadscope). The gray zone is between 40-60% and the threshold is 50%.

QSAR models	Photo-TPs	Alert ID/ highlighted molecule part	Prediction: positive, negative, IN
Human Carcinogenicity (A0J)	EHMC	–	The calculated probability of being positive for this compound is **29.0%**. The calculated probability is LOWER than the model's current classification threshold and not within the gray zone, therefore, the compound is predicted to be **NEGATIVE**.
	TP_{199}	13	The calculated probability of being positive for this compound is **53.8%.** The calculated probability falls inside the gray zone around the model's classification threshold, therefore, the results of activity prediction is inconclusive.
	TP_{305f}	165	The calculated probability of being positive for this compound is **48.4 %.** The calculated probability falls inside the gray zone around the model's classification threshold, therefore, the results of activity prediction is inconclusive.
	TP_{305g}	165	The calculated probability of being positive for this compound is **48.4%.** The calculated probability falls inside the gray zone around the model's classification threshold, therefore, the results of activity prediction is inconclusive.
Micronucleus Formation *in vivo* Mouse (A7T)	EHMC	–	The calculated probability of being positive for this compound is **26.4%**. The calculated probability is LOWER than the model's current classification threshold and not within the gray zone, therefore, the compound is predicted to be **NEGATIVE**.
	TP_{199}	57	The calculated probability of being positive for this compound is **42.1%.** The calculated probability falls inside the gray zone around the model's classification threshold, therefore, the results of activity prediction is inconclusive.

Table S8, SM: continued

In vivo micronucleus (IVMN, Leadscope)	EHMC	–	–
	TP_{199}		Positive
Chromosome Aberrations *in vitro* composite (A7U)	EHMC	100	The calculated probability of being positive for this compound is **49.0%**. The calculated probability falls inside the gray zone around the model's classification threshold, therefore, the results of activity prediction is inconclusive.
	TP_{137c}	91	Positive
	TP_{305a}	100, 376	Positive
	TP_{305b}	100	The calculated probability of being positive for this compound is **49.0%**. The calculated probability falls inside the gray zone around the model's classification threshold, therefore, the results of activity prediction is inconclusive.
	TP_{305c}	100	The calculated probability of being positive for this compound is **49.0%**. The calculated probability falls inside the gray zone around the model's classification threshold, therefore, the results of activity prediction is inconclusive.
	TP_{305d}	100	The calculated probability of being positive for this compound is **49.0%**. The calculated probability falls inside the gray zone around the model's classification threshold, therefore, the results of activity prediction is inconclusive.
	TP_{305e}	100	The calculated probability of being positive for this compound is **49.0%**. The calculated probability falls inside the gray zone around the model's classification threshold, therefore, the results of activity prediction is inconclusive.

Table S8, SM: continued

Chromosome Aberrations *in vitro* composite (A7U)	TP_{305f}	100	The calculated probability of being positive for this compound is **49.0%**. The calculated probability falls inside the gray zone around the model's classification threshold, therefore, the results of activity prediction is inconclusive.
	TP_{305g}	100	The calculated probability of being positive for this compound is **49.0%**. The calculated probability falls inside the gray zone around the model's classification threshold, therefore, the results of activity prediction is inconclusive.
	TP_{307e}	100	The calculated probability of being positive for this compound is **49.0%**. The calculated probability falls inside the gray zone around the model's classification threshold, therefore, the results of activity prediction is inconclusive.
	TP_{307f}	100	The calculated probability of being positive for this compound is **49.0%**. The calculated probability falls inside the gray zone around the model's classification threshold, therefore, the results of activity prediction is inconclusive.
Chromosome Aberrations *in vitro* CHO cells (A7V)	EHMC	20	The calculated probability of being positive for this compound is **56.1%**. The calculated probability falls inside the gray zone around the model's classification threshold, therefore, the results of activity prediction is inconclusive.
	TP_{305a}	20	The calculated probability of being positive for this compound is **56.1%**. The calculated probability falls inside the gray zone around the model's classification threshold, therefore, the results of activity prediction is inconclusive.
	TP_{305b}	20	The calculated probability of being positive for this compound is **56.1%**. The calculated probability falls inside the gray zone around the model's classification threshold, therefore, the results of activity prediction is inconclusive.

Table S8, SM: continued

	TP_{305c}	20	The calculated probability of being positive for this compound is **56.1%**. The calculated probability falls inside the gray zone around the model's classification threshold, therefore, the results of activity prediction is inconclusive.
	TP_{305d}	20	The calculated probability of being positive for this compound is **56.1%**. The calculated probability falls inside the gray zone around the model's classification threshold, therefore, the results of activity prediction is inconclusive.
	TP_{305e}	20, 211	Positive
Chromosome Aberrations *in vitro* CHO cells (A7V)	TP_{305f}	20	The calculated probability of being positive for this compound is **56.1%**. The calculated probability falls inside the gray zone around the model's classification threshold, therefore, the results of activity prediction is inconclusive.
	TP_{305g}	20, 211	Positive
	TP_{307e}	20	The calculated probability of being positive for this compound is **56.1%**. The calculated probability falls inside the gray zone around the model's classification threshold, therefore, the results of activity prediction is inconclusive.
	TP_{307f}	20	The calculated probability of being positive for this compound is **56.1%**. The calculated probability falls inside the gray zone around the model's classification threshold), therefore, the results of activity prediction is inconclusive.

Table S8, SM: continued

	EHMC	98	The calculated probability of being positive for this compound is **41.1%**. The calculated probability falls inside the gray zone around the model's classification threshold, therefore, the results of activity prediction is inconclusive.
	TP_{137c}	98	The calculated probability of being positive for this compound is **41.1%**. The calculated probability falls inside the gray zone around the model's classification threshold, therefore, the results of activity prediction is inconclusive.
	TP_{305a}	98	The calculated probability of being positive for this compound is **41.1%**. The calculated probability falls inside the gray zone around the model's classification threshold, therefore, the results of activity prediction is inconclusive.
UDS Induction (A64)	TP_{305b}	98 Unknown fragment: 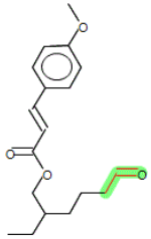 98	The calculated probability of being positive for this compound is **41.1%**. The calculated probability falls inside the gray zone around the model's classification threshold, therefore, the results of activity prediction is inconclusive.
	TP_{305c}	Unknown fragment: 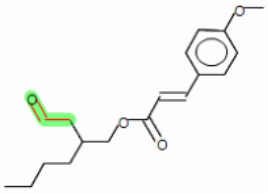	The calculated probability of being positive for this compound is **41.1%**. The calculated probability falls inside the gray zone around the model's classification threshold, therefore, the results of activity prediction is inconclusive.

UDS Induction (A64)	TP_{305d}	98	The calculated probability of being positive for this compound is **41.1%**. The calculated probability falls inside the gray zone around the model's classification threshold, therefore, the results of activity prediction is inconclusive.
	TP_{305e}	98	The calculated probability of being positive for this compound is **41.1%**. The calculated probability falls inside the gray zone around the model's classification threshold, therefore, the results of activity prediction is inconclusive.
	TP_{305f}	81, 98	Positive
	TP_{305g}	81, 98	Positive
	TP_{307e}	98	The calculated probability of being positive for this compound is **41.1%**. The calculated probability falls inside the gray zone around the model's classification threshold, therefore, the results of activity prediction is inconclusive.
	TP_{307f}	98	The calculated probability of being positive for this compound is **41.1%**. The calculated probability falls inside the gray zone around the model's classification threshold, therefore, the results of activity prediction is inconclusive.

References

Chakravarti, S.K.; Saiakhov, R.D.; Klopman, G. (2012) **Optimizing predictive performance of CASE Ultra expert system models using the applicability domains of individual toxicity alerts** *J Chem Inf Model* 52: 2609–8; doi:10.1021/ci300111r.

OECD - OECD guidelines for the testing of chemicals: ready biodegradability 301C: MITI (I) test. OECD Publication (1992) 1-62.

Palm, W. U.; Zetzsch, C. (1996) **Investigation of the photochemistry and quantum yields of triazines using polychromatic irradiation and UV-spectroscopy as analytical tool** *International Journal of Environmental Analytical Chemistry* 65(1-4): 313–29; doi:10.1080/03067319608045564.

Palm, W. U.; Millet, M.; Zetzsch, C. (1997) **Photochemical reactions of metamitron** *Chemosphere* 35(5): 1117–30; doi:10.1016/S0045-6535(97)00176-8.

Roberts, G.; Myatt, G.; Johnson, W.; Cross, K.; Blower, P. (2000) **LeadScope: software for exploring large sets of screening data** *J Chem Inf Model* 40: 1302–14; doi:10.1021/ci0000631.

Saiakhov, R.; Chakravarti, S.; Klopman, G. (2013) **Effectiveness of CASE Ultra expert system in evaluating adverse effects of drugs** *Mol Inf* 32: 87–7; doi:10.1002/minf.201200081.

Sedykh, A.; Saiakhov, R.; Klopman, G. META V. (2001) **A model of photodegradation for the prediction of photoproducts of chemicals under natural-like conditions** *Chemosphere* 45: 971–1.

Artikel 2

Franziska Jentzsch, Marco Reich, Klaus Kümmerer, Oliver Olsson

Photolysis of mixtures of UV filters octocrylene and ethylhexyl methoxycinnamate leads to formation of mixed transformation products and different kinetics

Science of the Total Environment (2019) 134048.

DOI: https://doi.org/10.1016/j.scitotenv.2019.134048

Science of the Total Environment 697 (2019) 134048

Contents lists available at ScienceDirect

Science of the Total Environment

journal homepage: www.elsevier.com/locate/scitotenv

Photolysis of mixtures of UV filters octocrylene and ethylhexyl methoxycinnamate leads to formation of mixed transformation products and different kinetics

F. Jentzsch, M. Reich, K. Kümmerer, O. Olsson *

Sustainable Chemistry and Material Resources, Institute of Sustainable and Environmental Chemistry, Faculty of Sustainability, Leuphana University of Lüneburg, Universitätsallee 1, DE-21335 Lüneburg, Germany

HIGHLIGHTS

- Octocrylene (OCR) was primary eliminated during aqueous photolysis.
- Incomplete mineralization of OCR by formation of possible photo transformation products (TPs)
- Ethylhexyl methoxycinnamate (EHMC) was degraded faster than OCR.
- Degradation kinetics in mixture differ from the kinetics of the separate tested substances.
- Indications that during aqueous photolysis of the OCR-EHMC-mixture mixed photo TPs could have been formed.

GRAPHICAL ABSTRACT

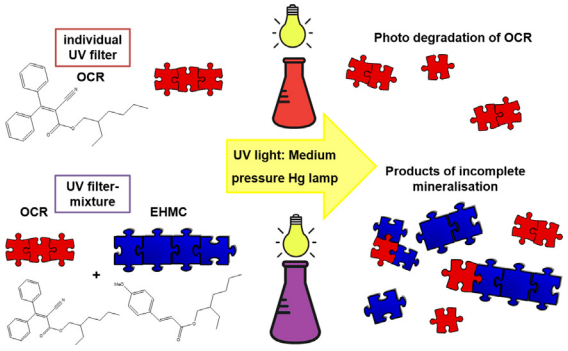

ARTICLE INFO

Article history:
Received 18 April 2019
Received in revised form 6 August 2019
Accepted 21 August 2019
Available online 22 August 2019

Editor: Paola Verlicchi

Keywords:
Personal care products (PCPs)
Octocrylene (OCR)
Ethylhexyl methoxycinnamate (EHMC)
Micropollutant
Mixture
Photo transformation product

ABSTRACT

The treatment with ultraviolet (UV) light is a well-known technique for water disinfection. Photodegradation by UV light is in discussion as measure for advanced water treatment that could provide a potential removal option for micropollutants. Micropollutants such as ingredients from personal care products are also present in grey water. Grey water gets increasingly attention as a source for water reuse. For that purpose it has to be treated. UV-treatment is an option. However, the knowledge on the fate of micropollutants within such a treatment is little. Therefore, we investigated the fate of the UV filters ethylhexyl methoxycinnamate (EHMC), and octocrylene (OCR) as for both UV filters the presence in grey water was reported. OCR as a single compound was investigated with regard to its degradation kinetics and possible photo-transformation products (photo-TPs). These results were compared with those of EHMC previously reported in literature. The mixture of the two UV filters was also investigated to reveal if mixture effects occur regarding the elimination of the UV filters and the formation of TPs. A medium pressure mercury vapor lamp (200–400 nm) was employed for photolysis. This study shows that OCR itself was eliminated below the limit of detection after 256 min and that photo-TPs were formed. The photolysis of the mixture demonstrated alterations of the degradation rates and patterns. Additional TPs were

* Corresponding author at: Institute of Sustainable and Environmental Chemistry, Faculty of Sustainability, Leuphana University of Lüneburg, Universitätsallee 1 – C.13.313a, DE–21335 Lüneburg, Germany.
E-mail addresses: Franziska.Jentzsch@leuphana.de (F. Jentzsch), marco.reich@leuphana.de (M. Reich), klaus.kuemmerer@leuphana.de (K. Kümmerer), oliver.olsson@leuphana.de (O. Olsson).

https://doi.org/10.1016/j.scitotenv.2019.134048

formed by the reaction of the UV filters or TPs with each other. The study shows that more attention should be paid to mixture-effects and mixture-TPs that may cause further follow-up effects.

1. Introduction

On-site grey water (GW) reuse serves as alternative water source that can replace potable water for non-potable water uses such as toilet flushing and garden irrigation. GW treatment systems should result in complete mineralization of contaminants. Conventional (biological) treatment of GW turned out to be less effective in removing emerging micropollutants (MP) (e.g., Eriksson et al., 2010; Hernández-Leal et al., 2010; Martinez-Hernandez et al., 2014). If GW treatment does not result in complete mineralization of pollutants, issues, such as groundwater contamination by products of incomplete mineralization (so called transformation products, TPs) or the parent compounds could arise (Fatta-Kassinos et al., 2011; Salgado et al., 2013; Haddad and Kümmerer, 2014; Mahmoud et al., 2014; Jentzsch et al., 2016; Mathon et al., 2016; Alfiya et al., 2017; Kümmerer et al., 2019). If TPs occur during GW treatment, it is important that they will undergo further (complete) degradation.

The majority of MPs present in treated GW originates from personal care products (PCPs), e.g. UV filters such as octocrylene (OCR) and ethylhexyl methoxycinnamte (EHMC), which are typically used in sunscreen products, lipsticks, shampoos and hair sprays (Díaz-Cruz et al., 2008). Those UV filters have been found in the aquatic environment (Balmer et al., 2005; Poiger et al., 2004). In addition, OCR and EHMC have the potential to bioaccumulate in fish (Buser et al., 2006; Balmer et al., 2005) and show hormonal activities (Kunz and Fent, 2006; Fent et al., 2008). In recent work Jentzsch et al. (2016) showed that EHMC degraded and that TPs were formed under multiwavelength irradiation (200–400 nm). The subsequent quantitative structural activity relationships (QSAR) analysis showed that some TPs of EHMC could have more toxic effects than the parent compound (Jentzsch et al., 2016). Since, OCR and EHMC have some structural similarities (Table 1) the hypothesis arose that both UV filters react in a similar way during photolysis. Photolysis of OCR in aqueous solution was already performed with artificial sunlight provided by a halogen lamp (290–800 nm) (Rodil et al., 2009) or by irradiation with a UV-A lamp (Ricci et al., 2003). In both cases, OCR appeared to be photostable. In contrast, Allen et al. (1998) determined a photolysis half-life of OCR in water of 96 h during irradiation in a sun light simulator equipped with a 1000 W Xe arc lamp that emits light >290 nm. So far, no research detected photo-TPs formed during irradiation of OCR because of its high photostability. Besides, no study investigated the photolysis of OCR with medium pressure mercury (Hg) vapor lamp that emits light in the range of 200–400 nm, as potential post-treatment technology, which could lead to the formation of photodegradation products. The high lipophilicity of OCR (Table 1) entails the use of solubilizers in order to improve the solubility in water. In literature, both solvents - acetonitrile (ACN) and methanol (MeOH) - were applied to spike OCR in water (Allen et al., 1998; Ricci et al., 2003; Rodil et al., 2009). Literature provided no data of quantum yields of photolysis of OCR in aqueous solution. Only Allen et al. (1998) reported the determination of a quantum yield for 313 nm but due to the long half-life (96 h) the quantum yield was 0.

In general, photolysis of mixtures was described for formulations (Gaspar and Maia Campos, 2006), model creams (oil-in-water emulsion) with liquid microparticles (Scalia and Mezzena, 2009), neat UV filters (Dondi et al., 2006) or solutions in organic solvents (Dondi et al., 2006). The analysis of the behavior of a mixture of UV filters in water as well as the study of the kinetics of the mixed substances setting compared with the kinetics of the single substances analyzed separately remains to be done. On the one hand, it is important to understand photodegradation and transformation of individual MPs (Zeng et al., 2017), on the other hand, GW contains a mixture of many MPs, which could affect the photolysis behavior of the individual contaminants. Within these mixtures, fragmentation or degradation could form new compounds with unknown environmental behavior. To address such a complex situation using a combination of two compounds is a good starting points. Against UV-A and UV-A/UV-B radiation OCR showed a photostabilizing effect on EHMC and other UV filters which were irradiated as formulations (Gaspar and Maia Campos, 2006; Scalia and Mezzena, 2009). Moreover, Dondi et al. (2006) reported the photolysis of the mixture of another UV filter avobenzone and EHMC tested in different solvents. In acetonitrile, the transformation products were the same resulting from unimolecular photoreactions in the mixture as for the photolysis of the individual substances; whereas the same experiment in cyclohexane lead to additional cross-reaction products, which

Table 1
Properties of OCR and EHMC: solubility in water, logP - octanol-water coefficient; λmax–absorption maximum; cGW–concentration in GW.

UV filter	Structure	Solubility in water [mg L^{-1}][a]	logP[a]	λ_{max} [nm][b,c,d]	c_{GW} [μg L^{-1}][a]
Octocrylene (OCR)	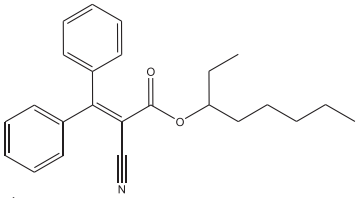	0.004	6.9	300[b] 305[c]	2.3–146
Ethylhexyl methoxycinnamate (EHMC)	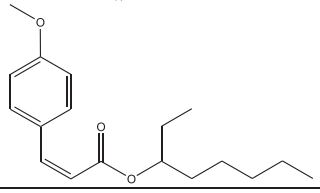	0.155	5.8	310[b] 306[d]	0.16–1.5

[a] Hernández-Leal et al., 2010.
[b] De Orsi et al., 2006: in HPLC eluent (mobile phase: acetonitrile/water (adjusted at pH 3.0 with 1 M perchloric acid) 10:90 (v/v)).
[c] In 100% acetonitrile (see Fig. S1, Supplementary material).
[d] Díaz-Cruz et al., 2008

were formed by the reaction between the enol form of avobenzone and a cinnamate of EHMC (Dondi et al., 2006). In consequence, new dimers and subsequent transformation and degradation products were found compared to the photolysis in acetonitrile (Dondi et al., 2006). For EHMC dimerization via [2 + 2]-cycloaddition was reported frequently (Broadbent et al., 1996; Jentzsch et al., 2016; MacManus-Spencer et al., 2011). However, previous studies did not investigate the mixture effects of the UV filters OCR and EHMC in aqueous solution. Therefore, the effects on the photolysis kinetics and TP formation of a mixture of UV filters in water was done in this study using OCR and EHMC. They were selected because they are (a) both present in GW and (b) share structural features such as cinnamate and the ethylhexyl moiety (Table 1). Consequently, for the photolysis of a mixture of OCR and EHMC reactions between the molecules such as the formation of cyclobutane dimers by the reaction of the double bonds, which leads to non-stable substances, were expected.

The lack of knowledge for the elucidation of photo-TPs of OCR in water illustrates the challenge of structural analysis of TPs of OCR. This study focused on new insights of photolysis of OCR in water and the interaction of two substances during photolysis. The main objectives of this study were an investigation of the behavior of OCR alone and of a mixture of OCR and EHMC in aquatic solution under UV irradiation. The photo transformations of EHMC were investigated in a previous study (Jentzsch et al., 2016). A first step was the determination of the elimination efficiency of OCR as single compound, than studying the elimination of OCR and EHMC in the mixture and the detection and comparison of transformation products of OCR, EHMC and the OCR-EHMC-mixture. HPLC with UV detection was used to determine the elimination efficiency of OCR as well as the formation of photo-TPs of OCR and the mixture of both UV filters, OCR and EHMC. Since the electrospray ionization (ESI) in LC-MS tests for TP identification showed problems in positive ionization structural analysis of photo-TPs was no part of this study. For the photolysis experiments, ACN was chosen as co-solvent because OCR showed no hydrolysis in water-ACN-solutions. Accordingly, the effect of the concentration of ACN on the photodegradation kinetics was investigated too. Since the results of the study should become compared with literature data on the photolysis of EHMC the experimental conditions of EHMC (concentrations of ACN and the initial concentration of the UV filter (Jentzsch et al., 2016)) were adapted to 1 mg L^{-1} and 5 mg L^{-1} for this study.

2. Materials and method

2.1. Chemicals and reagents

Octocrylene (OCR, purity: 97%, CAS: 6197-30-4) was purchased from VWR International GmbH (Darmstadt, Germany) and ethylhexyl methoxycinnamate (EHMC, purity: 98%, racemate, CAS 5466-77-3) from Sigma Aldrich (Germany). Acetonitrile (ACN, HiPerSolv CHROMANORM®; LC-MS grade) and ammonium acetate (HiPerSolv CHROMANORM® for HPLC) were obtained from VWR International GmbH (Darmstadt, Germany). 2-propanol (ROTISOLV® HPLC) was obtained from Carl Roth (Karlsruhe, Germany). OCR and EHMC stock solutions were prepared in ACN (1 g L^{-1}). All chemicals were analytical grade and were used without further purification. Ultrapure water (Q_1:16.6 mΩ and Q_2: 18.2mΩ) was used for the preparation of the diluted stock solutions for analytical measurement and as solvent in photolysis experiments.

2.2. Analytical methods

Since this study focused on photolysis behavior of OCR and mixture effects of OCR-EHMC-mixtures HPLC-UV analysis was selected as analytical method. Due to ionization problems in LC-ESI-MS tests structural analysis of photo-TPs was no part of this study. Thus, HPLC-UV analysis was applied to monitor the primary elimination and its kinetics of OCR and OCR-EHMC-mixture and to detect UV active TPs. Furthermore, HPLC-UV detection was applied to analyze the quantum yield. Therefore, the concentration of the quantum yield samples were quantified by measuring the absorption spectra to obtain the molar absorption coefficient of OCR. This study applied HPLC-UV detection in accordance to the analysis of the degradation kinetics of EHMC described by Jentzsch et al. (2016) in order to enable a comparison of the retention times of the HPLC-UV signals of EHMC, OCR, and of the OCR-EHMC-mixture. The TPs were expected to elute before OCR and EHMC on the applied reversed phase columns due to a higher polarity compared to parent compounds. A Shimadzu Prominence-20 HPLC system (Duisburg, Germany) equipped with a UV/vis-detector was used. The chromatographic separation was achieved on a RP 18plus column (EC 150/3 NUCLEOSHELL® 2.7 μm, Macherey-Nagel, Düren, Germany). A binary gradient program was applied that consisted of 10 mM ammonium acetate in ultrapure water (eluent A) and ACN (eluent B). The gradient started at 20% B and was held for 1 min. Until 15 min, the gradient raised to 97% B and was held for 2 min, then decreased back to 20% B until 25 min, and ended with a 2 min equilibration. The injection volume, flow rate, and column oven temperature were set to 10 μL, 0.3 mL min^{-1}, and 20 °C, respectively. For the quantification, the detection wavelength of 305 nm was chosen because it showed the highest signal intensities (see Fig. S1, Supplementary material). For quantitative analysis via external calibration, calibration standards of OCR were made up at eight different concentration levels, ranging from 78.125 μg L^{-1} to 10 mg L^{-1}. The final concentrations were achieved by diluting the stock solution with ACN. The method showed good linearity for OCR between 78.125 μg L^{-1} and 10 mg L^{-1} (correlation coefficient 0.999) and reproducibility RSD <2.0%. The limit of detection for OCR was found to be 10 μg L^{-1} at 305 nm.

The absorption spectrum of OCR (in acetonitrile) was measured with a Lambda 20 spectrometer (Perkin Elmer Inc., Waltham, Massachusetts, USA) (see Supplementary material).

Jentzsch et al. (2016) identified TPs of EHMC by LC-MS analysis, but due to poor ionization of OCR and its TPs this study focused on the comparison of the retention times of the TPs determined by HPLC-UV. Consequently, photolysis samples with an initial concentration of 5 mg L^{-1} EHMC in water with an ACN concentration of 0.5% (v/v) were used to investigate the peaks of the TPs via HPLC-UV and to compare them with the peaks in the experiment with the UV filter mixture.

2.3. Direct UV photolysis

In a pretest, the photolysis experiment was performed with OCR in 800 mL ultrapure water, but OCR and EHMC were only poorly soluble in water. Thus, the photolysis experiments were performed with 800 mL water spiked with either OCR or both dissolved in the co-solvent ACN (according to OECD 316) to improve the solubility of the UV filters. Methanol was not used as solubilizer because pretests showed changes in absorption (maximum) and methanolysis could occur. For usage of acetonitrile as solubilizer during photolysis no reaction of acetonitrile with the UV filters or the TPs was expected. Nevertheless, it was investigated if acetonitrile conducts when photolysed. Therefore, an acetonitrile-water mixture was photolysed and samples were taken and tested for its non purgeable organic carbon (NPOC) content using a Shimadzu TOC-V_{CPN} analyzer equipped with an ASI-V auto sampler. To study the influence of the co-solvent content on the degradation kinetics, different concentrations of ACN (0.1 and 0.5% (v/v)) were analyzed.

The initial nominal concentration of OCR was (i) 1 mg L^{-1}, in order to investigate the kinetics and to determine the quantum yield, and (ii) 5 mg L^{-1}, in order to be able to detect also TPs that were formed in a minor share only. To analyze the role of reactive oxygen species (ROS) during the photolysis process OCR was prepared with 1 mg L^{-1} but with OCR dissolved in ultrapure water dosed with 0.1% (v/v) 2-propanol. UV photolysis experiments were performed with a

polychromatic medium pressure Hg lamp (TQ150, 150 W, UV Consulting Peschl, Mainz, Germany) emitting light mainly in the range of UVA, B and C (200–400 nm). The samples were analyzed by HPLC-UV in order to monitor the primary elimination of OCR and potential TPs. Peroxide test stripes were used to screen hydrogen peroxide formation, an indicator for ROS (MQuant, Merck Chemicals GmbH, Schwalbach, Germany) during the photolysis experiments. The peroxide concentration is measured semi quantitatively by visual comparison of the reaction zone of the test strip with a color scale.

The first-order degradation rate constant k was calculated from the slope of the logarithm plot of the concentration ratio $c_t\,c_0^{-1}$ versus (irradiation) time in min according to Eq. (1):

$$\ln\frac{c_t}{c_0} = -k\cdot t \tag{1}$$

c_0 is the initial concentration and c_t is the remaining concentration of OCR at time t. In addition, the half-life $t_{1/2}$ was calculated from the photolysis constant k with Eq. (2).

$$t\frac{1}{2} = \frac{\ln(2)}{k} \tag{2}$$

Data on the kinetic of this EHMC photolysis experiment could be found in Jentzsch et al. (2016).

To investigate the photolysis of the mixture of OCR/EHMC two experiments were performed with an aqueous solution that was spiked with (i) 2.5 mg L^{-1} and (ii) 5 mg L^{-1} of each UV filter, respectively. In order to examine if EHMC, OCR, and possibly formed TPs would interact during a combined photolysis, the kinetic of the substances in mixture and the TPs formed during the photolysis of 5 mg L^{-1} OCR, 5 mg L^{-1} EHMC and a mixture of OCR and EHMC were determined via HPLC-UV. Due to the co-elution OCR and EHMC the peak was analyzed for the degradation kinetics in mixture measuring the whole peak area A at all time intervals. The plot was performed as natural logarithm of A_0 (peak area at time point 0 min) divided by natural logarithm of A versus time in minutes. For a single substance, which degrades with first order kinetic a linear graph, would be expected. The plot of the co-eluting peak area was a curve with two linear sections for which a linear regression was performed. In accordance with Eqs. (1) and (2), this approach delivered $t_{1/2}$ and k for OCR and EHMC in mixture. This approach was possible because the order of elution of the substances individually was known as well as the clearly different degradation kinetics. In consequence, it could be observed that the fast elimination of EHMC resulted in a separated peak for OCR whose degradation started later. Thus, the general condition (slightly different retention times and clearly different degradation kinetics) were urgently required if an evaluation as described above wants to be performed. A slight error of the result cannot be excluded as for this approach no degradation of OCR before 32 min was assumed.

2.4. Determination of quantum yield

The absolute photon flux (J_{abs}) of the source of radiation was examined by combining chemical actinometry and UV-VIS spectroscopy. A BlackComet UV-VIS spectrometer (StellartNet Inc., Tampa, USA) was applied to measure the relative photon flux (J_{rel}) from a distance of 5 cm and an integration time of 10 ms. The chemical actinometer metamitrone was treated with the UV lamp. J_{rel} was converted into J_{abs} via Eqs. (3) and (4) using the data of the actinometer experiment:

$$\mathrm{FACTOR} = \frac{\frac{dc}{dt}}{\Phi\cdot\sum_{200\ nm}^{400\ nm} J_{rel}\cdot 2.303\cdot c_0\cdot\varepsilon\cdot l} \tag{3}$$

$$J_{abs} = \mathrm{FACTOR}\cdot J_{rel} \tag{4}$$

FACTOR is the conversion factor, dc/dt is the initial elimination rate of the actinometer, Φ is a literature value of the quantum yield of the actinometer (Palm and Zetzsch, 1996; Palm et al., 1997), c_0 is the initial concentration of the actinometer, ε is the molar absorption coefficient of the actinometer and l is the path length (1 cm).

ε_{OCR}, the extinction of OCR (dissolved in 0.1% and 0.5% (v/v) ACN, respectively) in different concentrations was determined for every wavelength with a Perkin Elmer LAMBDA 20 UV-VIS spectral photometer (PerkinElmer LAS GmbH, Rodgau, Germany). As consequence of the sparse solubility, the measured concentrations of OCR differed from the initial nominal concentrations of all samples. Therefore, the exact concentrations were analyzed by HPLC-UV. The obtained data were used to calculate the molar extinction coefficient.

Due to the overlap of the emitted light of the lamp and the absorption spectra of OCR Eq. (5) was applied for a wavelength range from 200 to 400 nm, to calculate the quantum yield of OCR (Φ_{OCR}) for 0.1 and 0.5% ACN (v/v) concentration:

$$\Phi_{OCR} = \frac{\frac{dc}{dt}}{2.303\cdot\sum_{200\ nm}^{400\ nm}\varepsilon_{OCR}\cdot J_{abs}\cdot c_0\cdot l} \tag{5}$$

In Eq. (5), dc/dt represents the initial elimination rate of OCR, ε_{OCR} the molar absorption coefficient of OCR, J_{abs} is the absolute photon flux, c_0 is the initial concentration of OCR, and l is the path length (1 cm).

3. Results and discussion

3.1. Photolysis of OCR

Testing the photolysis of acetonitrile in water and analyzing the non purgeable organic carbon (NPOC) revealed constant values during 256 min irradiation. Therefore, no reaction of acetonitrile with the UV filters or the TPs was expected. So far, literature reported that OCR is photostable because another lamp was used (Gaspar and Maia Campos, 2006). All photolysis experiments followed first-order kinetics (Fig. 1). Comparing the photolysis of OCR at an initial concentration of 1 mg·L^{-1} which contained 0.1% and 0.5% ACN (v/v) there was no difference in photolysis rate constants and half-lives (Table 2). Fig. 1A illustrates also that at a concentration of 0.1% ACN OCR was completely eliminated after 192 min while the experiment with 0.5% ACN needed 256 min for the elimination of the parent compound below the limit of detection (LOD). This indicates that a higher concentration of ACN slightly slows down the degradation rate. The photolysis experiment with a start concentration about 5 mg L^{-1} OCR demonstrated a high but incomplete removal during 256 min irradiation (Fig. 1A) which leads to a lower rate constant and a notable higher half-life (Table 2). The reduction of the degradation rate at the higher concentration of OCR might be ascribed to a shielding effect of the molecules, meaning that molecules that are closer to the lamp become irradiated first. Another reason could be the limited solubility of OCR in water and due a bit by bit solution further photolysis could take place. In contrast to our results, literature stated high photostability for OCR which was irradiated by artificial sunlight (halogen lamp, 290–800 nm, Rodil et al., 2009) or UV-A lamp (Ricci et al., 2003) or at least very high half-lives about 96 h in experiments with a sun simulator (Allen et al., 1998). The reported photostabilities result from the emission spectra of the used lamps which were >290 nm while OCR also absorbs below 290 nm (see Fig. S1). Thus, irradiation with a lamp emitting radiation below 290 nm (e.g. the applied medium pressure Hg vapor lamp) is better able to induce photolysis of OCR. This can be explained due to a better overlapping of the absorption spectrum of OCR with the emission spectrum of the lamp used (200–400 nm). The calculated quantum yields at 200–400 nm for OCR dissolved in 0.1% and 0.5% (v/v) ACN

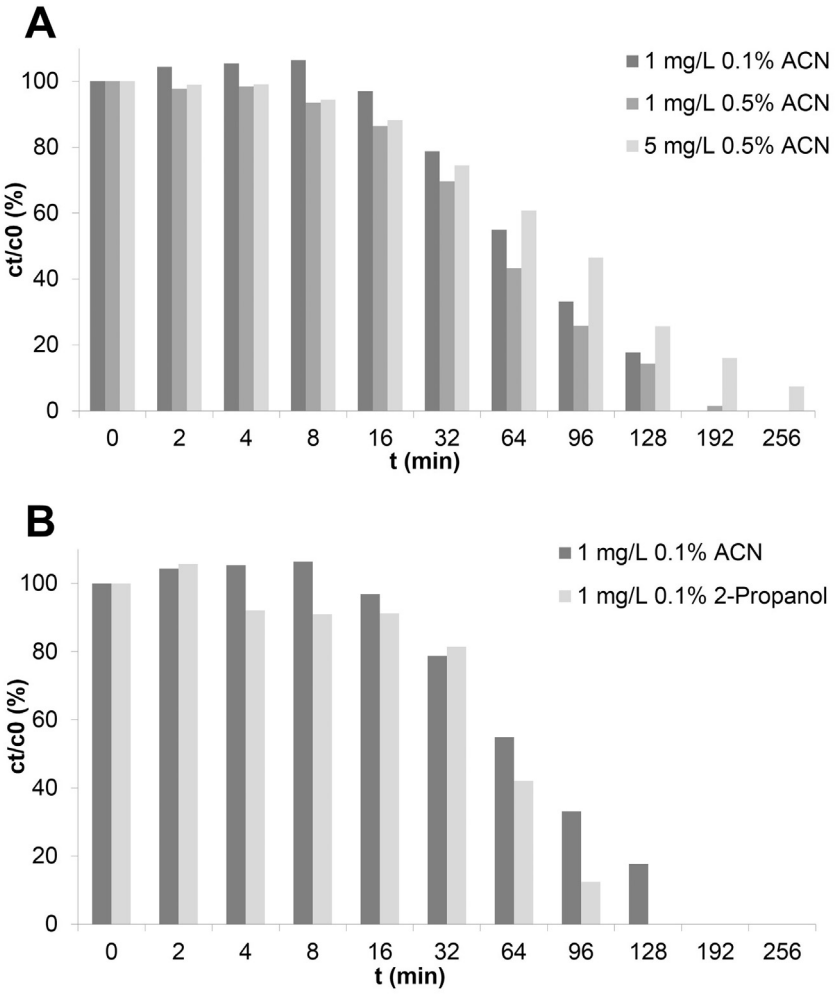

Fig. 1. The elimination of OCR during photolysis with A: 1 mg·L^{-1} and 5 mg·L^{-1} initial nominal concentrations of OCR in aqueous solution and varying ACN concentrations (0.1 and 0.5%) and for B: 1 mg L^{-1} OCR in aqueous solution with 0.1% (*v*/v) of ACN and 2-propanol; performed in duplicates.

were 0.0025 mol·Einstein^{-1} and 0.0033 mol·Einstein^{-1}, respectively (Table 2).

At the beginning of all photolysis experiments, no hydrogen peroxide could be determined. Between 32 min and 256 min the formation of H_2O_2 with a concentration up to 0.5 mg L^{-1} was detected indicating that ·OH were generated and formed H_2O_2. The generation of H_2O_2 under irradiation of the applied lamp was also reported e.g. for the photolysis of gabapentin and EHMC (Herrmann et al., 2015; Jentzsch et al., 2016).

To confirm the impact of photolysis by ROS, photolysis with the radical scavenger 2-propanol (Adam et al., 2000; Georgaki et al., 2014) was performed. The rate constant of OCR photolysis in 0.1% 2-propanol (v/v) was higher than for 0.1% ACN (Fig. 1B). Hence, ROS such as hydroxyl radicals (·OH) do not have a notable influence of the degradation.

Table 2
Overview of kinetic rate constants, half-lives and quantum yields of the photolysis of OCR under various experimental conditions with medium pressure Hg lamp (mean, $n = 2$).

C_{OCR} [mg L^{-1}]	solvent	amount of solvent [%] (v/v)	k [min^{-1}]	$t_{1/2}$ [min]	Φ [mol·Einstein^{-1}]
1	ACN	0.1	0.012	58.9	0.0025
1	ACN	0.5	0.016	46.3	0.0033
5	ACN	0.5	0.006	119.0	n.a.
1	2-propanol	0.1	0.022	31.8	n.a.

n.a.: not applicable.

Moreover, the used lamp emits light also in a wavelength range <200 nm and thus water separates hemolytically into hydroxyl and hydrogen radicals (Heit et al., 1998).

3.2. OCR's photo-TPs

The generation of photo-TPs was monitored for an initial concentration of 5 mg L^{-1} OCR in 0.5% ACN (v/v). By HPLC-UV analysis, four new peaks at retention times shorter than that of OCR were detected indicating that the TPs are more polar compared to OCR. To our best knowledge, this was the first time that TPs of OCR were detected after photolysis of an aqueous OCR solution. The higher polarity of a TP leads to a higher mobility of the substance in the aquatic environment compared to the parent compound (Boxall, 2009; Knepper et al., 2003; Reemtsma et al., 2016) which result in a hazard for humans or the environment. As TPs are usually unknown, TPs as new molecules could be more toxic than the parent compound (Stein et al., 2017; Kümmerer et al., 2018; Kümmerer et al., 2019). Fig. 2 illustrates the elimination of OCR (solid line) in comparison to the gradients of the photo-TPs (dashed lines). The TPs are represented by their relative peak areas A/A_0, whereas A is the UV peak area of the photo-TP being related to A_0 which is OCR's UV peak area at time point 0 min. After their formation, all TPs are further transformed but only two of them ($TP_{8.1}$ and $TP_{14.7}$) reached a concentration below their LOD within 256 min, respectively. An adequate irradiation time is needed to eliminate all TPs completely.

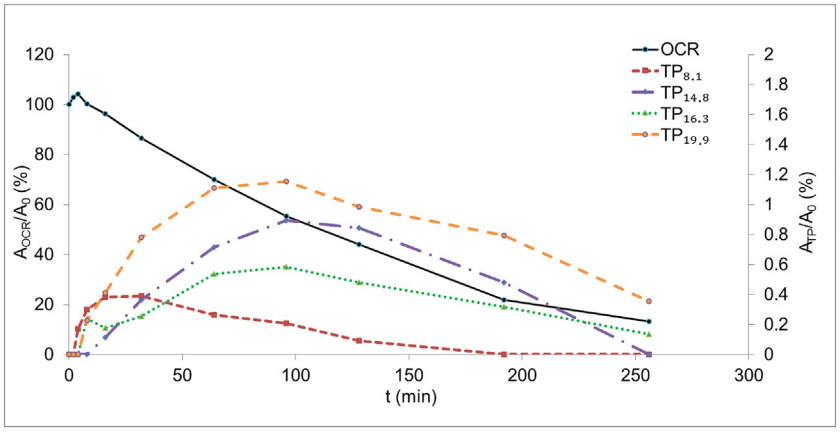

Fig. 2. Gradients (peak area over time) of the photo-TPs ($TP_{retention\ time\ (min)}$) of OCR and the primary elimination of OCR monitored by HPLC-UV analysis.

3.3. Comparison of OCR and EHMC photolysis

Fig. 3 shows that the multiwavelength UV irradiation method was suitable to degrade the individually tested UV filters. In addition, the data show that EHMC was eliminated faster than OCR. To be more precise, EHMC was completely eliminated within 64 min while some OCR was still remaining after 256 min irradiation. This difference is reflected in the elimination rate constants, too: For example, EHMC with an initial concentration of 5 mg·L^{-1} (in 0.5% ACN (v/v)) has an elimination rate constant about 0.33 min^{-1} which translated to a half-life of 2.1 min (Jentzsch et al., 2016) whereas the same experiment with OCR lead to a degradation rate constant about 0.006 min^{-1} and a corresponding half-life of 119.0 min (Table 2). This stems from the different overlapping of the absorption spectra with the emission spectra of the lamp (Supplementary material, Fig. S1). The investigation of the influence of the applied concentration of ACN on the degradation kinetics showed that a higher ACN concentration during the photolysis of 1 mg L^{-1} EHMC had a notable slowing down effect on the degradation (Fig. 3). In contrast, there was no difference in the degradation of OCR at a concentration 1 mg L^{-1} in presence of 0.1% and 0.5% ACN (Figs. 1A and 3). The stronger influence of ACN on the photodegradation of EHMC than on the degradation of OCR is reducible to the higher degradation rate of EHMC. Comparing the quantum yield of the experiment with 1 mg·L^{-1} initial concentration in 0.5% ACN demonstrates that they had the same order of magnitude and no difference with a quantum yield about 0.0023 ± 0.0001 mol·$Einstein^{-1}$ for EHMC (Jentzsch et al., 2016) and 0.0033 ± 0.0010 mol·$Einstein^{-1}$ for OCR (Table 2). Just as the above mentioned elimination rates vary for the two individual UV filters, the occurrence of the TPs and their gradients (illustrated in Fig. 2 and Table 4) likewise differ depending on the tested UV filter. In particular, the TPs of EHMC detected by HPLC-UV were formed and subsequently degraded within 64 min (Table 4 and Jentzsch et al., 2016). In contrast, the four TPs of OCR had their peak maximum between 16 and 64 min and were either completely eliminated ($TP_{8.1}$ and $TP_{14.7}$) or eliminated with some, undefined amounts remaining after 256 min irradiation ($TP_{16.2}$ and $TP_{19.8}$). In general, the comparison of TPs generated during the photolysis of OCR alone and EHMC alone shows that all retention times are different indicating that the TPs of OCR and for EHMC are different.

During photolysis of both substances the formation of H_2O_2 was detected. For EHMC, LC-MS analysis of the TPs proved the formation of oxidized and hydroxylated EHMC (Jentzsch et al., 2016) indicating a reaction of EHMC with ·OH.

3.4. Mixture effects in photolysis

Fig. 4 illustrates the course of the relative peak area of the co-eluting peaks ($A_t/A_{peak,total}$ x 100%) with time and how the plots were used for the evaluation of k and $t_{1/2}$. Table 3 concludes the kinetic values, which were evaluated in Fig. 4. In mixture, both UV filters behave kinetically the same way as reported for the individual kinetics. The photolysis of EHMC in mixture led to a reduction of the degradation kinetics of EHMC compared to the degradation of the single compound. The photolysis of the single substance EHMC has a half-life about 2 min at an

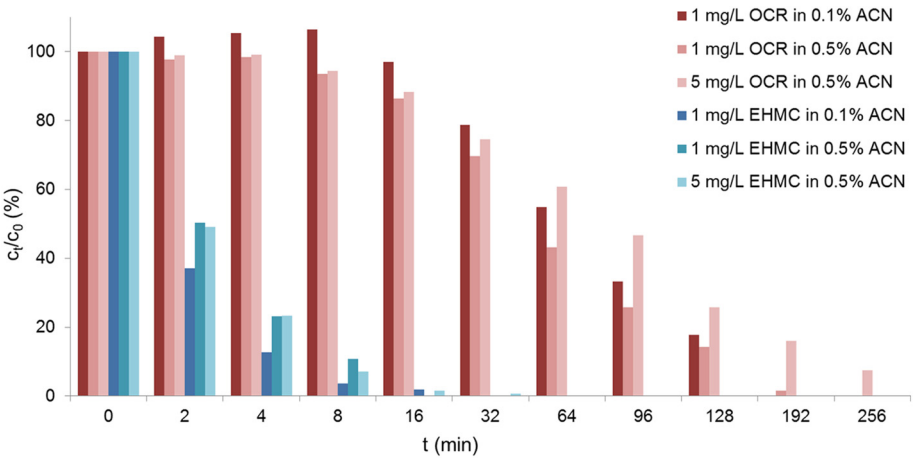

Fig. 3. Comparison of the degradation of OCR (red) and EHMC (blue) under different conditions with varying initial concentrations and varying ACN concentrations. (For interpretation of the references to color in this figure legend, the reader is referred to the web version of this article.)

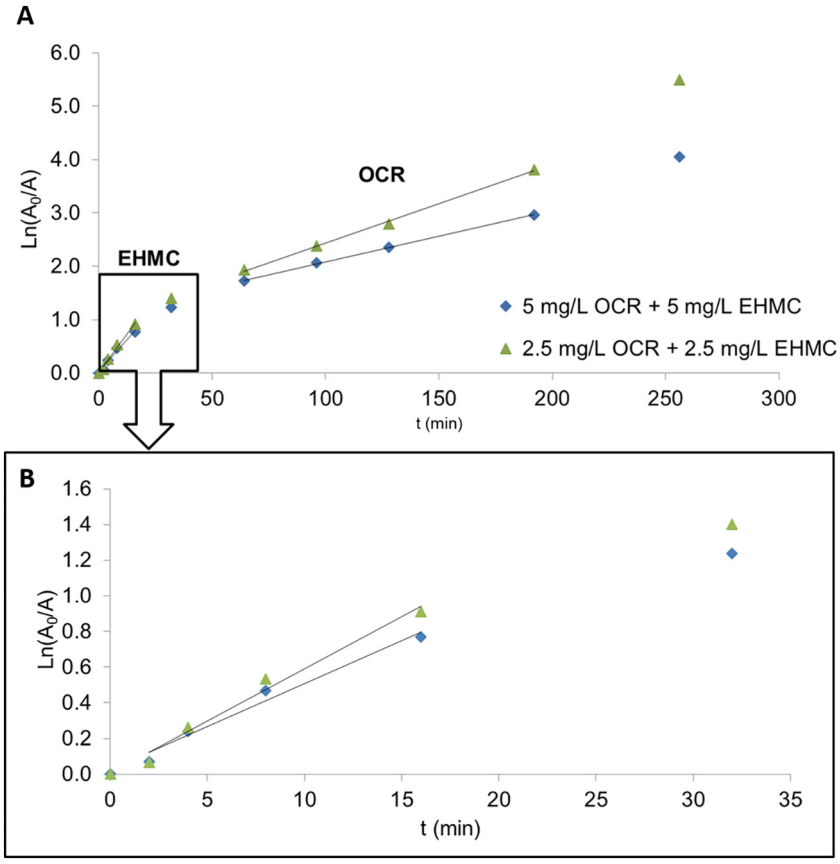

Fig. 4. Photo degradation of the mixture of OCR and EHMC with an initial concentration of 2.5 ppm each (green triangles) and 5 ppm each (blue diamond). (A): Natural logarithm of the areas of the peak of the parent compounds which co-elute when measured with HPLC-UV plotted against the sampling times; comparison of the curves with different initial concentrations; Linear fittings for the determination of k_{EHMC} and k_{OCR}. (B): Magnification of the linear trend curves for EHMC. (For interpretation of the references to color in this figure legend, the reader is referred to the web version of this article.)

initial concentration of 5 mg·L^{-1} EHMC (Jentzsch et al., 2016) while the half-lives in mixture range from 11.8 min to 14.3 min depending on the initial concentration (Table 3). This slower photolysis substances in presence of OCR is in accordance with Gaspar and Maia Campos (2006). For OCR a conversely effect was observed. While the photolysis of 5 mg·L^{-1} OCR alone led to a half-life about 119.0 ± 35.9 min (Table 2) the half-lives of the photolysis of the mixture revealed lower half-lives for OCR ranging from 47.2 min to 72.1 min (Table 3). A possible reason for the faster degradation of OCR might be the formation of radicals of EHMC that react with OCR. In consequence, the post-treatment of GW containing a mixture of MPs by UV irradiation needs to take interactions between the MPs into consideration. Results received for single compounds cannot be transferred to the mixtures directly, data on mixtures themselves are essential.

In order to allow a comparison of the TPs generated in the different photolysis experiments Table 4 lists the detected TPs named by retention time and sorted by their increasing retention time. The kinetics of each TP in Table 4 is characterized by displaying the sampling points at which it was detected and highlighting the peak maximum (in bold). These different kinetics of the TPs help correlate of UV peaks that appear during the photolysis of the mixture of OCR and EHMC with the TP peaks with those that were detected in the experiment with the individual UV filters. For example, the later formation of the TPs in mixture could be explained by the lower degradation rate of EHMC in the mixture experiment.

The comparison of TPs generated during the photolysis of the individual UV filters and of the OCR-EHMC-mixture shows that some TPs ($TP_{11.2}$, $TP_{12.4}$, $TP_{14.6}$, $TP_{16.1}$ and $TP_{19.8}$) were formed when photolysed alone as well as in mixture. More precisely, OCR has four TPs ($TP_{8.1}$, $TP_{14.7}$, $TP_{16.2}$ and $TP_{19.8}$) and EHMC has six TPs ($TP_{6.4}$, $TP_{11.2}$, $TP_{12.4}$, $TP_{12.7}$, $TP_{17.6}$ and $TP_{19.1}$) when analyzed alone (Fig. 5 and Table 4) while during the photolysis of the mixture with 5 mg·L^{-1} of each UV filter 12 peaks appeared. Two of the TPs formed in the mixture experiment had exactly the same retention time as the TPs of EHMC ($TP_{11.2}$ and $TP_{12.4}$). The gradients are similar although the TPs in the OCR-EHMC-mixture experiment were formed slightly later and thus the maximum is shifted slightly from 8 min to 16 min for $TP_{11.2}$ or from 8 min to 32 min for $TP_{12.4}$. Three TPs that were formed in the mixture experiment were suggested to be ascribed to OCR (t_R: 14.6/14.7 min ($TP_{14.6}$), 16.1/16.2 min ($TP_{16.1}$), 19.8 min ($TP_{19.8}$)). Two of them showed a minimal shift in retention time but all of them are in good agreement regarding the gradients. Besides $TP_{11.2}$, $TP_{12.4}$, $TP_{14.6}$, $TP_{16.1}$ and $TP_{19.8}$ the photolyzed mixture of OCR and EHMC contains further seven additional TPs ($TP_{15.0}$, $TP_{17.2}$, $TP_{17.4}$, $TP_{17.7}$, $TP_{18.1}$, $TP_{18.7}$ and $TP_{20.3}$) which could not be directly associated with OCR or EHMC. The number of TPs that could be ascribed to EHMC or OCR decrease comparing the individual UV filter experiments with the mixture experiments (Fig. 5).

Table 3
Kinetic rate constants and half-lives for the photolysis of OCR (Table 2; n = 2) and EHMC (Jentzsch et al., 2016) as single compounds, respectively, and in as a mixture of OCR and EHMC (with medium pressure Hg lamp at two different initial concentrations calculated as presented in Fig. 4).

Tested system	Photolyzed individually (5 mg·L^{-1})		Photolyzed as mixture			
			2.5 mg·L^{-1} of each UV filter		5 mg·L^{-1} of each UV filter	
	EHMC	OCR	EHMC	OCR	EHMC	OCR
k [min^{-1}]	0.33	0.006 ± 0.002	0.059	0.015	0.048	0.010
$t_{1/2}$ [min]	2	119.0 ± 35.9	11.8	47.2	14.3	72.2

Table 4
Occurrence of HPLC peaks of possible TPs generated during photolysis of OCR individually, EHMC individually and a combination of both (OCR/EHMC, at two initial concentrations). The TPs are sorted by their retention time t_R and their gradients are displayed by the samples in which they were detected with the value of the peak maximum in bold.

Name	t_R (min)	OCR 5 mg·L^{-1}	EHMC 5 mg·L^{-1}	OCR/EHMC each 5 mg·L^{-1}	OCR/EHMC each 2.5 mg·L^{-1}
$TP_{6.4}$	6.4	–	8, **16**	–	–
$TP_{8.1}$	8.1	4, 8, **16**, **32**, 64, 96, 128	–	–	–
$TP_{11.2}$	11.2	–	0, 2, 4, **8**, 16, 32	0, 2, 4, 8, **16**, 32, 64	0, 2, 4, 8, **16**, 32, 64
$TP_{12.4}$	12.4	–	4, **8**, 16, 32	4, 8, 16, **32**, 64, 96	8, **16**, **32**
$TP_{12.7}$	12.7	–	4, **8**, **16**, 32	–	–
$TP_{14.6}$	14.6	–	–	32, **64**, 96, 128	**32**, 64, 96
$TP_{14.6}$	14.7	8, 16, 32, **64**, 96, 128	–	–	–
$TP_{15.0}$	15.0	–	–	**32**, 64, 96, 128	–
$TP_{16.1}$	16.1	–	–	16, 32, **64**, 96, 128, 192	32, **64**, 96
$TP_{16.1}$	16.2	4, 8, 16, 32, **64**, 96, 128, 192, 256	–	–	–
$TP_{17.2}$	17.2	–	–	32, 64, **96**, 128	–
$TP_{17.4}$	17.4	–	–	**8**, 16	–
$TP_{17.6}$	17.6	–	**4**, 8	–	–
$TP_{17.7}$	17.7	–	–	16, 32, **64**, 96, 128	–
$TP_{18.1}$	18.1	–	–	32, **64**, 96, 128	–
$TP_{18.7}$	18.7	–	–	16, **32**, 64	–
$TP_{19.1}$	19.1	–	**2**, 4	–	–
$TP_{19.8}$	19.8	4, 8, 16, 32, **64**, 96, 128, 192, 256	–	8, 16, 32, **64**, 96, 128, 192	8, 16, **32**, 64, 96, 128
$TP_{20.3}$	20.3	–	–	8, **16**, 32, 64	–

This could possibly be caused by reactions of TPs with each other or with other TPs or with the parent compound. Moreover, $TP_{11.2}$, $TP_{12.4}$, $TP_{14.6}$, $TP_{16.1}$ and $TP_{19.8}$ were detected at both concentrations in the photolysis of the mixture. These seven TPs indicate that mixture effects such as interactions of OCR and EHMC and/or interactions of TPs and parent compounds took place during the photolysis of the mixture (Fig. 5). In general, the peak size of UV peaks does not allow a statement on the concentration of the TP as long as the standard substances are not available for a calibration. But nevertheless, the appearance of the five TPs $TP_{11.2}$, $TP_{12.4}$, $TP_{14.6}$, $TP_{16.1}$ and $TP_{19.8}$ in the mixture experiment with the initial concentration of 2.5 mg L^{-1} indicates, that these TPs are the higher concentrated than the TPs $TP_{15.0}$, $TP_{17.2}$, $TP_{17.4}$, $TP_{17.7}$, $TP_{18.1}$, $TP_{18.7}$ and $TP_{20.3}$. During the photolysis of the mixtures no dead end

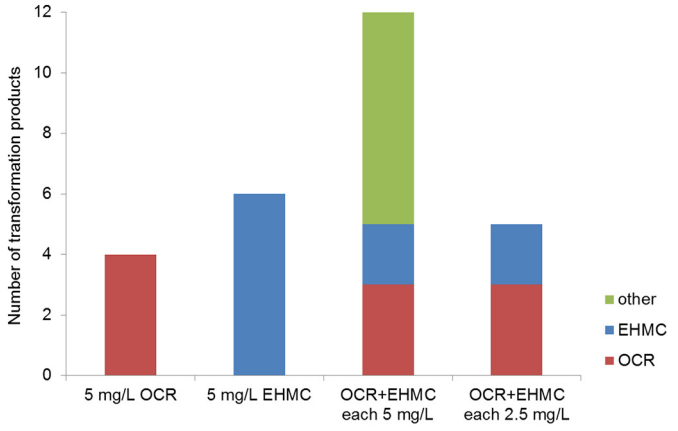

Fig. 5. Distribution of the formed TPs. Some TPs were formed directly from the parent compounds OCR (red) or EHMC (blue) and some result e.g. from mixture effects (green). (For interpretation of the references to color in this figure legend, the reader is referred to the web version of this article.)

TPs were found with the analytical method applied as they were all degraded after 256 min under the given experimental conditions. This indicates that UV irradiation as post-treatment of GW will generate more and new TPs. These could be eliminated if treatment time is long enough and spectra of compounds and of lamp used fit well enough.

4. Conclusions

In the present study OCR and a mixture of OCR and EHMC were irradiated with a medium pressure Hg lamp and compared with photolysis of single compounds. EHMC photolysed faster than OCR. For the first time, it was shown that in the mixture of OCR/EHMC EHMC was slower eliminated whereas OCR's elimination was quicker. Firstly, in the photolysed mixture TPs were detected which were also formed in the photolysis of the single compounds. Secondly, new TPs, possibly formed from reactions of TPs with each other and parent compounds, were formed. Eliminations of GW constituents depend on the type, i.e. spectrum of the lam applied as well as on treatment time. With the applied analytical method only UV active TPs were detectable. For a detection of all possible TPs analysis by HR-LC-MS (high resolution LC-MS) is recommended (Celeiro et al. (2019)). Therefore, the disappearance of TPs in photolysis does not exclude incomplete mineralization. Taken all this points together, it can be concluded that UV-photolysis may remove some more parent compounds and TPs on the one hand, however not all of them. Given the high energy input and need for long treatment advises to take measures at the source to prevent input of not mineralizable MPs into grey water in order to avoid follow up problems.

CRediT authorship contribution statement

F. Jentzsch: Writing - original draft **M. Reich:** Writing - review & editing. **K. Kümmerer:** Supervision, Writing - review & editing.**O. Olsson:** Supervision, Conceptualization, Funding acquisition, Project administration, Writing - review & editing.

Declaration of Competing Interest

The authors declare that they have no known competing financial interests or personal relationships that could have appeared to influence the work reported in this paper.

Acknowledgement

These results derive from a collaborative project in Lower Saxony and Israel with financial support from the Ministry of Science and Culture, Lower Saxony, Germany to research “Personal care products (PCPs) as source for micropollutants in Greywater – Identification, quantification and on-site treatment”, Project No. VWZN 2830.

Appendix A. Supplementary data

Supplementary data to this article can be found online at https://doi.org/10.1016/j.scitotenv.2019.134048.

References

Adam, W., Hartung, J., Okamoto, H., Saha-Möller, C.R., Špehar, K., 2000. N-Hydroxy-4-(4-chlorophenyl)thiazole-2(3H)-thione as a photochemical hydroxyl-radical source: photochemistry and oxidative damage of DNA (strand breaks) and 2′-deoxyguanosine (8-oxodG formation). Photochem. Photobiol. 72 (5), 619–624. https://doi.org/10.1562/0031-8655(2000)0720619NHCTHT2.0.CO2.

Alfiya, Y., Friedler, E., Westphal, J., Olsson, O., Dubowski, Y., 2017. Photodegradation of micropollutants using V-UV/UV-C processes; Tricloson as a model compound. Sci. Total Environ. 601–602, 397–404. https://doi.org/10.1016/j.scitotenv.2017.05.172.

Allen, J.M.; Allen, S.K.; Lingg, B. (1998) Photostabilities of several chemical compounds used as active ingredients in sunscreens In: Drugs: Photochemistry and Photostability; by: Albini, A.; Fasani, E.; Allen, J.M.; Allen, S.K.; Lingg, B. *Spec. Publ.-R. Soc. Chem.* (225) 171–181; doi:https://doi.org/10.1039/9781847550712-00171.

Balmer, M.E., Buser, H.-R., Müller, M.D., Poiger, T., 2005. Occurrence of some organic UV filters in wastewater, in surface waters, and in fish from Swiss Lakes. Environ. Sci. Technol. 39 (4), 953–962. https://doi.org/10.1021/es040055r.

Boxall, A., 2009. Transformation products of synthetic chemicals in the environment. Handb. Environ. Chem. 2 (Part P), 194 Springer, Berlin Heidelberg.

Broadbent, J.K., Martincigh, B.S., Raynor, M.W., Salter, L.F., Moulder, R., Sjöberg, P., Markides, K.E., 1996. Capillary supercritical fluid chromatography combined with atmospheric pressure chemical ionisation mass spectrometry for the investigation of photoproduct formation in the sunscreen absorber 2-ethylhexyl-p-methoxycinnamate. J. Chromatogr. A 732, 101–110. https://doi.org/10.1016/0021-9673(95)01199-4.

Buser, H.-R., Balmer, M.E., Schmid, P., Kohler, M., 2006. Occurrence of UV filters 4-methylbenzylidene camphor and octocrylene in fish from various Swiss Rivers with inputs from wastewater treatment plants. Environ. Sci. Technol. 40, 1427–1431. https://doi.org/10.1021/es052088s.

Celeiro, M., Rocio, Facorro, Dagnac, T., Vilar, V.J.P., Llopart, M., 2019. Photodegradation behavior of multiclass ultraviolet filters in the aquatic environment: removal strategies and photoproduct identification by liquid chromatography-high resolution mass spectrometry. J. Chromatogr. A 1596, 8–19. https://doi.org/10.1016/j.chroma.2019.02.065.

De Orsi, D., Giannini, G., Gagliardi, L., Porrà, R., Berri, S., Bolasco, A., Carpani, I., Tonelli, D., 2006. Simple extraction and HPLC determination of UV-A and UV-B filters in sunscreen products. Chromatographia 64 (9/10), 509–515. https://doi.org/10.1365/s10337-006-0074-9.

Díaz-Cruz, M.S., Llorca, M., Barceló, D., 2008. Organic UV filters and their photodegradates, metabolites and disinfection by-products in the aquatic environment. Trends Anal. Chem. 27 (10), 873–887. https://doi.org/10.1016/j.trac.2008.08.012.

Dondi, D., Albini, A., Serpone, N., 2006. Interactions between different solar UVB/UVA filters contained in commercial suncreams and consequent loss of UV protection. Photochem. Photobiol. Sci. 5, 835–843. https://doi.org/10.1039/B606768A.

Eriksson, E., Donner, E., Ledin, A., 2010. Presence of selected priority and personal care substances in an onsite bathroom greywater treatment facility. Water Sci. Technol. 62 (12), 2889–2898. https://doi.org/10.2166/wst.2010.988.

Fatta-Kassinos, D., Vasquez, M.I., Kümmerer, K., 2011. Transformation products of pharmaceuticals in surface waters and wastewater formed during photolysis and advanced oxidation processes – degradation, elucidation of byproducts and assessment of their biological potency. Chemosphere 85 (5), 693–709. https://doi.org/10.1016/j.chemosphere.2011.06.082.

Fent, K., Kunz, P.Y., Gomez, E., 2008. UV filters in the aquatic environment induce hormonal effects and affect fertility and reproduction in fish. Chimia 62 (5), 368–375. https://doi.org/10.2533/chimia.2008.368.

Gaspar, L.R., Maia Campos, P.M.B.G., 2006. Evaluation of the photostability of different UV filter combinations in a sunscreen. Int. J. Pharm. 307, 123–128. https://doi.org/10.1016/j.ijpharm.2005.08.029.

Georgaki, I., Vasilaki, E., Katsarakis, N., 2014. A study on the degradation of carbamazepine and ibuprofen by TiO_2 & ZnO photocatalysis upon UV/visible-light irradiation. Am. J. Anal. Chem. 5, 518–534. https://doi.org/10.4236/ajac.2014.58060.

Haddad, T., Kümmerer, K., 2014. Characterization of photo-transformation products of the antibiotic drug ciprofloxacin with liquid chromatography–tandem mass spectrometry in combination with accurate mass determination using an LTQ-Orbitrap. Chemposphere 115, 40–46. https://doi.org/10.1016/j.chemosphere.2014.02.013.

Heit, G., Neuner, A., Saugy, P.-Y., Braun, A.-m., 1998. Vacuum-UV (172 nm) actinometry. The quantum yield of the photolysis of water. J. Phys. Chem. A 102, 5551–5561. https://doi.org/10.1021/jp980130i.

Hernández-Leal, L., Vieno, N., Temmink, H., Zeeman, G., Buisman, C.J.N., 2010. Occurrence of xenobiotics in gray water and removal in three biological treatment systems. Environ. Sci. Technol. 44 (17), 6835–6842. https://doi.org/10.1021/es101509e.

Herrmann, M., Menz, J., Olsson, O., Kümmerer, K., 2015. Identification of phototransformation products of the antiepileptic drug gabapentin: biodegradability and initial assessment of toxicity. Water Res. 85 (11451), 11–21. https://doi.org/10.1016/j.watres.2015.08.004.

Jentzsch, F., Olsson, O., Westphal, J., Reich, M., Leder, C., Kümmerer, K., 2016. Photodegradation of the UV filter ethylhexyl methoxycinnamate under ultraviolet light: identification and in silico assessment of photo-transformation products in the context of grey water reuse. Sci. Total Environ. (16), 31701–31706 https://doi.org/10.1016/j.scitotenv.2016.08.017.

Knepper, T.P., de Voogt, P., Barceló, D., 2003. Analysis and fate of surfactants in the aquatic environment. Comprehensive Analytical Chemistry. vol. XL. Elsevier Science, Amsterdam, p. 808.

Kümmerer, K., Dionysiou, D.D., Olsson, O., Fatta-Kassions, D., 2018. **A** path to clean water. Science 361 (6399), 222–224. https://doi.org/10.1126/science.aau2405.

Kümmerer, K., Dionysiou, D.D., Olsson, O., Fatta-Kassions, D., 2019. Reducing aquatic micropollutants – increasing the focus on input prevention and integrated emission management. Sci. Total Environ. 652, 836–850. https://doi.org/10.1016/j.scitotenv.2018.10.219.

Kunz, P.Y., Fent, K., 2006. Multiple hormonal activities of UV filters and comparison of in vivo and in vitro estrogenic activity of ethyl-4-aminobenzoate in fish. Aquat. Toxicol. 79, 305–324. https://doi.org/10.1016/j.aquatox.2006.06.016.

MacManus-Spencer, L.A., Tse, M.L., Klein, J.L., Kracunas, A.E., 2011. Aqueous photolysis of the organic ultraviolet filter chemical octyl methoxycinnamate. Environ. Sci. Technol. 45, 3931–3937. https://doi.org/10.1021/es103682a.

Mahmoud, W.M.M., Toolaram, A.P., Menz, J., Leder, C., Schneider, M., Kümmerer, K., 2014. Identification of Phototransformation products of thalidomide and mixture toxicity assessment: an experimental and quantitative structural activity relationships (QSAR) approach. Water Res. 4, 11–22. https://doi.org/10.1016/j.watres.2013.11.014.

Martinez-Hernandez, V., Meffe, R., Herrera, S., Arranz, E., de Bustamante, I., 2014. Sorption/desorption of non-hydrophobic and ionisable pharmaceutical and personal care products from reclaimed water onto/from a natural sediment. Sci. Total Environ. 472, 273–281. https://doi.org/10.1016/j.scitotenv.2013.11.036.

Mathon, B., Choubert, J.-M., Miege, C., Coquery, M., 2016. A review of the photodegradability and transformation products of 13 pharmaceuticals and pesticides relevant to sewage polishing treatment. Sci. Total Environ. 551–552, 712–724. https://doi.org/10.1016/j.scitotenv.2016.02.009.

OECD, 2008. Test No. 316: Phototransformation of Chemicals in Water – Direct Photolysis, OECD Guidelines for the Testing of Chemicals, Section 3. OECD Publishing, Paris https://doi.org/10.1787/2074577x.

Palm, W.U., Zetzsch, C., 1996. Investigation of the photochemistry and quantum yields of triazines using polychromatic irradiation and UV-spectroscopy as analytical tool. Int. J. Environ. Anal. Chem. 65 (1–4), 313–329. https://doi.org/10.1080/03067319608045564.

Palm, W.U., Millet, M., Zetzsch, C., 1997. Photochemical reactions of metamitron. Chemosphere 35 (5), 1117–1130. https://doi.org/10.1016/S0045-6535(97)00176-8.

Poiger, T., Buser, H.-R., Balmer, M.E., Bergqvist, P.-A., Müller, M.D., 2004. Occurrence of UV filter compounds from sunscreens in surface waters: regional mass balance in two Swiss lakes. Chemosphere 55 (7), 951–963. https://doi.org/10.1016/j.chemosphere.2004.01.012.

Reemtsma, T., Berger, U., Arp, H.P.H., Gallard, H., Knepper, T.P., Neumann, M., Quintana, J.B., de Voogt, P., 2016. Mind the gap: persistent and mobile organic compounds — water contaminants that slip through. Environ. Sci. Technol. 50 (19), 10308–10315. https://doi.org/10.1021/acs.est.6b03338.

Ricci, A., Chrétien, M.N., Maretti, L., Scaiano, J.C., 2003. TiO_2-promoted mineralization of organic sunscreens in water suspension and sodium dodecyl sulfate micelles. Photochem. Photobiol. Sci. 2, 487–492. https://doi.org/10.1039/b212815b.

Rodil, R., Möder, M., Altenburger, R., Schmitt-Jansen, M., 2009. Photostability and phytotoxicity of selected sunscreen agents and their degradation mixtures in water. Anal. Bioanal. Chem. 395, 1513–1524. https://doi.org/10.1007/s00216-009-3113-1.

Salgado, R., Pereira, V.J., Carvalho, G., Soeiro, R., Gaffney, V., Almeida, C., Vale Cardoso, V., Ferreira, E., Benoliel, M.J., Ternes, T.A., Oehmen, A., Reis, M.A.M., Noronha, J.P., 2013. Photodegradation kinetics and transformation products of ketoprofen, diclofenac and atenolol in pure water and treated wastewater. J. Hazard. Mater. 244-245, 516–527. https://doi.org/10.1016/j.jhazmat.2012.10.039.

Scalia, S., Mezzena, M., 2009. Incorporation in lipid microparticles of the UVA filter, butyl methoxydibenzoylmethane combined with the UVB filter, octocrylene: effect on photostability. AAPS PharmSciTech 10 (2), 384–390. https://doi.org/10.1208/s12249-009-9217-2.

Stein, H.V., Berg, C.J., Maung, J.N., O'Connor, L.E., Pagano, A.E., MacManus-Spencer, L.A., Paulick, M.G., 2017. Photolysis and cellular toxicities of the organic ultraviolet filter chemical octyl methoxycinnamate and its photoproducts. Environ. Sci.: Processes Impacts 19, 851–860. https://doi.org/10.1039/C7EM00059F.

Zeng, X., Chen, J., Qu, R., Feng, M., Wang, Z., 2017. Degradation of octafluorodibenzo-p-dioxin by UV/Fe(II)/potassium monopersulfate system: kinetics, influence of coexisting chemicals, degradation products and pathways. Chem. Eng. J. 319, 98–107. https://doi.org/10.1016/j.cej.2017.02.152.

Supplementary materials

Photolysis of mixtures of UV filters octocrylene and ethylhexyl methoxycinnamate leads to formation of mixed transformation products and different kinetics

F. Jentzsch, M. Reich, K. Kümmerer, O. Olsson*

Sustainable Chemistry and Material Resources, Institute of Sustainable and Environmental Chemistry, Faculty of Sustainability, Leuphana University of Lüneburg, Universitätsallee 1, DE – 21335 Lüneburg, Germany

* Corresponding author address: O. Olsson, Sustainable Chemistry and Material Resources, Institute of Sustainable and Environmental Chemistry, C.13.313a, Universitätsallee 1, DE – 21335 Lüneburg, Germany. Tel.: +49 4131 677-2291.

E-mail addresses: Franziska.Jentzsch@leuphana.de (F. Jentzsch), marco.reich@leuphana.de (M. Reich), klaus.kuemmerer@leuphana.de (K. Kümmerer), oliver.olsson@leuphana.de (O. Olsson).

Characteristics of the medium pressure UV lamp and UV/vis spectra of OCR and EHMC

The relative photon flux of UV lamp was measured with a radiometer (Black Comet, Stellar.Net, Tampa, USA) and a chemical actinometers (metamitrone) was treated with the UV lamp to calculate the absolute photon flux (Figure S1) as described in the method part. The absorption spectrum of OCR and EHMC (in acetonitrile) was measured with a *Lambda 20* spectrometer (Perkin Elmer Inc., Waltham, Massachusetts, USA) (Figure S1).

Fig. S1 shows the absorption spectrum of OCR and EHMC dissolved in ACN and the absolute photon flux J_{abs} which was determined for the applied medium pressure Hg vapor lamp. Comparing the spectra displays good overlapping of the local maxima of the photon flux with the absorption maximum of OCR. This indicates a high potential of photo degradation of OCR during irradiation with the applied lamp. The absorption maximum of OCR at 303 nm matches with λ_{max} found in literature (Santos et al. 2012) and was the reason why the UV detection during HPLC analysis was set to 305 nm.

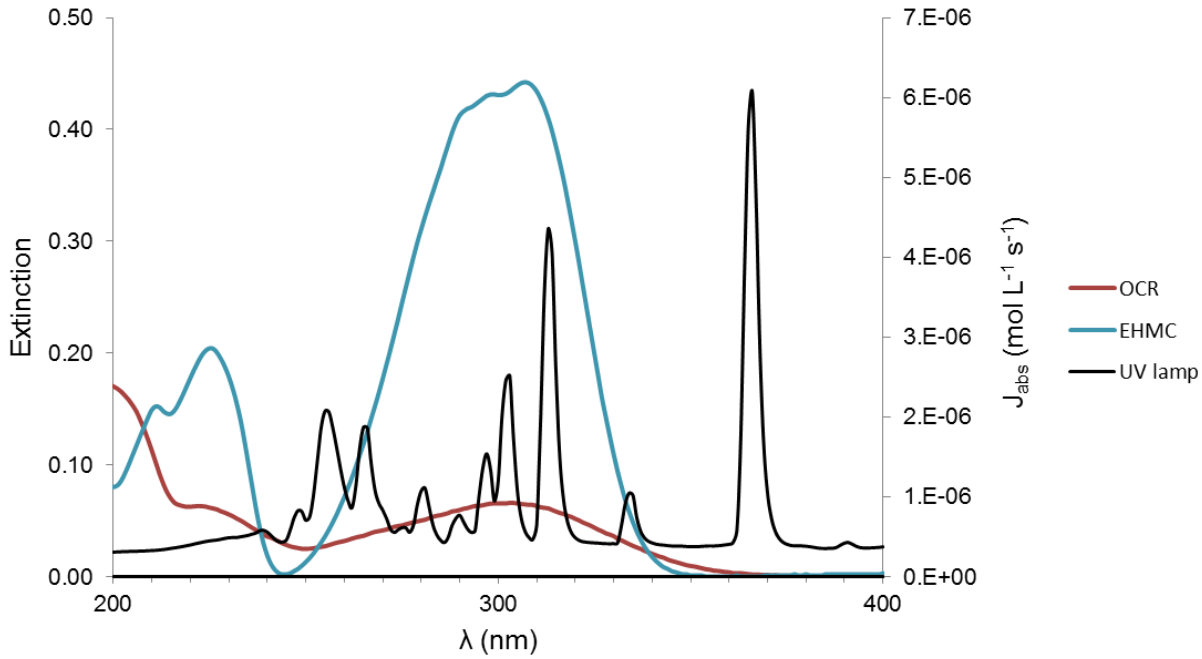

Figure S1, SM: Absolute photon flux J_{abs} of the medium pressure mercury vapor lamp (black line) and UV/vis absorption spectra of OCR (red) and EHMC (blue) in 100% acetonitrile.

The emission of the used medium pressure UV lamp was measured with UVpad (Opsytec Dr. Gröbel GmbH, Ettlingen, Germany) at a distance of 4 cm from the emission source in a black box within the range of 200 nm to 440 nm.

Table S1, SM: Light intensity emitted by the UV lamp measured with UVpad.

Radiation Intensity (D)	[mJ/(cm² · s)]
D (total)	2057
D (VIS)	642
D (UVA)	711
D (UVB)	606
D (UVC)	98

References

Santos, A. J. M.; Miranda, M. S.; Esteves da Silva, J. C. G. (2012) **The degradation products of UV filters in aqueous and chlorinated aqueous solutions** *Water Research* 46: 3167-3176

Artikel 3

Franziska Jentzsch, Klaus Kümmerer, Oliver Olsson

Status quo on identified transformation products of organic ultraviolet filters and their persistence.

International Journal of Cosmetic Science (2023) 45 (Suppl. 1): 101–126.

DOI: https://doi.org/10.1111/ics.12908

Received: 7 November 2022 | Accepted: 22 March 2023

DOI: 10.1111/ics.12908

International Journal of Cosmetic Science
SOCIÉTÉ FRANÇAISE DE COSMÉTOLOGIE

REVIEW ARTICLE

Status quo on identified transformation products of organic ultraviolet filters and their persistence

Franziska Jentzsch | **Klaus Kümmerer** | **Oliver Olsson**

Institute of Sustainable Chemistry, Faculty of Sustainability, Leuphana University of Lüneburg, Lüneburg, Germany

Correspondence
Oliver Olsson, Institute of Sustainable Chemistry, Faculty of Sustainability, Leuphana University of Lüneburg, Universitätsallee 1, DE-21335 Lüneburg, Germany.
Email: oliver.olsson@leuphana.de

Funding information
Ministry of Science and Culture, Lower Saxony, Germany, Grant/Award Number: VWZN 2830

Abstract

Organic micropollutants of concern—including organic UV filters (UVF)—are getting increasing attention. Personal care products such as sunscreens or cosmetic articles often contain large quantities of UVF. These substances enter the environment either directly (during outdoor activities) or indirectly (via sewages from households). Therefore, the removal or degradation of UVF by natural or technical treatment processes is important to understand. UVF are often incompletely removed and transformed to side products of incomplete mineralization by abiotic and biotic processes. An extensive overview on transformation products (TPs) is essential to systematically identify knowledge gaps and to derive research needs. While there are many reviews on the UVF themselves, the number of reviews which focus on their TPs is limited. Consequently, this review gives an overview on the latest findings regarding TPs of UVF. In this publication, known TPs of UVF, which were formed during abiotic and biotic processes, are reviewed. Target substances were defined and a literature database was reviewed for studies on TPs of the target substances. The first list of studies was shortened stepwise, thus generating a final list of studies which contained only the relevant studies. Since biodegradation is one of the most important pathways for removal of organic compounds from the environment, this review presents an overview on known TPs of organic UVF and their biodegradability, which determines their environmental fate. In this way, all identified TPs of UVF were listed and checked for information on their biodegradability. A total of 2731 records of studies were assessed. Forty-two studies, which assessed 46 processes that lead to the formation of identified TPs, were included in this review. One hundred and seventyseven different TPs resulting from 11 different UVF were identified. Little to no data on the biodegradability was found for TPs. This indicates a severe lack of data on the biodegradability of TPs of organic UVF substances. Since most TPs lack information on biodegradability, further research should provide information

on both—identity and biodegradability—of formed TPs to be able to assess their hazardousness for the environment.

KEYWORDS

abiotic/ biotic processes, fate, micropollutants, stability, suncare/ UV protection

Résumé

Les micropolluants organiques préoccupants, y compris les filtres UV organiques (UVF), font l'objet d'une attention croissante. Les produits de soins personnels tels que les écrans solaires ou les articles cosmétiques contiennent souvent de grandes quantités de filtres UV. Ces substances pénètrent dans l'environnement soit directement (lors d'activités de plein air), soit indirectement (via les eaux usées ménagères). Il est donc important de comprendre l'élimination ou la dégradation des UVF par des processus de traitement naturels ou techniques. Les UVF sont souvent éliminés de manière incomplète et transformés en produits secondaires de minéralisation incomplète par des processus abiotiques et biotiques. Il est essentiel de disposer d'une vue d'ensemble des produits de transformation pour identifier systématiquement les lacunes dans les connaissances et déterminer les besoins en matière de recherche. S'il existe de nombreuses études sur les UVF eux-mêmes, le nombre d'études portant sur leurs produits de transformation est limité. Par conséquent, cette étude donne un aperçu des dernières découvertes concernant les produits de transformation des UVF. Dans cette publication, les TP connus des UVF, qui ont été formés au cours de processus abiotiques et biotiques, sont passés en revue. Des substances cibles ont été définies et une base de données bibliographiques a été examinée pour trouver des études sur les PT des substances cibles. La première liste d'études a été raccourcie progressivement, ce qui a permis d'obtenir une liste finale d'études qui ne contenait que les études pertinentes. La biodégradation étant l'une des voies les plus importantes pour l'élimination des composés organiques de l'environnement, cette étude présente une vue d'ensemble des PT connus des UVF organiques et de leur biodégradabilité, qui détermine leur devenir dans l'environnement. Ainsi, tous les PT identifiés d'UVF ont été répertoriés et des informations sur leur biodégradabilité ont été vérifiées. Au total, 2731 enregistrements d'études ont été évalués. Quarante-deux études, qui ont évalué 46 processus conduisant à la formation des polluants organiques persistants identifiés, ont été incluses dans cette analyse. Cent soixante-dix- sept TP différents résultant de 11 UVF différents ont été identifiés. Peu ou pas de données sur la biodégradabilité ont été trouvées pour les PT. Cela indique un manque important de données sur la biodégradabilité des produits finis des substances UVF organiques. Étant donné que la plupart des PT manquent d'informations sur la biodégradabilité, les recherches futures devraient fournir des informations sur l'identité et la biodégradabilité des PT formés afin de pouvoir évaluer leur dangerosité pour l'environnement.

INTRODUCTION

Generally, ultraviolet filters (UVF) are divided into organic and inorganic UVF substances. This review includes only the commonly used organic UVF substances and their abiotic and biotic transformation.

The substance class of UVF shows a risk for the environment on the one hand, as UVF are included in the list of emerging contaminants [1], while its benefits (e.g. protection of human skin against solar radiation) are important for human health. However, the risk to human health should not be underestimated since the ubiquitous presence and the (often) high lipophilicity of UVF results in the potential of bioaccumulation and biomagnification of UVF in tissues of organisms along the food chain until they reach human tissues, for example, if people consume contaminated freshwater fish [2–4].

UVF are often applied in personal care products [1] or sunscreens [5]. After application, UVF are introduced into the environment directly by washing the UVF off of the skin [6] or clothes during recreational activities [7, 8]. Alternatively, UVF can enter the environment indirectly via waste water discharges [8], for example, after entering sewage systems following bathing [9], domestic uses [7] or from industrial discharge [10]. In consequence to their indirect input, UVF were frequently found in the wastewater recirculation system (in raw wastewater, treated wastewater or sewage sludge) [11–13]. Therefore, the indirect input of UVF represents one important path of how these substances reach the environment and explain their ubiquitous presence. On account of their chemical properties, UVF are not completely removed by applied treatment and removal techniques of wastewater [14–18] or greywater [19]. Nevertheless, the chemical properties are needed for the functionality of UVF. The reuse of waste and grey waters is becoming increasingly important in view of the climate change and the accompanying increasing water shortage. The occurrence of UVF in the aquatic environment has been studied frequently all around the world. In this way, many UVF have been detected in aqueous matrices: lake water [6, 9, 11, 20], river water [6, 11, 20, 21], seawater (beach) [7, 14, 20–22] or raw drinking water [12, 20]. A Spanish study detected the UVF ethylhexyl methoxycinnamate (EHMC) in groundwater [23]. Once UVF are present in the environment, their fate becomes an important issue. UVF were not only detected in the aquatic environment, but also in soil [24], sediments [25, 26] and biota such as corals [10], fish [11, 27–29], oyster tissue [25] or marine mussels [30]. Analysis of human samples showed that UVF are even present in urine and breast milk [31–33].

Conventional and advanced wastewater treatment often does not achieve full mineralization. Recently, the incomplete mineralization of organic contaminants within treatment and the environment progressively moved into environmental researcher's focus [34–39]. During transport and on introduction to the environment, various processes may alter the molecules of organic contaminants. These processes can either mineralize the contaminant, that is, complete degradation under formation of simple inorganic compounds such as carbon dioxide and water, or incomplete degradation of the molecule leading to the formation of transformation products (TPs), which could be found in the environment [40, 41]. TPs can be formed in abiotic or in biotic processes. Biotic processes are linked to living organisms and their metabolism and catabolism. Important abiotic processes are the degradation or transformation by hydrolysis, photolysis and redox processes [42, 43]. These processes can occur both in nature or within technical (treatment) systems [44–46]. TPs often differ from their parent compounds in properties such as persistence, mobility and toxicological potential [47–50]. The degradation of one substance with critical concerns could lead to the formation of one or more TPs with properties that are unknown or even worse compared to their parent compound. While the UVF themselves pose risks, their TPs may also have an impact [51–53]. In line with the Zero Pollution Ambition [54] both, parent compounds and TPs, should completely mineralize after their introduction into the environment latest to ensure a non-toxic environment [55]. That is to say both parent compounds and TPs, if introduced or formed in the environment, should not be persistent nor cause harmful effects.

Santos et al. (2012) reviewed the TPs of UVF formed during photolysis in aqueous solution [56]. They concluded that UVF can undergo photoisomerization and photodegradation processes under natural or artificial sunlight. The fact that the formed by-products do not have the same UV-protecting capabilities nor the same toxicological profiles compared to the parent compounds emphasizes the importance of a comprehensive review, which summarize the properties of (known) TPs. Apart from this review, further reviews have focused on analytical aspects and environmental levels of selected organic UVF [57] as well as their photostability [58]. The few studies which reviewed TPs did not concentrate on the properties of TPs such as biodegradation [56, 59, 60]. This gap is addressed in this review. All identified TPs of UVF are listed in this review, including the formation process (abiotic or biotic) under which the TPs of UVF were formed, and concludes with the current state of knowledge on the biodegradability of the identified TPs of UVF. For this, a list of all known TPs of UVF formed during water and wastewater treatment processes was established. Then, the kind of process (abiotic, biotic or both, except halogenation processes) for formation of individual TPs was

identified and subsequently the stability of the formed TPs was assessed. Based on this inventory, this review draws conclusions on how to handle and close these gaps.

METHODS

Target substance selection

The representative UVF included in this review were chosen according to two criteria: (i) if the UVF is authorized in the European Union (EU), whereas Table S1 (supplementary material, SM) lists all organic UVF, which fulfil this criterion (in accordance to a previous published list [61]), and (ii) those UVF, which do not fulfil the first criterion, but have been used frequently in products in the past and/or are found frequently in the environment. Table S2 (SM) lists these additional UVF which were included in the review to complement the EU-wide data sets. The review only includes those studies (or those TPs of UVF) for which the criteria and rules described hereafter are fulfilled.

For evaluation, the representative UVF were classified according to their structure in the following categories: (a) dibenzoylmethane derivatives, (b) benzophenone derivatives, (c) *p*-aminobenzoic acid and its derivatives, (d) benzimidazole derivatives, (e) camphor derivatives, (f) cinnamate derivatives and (g) octocrylene.

Generation of the final data set

Figure 1 illustrates the steps which were performed to generate the final literature data set. Hereafter, the applied criteria for each step will be explained in detail.

Step 1 | identification

During the pre-assessment, an initial set of records (Figure 1) was generated by reviewing the literature database Scopus from ELSEVIER with the keyword 'UV filter'. The search term 'UV filter' was combined with the terms 'biotic', 'abiotic', 'degradation', 'photolysis', 'biodegradation', 'biodegradability', 'transformation product', 'photoproduct', 'breakdown-product' or 'intermediate'. After step 1, the data set contains all studies, which are found in the above-mentioned data base using the above-mentioned keyword or keyword combinations.

Step 2 | screening

During the screening step, study duplicates were removed from the initial data set (Figure 1, second row) and the records were screened by title (Figure 1, third row) to remove those studies which clearly deal with other topics, for example, the term 'UV filter' also refers to glass lenses used in the field of photography.

Step 3 | eligibility examination

To examine the eligibility of the studies in the data set, some inclusion and exclusion rules were defined (Figure 1):

(i) to gain a more comprehensive data set, studies which tested only one UVF, as well as studies which identified TPs after exposure of mixtures of UVF, were considered;

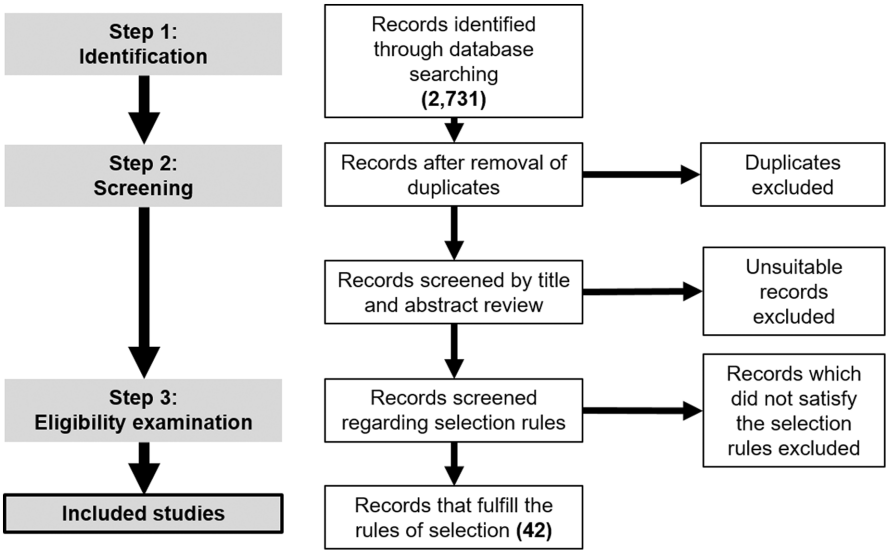

FIGURE 1 Procedure of how the studies were included in the preliminary record set.

(ii) studies which did not focus on abiotic and/or biotic processes of UVF, were removed from the list of studies reviewed;
(iii) studies which investigated TPs formed by halogenation were rejected, because this review does not focus on halogenation processes and TPs formed during these processes have already been reviewed [56–60];
(iv) studies which did not show a degradation of the parent compound or did not show the formation of TPs were rejected from the list;
(v) studies were filtered based on the presented information on the proposed TP reported in the study. Studies were included if they elucidated the structure of the TP (clear structures and/or explicit names and/or CAS (Chemical Abstracts Service) number). Studies with poor documentation (e.g. only the sum formula or only the molecular masses of TP were provided) were removed.

Documentation and handling of the final data set

For documentation purposes, a list of all found TPs was generated, which provides consistent information: the explicit name and if available the CAS No. as an identifier. If the documentation of the TP only included chemical structures, the names (and CAS No.) were searched using the database Scifinder or generated by the programs ChemDraw Professional (v19.0.1.28) and ACD/ChemSketch (ACD/Labs v2021.1.1). The resulting provisional list contained all found TPs sorted by the parent UVF substance(s) used in the experiments.

Refactoring of the final data set

Those TPs which were formed by the transformation of one and the same UVF and which had the same chemical structure, were combined as one entry including the corresponding references. In doing so, a total number of found TPs was gained (TP_{total}). Each identified TP was assigned a unique code which includes the abbreviation of the parent compound and a consecutive number, for example, 'BP-3 1' was the first listed TP of BP-3 (the latter being the code for the parent compound which is benzophenone-3 in this case). In a final step, TP_{total} was cleared of duplicates and triplicates to gain a total number of individual TPs (TP_{indiv}). This was necessary, since a comparison of the chemical structures of the TPs of different UVF showed that some TPs (the abovementioned duplicates and triplicates), were formed by transformation of different UVF. TP_{total} was subtracted by the total number of duplicates and triplicates to receive TP_{indiv}.

Addition of quality markers to the final data set

The data collected from the literature review were complemented by the addition of a quality marker which gives information on the kind of TPs generation and the transformation processes. This quality marker was introduced into the final list and gives additional information about the process type(s) (biotic or abiotic or both) in which the TP was formed. In addition, it was checked whether a degradation test was performed according to a published or adopted guideline (e.g. testing guideline No. 307 [62] of the Organization for Economic Co-operation and Development [OECD]), respectively, to be able to analyse the degree of harmonization and comparability.

Biodegradability of the TPs listed in the final literature data set

The available data of identified TPs were analysed concerning their biodegradability. Among others, the data analysis focused on the specific information about the examination or derivation of the biodegradability of the TP, for example, from experimental data, in agreement with OECD testing guidelines or modelled data from in silico analysis. Additionally, the European Chemicals Agency (ECHA) database (in particular the appropriate registration dossier provided by the ECHA) was used to collect more information on experimental biodegradability data of the identified TP, by using the CAS numbers or 'Simplified Molecular Input Line Entry Specification' (SMILES) codes. SMILES codes were generated from structures or names of the TPs using online available software [63, 64] or by using the programs ChemDraw Professional (v19.0.1.28) and ACD/ChemSketch (ACD/Labs v2021.1.1).

DEVELOPMENT OF AVAILABLE INTERNATIONAL SCIENTIFIC STUDIES ON UV FILTERS AND THEIR TRANSFORMATION PRODUCTS

Analysing the records for certain keywords ('UV filter' as well as 'UV filter' AND 'transformation product' OR

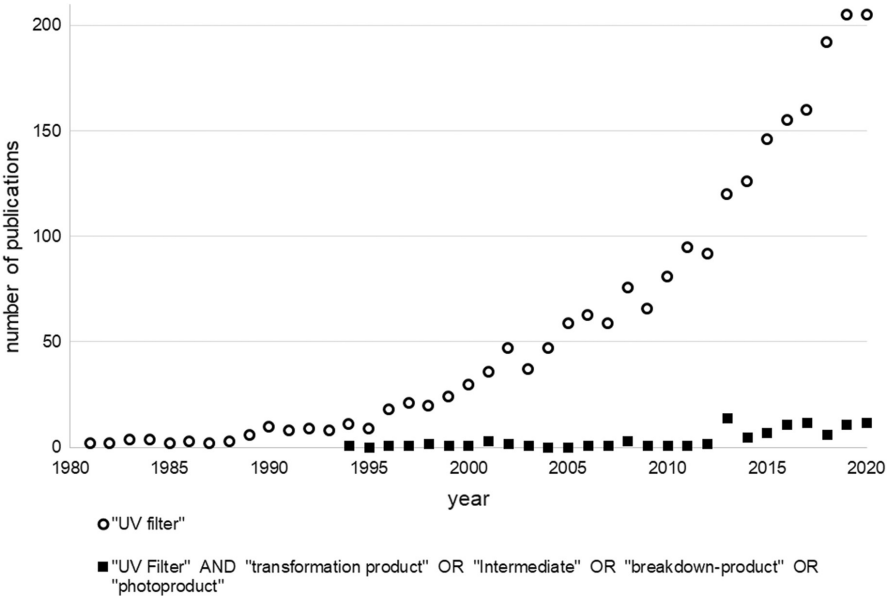

FIGURE 2 Analysis of the search results from 1980 to 2020 for the keywords 'UV filter' (black circles, total: 2268 publications per year) and from 1994 to 2020 (no entries before 1994) for the keyword combination 'UV Filter' AND 'transformation product' OR 'intermediate' OR 'breakdown-product' OR 'photoproduct' (filled squares, total: 100 publications per year) used in the review.

'intermediate' OR 'breakdown-product' OR 'photoproduct') in the applied database illustrates that the interest in studying (organic) UVF and their TPs has increased in recent years (Figure 2); more specifically, the number of publications on 'UV filter' per year doubled in the last 10 years (see black dots in Figure 2). In total, 2268 publications were listed for the time period between 1980 and 2020.

In contrast, the combination of the keywords 'UV filter' and 'TP' (and synonyms) yielded 100 publications which were published in the period from 1994 to 2020 (no entries before 1994). In 2020, the percentage of publications on UV filters which investigated TPs was recorded to be 5%. In 1994, the term 'intermediate', which was synonymously used for TP, was used in the context of research on UVF for the first time [65]. Since 2008, research has been using the term TP in the context of UVF [66] as the term TP gained more acceptance. One explanation for the increasing trend of using the term TP could be that in 2008, the Council Directive 76/768/EEC from 1976 was adjusted due to technological progress. Since then, compounds which could be used as UVF in cosmetic products had to be regulated applying the amendment from 2008. Furthermore, this regulation was implemented, for example, in national law in the United Kingdom (Cosmetic Products (Safety) Regulations 2008, Si 2008/1284) during this time. In addition, the technological development of analytical methods such as reverse phase liquid-chromatography coupled with mass spectrometry (LC-MS) for target and non-target analysis in environmental science [67] should not be neglected in context of TP analysis. In 2012, the number of publications on UVF and their TPs (and synonyms) began to rise strongly (see red squares in Figure 2). This is because TPs of UVF became more relevant in the environmental context in general and environmental laws and regulations in particular. An example is the US state of Hawaii. Here, the government passed a law in 2018 to ban sales of sunscreens which contain oxybenzone (BP-3) and EHMC to protect coral reefs from bleaching [68].

In comparison, the analogue evaluation of the term 'antibiotics' and its combination with TP (and synonyms) for the years 1980–2020 resulted in 335 times more publications on antibiotics compared to UVF. Therefore, the ratio of the publications per year in 2020 for the keyword itself and the combination with TP (and its synonyms) was calculated and resulted to be 1.5% for the term antibiotics; which is a notably lower percentage than for the term combination UVF and TP (4.4%). This shows, that compared to the research field of antibiotics, UVF on its own is a less researched topic within the universal field of UVF studies. The combination of UVF with TPs takes a larger space in this field which underlines the importance of TPs of UVF.

OUTCOME AND INSIGHTS OF THE LITERATURE SEARCH

A total of 2731 studies were identified in the literature database. The analysis showed that 42 studies met the applied criteria to be included in the further data assessment of this review (Table S3, SM). In these 42 studies, 46 abiotic and biotic processes of 11 UVF were investigated. One hundred and seventy-seven individual TPs were reported by the studies. One fifth of the surveyed studies focused on biological treatments of the UVF while more than half of the processes were light induced and about one quarter of the studies used advanced oxidation processes (AOP) or photocatalysis.

INCOMPLETE DEGRADATION OF UV FILTERS BY ABIOTIC AND BIOTIC PROCESSES

Table 1 summarizes the results of the reviewed abiotic and biotic processes (46 processes within 42 studies) which lead to an incomplete degradation of 11 UVF and potential generation of (stable) TPs. According to step 3 point (v), the applied selection rules include the requirement of a structural identification of the detected TPs. Therefore, Table 1 represents only those processes from studies which showed the formation of TPs of UVF and in addition identified the structure of the TPs. Studies which did not focus on the structural elucidation of the TPs were not included (e.g. [69]).

In general, abiotic processes were predominantly studied. The processes studied are quite diverse: The photolytic behaviour of some UVF (butyl methoxydibenzoylmethane [BMDM], ethylhexyl dimethyl 4-aminobenzoate [EHDP] and EHMC) was studied extensively. By contrast, no photolysis studies exist for other UVF (ethyl-4-aminobenzoate [Et-PABA], 4-methylbenzylidene camphor [MBC] and octocrylene [OCR]). Only 22% of the 42 reviewed studies focused on the degradation in biotic processes. Several studies investigated both abiotic and biotic degradation but only for few UVF. BP-3 was the substance, which was studied in most processes (11 processes) followed by EHDP (nine processes) and EHMC (eight processes). In contrast, for most UVF, only one (diethylamino hydroxybenzoyl hexyl benzoate [DHHB], Et-PABA and isoamyl *p*-methoxycinnamate [IMC]) or two (phenylbenzimidazole sulphonic acid [PBSA], MBC and OCR) processes were investigated. Furthermore, only two out of 42 studies documented that the degradation of the parent compounds was performed in line with OECD test guidelines. Thus, a harmonized approach is missing and complicates the comparison of the results.

The biotic processes included biodegradation with activated sludge [70], digested sludge under oxic and anoxic conditions [71] or sewage sludge [72], fungal biodegradation in sewage sludge by ligninolytic fungus *Trametes versicolor* [73, 74], biodegradation with green algae *Scenedesmus obliquus* [75], marine sediments usage [76] and microbial biofilm degradation with *Mycobacterium agri* [77].

TRANSFORMATION PRODUCTS OF UV FILTER AND UV FILTER MIXTURES

The reviewed studies demonstrate that UV filters become altered during biotic and abiotic processes and result in TP formation. In total, 187 TPs of 11 UVF and one UVF mixture were reviewed (TP_{total}). Figure 3 shows the number of listed TPs (TP_{total}: 187) per UVF. A strong variation in the number of TPs per UVF was found. This observation could be explained in different ways and strongly depends on the circumstances. For instance, if the parent compound does not form many TPs (e.g. IMC or OCR) or if a parent compound was investigated several times under several conditions (e.g. BP-3 and EHMC) or if the UVF was investigated few times or only once but forms a lot of TPs (e.g. Et-PABA).

Table 2 gives an overview on all 187 identified UVF-TPs (TP_{total}) which result from the review of 42 studies reporting 46 processes. An overview on the structures of the 187 TPs of the 11 UVF and the mixture of two UVF can be found in the supplementary (Figure S1–S12, SM).

According to the described method, this list of 187 found TPs (TP_{total}) was checked for TPs' redundancies. In doing so, several TPs which were formed by transformation of more than one substance (i.e. it is a TP common to more than one parent compound) under individual conditions (so-called duplicates and triplicates) were identified (for details, see text S1, SM). Furthermore, one (in the literature) wrongly assigned TP (EHMC 20 is IMC 1) was found. After exclusion of duplicates, triplicates and the wrong assignment a number of 177 identified, individual TPs (TP_{indiv}), resulted.

A comparison of the process type, under which individual TPs were formed, showed that out of the 177 individual TPs (TP_{indiv}), six TPs (BP-3 1, BP-3 18, EHDP 4, EHDP 5, EHMC 2 and EHMC 4) were formed in both—biotic *and* abiotic—processes. Consequently, the remaining TPs (97% of TP_{indiv}) were formed either in biotic *or* abiotic processes.

STABILITY OF TRANSFORMATION PRODUCTS OF UV FILTER

Biodegradability

Eight out of 42 studies that were included in the review dealt not only with the formation and identification of the TPs but also with their stability [19, 51, 71, 74, 85, 96, 97, 99]. Table 3 lists the reviewed literature which provides information on the stability of some TPs (of the UVF BP-3, EHMC and PBSA) regarding biodegradability and stability of TPs during photolytic or photocatalytic processes [19, 51, 71, 74, 85, 96, 97, 99]. Only three studies investigated the biodegradability of TPs, and it is noteworthy that all three studies were on TPs of BP-3 [71, 74, 85]. These studies showed that TPs of BP-3 were not stable: BP-3 1 and BP-3 2 were formed and subsequently degraded during photolytic processes [19]; BP-3 9 and BP-3 10 showed

TABLE 1 Overview of 46 abiotic and biotic processes of 11 UVF reported in 42 studies (n = number of studied processes).

	Processes													
	Photolysis		Advanced oxidation processes (AOP)						Biodegradation					
UV filter	Artificial UV-light[a]	Sun simulator	Light/TiO_2/H_2O_2	Light/H_2O_2	Light/TiO_2	Photo-Fenton (Fe^{3+})	Light/O_3	O_3	Algae	Fungus	Biofilm	Sludge	Marine sediment	Sum of studied processes
BMDM	4	2	0	0	0	0	0	0	0	0	0	0	0	6
BP-3	2	0	2	2	0	0	0	1	1	1	0	2	0	11
DHHB	1	0	0	0	0	0	0	0	0	0	0	0	0	1
PABA	1	0	1	0	0	1	0	0	0	0	0	0	0	3
EHDP	4	1	0	1	0	0	1	0	0	0	0	1	1	9
Et-PABA	0	0	0	0	1	0	0	0	0	0	0	0	0	1
PBSA	2	0	0	0	0	0	0	0	0	0	0	0	0	2
MBC	0	0	0	0	0	0	0	0	0	1	0	0	1	2
EHMC	5	1	0	0	0	0	0	1	0	0	0	1	0	8
IMC	1	0	0	0	0	0	0	0	0	0	0	0	0	1
OCR	0	0	0	0	0	0	0	1	0	0	1	0	0	2
Sum	20	4	3	3	1	1	1	3	1	2	1	4	2	46

[a]Especially: UV-A, UV-C or UV-C/V-UV.

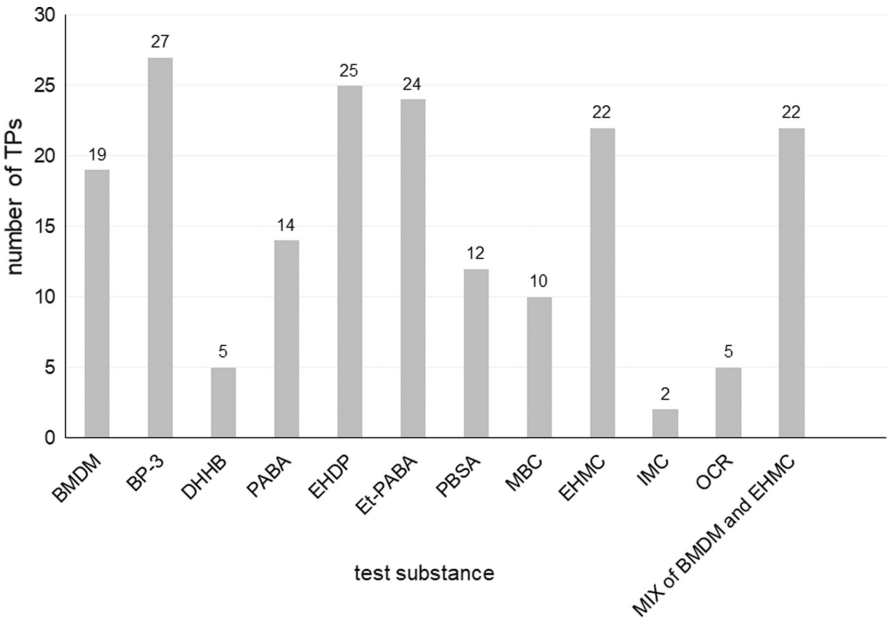

FIGURE 3 Number of known TPs per UVF (based on the total number TP_{total}: 187) for 11 UVF and a mixture of BMDM and EHMC (called 'MIX of BMDM and EHMC') based on 46 investigated processes from 42 reviewed studies.

biodegradability during biodegradation experiments with a fungus [74]; and the TPs of BP-3 (BP-3 1, BP-3 2, BP-3 3, BP-3 4, BP-3 5, BP-3 18, BP-3 21, BP-3 22, BP-3 23 and BP-3 24) formed during photocatalytic treatment (with TiO_2 and hydrogen peroxide) showed an increased biodegradability compared to the parent BP-3 [85]. In contrast, biodegradation of the TPs BP-3 1 and BP-3 18 was investigated under redox conditions: biodegradation was inhibited under oxic, nitrate-reducing and sulphate-reducing conditions [71].

Photostability

Two photolysis studies with EHMC showed contrary results for the dimeric TPs formed: Direct photolysis of EHMC lead to the formation of various TP, which showed different stability as several dimers appeared to be transient and some were photostable [97]. In contrast, a recent study on photolysis of EHMC showed that the formed and identified TPs of EHMC were non-persistent and subsequently degraded during the photolysis process [99].

In silico assessment of stability

A different approach to gain information on the stability of UVF-TPs was applied in the two studies on TPs of EHMC and PBSA: In a photolysis study, TPs of PBSA were identified and assessed with in silico methods. In the PBSA study, the software tool CASE Ultra from MultiCASE was used (short-term bacterial luminescence inhibition in the microtox assay, bacterial mutagenicity with two models a statistical model and an expert rule-based model). For all TPs, there were higher probabilities for bioconcentration and the same or lower biodegradability compared to the UVF PBSA itself were observed, suggesting that it is likely that PBSA TPs could be more persistent than PBSA [96]. In another study, the physicochemical properties of 33 TPs of the UVF EHMC, which were gathered from literature review, were estimated [51]. QSAR analysis of the reviewed TPs of EHMC were performed among other properties (molecular weight, melting point, boiling point, solubility, vapour pressure, bioconcentration factor, octanol–water partition coefficient, half-lives and long-range transport potential) concerning overall persistence [51] using the software tool EPI Suit™. Within the listed TPs of EHMC in this study on the properties, 17 TPs were relevant for this review (Table 3). The comparison of the predicted overall persistence (P_{OV}) of UVF (E)-EHMC and its TPs showed that three TPs (EHMC 4 (= (Z)-EHMC), EHMC 10 and EHMC 11) had the same P_{OV} as (E)-EHMC while six TPs (EHMC 1, EHMC 2, EHMC 7, EHMC 8, EHMC 9 and EHMC 16) had a lower P_{OV} than (E)-EHMC. This leads to the conclusion that for eight out of 17 TPs (47%), the persistence was predicted to be worse compared to the parent.

Interim conclusion on the stability of UVF-TPs according to the reviewed literature

In conclusion, information on the stability of TPs of UVF is very scarce in the literature. Moreover, the limited information that was available includes not only biodegradability but also non-biotic results (related to the stability of TPs under photolytic, photocatalytic and redox

TABLE 2 List of all reviewed TPs (TP_{total}: 187) of 11 UV filter substances and one mixture, assigned with name, CAS number and relevant transformation process.

Parent	Code	Name	CAS No.	Process	Reference
BMDM	BMDM 1	4-methoxybenzoic acid	100-09-4	Abiotic	[58, 78–82]
	BMDM 2	4-*tert*-buthylbenzoic acid	98-73-7	Abiotic	[58, 78–82]
	BMDM 3	3-hydroxy-1-(4-methoxy-2,4-cyclohexadien-1-yl)-3-(4-methoxyphenyl)-, (2Z)- 2-propen-1-one	2306713-02-8	Abiotic	[58, 80, 82]
	BMDM 4	1,4-bis(4-methoxyphenyl)-1,4-butanedione	15982-64-6	Abiotic	[58, 80, 82]
	BMDM 5	1,3-bis(4-methoxyphenyl)propane-1,3-dione	18362-51-1	Abiotic	[58, 78, 80, 83]
	BMDM 6	4-methoxybenzaldehyde (= anisaldehyde)	123-11-5	Abiotic	[58, 78, 81, 83]
	BMDM 7	4-*tert*-butylbenzaldehyde	939-97-9	Abiotic	[58, 78, 81, 83]
	BMDM 8	1-(4-methoxyphenyl)ethan-1-one	100-06-1	Abiotic	[58, 78, 83]
	BMDM 9	1-(4-*tert*-butylphenyl)-3-hydroxy-3-(4-methoxyphenyl)prop-2-en-1-one	1198075-35-2	Abiotic	[58]
	BMDM 10	*tert*-butylbenzene	98-06-6	Abiotic	[58]
	BMDM 11	2-(4-methoxyphenyl)-2-oxoacetaldehyde	1076-95-5	Abiotic	[58, 78]
	BMDM 12	2-(4-*tert*-butylphenyl)-2-oxoacetaldehyde	7062-64-8	Abiotic	[58, 78]
	BMDM 13	1-(4-*tert*-butylphenyl) ethanone (= p-*tert*-butylacetophenone = 1-(4-(1,1-dimethylethyl)phenyl)-ethanone)	943-27-1	Abiotic	[58, 78]
	BMDM 14	1,2-bis(4-*tert*-butylphenyl)ethane-1,2-dione (=1,2-bis(4-(1,1-dimethylethyl) phenyl)-1,2-ethanedione)	76471-78-8	Abiotic	[58, 78]
	BMDM 15	1-(4-*tert*-butylphenyl)-2-(4-methoxyphenyl)ethane-1,2-dione (= (4-(1,1-dimethylethyl)phenyl])(4-methoxyphenyl)- ethanedione)	166321-82-0	Abiotic	[58, 78, 80]
	BMDM 16	1-(4-(1,1-dimethylethyl)phenyl)-4-(4-methoxyphenyl)-1,4-butanedione	166321-83-1	Abiotic	[58, 78]
	BMDM 17	(Z)-1-(4-*tert*-butylphenyl)-3-hydroperoxy-3-(4-methoxyphenyl)prop-2-en-1-one	—	Abiotic	[58, 80]
	BMDM 18	4-methoxyphenol (= mequinol)	150-76-5	Abiotic	[58, 78, 81]
	BMDM 19	4-*tert*-butylphenol	98-54-4	Abiotic	[81]
BP-3	BP-3 1	2,4-dihydroxybenzophenone (= BP-1)	131-56-6	Abiotic, biotic	[19, 71, 74, 84, 85]
	BP-3 2	(2-hydroxy-4-methoxyphenyl)-(2-hydroxyphenyl)methanone (= dioxybenzone = 2,2′-dihydroxy-4-methoxy-benzophenone)	131-53-3	Abiotic	[19, 84–86]
	BP-3 3	1,3-benzenediol(= resorcinol)	108-46-3	Abiotic	[82, 85]
	BP-3 4	2-hydroxybenzaldehyde	90-02-8	Abiotic	[82, 85]
	BP-3 5	Benzoic acid	65-85-0	Abiotic	[82, 85]
	BP-3 6	1-methoxy-2,4-dimethylbenzene (= 2,4-dimethylanisole)	6738-23-4	Abiotic	[82, 87]
	BP-3 7	4,4′-dihydroxybenzophenone(=4DHB)	611-99-4	Biotic	[72, 74]
	BP-3 8	4-hydroxybenzophenone (=4HB)	1137-42-4	Biotic	[72, 74]

TABLE 2 (Continued)

Parent	Code	Name	CAS No.	Process	Reference
	BP-3 9	BP-3-hexose	—	Biotic	[74]
	BP-3 10	BP-3-pentose (xylose or ribose)	—	Biotic	[74]
	BP-3 11	3-methoxyphenol	150-19-6	Abiotic	[84]
	BP-3 12	3-methoxyxanthen-9-one	3722-52-9	Abiotic	[84]
	BP-3 13a	(2,5-dihydroxy-4-methoxyphenyl)-phenylmethanone	52811-37-7	Abiotic	[88]
	BP-3 13b	(2,6-dihydroxy-4-methoxyphenyl)-phenylmethanone	479-21-0	Abiotic	[88]
	BP-3 13c	(2,3-dihydroxy-4-methoxyphenyl)-phenylmethanone	3583641-0	Abiotic	[88]
	BP-3 14a	Phenyl(2,3,4,6-tetrahydroxyphenyl)methanone	—	Abiotic	[88]
	BP-3 14b	Phenyl(2,3,4,5-tetrahydroxyphenyl)methanone	—	Abiotic	[88]
	BP-3 15	2-hydroxy-4-methoxybenzoic acid (=4-methoxysalicylic acid)	2237-36-7	Biotic	[75]
	BP-3 16	4-methoxy-5-methylbenzene-1,2-diol	—	Biotic	[75]
	BP-3 17	(3,4,5-trimethylphenyl)methanol	39126-11-9	Biotic	[75]
	BP-3 18	4-methylphenol (= *p*-Cresol)	106-44-5	Abiotic, biotic	[71, 85]
	BP-3 19	(2-amino-4-methoxyphenyl)-phenylmethanone	37527-68-7	Abiotic	[86]
	BP-3 20	(4-methoxy-2-nitrophenyl)-phenylmethanone	1228191-31-8	Abiotic	[86]
	BP-3 21	Benzaldehyde	100-52-7	Abiotic	[85]
	BP-3 22	2-methylphenol (= o-cresol)	95-48-7	Abiotic	[85]
	BP-3 23	(2-methylphenyl) benzoate	617-02-7	Abiotic	[85]
	BP-3 24	Phenylmethanol (= benzyl alcohol)	100-51-6	Abiotic	[85]
DHHB	DHHB 1	Hexyl 2-(4-amino-2-hydroxybenzoyl)benzoate	—	Abiotic	[82]
	DHHB 2a	Hexyl 2-(4-(diethylamino)-2,3-dihydroxybenzoyl)benzoate	—	Abiotic	[82]
	DHHB 2b	Hexyl 2-(4-(diethylamino)-2,5-dihydroxybenzoyl)benzoate	—	Abiotic	[82]
	DHHB 2c	Hexyl 2-(4-(diethylamino)-2,6-dihydroxybenzoyl)benzoate	—	Abiotic	[82]
	DHHB 3	Hexyl 2-(4-(ethylamino)-2-hydroxybenzoyl)benzoate	—	Abiotic	[82]
PABA	PABA 1	Aniline (= benzenamine)	62-53-3	Abiotic	[89, 90]
	PABA 2	2-aminophenol	95-55-6	Abiotic	[89]
	PABA 3	Benzene-1,4-diol (= hydroquinone)	123-31-9	Abiotic	[89]
	PABA 4	Methyl 4-aminobenzoate	619-45-4	Abiotic	[82, 89]
	PABA 5a	4-amino-2-hydroxybenzoic acid	65-49-6	Abiotic	[82, 90]
	PABA 5b	4-amino-3-hydroxybenzoic acid	2374-03-0	Abiotic	[82, 90]
	PABA 6a	4-amino-2,6-dihydroxybenzoic acid	69727-10-2	Abiotic	[90]

(Continues)

TABLE 2 (Continued)

Parent	Code	Name	CAS No.	Process	Reference
	PABA 6b	4-amino-2,3-dihydroxybenzoic acid	742040-28-4	Abiotic	[90]
	PABA 6c	4-amino-2,5-dihydroxybenzoic acid	—	Abiotic	[90]
	PABA 6d	4-amino-3,5-dihydroxybenzoic acid	958232-24-1	Abiotic	[90]
	PABA 7a	3,4-dihydroxybenzoic acid	99-50-3	Abiotic	[90]
	PABA 7b	2,4-dihydroxybenzoic acid	89-86-1	Abiotic	[90]
	PABA 8	4-hydroxybenzoic acid	99-96-7	Abiotic	[82, 90]
	PABA 9	Benzoic acid	65-85-0	abiotic	[90]
EHDP	EHDP 1	2-ethylhexyl 4-(methylamino)benzoate (=4-(methylamino)-2-ethylhexyl ester benzoic acid)	158576-31-9	Abiotic	[58, 82, 91–93]
	EHDP 2	Methyl 4-(dimethylamino)benzoate (=4-(dimethylamino)-methyl ester benzoic acid)	1202-25-1	Abiotic	[82]
	EHDP 3	2-ethylhexyl 4-(*N*-methylformamido)benzoate	—	Abiotic	[58, 82]
	EHDP 4	4-(methylamino)benzoic acid	10541-83-0	Abiotic, biotic	[70, 76, 82, 93]
	EHDP 5	2-ethylhexyl 4-aminobenzoate (=4-amino-2-ethylhexyl ester benzoic acid)	26218-04-2	Abiotic, biotic	[58, 91–93]
	EHDP 6a	2-ethylhexyl 4-(dimethylamino)-2-methylbenzoate	—	Abiotic	[58, 92]
	EHDP 6b	2-ethylhexyl 4-(dimethylamino)-3-methylbenzoate	—	Abiotic	[58, 92]
	EHDP 7a	2-ethylhexyl 4-(dimethylamino)-2-hydroxybenzoate	—	Abiotic	[91]
	EHDP 7b	2-ethylhexyl 4-(dimethylamino)-3-hydroxybenzoate	—	Abiotic	[91]
	EHDP 8	2-ethylpentyl 4-(dimethylamino)benzoate	—	Biotic	[76]
	EHDP 9	2-(((cyclohexa-1,5-diene-1-carbonyl)oxy)methyl)butanedioic acid	—	Biotic	[76]
	EHDP 10	3-(((cyclohex-1-ene-1-carbonyl)oxy)methyl)pentanoic acid	—	Biotic	[76]
	EHDP 11	3-(((cyclohex-1-ene-1-carbonyl)oxy)methyl)-4-hydroxybutanoic acid (=4-((cyclohex-1-ene-1-carbonyl)oxy)-3-(hydroxymethyl)butanoic acid)	—	Biotic	[76]
	EHDP 12	2-ethylhexyl cyclohex-1-ene-1-carboxylate	—	Biotic	[76]
	EHDP 13	2-(((cyclohexanecarbonyl)oxy)methyl) butanoic acid	—	Biotic	[76]
	EHDP 14	2-(((cyclohexa-1,3-diene-1-carbonyl)oxy)methyl)-3-hydroxypropanoic acid (=3-((cyclohexa-1,3-diene-1-carbonyl)oxy)-2-(hydroxymethyl)propanoic acid)	—	Biotic	[76]
	EHDP 15	4-((cyclohexa-1,5-diene-1-carbonyl)oxy)butanoic acid	—	Biotic	[76]
	EHDP 16	2-hydroxybutyl cyclohexa-1,3-diene-1-carboxylate	—	Biotic	[76]
	EHDP 17	3-formylheptanedioic acid	—	Biotic	[76]
	EHDP 18	3-hydroxypropyl cyclohex-1-ene-1-carboxylate	—	Biotic	[76]

TABLE 2 (Continued)

Parent	Code	Name	CAS No.	Process	Reference
	EHDP 19	((cyclohex-1-ene-1-carbonyl)oxy)acetic acid	—	Biotic	[76]
	EHDP 20	3-hydroxypropyl cyclohexa-1,5-diene-1-carboxylate	—	Biotic	[76]
	EHDP 21	2-hydroxyethyl cyclohex-1-ene-1-carboxylate	—	Biotic	[76]
	EHDP 22	4-(dimethylamino)benzoic acid	619-84-1	Biotic	[76]
	EHDP 23	2-ethylhexan-1-ol	104-76-7	Abiotic	[93]
Et-PABA	Et-PABA 1	Aniline (= benzenamine)	62-53-3	Abiotic	[94]
	Et-PABA 2	4-aminobenzoic acid	150-13-0	Abiotic	[94]
	Et-PABA 3	(4-iminocyclohexa-2,5-dien-1-ylidene)methanone	—	Abiotic	[94]
	Et-PABA 4a	(2-hydroxy-4-iminocyclohexa-2,5-dien-1-ylidene)methanone	—	Abiotic	[94]
	Et-PABA 4b	(3-hydroxy-4-iminocyclohexa-2,5-dien-1-ylidene)methanone	—	Abiotic	[94]
	Et-PABA 5a	(2,3-dihydroxy-4-iminocyclohexa-2,5-dien-1-ylidene)methanone	—	Abiotic	[94]
	Et-PABA 5b	(2,5-dihydroxy-4-iminocyclohexa-2,5-dien-1-ylidene)methanone	—	Abiotic	[94]
	Et-PABA 5c	(2,6-dihydroxy-4-iminocyclohexa-2,5-dien-1-ylidene)methanone	—	Abiotic	[94]
	Et-PABA 5d	(3,5-dihydroxy-4-iminocyclohexa-2,5-dien-1-ylidene)methanone	—	Abiotic	[94]
	Et-PABA 6	Methyl 4-aminobenzoate	619-45-4	Abiotic	[94]
	Et-PABA 7a	4-amino-2-hydroxybenzoic acid	65-49-6	Abiotic	[94]
	Et-PABA 7b	4-amino-3-hydroxybenzoic acid	2374-03-0	Abiotic	[94]
	Et-PABA 8a	Methyl 4-amino-3-hydroxybenzoate	63435-16-5	Abiotic	[94]
	Et-PABA 8b	Methyl 4-amino-2-hydroxybenzoate	4136-97-4	Abiotic	[94]
	Et-PABA 9a	Ethyl 4-amino-2-hydroxybenzoate	6059-17-2	Abiotic	[94]
	Et-PABA 9b	Ethyl 4-amino-3-hydroxybenzoate	87081-52-5	Abiotic	[94]
	Et-PABA 10a	Methyl 4-amino-2,3-dihydroxybenzoate	—	Abiotic	[94]
	Et-PABA 10b	Methyl 4-amino-2,5-dihydroxybenzoate	—	Abiotic	[94]
	Et-PABA 10c	Methyl 4-amino-3,5-dihydroxybenzoate	—	Abiotic	[94]
	Et-PABA 10d	Methyl 4-amino-2,6-dihydroxybenzoate	—	Abiotic	[94]
	Et-PABA 11a	Ethyl 4-amino-2,6-dihydroxybenzoate	—	Abiotic	[94]
	Et-PABA 11b	Ethyl 4-amino-2,5-dihydroxybenzoate	—	Abiotic	[94]
	Et-PABA 11c	Ethyl 4-amino-3,5-dihydroxybenzoate	—	Abiotic	[94]
	Et-PABA 11d	Ethyl 4-amino-2,3-dihydroxybenzoate	—	Abiotic	[94]
PBSA	PBSA 1	2-phenyl-1*H*-benzimidazole	716-79-0	Abiotic	[95]
	PBSA 2	4-formyl-2-phenyl-1*H*-imidazole-5-carboxylic acid	—	Abiotic	[95]
	PBSA 3	2-phenyl-1*H*-imidazole-4,5-dicarboxylic acid	888-60-8	Abiotic	[95]

(Continues)

TABLE 2 (Continued)

Parent	Code	Name	CAS No.	Process	Reference
	PBSA 4	2-phenyl-1*H*-imidazole-5-carboxylic acid	77498-98-7	Abiotic	[95]
	PBSA 5	Benzenecarboximidamide	618-39-3	Abiotic	[95]
	PBSA 6	Benzamide	55-21-0	Abiotic	[95]
	PBSA 7	7-hydroxy-2-phenyl-1*H*-benzimidazole-6-sulfonic acid	—	Abiotic	[96]
	PBSA 8	5-hydroxy-2-phenyl-1*H*-benzimidazole-6-sulfonic acid	—	Abiotic	[96]
	PBSA 9	4-hydroxy-2-phenyl-1*H*-benzimidazole-6-sulfonic acid	—	Abiotic	[96]
	PBSA 10	2-(2-hydroxyphenyl)-1*H*-benzimidazole-6-sulfonic acid	—	Abiotic	[96]
	PBSA 11	2-(3-hydroxyphenyl)-1*H*-benzimidazole-6-sulfonic acid	—	Abiotic	[96]
	PBSA 12	2-(4-hydroxyphenyl)-1*H*-benzimidazole-6-sulfonic acid	—	Abiotic	[96]
MBC	MBC 1	(1*R*)-1,7-bis(hydroxymethyl)-2-oxobicyclo[2.2.1]heptane-7-carbaldehyde	—	Biotic	[76]
	MBC 2	2,3-dioxobicyclo[2.2.1]heptane-7,7-dicarbaldehyde	—	Biotic	[76]
	MBC 3	3-methyl-2-oxocyclohexane-1-carboxaldehyde	1194-91-8	Biotic	[76]
	MBC 4	6-(hydroxymethyl)cyclohex-2-en-1-one	—	Biotic	[76]
	MBC 5a	3-((2-hydroxy-4-methylphenyl)methylidene)-1,7,7-trimethylbicyclo[2.2.1]heptan-2-one	—	Biotic	[73]
	MBC 5b	3-((3-hydroxy-4-methylphenyl)methylidene)-1,7,7-trimethylbicyclo[2.2.1]heptan-2-one	—	Biotic	[73]
	MBC 6a	1,7,7-trimethyl-3-((2,3-dihydroxy-4-methylphenyl)methylidene)bicyclo[2.2.1]heptan-2-one	—	Biotic	[73]
	MBC 6b	1,7,7-trimethyl-3-((2,5-dihydroxy-4-methylphenyl)methylidene)bicyclo[2.2.1]heptan-2-one	—	Biotic	[73]
	MBC 6c	1,7,7-trimethyl-3-((2,6-dihydroxy-4-methylphenyl)methylidene)bicyclo[2.2.1]heptan-2-one	—	Biotic	[73]
	MBC 6d	1,7,7-trimethyl-3-((3,5-dihydroxy-4-methylphenyl)methylidene)bicyclo[2.2.1]heptan-2-one	—	Biotic	[73]
EHMC	EHMC 1	4-Methoxybenzaldehyde (= anisaldehyde)	123-11-5	Abiotic	[82, 88, 97–99]
	EHMC 2	2-Ethylhexan-1-ol	104-76-7	Abiotic, biotic	[51, 70, 82, 97]
	EHMC 3	2-(2-oxoethyl)hexyl 3-(4-methoxyphenyl)prop-2-enoate	—	Abiotic	[51, 82, 99]
	EHMC 4	2-Ethylhexyl (*Z*)-3-(4-methoxyphenyl)prop-2-enoate	177352-99-7	Abiotic, biotic	[56–58, 70, 97, 100, 101]
	EHMC 5	2-Ethylhexyl acetate	103-09-3	Abiotic	[83]
	EHMC 6	1-Ethenyl-4-methoxybenzene	637-69-4	Abiotic	[83]

TABLE 2 (Continued)

Parent	Code	Name	CAS No.	Process	Reference
	EHMC 7	(*E*)-3-(4-methoxyphenyl)prop-2-enoic acid (= *trans*-4-methoxycinnamic acid)	830-09-1	Abiotic	[51]
	EHMC 8	4-Methoxyphenol (= mequinol)	150-76-5	Abiotic	[51]
	EHMC 9	3-Ethenyl-6-methoxybenzene-1,2,4,5-tetrol (=1-ethenyl-2,3,5,6-tetrahydroxyl-4-methoxy-benzene)	—	Abiotic	[51, 99]
	EHMC 10	2-Ethylhexyl (2E)-3-(3-hydroxy-4-methoxyphenyl)prop-2-enoate	---	Abiotic	[51, 99]
	EHMC 11	2-Ethylhexyl 3-(2-hydroxy-4-methoxyphenyl)prop-2-enoate	—	Abiotic	[51, 99]
	EHMC 12	2-Ethyl-4-oxohexyl-3-(4-methoxyphenyl)prop-2-enoate (=3-(4-methoxyphenyl)prop-2-enoic acid 2-ethyl-4-oxohexyl ester)	—	Abiotic	[51, 99]
	EHMC 13	2-Ethylhexanoic-3-(4-methoxyphenyl)prop-2-enoic anhydride	—	Abiotic	[51, 99]
	EHMC 14	2-Ethyl-6-oxohexyl-3-(4-methoxyphenyl)prop-2-enoate (=3-(4-methoxyphenyl)prop-2-enoic acid 2-ethyl-6-oxohexyl ester)	—	Abiotic	[51, 99]
	EHMC 15	2-Ethyl-5-oxohexyl-3-(4-methoxyphenyl)prop-2-enoate (=3-(4-methoxyphenyl)prop-2-enoic acid 2-ethyl-5-oxohexyl ester)	—	Abiotic	[51, 99]
	EHMC 16	2-Ethyl-3-oxohexyl-3-(4-methoxyphenyl)prop-2-enoate (=3-(4-methoxyphenyl)prop-2-enoic acid 2-ethyl-3-oxohexyl ester)	—	Abiotic	[51, 99]
	EHMC 17	2-Acetylhexyl-3-(4-methoxyphenyl)prop-2-enoate	—	Abiotic	[99]
	EHMC 18	3-(((2-ethylhexyl)oxy)carbonyl)-2,4-bis(4-methoxyphenyl)cyclobutane-1-carboxylic acid	—	Abiotic	[51, 99]
	EHMC 19	2-(((2-ethylhexyl)oxy)carbonyl)-3,4- bis(4-methoxyphenyl)cyclobutane-1-carboxylic acid	—	Abiotic	[51, 97–99]
	EHMC 20[a]= IMC 1	2,4-bis((2Z,4E)-4-methoxyhepta-2,4,6-trienyl)cyclobutane-1,3-dicarboxylic acid bis(3-methylbutyl) ester	—	Abiotic	[51]
	EHMC 21	3,4-bis(4-methoxyphenyl)-1,2-bis(2-ethylhexyl) ester cyclobutane-1,2-dicarboxylic acid	—	Abiotic	[51, 57, 92, 97–99]
	EHMC 22	2,4-bis-((2Z,4E)-4-methoxyhepta-2,4,6-trienyl)-1,3-bis(2-ethylhexyl) ester cyclobutane-1,3-dicarboxylic acid	—	Abiotic	[57, 92]
IMC	IMC 1	dIAMC=2,4-bis((2Z,4E)-4-methoxyhepta-2,4,6-trienyl)cyclobutane-1,3-dicarboxylic acid bis(3-methylbutyl) ester	—	Abiotic	[51, 92]
	IMC 2	dIAMC=3,4-bis((2Z,4E)-4-methoxyhepta-2,4,6-trienyl)cyclobutane-1,2-dicarboxylic acid bis(3-methylbutyl) ester	—	Abiotic	[92]
OCR	OCR 1	3-(((2-cyano-3,3-diphenylprop-2-enoyl)oxy)methyl)pentanoic acid	—	Biotic	[77]
	OCR 2	2-Cyano-3,3-diphenylprop-2-enoic acid	10380-41-3	Biotic	[77]
	OCR 3	2-Ethyl-5-hydroxyhexyl 2-cyano-3,3-diphenylprop-2-enoate	—	Biotic	[77]
	OCR 4	2-Ethylhexyl 3-nitrilo-2-oxopropanoate	—	Abiotic	[88]
	OCR 5	Diphenylmethanone (=benzophenone)	119-61-9	Abiotic	[88]

(Continues)

TABLE 2 (Continued)

Parent	Code	Name	CAS No.	Process	Reference
BMDM + EHMC	MIX 1	Benzoic acid	65-85-0	Abiotic	[79]
	MIX 2	1,3-cyclobutanedicarboxylic acid 2,4-diphenyl-1,3-diethyl ester	56280-73-0	Abiotic	[79]
	MIX 3	(1α,2α,3β,4β)-1,3-cyclobutanedicarboxylic acid 2,4-diphenyl-1,3-diethyl ester	—	Abiotic	[79]
	MIX 4	(1α,2β,3α,4β)-1,3-cyclobutanedicarboxylic acid 2,4-diphenyl-1,3-diethyl ester	—	Abiotic	[79]
	MIX 5	(1α,2α,3α,4β)-1,3-Cyclobutanedicarboxylic acid 2,4-diphenyl-1,3-diethyl ester	—	Abiotic	[79]
	MIX 6	1,2-cyclobutanedicarboxylic acid 3,4-diphenyl-1,2-diethyl ester	—	Abiotic	[79]
	MIX 7	(1α,2α,3β,4β)-1,2-cyclobutanedicarboxylic acid 3,4-diphenyl-1,2-diethyl ester	—	Abiotic	[79]
	MIX 8	(1α,2β,3α,4β)-1,2-cyclobutanedicarboxylic acid 3,4-diphenyl-1,2-diethyl ester	—	Abiotic	[79]
	MIX 9	(1α,2β,3α,4α)-1,2-cyclobutanedicarboxylic acid 3,4-diphenyl-1,2-diethyl ester	—	Abiotic	[79]
	MIX 10	(1α,2α,3α,4β)-1,2-cyclobutanedicarboxylic acid 3,4-diphenyl-1,2-diethyl ester	—	Abiotic	[79]
	MIX 11	(1α,2β,3β,4α)-1,2-cyclobutanedicarboxylic acid 3,4-diphenyl-1,2-diethyl ester	—	Abiotic	[79]
	MIX 12	2-Ethylhexyl 2-(4-methoxybenzoyl)-3-(4-methoxyphenyl)-5-(4-*tert*-butylphenyl))-5-oxo-pentanoate	—	Abiotic	[79]
	MIX 13	2-Ethylhexyl 2-(4-*tert*-butylbenzoyl)-3,5-bis(4-methoxyphenyl)-5-oxo-pentanoate	—	Abiotic	[79]
	MIX 14	Ethyl (2*R*,3*R*)-2-benzoyl-5-oxo-3,5-diphenylpentanoate	—	Abiotic	[79]
	MIX 15	Ethyl 2-benzoyl-3,5-diphenyl-5-oxopentanoate (= 2-benzoyl-5-oxo-3,5-diphenylpentanoic acid ethyl ester)	117402-91-2	Abiotic	[79]
	MIX 16	Ethyl (2*R*,3*S*)-2-benzoyl-5-oxo-3,5-diphenylpentanoate (= (αR,βS) α-benzoyl-δ-oxo-β-phenyl benzenepentanoic acid ethyl ester)	—	Abiotic	[79]
	MIX 17	2-Ethylhexyl 2-(4-methoxybenzoylmethyl)-3-(4-methoxyphenyl)-4-(4-*tert*-butylphenyl)-4-oxobutanoate (=2-ethylhexyl 3,4-bis-(4-methoxyphenyl)-2-(4-*tert*-butylbenzoylmethyl)-4-oxobutanoate)	—	Abiotic	[79]
	MIX 18	2-Ethylhexyl 2-(4-*tert*-butylphenyl-2-oxoethyl)-3-(4-methoxyphenyl)-4-(4-methoxyphenyl)-4-oxobutanoate	—	Abiotic	[79]
	MIX 19	Ethyl (2*R*,3*S*)-4-oxo-2-(2-oxo-2-phenylethyl)-3,4-diphenylbutanoate	—	Abiotic	[79]
	MIX 20	Ethyl (2*S*,3*S*)-4-oxo-2-(2-oxo-2-phenylethyl)-3,4-diphenylbutanoate	—	Abiotic	[79]
	MIX 21	Ethyl 3-benzoyl-2-hydroxy-2,4-diphenylcyclobutane-1-carboxylate	—	Abiotic	[79]
	MIX 22	Ethyl 2-benzoyl-3-hydroxy-3,4-diphenylcyclobutane-1-carboxylate	927179-36-0	Abiotic	[79]

[a]This TP was wrongly assigned to the UV filter EHMC in [51]. The reference to the original study [92] was given and checked and revealed that this TP must be assigned to the UV filter IMC, TP IMC 1 in particular.

TABLE 3 Overview on the stability of certain TPs (extracted from literature, limited by data availability).

Kind of stability test	Statement on stability	Tested TP (TP code)	Reference
Photolytic laboratory experiment	(photo-)degradable (photolytically instable)	BP-3 1 and BP-3 2	[19]
Biodegradation (with fungus)	Biodegradable	BP-3 9 and BP-3 10	[74]
Biodegradability	Increased biodegradability	BP-3 1, BP-3 2, BP-3 3, BP-3 4, BP-3 5, BP-3 18, BP-3 21, BP-3 22, BP-3 23 and BP-3 24	[85]
Biodegradability under redox conditions	Inhibited biodegradation (under oxic, nitrate-reducing and sulphate-reducing conditions)	BP-3 1 and BP-3 18	[71]
Photolytic laboratory experiment	Transient photo-stability (photolytically instable)	EHMC 21	[97]
	Photostable	EHMC 19	[97]
Photolytic laboratory experiment	Photo-labile	EHMC 1, EHMC 3, EHMC 9, EHMC 10, EHMC 11, EHMC 12, EHMC 13, EHMC 14, EHMC 15, EHMC 16, EHMC 17, EHMC 18, EHMC 19 and EHMC 21	[99]
In silico prediction (QSAR)	Same or less for biodegradation compared to the UVF PBSA predicted	PBSA 7, PBSA 8, PBSA 9, PBSA 10, PBSA 11 and PBSA 12	[96]
In silico prediction (QSAR)	Higher overall persistence (P_{OV}) compared to UVF EHMC predicted	EHMC 3, EHMC 12, EHMC 13, EHMC 14, EHMC 15, EHMC 18, EHMC 19 and EHMC 21	[51]
	Same overall persistence (P_{OV}) as (*E*)-EHMC	EHMC 4 (= (*Z*)EHMC), EHMC 10 and EHMC 11	[51]
	Lower overall persistence (P_{OV}) than for UVF EHMC predicted	EHMC 1, EHMC 2, EHMC 7, EHMC 8, EHMC 9 and EHMC 16	[51]

conditions) or in silico predictions. Thus, a substantial data gap on the stability of known UVF-TPs was identified and hardly any information on biodegradability of TPs of UVF was available in the reviewed literature.

Biodegradability of UVF-TPs according to the ECHA (database) reports

In addition to the literature, the ECHA database was checked for information on biodegradability to extend the data set of biodegradability of TPs of UVF (see Table 4 and Table S4, SM). Table 4 gives a short summary of the 59 TPs (out of TP_{total}) for which an OECD 301 test result was found in the ECHA database (orange and green label) and/or a stability result was given in the literature (grey label for TPs without ECHA database entry). Out of all individual TP_{indiv} (in total: 177), six TPs (3.4%) were not biodegradable according to OECD testing guideline 301 [62], 23 TPs (13%) were biodegradable according to OECD 301 test results and more than 83% were not listed or listed without information on their biodegradability in the ECHA database. The exhaustive list with the biodegradability results for all TP_{total} can be found in Table S4 (SM). Based on the available results for stability and biodegradability, the ECHA results show in particular a trend that four out of five TPs are biodegradable. However, this trend towards better biodegradable TPs should not be considered as reliable evidence, since no statement was possible for more than 80% (of the individual TP_{indiv}) because of an incomplete data set.

Most of the identified TPs were not investigated regarding their biodegradability. An explanation could be that most of the substances are hard to isolate, commercially not available or a synthesis is very expensive. However, the data set was very small and more information on the biodegradability of all TPs is needed.

CHALLENGES REVIEWING TRANSFORMATION PRODUCTS OF UV FILTERS AND THEIR BIODE GRADABILITY

This review on TPs of UVF held certain challenges. For example, the terminology 'transformation product' changed over the years and older publications used terms such as 'intermediate', 'breakdown-product' or

TABLE 4 Shortened list of the TPs (based on list of TP_{total}) for which the literature and/or ECHA database (April 2022) provided information on the stability. Green highlights TP which were found to be readily biodegradable and orange highlights TPs which were found to be not readily biodegradable in OECD 301 tests as provided by ECHA database. TPs without entry or information on the biodegradability (OECD 301 tests) in the ECHA database are highlighted in grey if literature gave an information on their stability and not shown if no information on their stability was available. For full table with all TPs, see Table S4 (SM).

TP code	CAS	Stability (according to the literature, see Table 3)	Readily biodegradable: YES/NO (according to database entry)	Biodegradability test (according to ECHA database entry)
BMDM 1	100-09-4	—	YES (89% degradation after 28 days)	OECD 301F
BMDM 2	98-73-7	—	NO	OECD 301 B (CO_2 evolution) and OECD 301 D
BMDM 6 (= EHMC 1)	123-11-5	See EHMC 1: Photo-labile [99], lower overall persistence (P_{OV}) than for UVF EHMC (predicted) [51]	YES (measured DOC removal was 97% after 6 days)	OECD 301 E
BMDM 7	939-97-9	—	YES (84% after 14 days)	OECD 301 B (CO_2 evolution)
BMDM 8	100-06-1	—	YES (100% degraded within 28 days)	EU Method C.4-B (modified OECD screening test for ready biodegradability)
BMDM 10	98-06-6	—	NO (11% after 28 days)	OECD 301 B (CO_2 evolution)
BMDM 18 (= EHMC 8)	150-76-5	See EHMC 8: lower overall persistence compared to EHMC (predicted) [51]	YES (based on BOD criterion, biodegradation rate was 86% at 28 days)	OECD 301 C (MITI)
BMDM 19	98-54-4	—	YES, but failing the 10-day-window criterion	OECD 301 F (MRT)
BP-3 1	131-56-6	(photo-)degradable [19]; increased biodegradability [85]; inhibited biodegradation (under oxic, nitrate-reducing and sulphate-reducing conditions) [71]	NO (0% BOD after 28 days)	OECD 301 C (MITI)
BP-3 2	131-53-3	(photo-)degradable [19]; increased biodegradability [85]	NO (no degradation observed after 28 days)	OECD 301 B (CO_2 evolution)
BP-3 3	108-46-3	Increased biodegradability [85]	YES (elimination rates: 66.7% after 14 days)	OECD 301 C (MITI)
BP-3 4	90-02-8	Increased biodegradability [85]	NO (special case: transformation to 2-hydroxybenzoic acid after cultivation period of the test)	301 C (modified MITI test (I))
BP-3 5 (= MIX 1 = PABA 9)	65-85-0	Increased biodegradability [85]	YES (in several tests)	Inter alia OECD 301 B (CO_2 evolution) and OECD 301 C (MITI)
BP-3 7	611-99-4	—	YES (≥ 60% degradation relative to the $ThCO_2$ value)	OECD 301 B (CO_2 evolution)

TABLE 4 (Continued)

TP code	CAS	Stability (according to the literature, see Table 3)	Readily biodegradable: YES/NO (according to database entry)	Biodegradability test (according to ECHA database entry)
BP-3 8	1137-42-4	—	YES (87% and 73% biodegradation, respectively (based on ThOD))	OECD 301 F (MRT)
BP-3 9	—	Biodegradable [74]	—	—
BP-3 10	—	Biodegradable [74]	—	—
BP-3 18	106-44-5	Increased biodegradability [85]; inhibited biodegradation (under oxic, nitrate-reducing and sulphate-reducing conditions) [71]	YES (80%–95% degraded within 40 days)	OECD 301 C (modified MITI test (I))
BP-3 21	100-52-7	Increased biodegradability [85]	YES (in several tests)	OECD 301 B (CO_2 evolution), OECD 301 E
BP-3 22	95-48-7	Increased biodegradability [85]	YES (in several tests)	Inter alia OECD 301 C (modified MITI test (I))
BP-3 23	617-02-7	Increased biodegradability [85]	—	—
BP-3 24	100-51-6	Increased biodegradability [85]	YES (in several tests, e.g. MITI: 9296% after 14 days)	Inter alia OECD 301 C (modified MITI test (I))
PABA 1 (=Et-PABA 1)	62-53-3	—	YES (in several tests, e.g. CBT: 100% mineralization after 5 days)	Inter alia OECD 301 D (CBT)
PABA 2	95-55-6	—	NO (18%–27% after 14 days)	OECD 301 C
PABA 3	123-31-9	—	YES (fulfilling the 14 days window criterion (70% biodegradation after 14 days))	OECD 301C (MITI I)
PABA 7b	89-86-1	—	YES (76% biodegradation within 2 days)	OECD 301 A (DOC die away test)
PABA 8	99-96-7	—	YES (76.5% degradation within 4 days)	OECD 301 D (CBT)
PABA 9 (= BP-3 5 = MIX 1)	65-85-0	Increased biodegradability [85]	YES (in several tests)	Inter alia OECD 301 B (CO_2 evolution) and OECD 301 C (MITI)
EHDP 5	26 218-04-2	—	YES (72%–78% O_2 consumption)	OECD 301 F (MRT)
EHDP 23 (= EHMC 2)	104-76-7	See EHMC 2: lower overall persistence compared to EHMC (predicted) [51]	YES (complete removal of TOC (100%) and test substance (100%) within 2 weeks)	OECD 301 C (modified MITI test (I))
Et-PABA 1 (= PABA 1)	62-53-3	—	YES (in several tests, e.g. CBT: 100% mineralization after 5 days)	Inter alia OECD 301 D (CBT)
Et-PABA 2	150-13-0	—	YES (82% O_2 consumption after 28 days, but failing the 10-day-window criterion)	OECD 301 C (modified MITI test (I))

(Continues)

TABLE 4 (Continued)

TP code	CAS	Stability (according to the literature, see Table 3)	Readily biodegradable: YES/NO (according to database entry)	Biodegradability test (according to ECHA database entry)
PBSA 7	—	Same or less for biodegradation compared to the UVF PBSA (predicted) [96]	—	—
PBSA 8	—	Same or less for biodegradation compared to the UVF PBSA (predicted) [96]	—	—
PBSA 9	—	Same or less for biodegradation compared to the UVF PBSA (predicted) [96]	—	—
PBSA 10	—	Same or less for biodegradation compared to the UVF PBSA (predicted) [96]	—	—
PBSA 11	—	Same or less for biodegradation compared to the UVF PBSA (predicted) [96]	—	—
PBSA 12	—	Same or less for biodegradation compared to the UVF PBSA (predicted) [96]	—	—
EHMC 1 (= BMDM 6)	123-11-5	Photo-labile [99], lower overall persistence (P_{OV}) than for UVF EHMC (predicted) [51]	YES (measured DOC removal was 97% after 6 days)	OECD 301 E
EHMC 2 (= EHDP 23)	104-76-7	Lower overall persistence compared to EHMC (predicted) [51]	YES (complete removal of TOC (100%) and test substance (100%) within 2 weeks)	OECD 301 C (modified MITI test (I))
EHMC 3	—	Photo-labile [99], lower overall persistence (P_{OV}) than for UVF EHMC (predicted) [51]	—	—
EHMC 4	177352-99-7	Same overall persistence like (E)-EHMC (predicted) [51]	—	—
EHMC 5	103-09-3	—	YES (70% degradation after 28 days)	OECD 301 B (CO_2 evolution)
EHMC 7	830-09-1	Lower overall persistence (P_{OV}) than for UVF EHMC (predicted) [51]	—	—
EHMC 8 (= BMDM 18)	150-76-5	Lower overall persistence than EHMC (predicted) [51]	YES (Based on BOD criterion, biodegradation rate was 86% at 28 days)	OECD 301 C (MITI)
EHMC 9	—	Photo-labile [99], lower overall persistence (P_{OV}) than for UVF EHMC (predicted) [51]	—	—
EHMC 10	—	Photo-labile [99], same overall persistence (P_{OV}) like (E)-EHMC (predicted) [51]	—	—
EHMC 11	—	Photo-labile [99], same overall persistence (P_{OV}) like (E)-EHMC (predicted) [51]	—	—
EHMC 12	—	Photo-labile [99], higher overall persistence (P_{OV}) compared to EHMC (predicted) [51]	—	—

TABLE 4 (Continued)

TP code	CAS	Stability (according to the literature, see Table 3)	Readily biodegradable: YES/NO (according to database entry)	Biodegradability test (according to ECHA database entry)
EHMC 13	—	Photo-labile [99], higher overall persistence (P_{OV}) compared to EHMC (predicted) [51]	—	—
EHMC 14	—	Photo-labile [99], higher overall persistence (P_{OV}) compared to EHMC (predicted) [51]	—	—
EHMC 15	—	Photo-labile [99], higher overall persistence (P_{OV}) compared to EHMC (predicted) [51]	—	—
EHMC 16	—	Photo-labile [99], lower overall persistence (P_{OV}) than for EHMC (predicted) [51]	—	—
EHMC 17	—	Photo-labile [99]	—	—
EHMC 18	—	Photo-labile [99], higher overall persistence (P_{OV}) compared to EHMC (predicted) [51]	—	—
EHMC 19	—	Photo-labile [99], higher overall persistence (P_{OV}) compared to EHMC (predicted) [51], photostable [97]	—	—
EHMC 21	—	Photo-labile [99], higher overall persistence (P_{OV}) compared to EHMC (predicted) [51], transient photo-stability (photolytically instable) [97]	—	—
OCR 5	119-61-9	—	YES (66%–84% mineralization after 28 days)	OECD 301F (MRT)
MIX 1 (= BP-3 5 = PABA 9)	65-85-0	Increased biodegradability [85]	YES (in several tests)	Inter alia OECD 301 B (CO_2 evolution) and OECD 301 C (MITI)

Abbreviations: BOD, biochemical oxygen demand; CBT, closed bottle test; DOC, dissolved organic carbon; MITI, Ministry of International Trade and Industry, Japan; MRT, manometric respiratory test; $ThCO_2$, theoretical amount of CO_2; ThOD, theoretical oxygen demand; TOC, total organic carbon.

'photoproduct'. In addition, the structural identification and estimation of properties of TPs was often not the focus of the research. In many publications, the removal of parent compounds was often investigated more than the general analysis of whether TPs were formed and the identification of these. The transformation of UVF was observed very often. Applying a suitable analytical methodology, the elucidation of the structure of the TPs would be possible and an even more detailed list of known TPs of UVF could be generated. Such a list is important for further analysis of TP properties, for example, via in silico assessments or in laboratory experiments. Applying the selection rules on the data set of studies reviewed showed that the presentation or documentation of TPs was diverse and in parts incomplete in the studies. The check of the selected studies, regarding the availability of data on the biodegradation behaviour of the TPs demonstrated that only sparse information (for only few TPs and in a few studies reported in literature) was available which led to the incomplete biodegradability data set. A useful measure to overcome this insufficient situation is to implement a harmonized test system which encompasses the performance of all steps from the removal of UVF, over analysis of the transformation process including the structural elucidation of the TPs and a final assessment of the properties of the TPs.

CONSEQUENCES FOR THE ENVIRONMENTAL PERSPECTIVE AND RECOMMENDATIONS FOR FURTHER RESEARCH

If further research proceeds as it does now, the already well-investigated UVF will become investigated in even more detail, while knowledge on lesser known UVF will remain scarce. Moreover, if the focus remains on primary elimination only, a knowledge gap in the existence and identity of TPs of UVF can be expected. Additionally, the lack of knowledge regarding the properties (such as biodegradability) of TPs in the environment will persist and the body of knowledge of the fate of TPs of UVF in the environment will be insufficient both for risk assessment and regulation as well as future design for environmental mineralization [41, 102]. Even though, only studies in which TP have been identified were included in this review, it is clear that not only the properties of identified TPs should become further investigated, but also those TPs which were only detected so far should be identified, too.

If the applied procedures continue to vary as they do so far (e.g. for the determination of biodegradability of TPs of UVF), the strongly needed comparison of TPs with each other will be very limited as will the resulting insights. Since TPs could be either of the same or even of more concern than parent compounds, the assessment of the properties is important. In doing so, processes should be better aligned and/or standardized, to avoid the formation of those TPs. In addition, the knowledge gap represents an important issue, since it is not clear whether formed TPs are relevant for the environment and humans. Consequently, a potential risk due to the formation of TPs cannot be excluded.

Summarizing, this review clearly demonstrated that it is important to perform more extensive experiments to understand the significance of UVF and the possibly formed TPs presence in the environment. The (structural) identification of TPs as well as the assessment of their fate (persistence and biodegradation) and effects is urgently needed in the future to close knowledge gaps. It will also provide a better starting point for regulatory approaches by providing a fundamental and complete information base of higher quality. In that sense, the results of this review suggest establishing a harmonized and tiered procedure to systematically analyse the persistence including biodegradability of TPs of UVF. For instance, in the first tier, a method could be applied, which is easily accessible. In the higher tier, specific tests could be applied, which are more complex (see also [39]). In addition, the testing guidance should be re-evaluated to the current state of the art in science and technology. Nevertheless, we do not see a lack in test methodologies or missing of tiered test procedures. Those are, however, mainly applied to the parent compounds not to the TPs. UVF which have not been the focus of research so far should be investigated as well for the same reasons. However, in the view of the high efforts further investigation will have, a prioritization is deemed necessary, for example, by starting the investigation with highly used UVF.

A harmonized test system for TPs beyond UVF including their properties is needed to allow a systematic investigation of the stability of TPs. Standardized procedures, such as the procedures already established for biodegradability assessment should be applied or developed if not yet in place. If laboratory experiments are not feasible, structure–activity-relationships analysis or read across of the employment of computational methods are an option to perform a systematic investigation of the stability or other properties of TPs of UVF, including a pre-screening.

CONCLUSION

This article reviewed available literature data on the TPs of UVF, which were formed in abiotic and biotic processes. Data on the degradability of the identified TPs of UVF with a focus on biodegradability was assessed. By analysing literature data on the transformation of eleven UVF in aerobic and biotic processes, in total, 187 TPs (TP_{total})

were identified based on the literature research. It is notable, that a comparison of the structures of the 187 TP_{total} of the 11 UVF showed that 177 individual TP_{indiv} were identified (excluding structural duplicates and one triplicate). In addition, an overview was given on the distribution of processes that lead to the formation of TPs of UVF. It became clear, that information on biodegradability of TPs in the literature as well as in the ECHA database was very scarce (no information was available for more than 80% of the TP). Therefore, this study identified a data gap regarding biodegradability of TPs of UVF.

Further research should address not only the detection of TPs but also structure elucidation, and more importantly, an assessment of the biodegradability. The biodegradability assessment of identified TPs should follow a harmonized approach in order to allow a better reliability, understanding and comparison of the results. Furthermore, it turned out that it is important to generate knowledge on the biodegradability of the formed TPs to ensure that processes (e.g. [waste] water treatment) lead (in the best case) to fully environmentally mineralizing TPs. In doing so, goals such as non-toxic environment in accordance with strategies such as the EUs Zero Pollution Ambition might be reached eventually.

ACKNOWLEDGEMENTS

These results derive from a collaborative project in Lower Saxony and Israel with financial support from the Ministry of Science and Culture, Lower Saxony, Germany to research 'Personal care products (PCPs) as source for micropollutants in Greywater – Identification, quantification and on-site treatment', Project No. VWZN 2830. Open Access funding enabled and organized by Projekt DEAL.

CONFLICT OF INTEREST STATEMENT

The follwing statements do not apply to the authors: royalties or licenses; consulting fees; payment or honoraria for lectures, presentaions, speakers bureaus, manuscript writing or educational events; payment for expert testimony; support for attending meetings and/ or travel; plan, issue or pending patents; participation on a Data Safety Monitoring Board or Advisory Board; leadership or fiduciary role in other board, society, commitee or advocacy group, paid or unpaid; stock or stock options; receipt of equipment, materials, drugs, medical writing, gifts or other services; other financial or non-financial interests.

ORCID

Franziska Jentzsch https://orcid.org/0000-0002-4456-6693
Klaus Kümmerer https://orcid.org/0000-0003-2027-6488
Oliver Olsson https://orcid.org/0000-0003-0082-1442

REFERENCES

1. Magi E, Scapolla C, Di Carro M, Rivaro P, Ngoc Nguyen KT. Emerging pollutants in aquatic environments: monitoring of UV filters in urban wastewater treatment plants. Anal Methods. 2013;5(2):428–33.
2. Langford KH, Reid MJ, Fjeld E, Øxnevad S, Thomas KV. Environmental occurrence and risk of organic UV filters and stabilizers in multiple matrices in Norway. Environ Int. 2015;80:1–7.
3. Caloni S, Durazzano T, Franci G, Marsili L. Sunscreens' UV filters risk for coastal marine environment biodiversity: a review. Diversity. 2021;13(8):374.
4. Fivenson D, Sabzevari N, Qiblawi S, Blitz J, Norton BB, Norton SA. Sunscreens: UV filters to protect us: part 2-increasing awareness of UV filters and their potential toxicities to us and our environment. Int J Women's Dermatol. 2021;7(1):45–69.
5. Chisvert A, León-González Z, Tarazona I, Salvador A, Giokas D. An overview of the analytical methods for the determination of organic ultraviolet filters in biological fluids and tissues. Anal Chim Acta. 2012;752:11–29.
6. Cuderman P, Heath E. Determination of UV filters and antimicrobial agents in environmental water samples. Anal Bioanal Chem. 2007;387(4):1343–50.
7. Cadena-Aizaga MI, Montesdeoca-Esponda S, Torres-Padrón ME, Sosa-Ferrera Z, Santana-Rodríguez JJ. Organic UV filters in marine environments: an update of analytical methodologies, occurrence and distribution. Trends Environ Anal Chem. 2020;25:e00079.
8. Pintado-Herrera MG, Lara Martín PA. Fate and behavior of UV filters in the marine environment. In: Tovar-Sánchez A, Sánchez-Quiles D, Blasco J, editors. Sunscreens in coastal ecosystems. Volume 94. Cham: Springer International Publishing; 2020.
9. Poiger T, Buser H-R, Balmer ME, Bergqvist P-A, Müller MD. Occurrence of UV filter compounds from sunscreens in surface waters: regional mass balance in two Swiss lakes. Chemosphere. 2004;55(7):951–63.
10. Tsui MMP, Lam JCW, Ng TY, Ang PO, Murphy MB, Lam PKS. Occurrence, distribution, and fate of organic UV filters in coral communities. Environ Sci Technol. 2017;51(8):4182–90.
11. Balmer ME, Buser H-R, Müller MD, Poiger T. Occurrence of some organic UV filters in wastewater, in surface waters, and in fish from Swiss Lakes. Environ Sci Technol. 2005;39(4):953–62.
12. Loraine GA, Pettigrove ME. Seasonal variations in concentrations of pharmaceuticals and personal care products in drinking water and reclaimed wastewater in Southern California. Environ Sci Technol. 2006;40(3):687–95.
13. Plagellat C, Kupper T, Furrer R, de Alencastro LF, Grandjean D, Tarradellas J. Concentrations and specific loads of UV filters in sewage sludge originating from a monitoring network in Switzerland. Chemosphere. 2006;62(6):915–25.
14. Cadena-Aizaga MI, Montesdeoca-Esponda S, Sosa-Ferrera Z, Santana-Rodríguez JJ. Occurrence and environmental hazard of organic UV filters in seawater and wastewater from gran Canaria Island (Canary Islands, Spain). Environ Pollut. 2022;300:118843.
15. Gorito AM, Ribeiro AR, Gomes CR, Almeida CMR, Silva AMT. Constructed wetland microcosms for the removal of organic micropollutants from freshwater aquaculture effluents. Sci Total Environ. 2018;644:1171–80.

16. Zúñiga-Benítez H, Peñuela GA. Application of solar photo-Fenton for benzophenone-type UV filters removal. J Environ Manage. 2018;217:929–38.
17. Biel-Maeso M, Corada-Fernández C, Lara-Martín PA. Removal of personal care products (PCPs) in wastewater and sludge treatment and their occurrence in receiving soils. Water Res. 2019;150:129–39.
18. O'Malley E, O'Brien JW, Verhagen R, Mueller JF. Annual release of selected UV filters via effluent from wastewater treatment plants in Australia. Chemosphere. 2020;247:125887.
19. Dubowski Y, Alfiya Y, Gilboa Y, Sabach S, Friedler E. Removal of organic micropollutants from biologically treated greywater using continuous-flow vacuum-UV/UVC photo-reactor. Environ Sci Pollut Res. 2020;27(7):7578–87.
20. Fent K, Kunz PY, Gomez E. UV filters in the aquatic environment induce hormonal effects and affect fertility and reproduction in fish. Chimia. 2008;62(5):368.
21. Kim KY, Ekpeghere KI, Jeong H-J, Oh J-E. Effects of the summer holiday season on UV filter and illicit drug concentrations in the Korean wastewater system and aquatic environment. Environ Pollut. 2017;227:587–95.
22. Schaap I, Slijkerman DME. An environmental risk assessment of three organic UV-filters at Lac Bay, Bonaire, Southern Caribbean. Mar Pollut Bull. 2018;135:490–5.
23. Jurado A, Vàzquez-Suñé E, Carrera J, López de Alda M, Pujades E, Barceló D. Emerging organic contaminants in groundwater in Spain: a review of sources, recent occurrence and fate in a European context. Sci Total Environ. 2012;440:82–94.
24. Jeon H-K, Chung Y, Ryu J-C. Simultaneous determination of benzophenone-type UV filters in water and soil by gas chromatography–mass spectrometry. J Chromatogr A. 2006;1131(1–2):192–202.
25. He K, Hain E, Timm A, Tarnowski M, Blaney L. Occurrence of antibiotics, estrogenic hormones, and UV-filters in water, sediment, and oyster tissue from the Chesapeake Bay. Sci Total Environ. 2019;650:3101–9.
26. Fenni F, Sunyer-Caldú A, Ben Mansour H, Diaz-Cruz MS. Contaminants of emerging concern in marine areas: first evidence of UV filters and paraben preservatives in seawater and sediment on the eastern coast of Tunisia. Environ Pollut. 2022;309:119749.
27. Nagtegaal M, Ternes TA, Baumann W, Nagel R. UV-Filtersubstanzen in Wasser und Fischen. UWSF - Z Umweltchem Ökotox. 1997;9(2):79–86.
28. Buser H-R, Balmer ME, Schmid P, Kohler M. Occurrence of UV filters 4-methylbenzylidene camphor and octocrylene in fish from various Swiss rivers with inputs from wastewater treatment plants. Environ Sci Technol. 2006;40(5):1427–31.
29. Molins-Delgado D, Muñoz R, Nogueira S, Alonso MB, Torres JP, Malm O, et al. Occurrence of organic UV filters and metabolites in lebranche mullet (Mugil liza) from Brazil. Sci Total Environ. 2018;618:451–9.
30. Bachelot M, Li Z, Munaron D, Le Gall P, Casellas C, Fenet H, et al. Organic UV filter concentrations in marine mussels from French coastal regions. Sci Total Environ. 2012;420:273–9.
31. Krause M, Klit A, Blomberg Jensen M, Søeborg T, Frederiksen H, Schlumpf M, et al. Sunscreens: are they beneficial for health? An overview of endocrine disrupting properties of UV-filters: sunscreens and their adverse effects. Int J Androl. 2012;35(3):424–36.
32. Ao J, Yuan T, Gu J, Ma Y, Shen Z, Tian Y, et al. Organic UV filters in indoor dust and human urine: a study of characteristics, sources, associations and human exposure. Sci Total Environ. 2018;640–641:1157–64.
33. Tschersich C, Murawski A, Schwedler G, Rucic E, Moos RK, Kasper-Sonnenberg M, et al. Bisphenol a and six other environmental phenols in urine of children and adolescents in Germany – human biomonitoring results of the German environmental survey 2014–2017 (GerES V). Sci Total Environ. 2021;763:144615.
34. Helbling DE, Hollender J, Kohler H-PE, Singer H, Fenner K. High-throughput identification of microbial transformation products of organic micropollutants. Environ Sci Technol. 2010;44(17):6621–7.
35. Wilkinson J, Hooda PS, Barker J, Barton S, Swinden J. Occurrence, fate and transformation of emerging contaminants in water: an overarching review of the field. Environ Pollut. 2017;231:954–70.
36. Diehle M, Gebhardt W, Pinnekamp J, Schäffer A, Linnemann V. Ozonation of valsartan: structural elucidation and environmental properties of transformation products. Chemosphere. 2019;216:437–48.
37. Leusch FDL, Neale PA, Busetti F, Card M, Humpage A, Orbell JD, et al. Transformation of endocrine disrupting chemicals, pharmaceutical and personal care products during drinking water disinfection. Sci Total Environ. 2019;657:1480–90.
38. Porter AW, Wolfson SJ, Häggblom M, Young LY. Microbial transformation of widely used pharmaceutical and personal care product compounds. F1000Res. 2020;9:130.
39. Hensen B, Olsson O, Kümmerer K. A strategy for an initial assessment of the ecotoxicological effects of transformation products of pesticides in aquatic systems following a tiered approach. Environ Int. 2020;137:105533.
40. Fenner K, Canonica S, Wackett LP, Elsner M. Evaluating pesticide degradation in the environment: blind spots and emerging opportunities. Science. 2013;341(6147):752–8.
41. Kümmerer K, Dionysiou DD, Olsson O, Fatta-Kassinos D. Reducing aquatic micropollutants – increasing the focus on input prevention and integrated emission management. Sci Total Environ. 2019;652:836–50.
42. Voelskow H. abiotischer Abbau. 2011.
43. Klöpffer W. Verhalten und Abbau von Umweltchemikalien: Physikalisch-chemische Grundlagen. Weinheim, Germany: Wiley; 2012.
44. Li Z, Kaserzon SL, Plassmann MM, Sobek A, Gómez Ramos MJ, Radke M. A strategic screening approach to identify transformation products of organic micropollutants formed in natural waters. Environ Sci: Processes Impacts. 2017;19(4):488–98.
45. Bergheim M, Gminski R, Spangenberg B, Dębiak M, Bürkle A, Mersch-Sundermann V, et al. Recalcitrant pharmaceuticals in the aquatic environment: a comparative screening study of their occurrence, formation of phototransformation products and their in vitro toxicity. Environ Chem. 2014;11(4):431.
46. Gonzalez-Gil L, Krah D, Ghattas A-K, Carballa M, Wick A, Helmholz L, et al. Biotransformation of organic micropollutants by anaerobic sludge enzymes. Water Res. 2019;152:202–14.

47. Gutowski L, Baginska E, Olsson O, Leder C, Kümmerer K. Assessing the environmental fate of S-metolachlor, its commercial product Mercantor Gold® and their photoproducts using a water–sediment test and in silico methods. Chemosphere. 2015;138:847–55.
48. Herrmann M, Menz J, Olsson O, Kümmerer K. Identification of phototransformation products of the antiepileptic drug gabapentin: biodegradability and initial assessment of toxicity. Water Res. 2015;85:11–21.
49. Khaleel NDH, Mahmoud WMM, Olsson O, Kümmerer K. Initial fate assessment of teratogenic drug trimipramine and its photo-transformation products – role of pH, concentration and temperature. Water Res. 2017;108:197–211.
50. Menz J, Toolaram AP, Rastogi T, Leder C, Olsson O, Kümmerer K, et al. Transformation products in the water cycle and the unsolved problem of their proactive assessment: a combined in vitro/in silico approach. Environ Int. 2017;98:171–80.
51. Gackowska A, Studziński W, Kudlek E, Dudziak M, Gaca J. Estimation of physicochemical properties of 2-ethylhexyl-4-methoxycinnamate (EHMC) degradation products and their toxicological evaluation. Environ Sci Pollut Res. 2018;25(16):16037–49.
52. Nataraj B, Maharajan K, Hemalatha D, Rangasamy B, Arul N, Ramesh M. Comparative toxicity of UV-filter octyl methoxycinnamate and its photoproducts on zebrafish development. Sci Total Environ. 2020;718:134546.
53. Studziński W, Gackowska A, Kudlek E. Determination of environmental properties and toxicity of octyl-dimethyl-para-aminobenzoic acid and its degradation products. J Hazard Mater. 2021;403:123856.
54. European Commission. A European green Deal. European Commission - European Commission. https://ec.europa.eu/info/strategy/priorities-2019-2024/european-green-deal_en Accessed 5 Sep 2023.
55. European Commission. Zero pollution action plan. https://environment.ec.europa.eu/strategy/zero-pollution-action-plan_en Accessed 5 Sep 2023.
56. Santos AJM, Miranda MS, Esteves da Silva JCG. The degradation products of UV filters in aqueous and chlorinated aqueous solutions. Water Res. 2012;46(10):3167–76.
57. Díaz-Cruz MS, Llorca M, Barceló D, Barceló D. Organic UV filters and their photodegradates, metabolites and disinfection by-products in the aquatic environment. TrAC Trends Anal Chem. 2008;27(10):873–87.
58. Kockler J, Oelgemöller M, Robertson S, Glass BD. Photostability of sunscreens. J Photochem Photobiol C Photchem Rev. 2012;13(1):91–110.
59. Gago-Ferrero P, Díaz-Cruz MS, Barceló D. Liquid chromatography-tandem mass spectrometry for the multi-residue analysis of organic UV filters and their transformation products in the aquatic environment. Anal Methods. 2013;5(2):355–66.
60. Pestotnik K, Kosjek T, Heath E. Transformation products of personal care products: UV filters case studies. In: Lambropoulou DA, Nollet LML, editors. Transformation products of emerging contaminants in the environment. Chichester, United Kingdom: John Wiley and Sons Ltd; 2014.
61. Chisvert A, Salvador A. Ultraviolet filters in cosmetics. Analysis of Cosmetic Products. Amsterdam, The Netherlands; Oxford, UK; Cambridge, MA: Elsevier; 2018.
62. OECD. Test No. 301: Ready Biodegradability. Paris: OECD; 1992.
63. cheminfo.org. SMILES generator / checker. cheminfo.org, http://www.cheminfo.org/flavor/malaria/Utilities/SMILES_generator___checker/index.html# Accessed 5 Sep 2023.
64. Cactus.nci.nih.gov. Online SMILES Translator. Online SMILES Translator and Structure File Generator. https://cactus.nci.nih.gov/translate/ Accessed 5 Sep 2023.
65. Cufar A, Kristl J. Sun protection preparations. Part I: UV-radiation, protection mechanisms. UV-sunscreen substances. Farm Vestn. 1994;45(2):71–87.
66. Farré M, Pérez S, Kantiani L, Barceló D. Fate and toxicity of emerging pollutants, their metabolites and transformation products in the aquatic environment. TrAC -Trends Anal Chem. 2008;27(11):991–1007.
67. Hernández F, Sancho JV, Ibáñez M, Abad E, Portolés T, Mattioli L. Current use of high-resolution mass spectrometry in the environmental sciences. Anal Bioanal Chem. 2012;403(5):1251–64.
68. Narla S, Lim HW. Sunscreen: FDA regulation, and environmental and health impact. Photochem Photobiol Sci. 2020;19(1):66–70.
69. Jentzsch F, Reich M, Kümmerer K, Olsson O. Photolysis of mixtures of UV filters octocrylene and ethylhexyl methoxycinnamate leads to formation of mixed transformation products and different kinetics. Sci Total Environ. 2019;697:134048.
70. Gackowska A, Studziński W. Effect of activated sludge on the degradation of 2-Ethylhexyl 4-methoxycinnamate and 2-Ethylhexyl 4-(Dimethylamino)benzoate in wastewater. Water Air Soil Pollut. 2020;231(4):158.
71. Liu Y-S, Ying G-G, Shareef A, Kookana RS. Biodegradation of the ultraviolet filter benzophenone-3 under different redox conditions. Environ Toxicol Chem. 2012;31(2):289–95.
72. Gago-Ferrero P, Díaz-Cruz MS, Barceló D. Occurrence of multiclass UV filters in treated sewage sludge from wastewater treatment plants. Chemosphere. 2011;84(8):1158–65.
73. Badia-Fabregat M, Rodríguez-Rodríguez CE, Gago-Ferrero P, Olivares A, Piña B, Díaz-Cruz MS, et al. Degradation of UV filters in sewage sludge and 4-MBC in liquid medium by the ligninolytic fungus Trametes versicolor. J Environ Manage. 2012;104:114–20.
74. Gago-Ferrero P, Badia-Fabregat M, Olivares A, Piña B, Blánquez P, Vicent T, et al. Evaluation of fungal- and photo-degradation as potential treatments for the removal of sunscreens BP3 and BP1. Sci Total Environ. 2012;427–428:355–63.
75. Lee S-H, Xiong J-Q, Ru S, Patil SM, Kurade MB, Govindwar SP, et al. Toxicity of benzophenone-3 and its biodegradation in a freshwater microalga Scenedesmus obliquus. J Hazard Mater. 2020;389:122149.
76. Volpe A, Pagano M, Mascolo G, Grenni P, Rossetti S. Biodegradation of UV-filters in marine sediments. Sci Total Environ. 2017;575:448–57.
77. Suleiman M, Schröder C, Kuhn M, Simon A, Stahl A, Frerichs H, et al. Microbial biofilm formation and degradation of octocrylene, a UV absorber found in sunscreen. Commun Biol. 2019;2(1):430.
78. Schwack W, Rudolph T. Photochemistry of dibenzoyl methane UVA filters part 1. J Photochem Photobiol B Biol. 1995;28(3):229–34.
79. Dondi D, Albini A, Serpone N. Interactions between different solar UVB/UVA filters contained in commercial suncreams

and consequent loss of UV protection. Photochem Photobiol Sci. 2006;5(9):835–43.
80. Huong SP, Rocher E, Fourneron J-D, Charles L, Monnier V, Bun H, et al. Photoreactivity of the sunscreen butylmethoxydibenzoylmethane (DBM) under various experimental conditions. J Photochem Photobiol A Chem. 2008;196(1):106–12.
81. Trebše P, Polyakova OV, Baranova M, Kralj MB, Dolenc D, Sarakha M, et al. Transformation of avobenzone in conditions of aquatic chlorination and UV-irradiation. Water Res. 2016;101:95–102.
82. Celeiro M, Facorro R, Dagnac T, Vilar VJP, Llompart M. Photodegradation behaviour of multiclass ultraviolet filters in the aquatic environment: removal strategies and photoproduct identification by liquid chromatography–high resolution mass spectrometry. J Chromatogr A. 2019;1596:8–19.
83. Freitas JV, Lopes NP, Gaspar LR. Photostability evaluation of five UV-filters, trans-resveratrol and beta-carotene in sunscreens. Eur J Pharm Sci. 2015;78:79–89.
84. Gong P, Yuan H, Zhai P, Xue Y, Li H, Dong W, et al. Investigation on the degradation of benzophenone-3 by UV/H2O2 in aqueous solution. Chem Eng J. 2015;277:97–103.
85. Zúñiga-Benítez H, Aristizábal-Ciro C, Peñuela GA. Heterogeneous photocatalytic degradation of the endocrine-disrupting chemical Benzophenone-3: parameters optimization and by-products identification. J Environ Manage. 2016;167:246–58.
86. Luo J, Liu T, Zhang D, Yin K, Wang D, Zhang W, et al. The individual and Co-exposure degradation of benzophenone derivatives by UV/H2O2 and UV/PDS in different water matrices. Water Res. 2019;159:102–10.
87. Liu Y-S, Ying G-G, Shareef A, Kookana RS. Photostability of the UV filter benzophenone-3 and its effect on the photodegradation of benzotriazole in water. Environ Chem. 2011;8(6):581.
88. Hopkins ZR, Snowberger S, Blaney L. Ozonation of the oxybenzone, octinoxate, and octocrylene UV-filters: reaction kinetics, absorbance characteristics, and transformation products. J Hazard Mater. 2017;338:23–32.
89. Tsoumachidou S, Velegraki T, Poulios I. TiO $_2$ photocatalytic degradation of UV filter para-aminobenzoic acid under artificial and solar illumination: TiO $_2$ photocatalytic degradation of UV filter PABA. J Chem Technol Biotechnol. 2016;91(6):1773–81.
90. Tsoumachidou S, Lambropoulou D, Poulios I. Homogeneous photocatalytic oxidation of UV filter para-aminobenzoic acid in aqueous solutions. Environ Sci Pollut Res. 2017;24(2):1113–21.
91. Sakkas VA, Giokas DL, Lambropoulou DA, Albanis TA. Aqueous photolysis of the sunscreen agent octyl-dimethyl-p-aminobenzoic acid. J Chromatogr A. 2003;1016(2):211–22.
92. Rodil R, Moeder M, Altenburger R, Schmitt-Jansen M. Photostability and phytotoxicity of selected sunscreen agents and their degradation mixtures in water. Anal Bioanal Chem. 2009;395(5):1513–24.
93. Studziński W, Gackowska A. Evaluation of degradation efficiency of 2′-Ethylhexyl 4-(Dimethylamino)benzoate under the influence of oxidizing agents. J Ecol Eng. 2018;19(4):236–41.
94. Li AJ, Sang Z, Chow C-H, Law JC-F, Guo Y, Leung KS-Y. Environmental behavior of 12 UV filters and photocatalytic profile of ethyl-4-aminobenzoate. J Hazard Mater. 2017;337:115–25.
95. Zhang S, Chen J, Qiao X, Ge L, Cai X, Na G. Quantum chemical investigation and experimental verification on the aquatic photochemistry of the sunscreen 2-phenylbenzimidazole-5-sulfonic acid. Environ Sci Technol. 2010;44(19):7484–90.
96. Westphal J, Kümmerer K, Olsson O. Experimental and in silico assessment of fate and effects of the UV filter 2-phenylbenzimidazole 5-sulfonic acid and its phototransformation products in aquatic solutions. Water Res. 2020;171:115393.
97. MacManus-Spencer LA, Tse ML, Klein JL, Kracunas AE. Aqueous photolysis of the organic ultraviolet filter chemical octyl methoxycinnamate. Environ Sci Technol. 2011;45(9):3931–7.
98. Vione D, Calza P, Galli F, Fabbri D, Santoro V, Medana C. The role of direct photolysis and indirect photochemistry in the environmental fate of ethylhexyl methoxy cinnamate (EHMC) in surface waters. Sci Total Environ. 2015;537:58–68.
99. Jentzsch F, Olsson O, Westphal J, Reich M, Leder C, Kümmerer K. Photodegradation of the UV filter ethylhexyl methoxycinnamate under ultraviolet light: identification and in silico assessment of photo-transformation products in the context of grey water reuse. Sci Total Environ. 2016;572:1092–100.
100. Broadbent KK, Martincigh BS, Raynor MW, Salter LF, Moulder R, Sjöberg P, et al. Capillary supercritical fluid chromatography combined with atmospheric pressure chemical ionisation mass spectrometry for the investigation of photoproduct formation in the sunscreen absorber 2-ethylhexyl-p-methoxycinnamate. J Chromatogr A. 1996;732(1):101–10.
101. Serpone N, Salinaro A, Emeline AV, Horikoshi S, Hidaka H, Zhao J. An in vitro systematic spectroscopic examination of the photostabilities of a random set of commercial sunscreen lotions and their chemical UVB/UVA active agents. Photochem Photobiol Sci. 2002;1(12):970–81.
102. Puhlmann N, Olsson O, Kümmerer K. Transformation products of sulfonamides in aquatic systems: lessons learned from available environmental fate and behaviour data. Sci Total Environ. 2022;830:154744.

SUPPORTING INFORMATION

Additional supporting information can be found online in the Supporting Information section at the end of this article.

How to cite this article: Jentzsch F, Kümmerer K, Olsson O. Status quo on identified transformation products of organic ultraviolet filters and their persistence. Int J Cosmet Sci. 2023;45(Suppl. 1):101–126. https://doi.org/10.1111/ics.12908

Supplementary material

Status quo on identified transformation products of organic ultraviolet filters and their persistence

Table SI: Overview on organic UV filter substances (alphabetical order) which are allowed in cosmetics according to European legislation (Regulation EC 1223/2009).

INCI name	Abbreviation	Chemical structure	CAS No.	Synonyms
4-Methylbenzylidene camphor	MBC	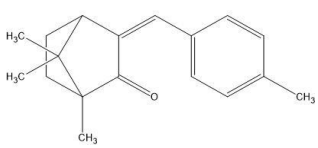	36861-47-9	Enzacamene; 3-(4-Methylbenzylidene)-di-camphor
Benzophenone-3	BP-3	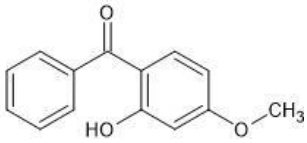	131-57-7	BZ3 Oxybenzone; 2-Hydroxy-4-methoxybenzophenone
Benzophenone-4 and/or its sodium salt	BP-4	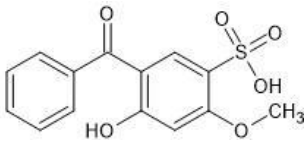	4065-45-6 6628-37-1 (sodium salt)	BZ4; Sulisobenzone
Benzylidene camphor sulphonic acid	BCSA	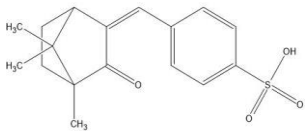	56039-58-8	-
Bis-ethylhexyloxyphenol methoxyphenyl triazine	BEMT	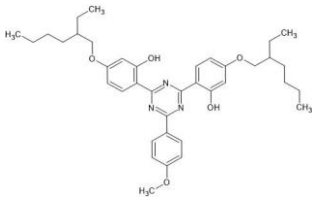	187393-00-6	Tinosorb S; Anisotriazine; 2,2′-[6-(4-Methoxyphenyl)-1,3,5-triazine-2,4-diyl] bis{5-[(2-ethylhexyl)oxy]phenol}

INCI name	Abbreviation	Chemical structure	CAS No.	Synonyms
Butyl methoxydibenzoylmethane	BMDM	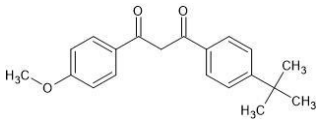	70356-09-1	Avobenzone; 1-(4-Methoxyphenyl)-3-(4-tert-butylphenyl)propane-1,3-dione
Camphor benzalkonium methosulfate	CBM	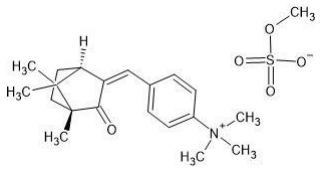	52793-97-2	-
Diethylamino hydroxybenzoyl hexyl Benzoate	DHHB	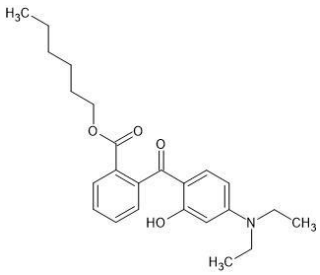	302776-68-7	Hexyl 2-[4-(diethylamino)-2-hydroxybenzoyl]benzoate; Uvinul A Plus
Diethylhexyl butamido triazone	DEBT	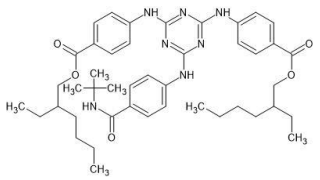	154702-15-5	Iscotrizinol
Disodium phenyl dibenzimidazole tetrasulfonate	PDTA	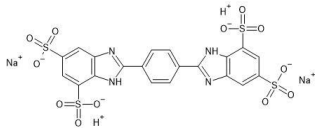	180898-37-7	Bisdisulizole disodium
Drometrizole trisiloxane	DTS	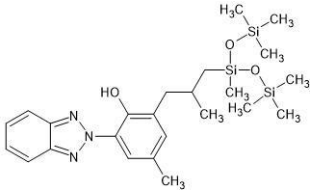	155633-54-8	-

INCI name	Abbreviation	Chemical structure	CAS No.	Synonyms
Ethylhexyl dimethyl PABA	EHDP	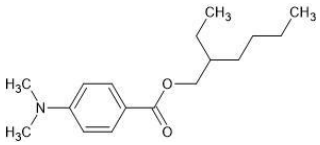	21245-02-3	OD-PABA; Padimate-O; 2-Ethylhexyl 4-(dimethylamino)benzoate
2-Ethoxyethyl (2Z)-2-cyano-2-[3-(3-methoxypropylamino) cyclohex-2-en-1-ylidene]acetate	-	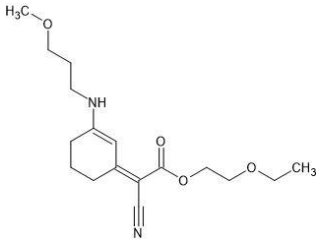	1419401-88-9	2-Ethoxyethyl (2Z)-2-cyano-2-[3-(3-methoxypropylamino) cyclohex-2-en-1-ylidene]acetate
Ethylhexyl methoxycinnamate	EHMC	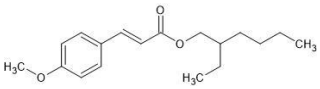	5466-77-3	OMC, Octinoxate
Ethylhexyl salicylate	EHS	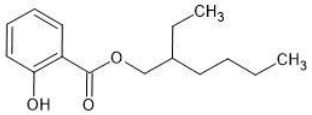	118-60-5	2-ethylhexyl salicylate; Octyl salicylate
Ethylhexyl triazone	EHT	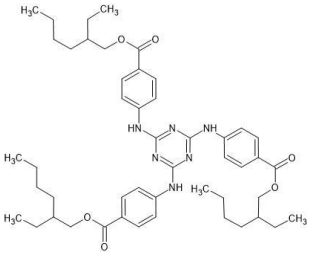	88122-99-0	Octyltriazon
Homosalate	HMS	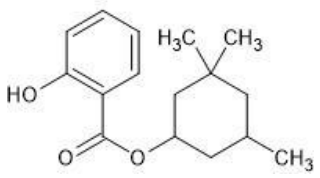	118-56-9	3,3,5-Trimethylcyclohexyl 2-hydroxybenzoate

INCI name	Abbreviation	Chemical structure	CAS No.	Synonyms
Isoamyl *p*-methoxycinnamate	IMC	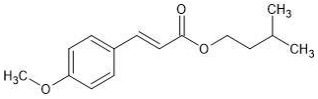	71617-10-2	Amiloxate
Methylene bisbenzotriazolyl tetramethylbutylphenol	MBBT	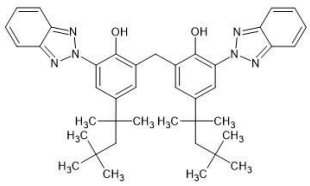	103597-45-1	Tinosorb M; Milestab 360
Octocrylene	OCR	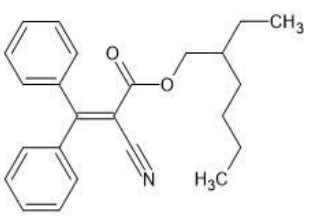	6197-30-4	OC; 2-ethylhexyl 2-cyano-3,3-diphenyl-2-propenoate
PEG-25 PABA	P25	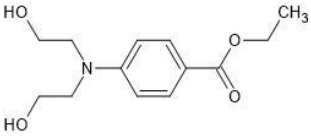	116242-27-4	Uvinul P 25; Ethyl p-bis(2-hydroxyethyl)aminobenzoate
Phenylbenzimidazole sulphonic acid	PBSA	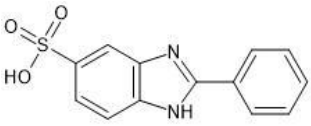	27503-81-7	Phenylbenzimidazole sulfonic acid; 2-Phenyl-3H-benzimida-zole-5-sulfonic acid
Phenylene Bis-Diphenyltriazine	S86	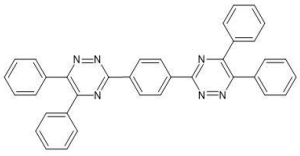	55514-22-2	-

INCI name	Abbreviation	Chemical structure	CAS No.	Synonyms
Polyacrylamidomethyl benzylidene camphor	PBC	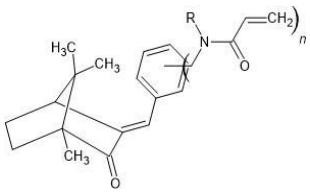	113783-61-2	-
Polysilicone-15	P15	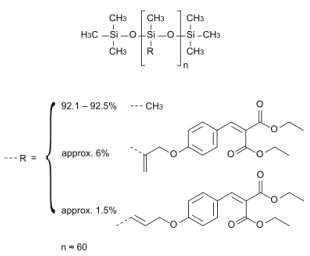	207574-74-1	Parsol SLX; Dimethiocodiethylbenzalmalonate
Terephthalylidene dicamphor sulphonic acid	TDSA	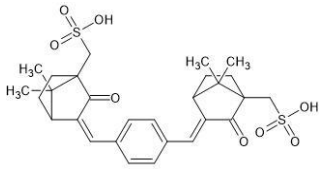	92761-26-7	Ecamsule; Mexoryl SX
Tris-biphenyl triazine	TBT	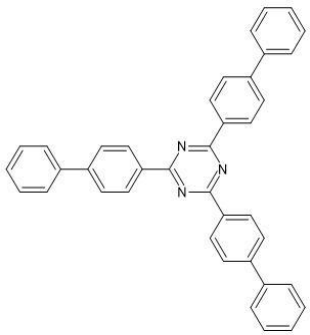	31274-51-8	2,4,6-Tris(biphenyl-4-yl)-1,3,5-triazin; Tinosorb A2B; ETH50

Table SII: Organic UV filter substances which's usage in cosmetics is at present not allowed according to European legislation (Regulation EC 1223/2009).

INCI name	Abbreviation	Structure	CAS No.	Synonyms	Authorization
3-benzylidene camphor	3-BC	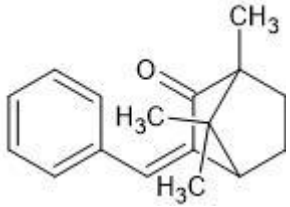	15087-24-8: undefined configuration	-	Until 2016: European union
		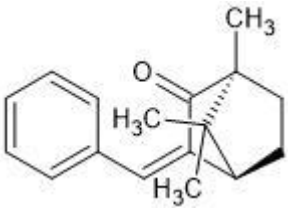	36275-29-3: (1S,4R) but unknown geometry at C=C-moiety		
4-aminobenzoic acid	PABA	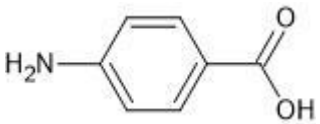	150-13-0	4-p-aminobenzoic acid, Para-aminobenzoic acid	USA, Japan and Mercosur*

* Mercosur (Spanish *Mercado Común del Sur*, "*Southern Common Market*", a South American trade block)

Table SIII: Metadata summary.

Search term	**No. of records (until the end of year 2020)**
“UV filter”	2,276
“UV filter” AND “transformation product”	45
“UV filter” AND “biotic”	4
“UV filter” AND “abiotic”	9
“UV filter” AND “degradation”	218
“UV filter” AND “photolysis”	62
“UV filter” AND “biodegradation”	46
“UV filter” AND “biodegradability”	9
“UV filter” AND “photoproduct”	8
“UV filter” AND “breakdown-product”	1
“UV filter” AND “intermediate”	53
Sum of found studies	2,731
Sum of studies the review relied upon	42

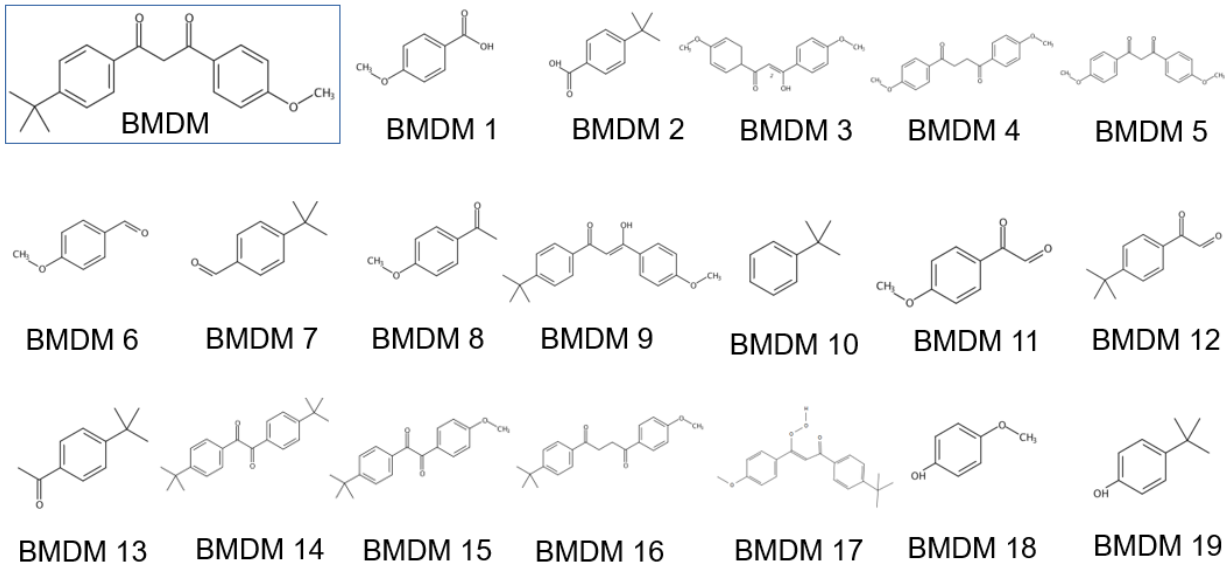

Figure S1: TPs of BMDM formed during photolysis experiments.

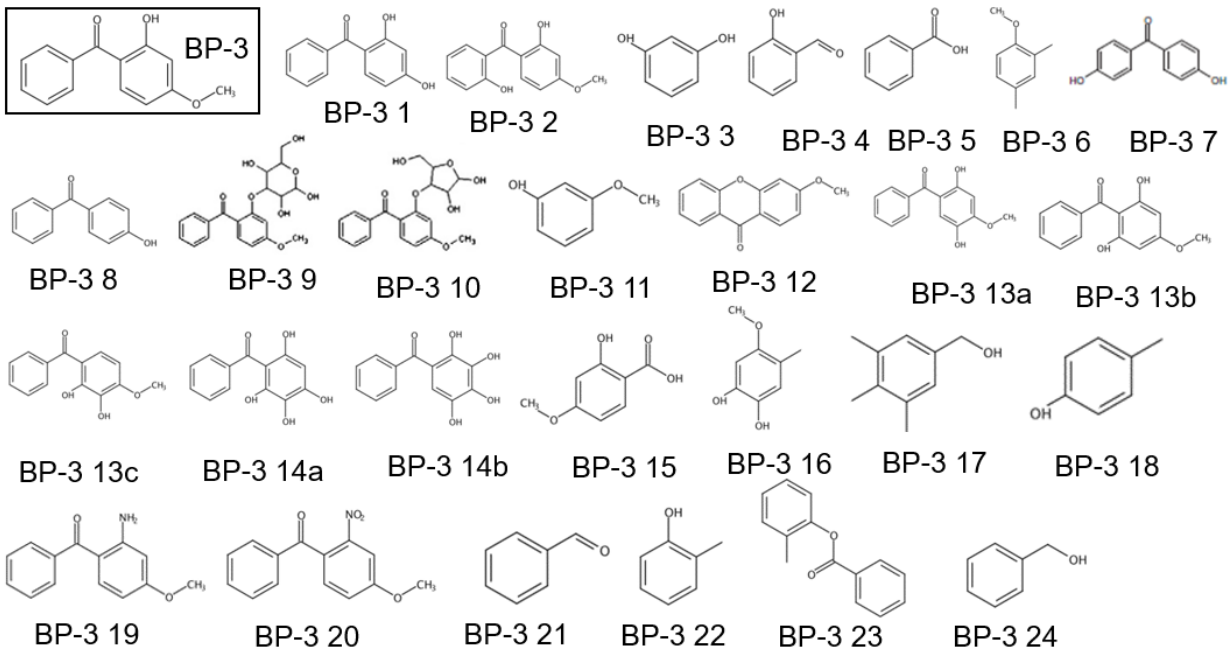

Figure S2: TPs of BP-3 formed during abiotic and biotic processes.

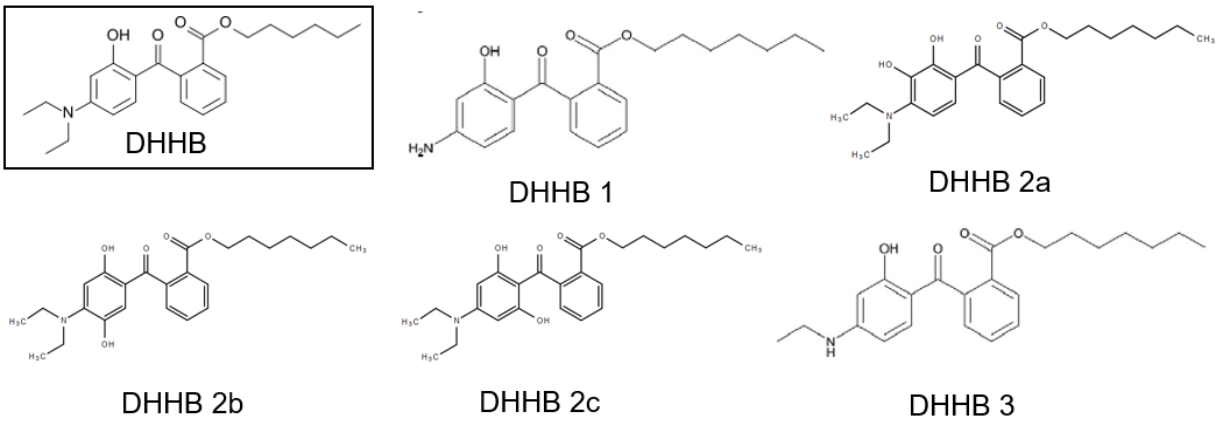

Figure S3: Photo-TPs of DHHB formed after irradiation by UV-C light (λ = 254 nm, 8 W) in aqueous solutions [1]. Note: the shown TP structures deviate from the structures presented in [1] since all TP structures included a heptyl (C_7) function in the mentioned reference. Noticeably, the UVF DHHB contains a hexyl (C_6) function. In addition, names and sum formula provided in the reference indicate that hexyl (C_6) must be the correct group. The structures in [1] seem to be misrepresented accidently.

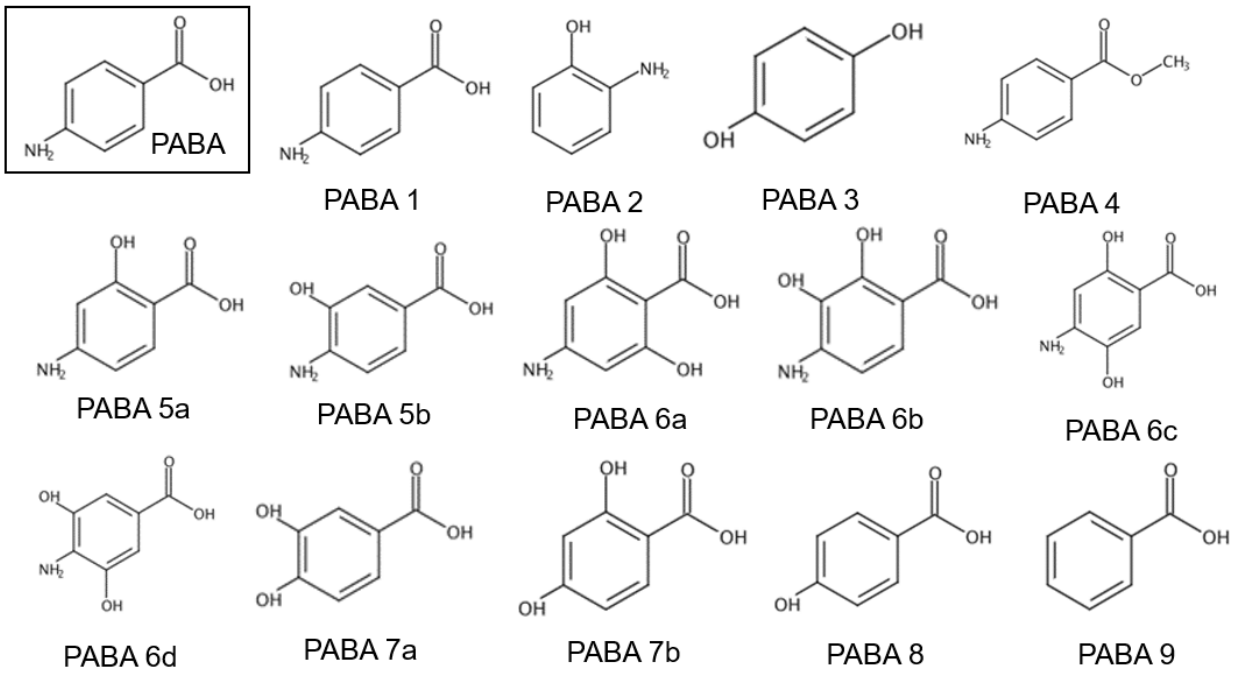

Figure S4: TPs of PABA formed during abiotic processes (photolysis and AOP experiments).

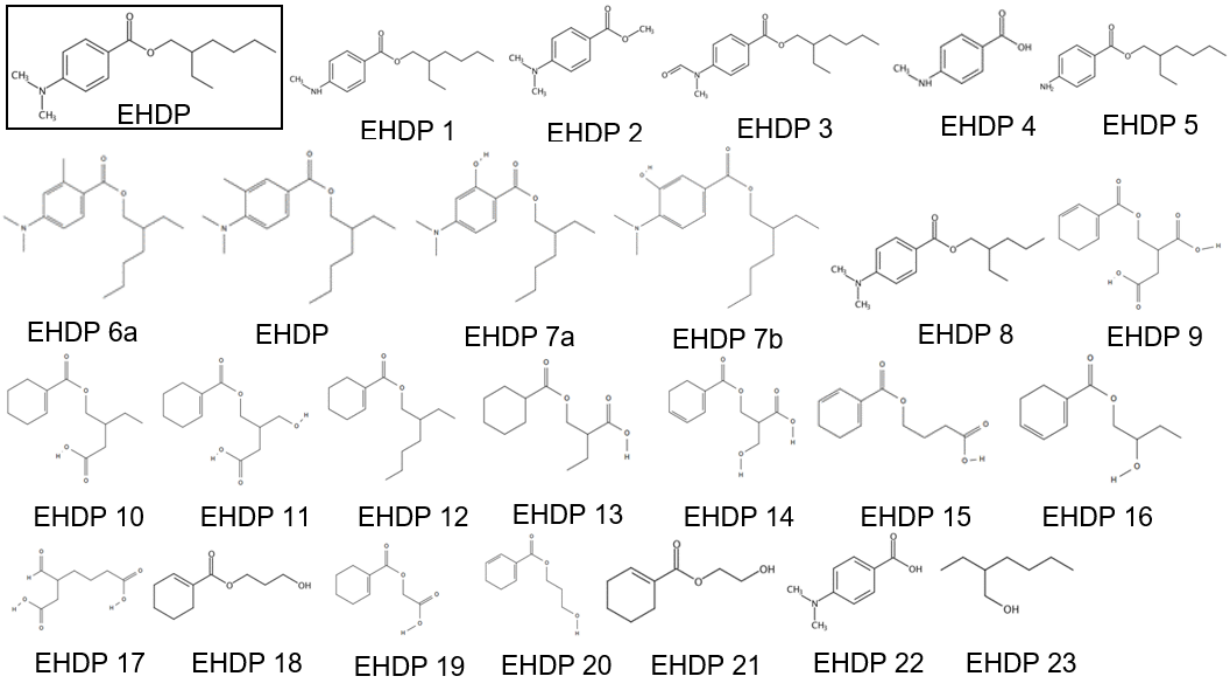

Figure S5: TPs of EHDP formed during abiotic and biotic processes.

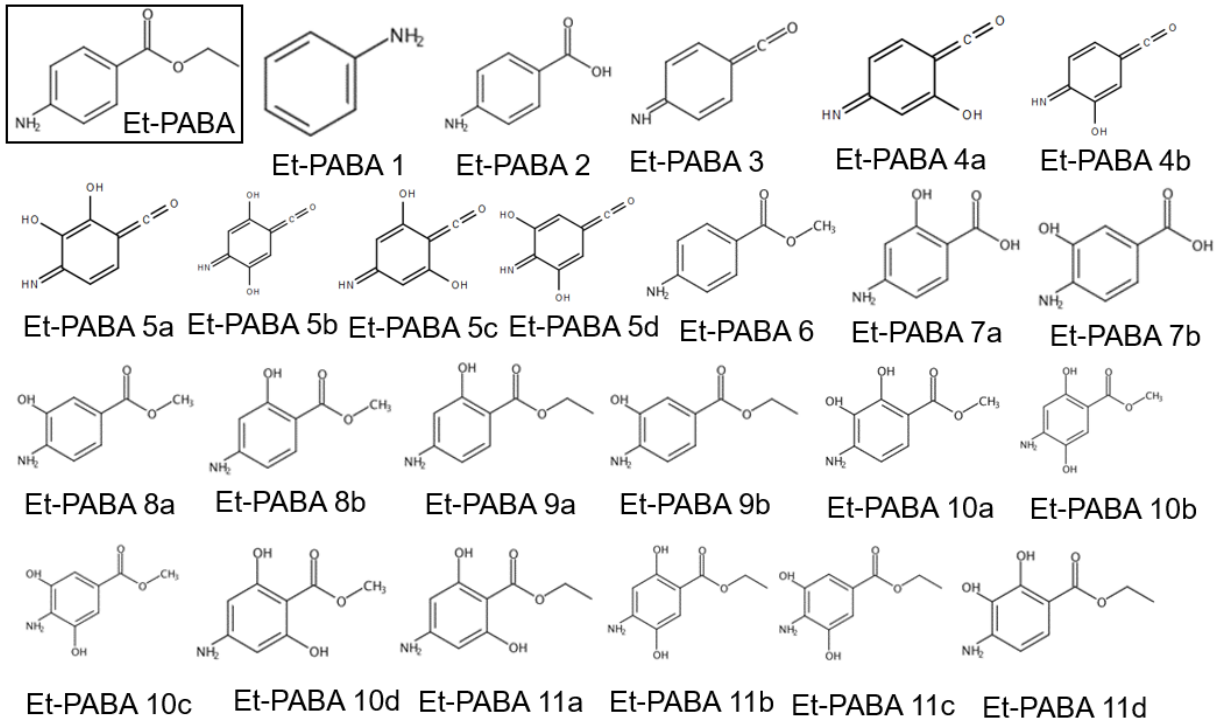

Figure S6: TPs of Et-PABA formed during direct photolysis with an UV-C lamp and under photocatalytic conditions using UV-C light in presence of TiO_2 [2].

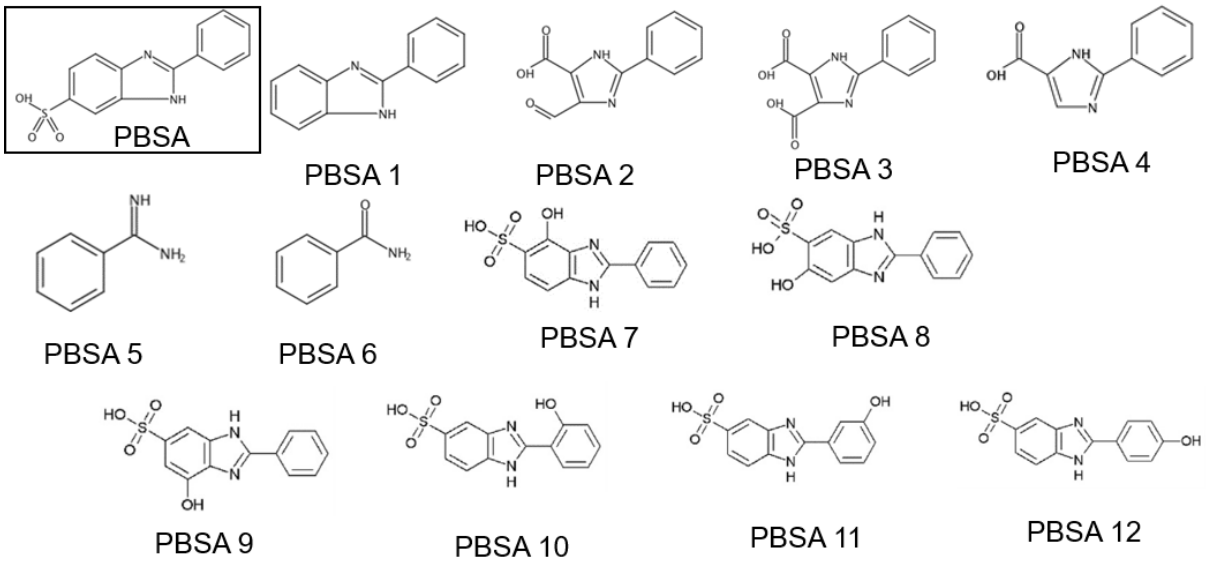

Figure S7: TPs of PBSA resulting from abiotic processes (photolysis using an UV-A/ UV-B lamp [3] or irradiation with UV-light and simulated sun light [4].

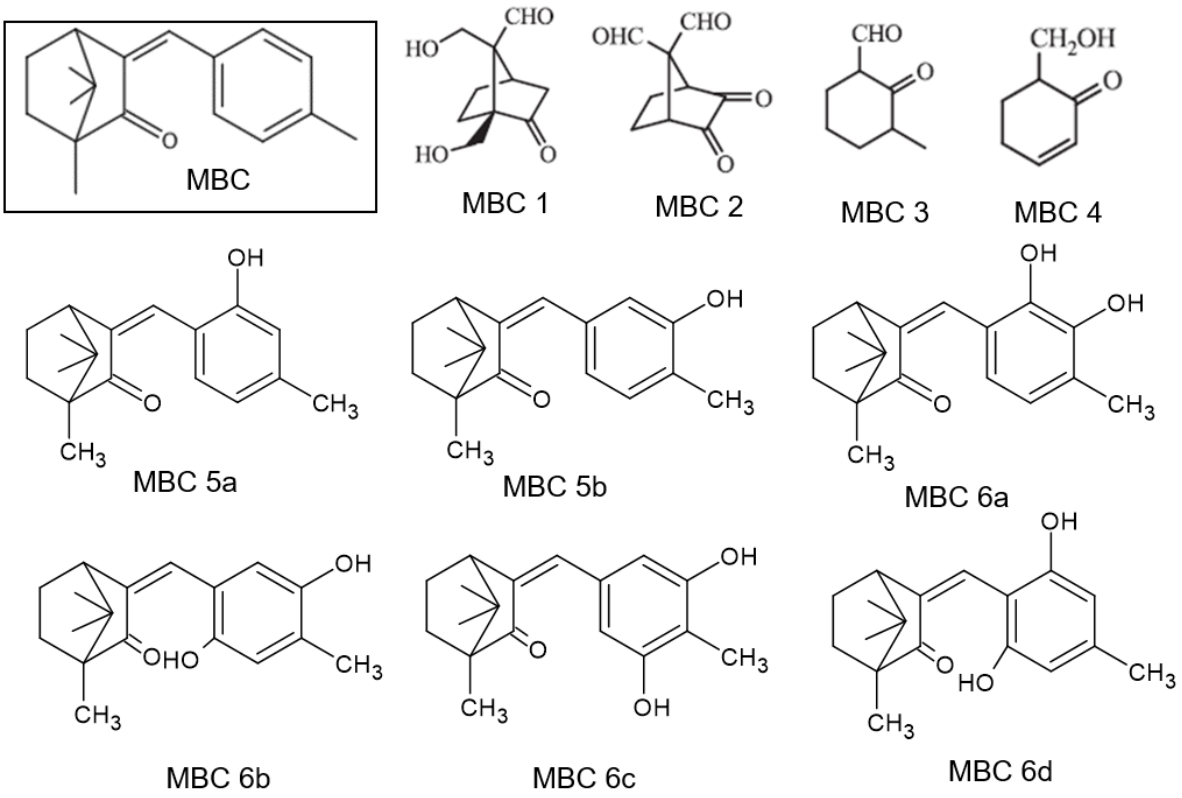

Figure S8: TPs of MBC formed during biotic processes [5, 6].

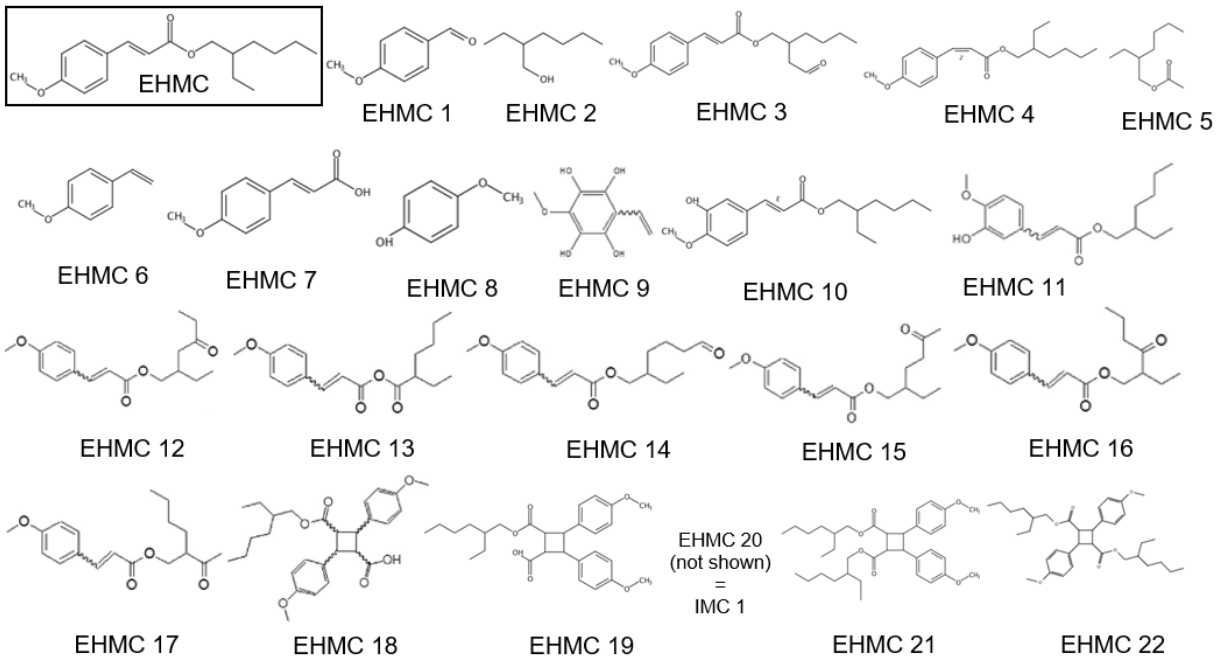

Figure S9: TPs of EHMC formed under abiotic and biotic conditions.

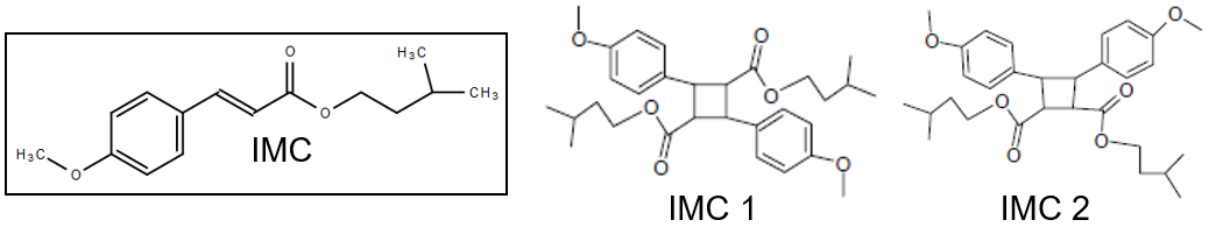

Figure S10: Photo-TPs of IMC formed under abiotic conditions (photolysis in aqueous solution under artificial sunlight [7]. IMC *E-Z*-isomerizes fast and dimerizes during photolysis [7].

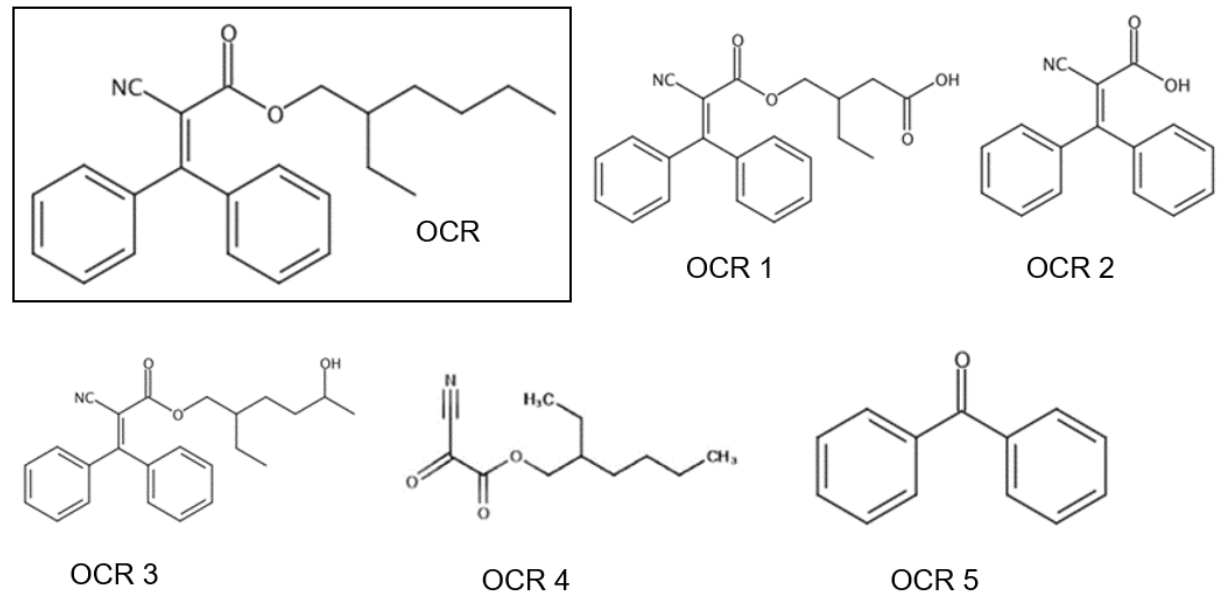

Figure S11: TP of OCR formed in abiotic (ozonation [8] and biotic (with microbial biofilm of *Mycobacterium agri* [9] processes.

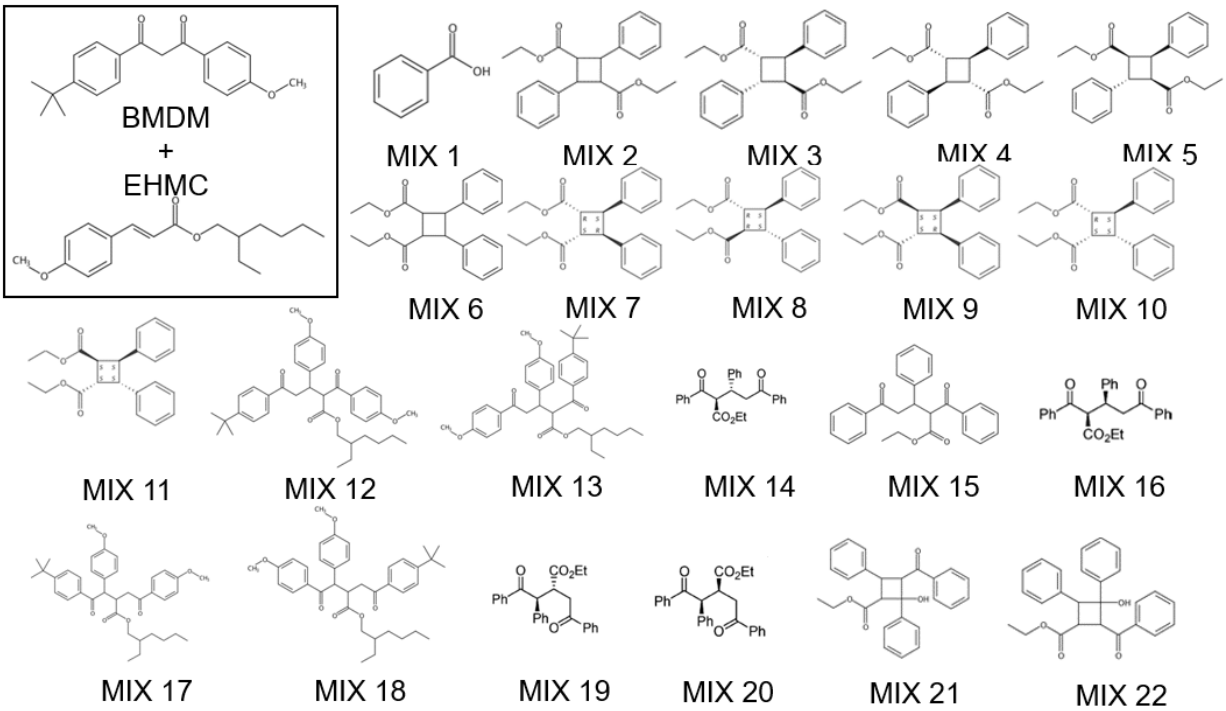

Figure S12: TPs formed during an abiotic process (photolysis performed by a solar simulator), in which two UVF (BMDM and EHMC) were applied as mixture [10].

Text S1: Overview on duplicates and triplicates of the reviewed TPs in Table II

The following duplicates and one triplicate were identified in Table II:

- EHDP 23 = EHMC 2;
- BMDM 6 = EHMC 1;
- BMDM 18 = EHMC 8;
- PABA 5b = Et-PABA 7b;
- PABA 4 = Et-PABA 6;
- PABA 1 = Et-PABA 1;
- PABA 5a = Et-PABA 7a;
- PB-3 5 = PABA 9 = MIX 1
- and special case: EHMC 20 (which was wrongly assigned to EHMC in [11]) = IMC 1. For details see annotation in Table II.

Table SIV: Complete list of all TP_{total} (187) which were evaluated regarding the information on their stability in literature and in the ECHA database (latest update in April 2022). If the ECHA database provided OECD 301 test results the TP was highlighted in green (if readily biodegradable in at least one OECD 301 test) or orange (not readily biodegradable in at least one OECD 301 test). Grey highlighted those TPs without entries or without information on the biodegradability (OECD 301 tests) in the ECHA database, respectively. The availability of literature data on stability of the TP has no influence on the color highlighting.

TP code	CAS	Stability (according to literature, see Table III)	Readily biodegradable: YES/ NO (according to database entry)	Biodegradability test (according to ECHA database entry or dossier, respectively)
BMDM 1	100-09-4	-	YES (89% degradation after 28 days)	OECD 301F
BMDM 2	98-73-7	-	NO	OECD 301 B (CO_2 evolution) and OECD 301 D
BMDM 3	2306713-02-8	-	-	-
BMDM 4	15982-64-6	-	-	-
BMDM 5	18362-51-1	-	-	-
BMDM 6 (= EHMC 1)	123-11-5	see EHMC 1: photo-labile [12], lower overall persistence (P_{OV}) than for UVF EHMC (predicted) [11]	YES (measured DOC removal was 97% after 6 days)	OECD 301 E
BMDM 7	939-97-9	-	YES (84% after 14 days)	OECD 301 B (CO_2 evolution)
BMDM 8	100-06-1	-	YES (100% degraded within 28 days)	EU Method C.4-B (modified OECD screening test for ready biodegradability)

TP code	CAS	Stability (according to literature, see Table III)	Readily biodegradable: YES/ NO (according to database entry)	Biodegradability test (according to ECHA database entry or dossier, respectively)
BMDM 9	1198075-35-2	-	-	-
BMDM 10	98-06-6	-	NO (11% after 28 days)	OECD 301 B (CO_2 evolution)
BMDM 11	1076-95-5	-	-	-
BMDM 12	7062-64-8	-	-	-
BMDM 13	943-27-1	-	-	-
BMDM 14	76471-78-8	-	-	-
BMDM 15	166321-82-0	-	-	-
BMDM 16	166321-83-1	-	-	-
BMDM 17	-	-	-	-
BMDM 18 (= EHMC 8)	150-76-5	see EHMC 8: lower overall persistence compared to EHMC (predicted) [11]	YES (based on BOD criterion, biodegradation rate was 86% at 28 days)	OECD 301 C (MITI)
BMDM 19	98-54-4	-	YES, but failing the 10-day-window criterion	OECD 301 F (MRT)
BP-3 1	131-56-6	(photo-)degradable [13]; increased biodegradability [14]; inhibited biodegradation (under oxic, nitrate-reducing and sulfate-reducing conditions) [15]	NO (0% BOD after 28 days)	OECD 301 C (MITI)

TP code	CAS	Stability (according to literature, see Table III)	Readily biodegradable: YES/ NO (according to database entry)	Biodegradability test (according to ECHA database entry or dossier, respectively)
BP-3 2	131-53-3	(photo-)degradable [13]; increased biodegradability [14]	NO (no degradation observed after 28 days)	OECD 301 B (CO_2 evolution)
BP-3 3	108-46-3	increased biodegradability [14]	YES (elimination rates: 66.7% after 14 days)	OECD 301 C (MITI)
BP-3 4	90-02-8	increased biodegradability [14]	NO (special case: transformation to 2-hydroxybenzoic acid after cultivation period of the test)	301 C (modified MITI test (I))
BP-3 5 (= MIX 1 = PABA 9)	65-85-0	increased biodegradability [14]	YES (in several tests)	*inter alia* OECD 301 B (CO_2 evolution) and OECD 301 C (MITI)
BP-3 6	6738-23-4	-	-	-
BP-3 7	611-99-4	-	YES (≥ 60% degradation relative to the $ThCO_2$ value)	OECD 301 B (CO_2 evolution)
BP-3 8	1137-42-4	-	YES (87% and 73% biodegradation, respectively (based on ThOD))	OECD 301 F (MRT)
BP-3 9	-	biodegradable [16]	-	-

TP code	CAS	Stability (according to literature, see Table III)	Readily biodegradable: YES/ NO (according to database entry)	Biodegradability test (according to ECHA database entry or dossier, respectively)
BP-3 10	-	biodegradable [16]	-	-
BP-3 11	150-19-6	-	-	-
BP-3 12	3722-52-9	-	-	-
BP-3 13a	52811-37-7	-	-	-
BP-3 13b	479-21-0	-	-	-
BP-3 13c	35836-41-0	-	-	-
BP-3 14a	-	-	-	-
BP-3 14b	-	-	-	-
BP-3 15	2237-36-7	-	-	-
BP-3 16	-	-	-	-
BP-3 17	39126-11-9	-	-	-
BP-3 18	106-44-5	increased biodegradability [14]; inhibited biodegradation (under oxic, nitrate-reducing and sulfate-reducing conditions) [15]	YES (80–95% degraded within 40 days)	OECD 301 C (modified MITI test (I))
BP-3 19	37527-68-7	-	-	-
BP-3 20	1228191-31-8	-	-	-

TP code	CAS	Stability (according to literature, see Table III)	Readily biodegradable: YES/ NO (according to database entry)	Biodegradability test (according to ECHA database entry or dossier, respectively)
BP-3 21	100-52-7	increased biodegradability [14]	YES (in several tests)	OECD 301 B (CO_2 evolution), OECD 301 E
BP-3 22	95-48-7	increased biodegradability [14]	YES (in several tests)	*inter alia* OECD 301 C (modified MITI test (I))
BP-3 23	617-02-7	increased biodegradability [14]	-	-
BP-3 24	100-51-6	increased biodegradability [14]	YES (in several tests, e.g. MITI: 9296% after 14 days)	*inter alia* OECD 301 C (modified MITI test (I))
DHHB 1	-	-	-	-
DHHB 2a	-	-	-	-
DHHB 2b	-	-	-	-
DHHB 2c	-	-	-	-
DHHB 3	-	-	-	-
PABA 1 (=Et-PABA 1)	62-53-3	-	YES (in several tests, e.g. CBT: 100% mineralization after 5 days)	*inter alia* OECD 301 D (CBT)
PABA 2	95-55-6	-	NO (18 – 27% after 14 days)	OECD 301 C

TP code	CAS	Stability (according to literature, see Table III)	Readily biodegradable: YES/ NO (according to database entry)	Biodegradability test (according to ECHA database entry or dossier, respectively)
PABA 3	123-31-9	-	YES (fulfilling the 14 day window criterion (70% biodegradation after 14 days))	OECD 301C (MITI I)
PABA 4 (= Et-PABA 6)	619-45-4	-	-	-
PABA 5a (= Et-PABA 7a)	65-49-6	-	-	-
PABA 5b (= Et-PABA 7b)	2374-03-0	-	-	-
PABA 6a	69727-10-2	-	-	-
PABA 6b	742040-28-4	-	-	-
PABA 6c	-	-	-	-
PABA 6d	958232-24-1	-	-	-
PABA 7a	99-50-3	-	-	-
PABA 7b	89-86-1	-	YES (76% biodegradation within 2 days)	OECD 301 A (DOC die away test)

TP code	CAS	Stability (according to literature, see Table III)	Readily biodegradable: YES/ NO (according to database entry)	Biodegradability test (according to ECHA database entry or dossier, respectively)
PABA 8	99-96-7	-	YES (76.5% degradation within 4 days)	OECD 301 D (CBT)
PABA 9 (= BP-3 5 = MIX 1)	65-85-0	increased biodegradability [14]	YES *(in several tests)*	*inter alia* OECD 301 B (CO_2 evolution) and OECD 301 C (MITI)
EHDP 1	158576-31-9	-	-	-
EHDP 2	1202-25-1	-	-	-
EHDP 3	-	-	-	-
EHDP 4	10541-83-0	-	-	-
EHDP 5	26218-04-2	-	YES (72-78% O_2 consumption)	OECD 301 F (MRT)
EHDP 6a	-	-	-	-
EHDP 6b	-	-	-	-
EHDP 7a	-	-	-	-
EHDP 7b	-	-	-	-
EHDP 8	-	-	-	-
EHDP 9	-	-	-	-

TP code	CAS	Stability (according to literature, see Table III)	Readily biodegradable: YES/ NO (according to database entry)	Biodegradability test (according to ECHA database entry or dossier, respectively)
EHDP 10	-	-	-	-
EHDP 11	-	-	-	-
EHDP 12	-	-	-	-
EHDP 13	-	-	-	-
EHDP 14	-	-	-	-
EHDP 15	-	-	-	-
EHDP 16	-	-	-	-
EHDP 17	-	-	-	-
EHDP 18	-	-	-	-
EHDP 19	-	-	-	-
EHDP 20	-	-	-	-
EHDP 21	-	-	-	-
EHDP 22	619-84-1	-	-	-
EHDP 23 (= EHMC 2)	104-76-7	see EHMC 2: lower overall persistence compared to EHMC (predicted) [11]	YES (complete removal of TOC (100%) and test substance (100%) within 2 weeks)	OECD 301 C (modified MITI test (I))

TP code	CAS	Stability (according to literature, see Table III)	Readily biodegradable: YES/ NO (according to database entry)	Biodegradability test (according to ECHA database entry or dossier, respectively)
Et-PABA 1 (= PABA 1)	62-53-3	-	YES (in several tests, e.g. CBT: 100% mineralization after 5 days)	*inter alia* OECD 301 D (CBT)
Et-PABA 2	150-13-0	-	YES (82% O_2 consumption after 28 days, but failing the 10-day-window criterion)	OECD 301 C (modified MITI test (I))
Et-PABA 3	-	-	-	-
Et-PABA 4a	-	-	-	-
Et-PABA 4b	-	-	-	-
Et-PABA 5a	-	-	-	-
Et-PABA 5b	-	-	-	-
Et-PABA 5c	-	-	-	-
Et-PABA 5d	-	-	-	-
Et-PABA 6 (= PABA 4)	619-45-4	-	-	-
Et-PABA 7a (= PABA 5a)	65-49-6	-	-	-

TP code	CAS	Stability (according to literature, see Table III)	Readily biodegradable: YES/ NO (according to database entry)	Biodegradability test (according to ECHA database entry or dossier, respectively)
Et-PABA 7b (=PABA 5b)	2374-03-0	-	-	-
Et-PABA 8a	63435-16-5	-	-	-
Et-PABA 8b	4136-97-4	-	-	-
Et-PABA 9a	6059-17-2	-	-	-
Et-PABA 9b	87081-52-5	-	-	-
Et-PABA 10a	-	-	-	-
Et-PABA 10b	-	-	-	-
Et-PABA 10c	-	-	-	-
Et-PABA 10d	-	-	-	-
Et-PABA 11a	-	-	-	-
Et-PABA 11b	-	-	-	-
Et-PABA 11c	-	-	-	-
Et-PABA 11d	-	-	-	-
PBSA 1	716-79-0	-	-	-
PBSA 2	-	-	-	-

TP code	CAS	Stability (according to literature, see Table III)	Readily biodegradable: YES/ NO (according to database entry)	Biodegradability test (according to ECHA database entry or dossier, respectively)
PBSA 3	888-60-8	-	-	-
PBSA 4	77498-98-7	-	-	-
PBSA 5	618-39-3	-	-	-
PBSA 6	55-21-0	-	-	-
PBSA 7	-	same or less for biodegradation compared to the UVF PBSA predicted [4]	-	-
PBSA 8	-	same or less for biodegradation compared to the UVF PBSA predicted [4]	-	-
PBSA 9	-	same or less for biodegradation compared to the UVF PBSA predicted [4]	-	-
PBSA 10	-	same or less for biodegradation compared to the UVF PBSA predicted [4]	-	-
PBSA 11	-	same or less for biodegradation compared to the UVF PBSA predicted [4]	-	-
PBSA 12	-	same or less for biodegradation compared to the UVF PBSA predicted [4]	-	-
MBC 1	-	-	-	-
MBC 2	-	-	-	-

TP code	CAS	Stability (according to literature, see Table III)	Readily biodegradable: YES/ NO (according to database entry)	Biodegradability test (according to ECHA database entry or dossier, respectively)
MBC 3	1194-91-8	-	-	-
MBC 4	-	-	-	-
MBC 5a	-	-	-	-
MBC 5b	-	-	-	-
MBC 6a	-	-	-	-
MBC 6b	-	-	-	-
MBC 6c	-	-	-	-
MBC 6d	-	-	-	-
EHMC 1 (= BMDM 6)	123-11-5	photo-labile [12], lower overall persistence (P_{OV}) than for UVF EHMC (predicted) [11]	YES (measured DOC removal was 97% after 6 days)	OECD 301 E
EHMC 2 (= EHDP 23)	104-76-7	lower overall persistence compared to EHMC (predicted) [11]	YES (complete removal of TOC (100%) and test substance (100%) within 2 weeks)	OECD 301 C (modified MITI test (I))
EHMC 3	-	photo-labile [12], lower overall persistence (POV) than for UVF EHMC (predicted) [11]	-	-
EHMC 4	177352-99-7	same overall persistence like (E)-EHMC (predicted) [11]	-	-

TP code	CAS	Stability (according to literature, see Table III)	Readily biodegradable: YES/ NO (according to database entry)	Biodegradability test (according to ECHA database entry or dossier, respectively)
EHMC 5	103-09-3	-	YES (70% degradation after 28 days)	OECD 301 B (CO_2 evolution)
EHMC 6	637-69-4	-	-	-
EHMC 7	830-09-1	lower overall persistence (POV) than for UVF EHMC (predicted) [11]	-	-
EHMC 8 (= BMDM 18)	150-76-5	lower overall persistence than EHMC (predicted) [11]	YES (Based on BOD criterion, biodegradation rate was 86% at 28 days)	OECD 301 C (MITI)
EHMC 9	-	photo-labile [12], lower overall persistence (POV) than for UVF EHMC (predicted) [11]	-	-
EHMC 10	-	photo-labile [12], same overall persistence (POV) like (E)-EHMC (predicted) [11]	-	-
EHMC 11	-	photo-labile [12], same overall persistence (POV) like (E)-EHMC (predicted) [11]	-	-
EHMC 12	-	photo-labile [12], higher overall persistence (POV) compared to UVF EHMC (predicted) [11]	-	-
EHMC 13	-	photo-labile [12], higher overall persistence (POV) compared to UVF EHMC (predicted) [11]	-	-

TP code	CAS	Stability (according to literature, see Table III)	Readily biodegradable: YES/ NO (according to database entry)	Biodegradability test (according to ECHA database entry or dossier, respectively)
EHMC 14	-	photo-labile [12], higher overall persistence (POV) compared to UVF EHMC (predicted) [11]	-	-
EHMC 15	-	photo-labile [12], higher overall persistence (POV) compared to UVF EHMC (predicted) [11]	-	-
EHMC 16	-	photo-labile [12], lower overall persistence (POV) than for UVF EHMC (predicted) [11]	-	-
EHMC 17	-	photo-labile [12]	-	-
EHMC 18	-	photo-labile [12], higher overall persistence (POV) compared to UVF EHMC (predicted) [11]	-	-
EHMC 19	-	photo-labile [12], higher overall persistence (POV) compared to UVF EHMC (predicted) [11], photostable [17]	-	-
EHMC 20* = IMC 1	-	-	-	-
EHMC 21	-	photo-labile [12], higher overall persistence (POV) compared to UVF EHMC (predicted) [11], transient photo-stability (photolytically instable) [17]	-	-

TP code	CAS	Stability (according to literature, see Table III)	Readily biodegradable: YES/ NO (according to database entry)	Biodegradability test (according to ECHA database entry or dossier, respectively)
EHMC 22	-	-	-	-
IMC 1	-	-	-	-
IMC 2	-	-	-	-
OCR 1	-	-	-	-
OCR 2	10380-41-3	-	-	-
OCR 3	-	-	-	-
OCR 4	-	-	-	-
OCR 5	119-61-9	-	YES (66-84% mineralization after 28 days)	OECD 301F (MRT)
MIX 1 (= BP-3 5 = PABA 9)	65-85-0	increased biodegradability [14]	YES (in several tests)	*inter alia* OECD 301 B (CO_2 evolution) and OECD 301 C (MITI)
MIX 2	56280-73-0	-	-	-
MIX 3	-	-	-	-
MIX 4	-	-	-	-
MIX 5	-	-	-	-
MIX 6	-	-	-	-

TP code	CAS	Stability (according to literature, see Table III)	Readily biodegradable: YES/ NO (according to database entry)	Biodegradability test (according to ECHA database entry or dossier, respectively)
MIX 7	-	-	-	-
MIX 8	-	-	-	-
MIX 9	-	-	-	-
MIX 10	-	-	-	-
MIX 11	-	-	-	-
MIX 12	-	-	-	-
MIX 13	-	-	-	-
MIX 14	-	-	-	-
MIX 15	117402-91-2	-	-	-
MIX 16	-	-	-	-
MIX 17	-	-	-	-
MIX 18	-	-	-	-
MIX 19	-	-	-	-
MIX 20	-	-	-	-
MIX 21	-	-	-	-
MIX 22	-	-	-	-

DOC – dissolved organic carbon; BOD – biochemical oxygen demand; MITI - Ministry of International Trade and Industry, Japan; MRT – manometric respiratory test; $ThCO_2$ - theoretical amount of CO_2; ThOD – theoretical oxygen demand; CBT – closed bottle test; TOC – total organic carbon.

References

1. Celeiro M, Facorro R, Dagnac T, Vilar VJP, and Llompart M. Photodegradation behaviour of multiclass ultraviolet filters in the aquatic environment: Removal strategies and photoproduct identification by liquid chromatography–high resolution mass spectrometry. Journal of Chromatography A. 2019;1596:8–19.

2. Li AJ, Sang Z, Chow C-H, Law JC-F, Guo Y, and Leung KS-Y. Environmental behavior of 12 UV filters and photocatalytic profile of ethyl-4-aminobenzoate. Journal of Hazardous Materials. 2017;337:115–25.

3. Zhang S, Chen J, Qiao X, Ge L, Cai X, and Na G. Quantum Chemical Investigation and Experimental Verification on the Aquatic Photochemistry of the Sunscreen 2-Phenylbenzimidazole-5-Sulfonic Acid. Environ Sci Technol. 2010;44(19):7484–90.

4. Westphal J, Kümmerer K, and Olsson O. Experimental and in silico assessment of fate and effects of the UV filter 2-phenylbenzimidazole 5-sulfonic acid and its phototransformation products in aquatic solutions. Water Research. 2020;171:115393.

5. Volpe A, Pagano M, Mascolo G, Grenni P, and Rossetti S. Biodegradation of UV-filters in marine sediments. Science of The Total Environment. 2017;575:448–57.

6. Badia-Fabregat M, Rodríguez-Rodríguez CE, Gago-Ferrero P, Olivares A, Piña B, Díaz-Cruz MS, Vicent T, Barceló D, and Caminal G. Degradation of UV filters in sewage sludge and 4-MBC in liquid medium by the ligninolytic fungus Trametes versicolor. Journal of Environmental Management. 2012;104:114–20.

7. Rodil R, Moeder M, Altenburger R, and Schmitt-Jansen M. Photostability and phytotoxicity of selected sunscreen agents and their degradation mixtures in water. Anal Bioanal Chem. 2009;395(5):1513–24.

8. Hopkins ZR, Snowberger S, and Blaney L. Ozonation of the oxybenzone, octinoxate, and octocrylene UV-filters: Reaction kinetics, absorbance characteristics, and transformation products. Journal of Hazardous Materials. 2017;338:23–32.

9. Suleiman M, Schröder C, Kuhn M, Simon A, Stahl A, Frerichs H, and Antranikian G. Microbial biofilm formation and degradation of octocrylene, a UV absorber found in sunscreen. Commun Biol. 2019;2(1):430.

10. Dondi D, Albini A, and Serpone N. Interactions between different solar UVB/UVA filters contained in commercial suncreams and consequent loss of UV protection. Photochem Photobiol Sci. 2006;5(9):835.

11. Gackowska A, Studziński W, Kudlek E, Dudziak M, and Gaca J. Estimation of physicochemical properties of 2-ethylhexyl-4-methoxycinnamate (EHMC) degradation products and their toxicological evaluation. Environ Sci Pollut Res. 2018;25(16):16037–49.

12. Jentzsch F, Olsson O, Westphal J, Reich M, Leder C, and Kümmerer K. Photodegradation of the UV filter ethylhexyl methoxycinnamate under ultraviolet light: Identification and in silico assessment of photo-transformation products in the context of grey water reuse. Science of The Total Environment. 2016;572:1092–100.

13. Dubowski Y, Alfiya Y, Gilboa Y, Sabach S, and Friedler E. Removal of organic micropollutants from biologically treated greywater using continuous-flow vacuum-UV/UVC photo-reactor. Environ Sci Pollut Res. 2020;27(7):7578–87.

14. Zúñiga-Benítez H, Aristizábal-Ciro C, and Peñuela GA. Heterogeneous photocatalytic degradation of the endocrine-disrupting chemical Benzophenone-3: Parameters optimization and by-products identification. Journal of Environmental Management. 2016;167:246–58.

15. Liu Y-S, Ying G-G, Shareef A, and Kookana RS. Biodegradation of the ultraviolet filter benzophenone-3 under different redox conditions. Environmental Toxicology and Chemistry. 2012;31(2):289–95.

16. Gago-Ferrero P, Badia-Fabregat M, Olivares A, Piña B, Blánquez P, Vicent T, Caminal G, Díaz-Cruz MS, and Barceló D. Evaluation of fungal- and photo-degradation as potential treatments for the removal of sunscreens BP3 and BP1. Science of The Total Environment. 2012;427–428:355–63.

17. MacManus-Spencer LA, Tse ML, Klein JL, and Kracunas AE. Aqueous Photolysis of the Organic Ultraviolet Filter Chemical Octyl Methoxycinnamate. Environ Sci Technol. 2011;45(9):3931–7.